The Utrophin-Actin Interface

Michael James Francis Broderick BSc (Hons).

Doctor of Philosophy

University of Glasgow
Division of Biochemistry and Molecular Biology
Faculty of Biomedical and Life Sciences
November 2005

Abstract

The spectrin superfamily is a diverse group of proteins variously involved in cross-linking, bundling and binding to the F-actin cytoskeleton. These proteins are modular in nature and interaction with actin occurs, at least in part, via CH domain containing ABDs. The actin-binding domains of the spectrin superfamily proteins are all very similar in overall structure however the functions of the individual proteins differ greatly. Utrophin is a member of the spectrin superfamily and has been used extensively to investigate and model the association of actin-binding domains with F-actin; however, much controversy exists as to whether binding occurs when the domain is in an open or a closed conformation.

The data herein specifically investigates the importance of the utrophin ABD inter-CH domain linker to the conformation of the domain and how this domain associates with F-actin. We provide evidence that this particular region of the ABD is particularly sensitive to mutation and that the conformation of the domain when in solution can not be altered by affecting the electrostatic environment surrounding the protein. It has been assumed previously that the utrophin ABD adopts a closed and compact configuration in solution similar to the fimbrin crystal structure conformation; however we present evidence that suggests this is not the case. It has been proposed that the utrophin ABD may open from this closed conformation to bind F-actin in a more open manner, we present data that demonstrates that opening of the domain is not essential to F-actin binding and that there is very little conformation change associated with the domain upon interaction with F-actin.

It appears that the utrophin ABD can bind F-actin in two conformations. This supports current models of utrophin ABD binding where interaction with F-actin occurs in either an open or closed conformation. The data presented here provides an interesting insight into the utrophin ABD/F-actin interaction and raises many questions regarding the evaluation of current binding models. Future research stemming from this work will serve to further the understanding of how utrophin and related actin-binding proteins interact with F-actin.

Table of Contents

Chapter 2: Materials and Methods

Chapter 3: pH Induced Conformational Change of the Utrophin ABD

Chapter 4: Utrophin ABD Linker Mutants

Chapter 5: Utrophin ABD Cysteine Mutants

List of Figures

List of Tables

Acknowledgements

I would like to express my sincerest thanks to Professor Steve Winder for his excellent supervision throughout the course of my PhD. I am very grateful for his advice, encouragement and constant support.

In addition, I wish to acknowledge the members of the Winder/Ayscough lab who have been a constant source of support and advice which I have found to be invaluable during the course of my project. I wish to thank Dr Sharon Kelly and Dr Rosie Stainforth for their assistance with circular dichroism and fluorescence analyses and Dr Olwyn Byron for her help with analytical ultracentrifugation. I would also like to thank Dr Andrey Bobkov for his help with the differential scanning calorimetry analyses. I would especially like to thank Professors Carl and Elizabeth Smythe who afforded me the use of space within their lab and were particularly accommodating of me during the final few months of my project. I would also like to thank the members of the Smythe lab but especially Barry and Richard who have helped keep me sane and were always at hand when a drink after work was required. I also wish to thank the University of Glasgow and the University of Sheffield for the opportunity to work at both institutions but also the MRC for providing the funding for my project.

Finally, I would also like to thank my family for their continued encouragement and support over the last four years, without which, I don't think I would be where I am today.

Declaration

I certify that this thesis is a result of my own work and that I have not been assisted in its production, except where acknowledged in the text. No part of the manuscript has been submitted for consideration for any other higher degree, and all references cited have been consulted.

Michael J. F. Broderick
Candidate

I certify that Michael J. F. Broderick is the author of this thesis and has complied with the regulations of the University of Glasgow appropriate to its submission.

Professor Steven J. Winder
Supervisor

November 2005

Abbreviations

ABD;	actin-binding domain
atm;	atmospheres
ATP;	adenosine tri-phosphate
BMD;	becker muscular dystrophy
CAPS;	3-(Cyclohexylamino)-1-propanesulfonic acid
CD;	circular dichroism
CH;	calponin homology
DMSO;	dimethyl sulphoxide
DNA;	deoxyribonucleic acid
dNTP;	deoxyribonucleotide triphosphate
DSC;	differential scanning calorimetry
DTT;	dithiothreitol
DTNB;	5,5'-Dithiobis(2-nitrobenzoic acid)
DMD;	duchenne muscular dystrophy
ε;	extinction coefficient ($cm^{-1}M^{-1}$)
ECL;	enhanced chemiluminescence
EDTA;	ethylenediaminetetraacetic acid
EGTA;	ethylene glycol-bis(2-aminoethylether)-*N,N,N',N'* -tetraacetic acid
F-actin;	filamentous actin
FRET;	fluorescence resonance energy transfer
g;	gravity
G-actin;	globular actin
HRP;	horseradish peroxidase
IPTG;	isopropyl-β-D-thiogalactopyranoside
K;	Kelvin
K_{av};	coefficient of partitioning
Kb;	kilobases
K_d;	dissociation constant
kDa;	kilo Daltons

Mb;	megabases
mdeg;	millidegrees
MES;	2-(N-Morpholino)ethanesulfonic acid
MW;	molecular weight
NTCB;	2-Nitro-5-thiocyanobenzoate
PCR;	polymerase chain reaction
PDZ;	protein interaction domain
PIP_2;	phosphatidylinositol bisphosphate
PIPES;	1,4-piperazinediethanesulfonic acid
rpm;	revolutions per minute
SDS;	sodium dodecylsulphate
SDS-PAGE;	sodium dodecyl sulphate polyacrylamide gel electrophoresis
SET;	sucrose, EDTA, tris
TCEP;	Tris(2-carboxyethyl)phosphine hydrochloride
TE;	Tris-HCl, EDTA
TED	Tris-HCl, EDTA, DTT
TEMED;	N, N, N', N'-tetramethylethylenediamine
θ;	mean residual molar ellipticity
T_m;	melting point temperature
Tris;	tris (hydroxymethyl) aminomethane
UV;	ultra violet
UTR261;	wild type utrophin actin-binding domain
$UTR^{\alpha\text{-actinin}}$;	utrophin α-actinin-like linker mutant
$UTR^{fimbrin}$;	utrophin fimbrin-like linker mutant
UTR^{T36C};	utrophin single cysteine mutant
$UTR^{T36C/S242C}$;	utrophin double cysteine mutant
V;	volts
v/v;	volume per volume
w/v;	weight per volume

Chapter 1:

Introduction

Chapter 1

Introduction

1.1 Introduction

The eukaryotic cytoskeletal network is formed from a number of filamentous systems composed of polymers of actin, tubulin or intermediate filament proteins. The actin stress fibres, microtubules and intermediate filaments generated are integrated in a highly organised manner that can be both dynamic as well as stable. The filamentous state and organisation of these proteins provides the cell with an internal scaffold essential to many cellular processes, including mechanical strength, cellular morphology, adhesion, motility, intracellular trafficking, cell division, and networks for inter- and intracellular communication. The cytoskeletal network allows rapid remodelling in response to altered mechanical needs facilitated by the dynamic exchange of protein subunits within the system and by the manner in which the network is linked through cross-linking proteins.

Interaction with filamentous actin (F-actin) requires a protein to possess motifs or domains that help to facilitate this association. One such domain is the calponin homology (CH) domain. This particular domain can be found within a wide range of proteins and may be present either singly, as a pair or a tandem pair. In any case almost all structural information about the domain has stemmed from work involving relatively few proteins that encompass all three of the CH domain families: namely calponin, containing a single CH domain; spectrin, α-actinin, dystrophin and utrophin, all of which contain a pair of CH domains referred to as an actin-binding domain (ABD); and fimbrin, which contains a tandem pair of CH domains (two ABDs). Of these proteins, α-actinin, dystrophin and utrophin are more closely related and form the bulk of a protein group referred to as the spectrin superfamily. This group of proteins is particularly interesting given that all members of the group have very different cellular functions even though they are essentially constructed from the same basic modules. These protein modules, most noticeably the spectrin repeat, are present to differing extents depending on the particular superfamily member and impart functionality specific to each protein. The following introduction aims to give

an overview of this superfamily and how the structure of these proteins is tied to their function within the cell.

1.2 *Spectrin family Proteins*

1.2.1 *Introduction to spectrin superfamily proteins*

The spectrin family of proteins are highly modular and share common structural elements including a calponin homology (CH) domain containing an actin-binding domain, spectrin repeats, EF-hands, and various other signalling domains and motifs (Fig. 1). The spectrin family of proteins arose from work that originally focused on understanding the role that spectrin played biochemically in the organisation and assembly of the cytoskeleton (reviewed in (Gratzer, 1982). Spectrin possesses the ability to self assemble but the molecular basis of this process could not be explained until more was known about the sequence and, ultimately, the structure of the protein. The work of Speicher and Marchesi (1984) provided the protein sequence of almost half of the α-spectrin chain. This work identified spectrin as being a highly modular protein composed of many repeating 106 amino acid units (Speicher and Marchesi, 1984). The helical nature of these units was predicted to form triple-helical coiled-coil bundles which were dubbed spectrin repeats. Continued investigation and DNA sequencing led to the determination of several α-spectrin sequences from erythrocyte, *Drosophila* and brain (Dubreuil et al., 1989; Sahr et al., 1990; Wasenius et al., 1989). It was around this time that the DNA sequences encoding the related proteins α-actinin and dystrophin were completed (Baron et al., 1987; Koenig et al., 1988). These proteins were found to contain repeating units similar to those found in spectrin (Davison and Critchley, 1988) and hence, the spectrin family of proteins was born.

The sequencing of α- and β-spectrin, α-actinin and dystrophin has revealed similarities not only within the spectrin repeat but also the other domains and motifs present within these proteins. Subsequent analyses have revealed an evolutionary pathway for the divergence of spectrin and dystrophin/utrophin from a common α-actinin ancestor via a series of rearrangements, duplications and evolution of repeats

and other domains, as well as the acquisition of unique domains such as PH, WW, and SH3 (Figure 2).

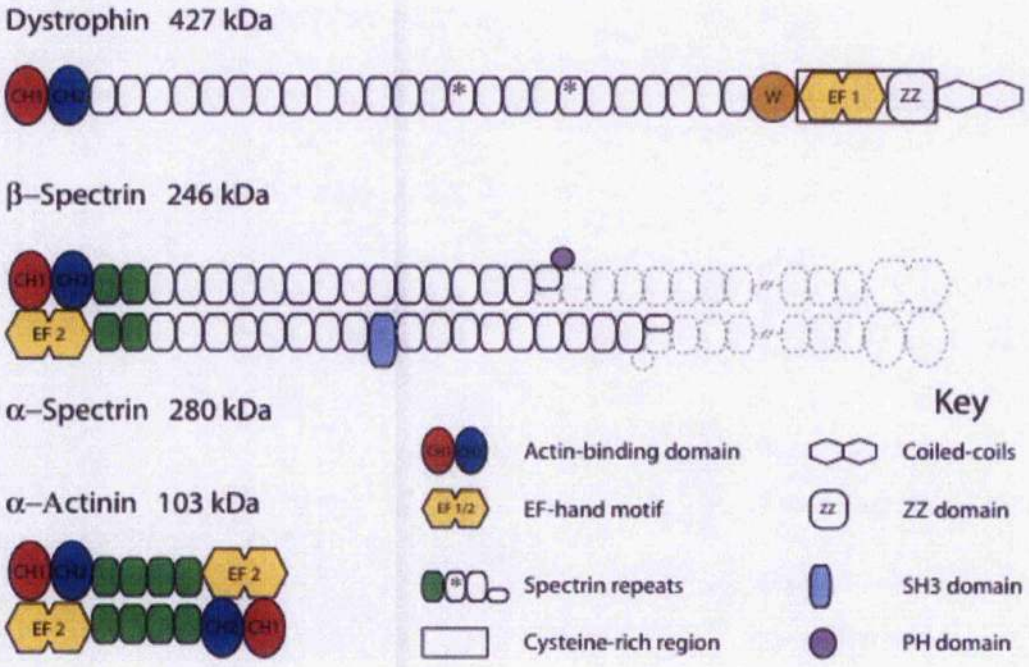

Figure 1.1: Structure of spectrin superfamily proteins. Modular domains within each protein are clearly defined. Shaded spectrin repeats represent coiled-coils involved in dimerisation events, incomplete repeats represent proportionally the number of coiled-coil helices contributed by α- and β-spectrin when generating a complete spectrin repeat during formation of the spectrin tetramer. The dashed lines indicate how two spectrin heterodimers interact to form a functional spectrin tetramer. Asterisks in the dystrophin spectrin repeats represent the position of the two greater repeats in dystrophin with respect to utrophin, which in all other respects has a similar overall structure. Numbers in the EF hand regions represent the number of EF hand motifs.

1.2.2 *Evolution of spectrin superfamily proteins*

The availability of complete sequences for α-actinin, spectrin and dystrophin has allowed the ancestry and evolution of the proteins to be traced. Multiple sequence alignments and phylogenetic trees have been combined with precise alignment of equivalent domains within each protein to provide details of the relationship that exist between each of the protein domains. Analysis of the amino

acid sequences from α-actinin, spectrin and dystrophin suggested that all three of the protein families have arisen from a common ancestral protein that was similar to α-actinin (Byers et al., 1992; Dubreuil, 1991) via a series of gene duplications and gene rearrangements (Baines, 2003; Pascual et al., 1997; Thomas et al., 1997; Viel, 1999). One of the diagnostic features of the spectrin superfamily of proteins is the presence of the 106-120 repetitive unit referred to as the spectrin repeat (Speicher and Marchesi, 1984). Sequence comparisons suggest that all three of these proteins share significant homology within their N-terminal actin-binding domains and in the spectrin repeats that form the rod domains (Davison and Critchley, 1988). The spectrin repeats are found in distinct multiples in each of the proteins resulting in a characteristic actin cross-linking distance. α-Actinin contains four repeats, β-spectrin 17, α-spectrin 20 and dystrophin 24. The sequences of some spectrin repeats of α- and β-spectrin are similar in many ways to the four repeats present in α-actinin (Dubreuil, 1991). Within the cell α-actinin and spectrin dimerise although the spectrins interact further to generate a functional tetramer (Figure 1.1). Most notable is that the ends of the native spectrin tetramer involved in the dimerisation event show remarkable similarity to the rod domain repeats of α-actinin that also mediate dimer formation. Indeed, homologous regions of all of the α-actinin protein domains can be found within the sequences of α- and β-spectrin. For example, the amino and carboxy terminal regions of α-actinin resemble the N-terminus of β-spectrin and the C-terminus of α-spectrin respectively (Byers et al., 1989; Dubreuil et al., 1989). Phylogenetic analysis shows a common ancestor for the first repeat of α-actinin and the first repeat of β-spectrin. Similarly, each of the remaining repeats in α-actinin (2-4), correspond to repeats 1 and 2 of β-spectrin and repeats 19 and 20 of α-spectrin respectively (Fig. 2). This may have relevance for the function of these repeats in the dimerisation of these proteins (Pascual et al., 1997). It is the similarity between these regions of α-actinin and the spectrins and the simpler domain organisation of α-actinin that have led to the hypothesis that these two protein families have evolved from an α-actinin like precursor.

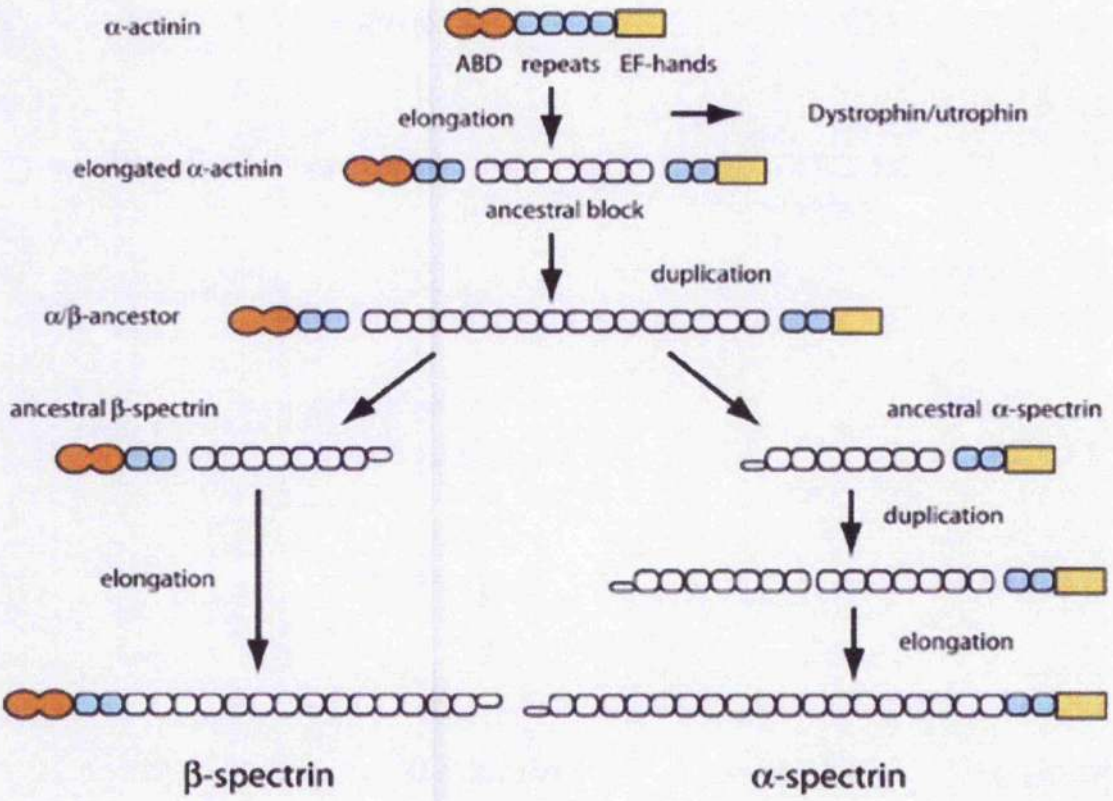

Figure 1.2: Evolution of the spectrin superfamily. Rounded rectangles represent spectrin repeats. Those that are shaded denote α-actinin-like repeats involved in dimerisation whereas un-shaded represent repeats that were involved in duplication and/or elongation events. The incomplete spectrin repeats involved in tetramer formation are proportionally represented depending on the number of repeat helices each protein contributes to the formation of a complete spectrin repeat (Adapted form Dubreuil, 1991 and Pascual, 1997). A dystrophin/utrophin ancestor probably diverged from α-actinin at a relatively early stage and then underwent their own series of duplications and acquisitions of new motifs.

Spectrin is a much more elongated protein compared to α-actinin due to the additional number of repeats. The additional repeats are more closely related to one another than repeats that seem to be common to both α-actinin and spectrin. The spectrin repeat sequences are the most divergent in dystrophin and its homologue utrophin (Winder et al., 1995), most likely reflecting an earlier divergent event when compared to spectrin (Pascual et al., 1997).

The additional molecular length of spectrin compared to the ancestral α-actinin is believed to have arisen through two major duplication events containing blocks of seven repeats (Pascual et al., 1997). The beginning of the process can be described as

the elongation of α-actinin by insertion of a seven repeat block between the second and third α-actinin repeats. That block of repeats was then duplicated and an ancestor of the tetramerisation repeat inserted between the blocks (Pascual et al., 1997) (Figure 1.2). Overall, the two stage evolution of the superfamily is believed to have involved an initial dynamic phase involving intragenic duplications and concerted evolution followed by a stable phase where repeat number became constant and their sequences evolved independently (Thomas et al., 1997). The first phase of evolution resulted in the α-actinin, spectrin and dystrophin lineages via a series of duplication events. This process gave rise to the necessary repeat lengths and number within the spectrin and dystrophin lineages. The α-actinin lineage continued to evolve. Phylogenetic analysis has indicated that the different isoforms found today in modern vertebrates have arisen after the vertebrate urochordate split with the muscle and non-muscle isoforms evolving separately (Virel and Backman, 2004). Thomas and colleagues (1997) hypothesised that during a transition period the new genes began to acquire distinct cross-linking distances and that subsequent selection against longer or shorter proteins would result in a stabilisation of protein length (Thomas et al., 1997). The current length of spectrin repeats is evidently very stable as there has been little change since the split of the arthropod vertebrate lineages.

1.2.3 *Structure of spectrin superfamily proteins*

The spectrin superfamily is an important group of cytoskeletal proteins that are involved in many functions that require cross-linking, bundling or binding to filamentous actin. Each of the proteins within this family differs greatly in their specific biological function. However, they all share a surprising level of structural homology. The members of this protein family are composed from a number of conserved domains; spectrin repeats, CH domain containing actin-binding domains, EF-hands, calcium-binding motifs and various signalling domains (Figure 1.1). The actin-binding domain (ABD) is the most N-terminal domain and can be found in α-actinin, β-spectrin, dystrophin and utrophin but not α-spectrin. The presence of the

ABD allows these proteins to interact with F-actin in a variety of different cellular situations.

The ABDs of these proteins comprise a tandem pair of CH domains although the manner in which this domain interacts with F-actin is still unclear even after extensive investigation and modelling. The spectrin repeats form the rod domains of these proteins. There are four repeats in α-actinin and between 17 and 24 in spectrin and dystrophin. In general the spectrin repeats are responsible for the overall length of the protein and they are usually recognised as modules for the generation of elongated molecules and the separation of the specific N-and C-terminal domains (Winder, 1997). Overall, the core structure of the spectrin repeats from each family member are very similar although the size of the repeating regions differs slightly. In α-actinin repeats are 122 residues in length, in spectrin 106 and in dystrophin and utrophin the repeating units are 109 residues in length. Within the spectrin family proteins each member contains a differing number of repeating elements. The four repeats in α-actinin are separated from the ABD by a linker that allows a significant degree of flexibility between the rigid rod and the ABD. In the functional α-actinin dimer it is the spectrin repeats that are responsible for the dimerisation. Crystal structures of the dimeric α-actinin rod domain have found that the rod bends slightly along its length but also the whole domain twists through approximately 90°. In conjunction with the rod domain and ABD the flexible linker that separates them contributes to α-actinin's ability to cross-link actin filaments that are oriented in either a parallel or antiparallel manner (Ylanne et al., 2001).

The rod domains of α- and β-spectrin are composed of 22 and 17 spectrin repeats respectively. At the N-terminus of α-spectrin the first repeating segment begins with the 'third helix' of what will become a complete triple helical coiled-coil structure analogous to a spectrin repeat when it interacts with the two helices that are found at the C-terminus of β-spectrin (Figure 1.1). This site allows the spectrin dimer to interact with another dimer to form a spectrin heterodimer or tetramer. This is the functional unit of spectrin within the erythrocyte. It has been shown that specific repeats in both α- and β-spectrin are not just present as structural modules that contribute to the length of the rod domain. Repeat 10 of α-spectrin has been found to be slightly shorter than a typical spectrin repeat and shows substantial homology to

the SH3 domain of the Src protein family (Wasenius et al., 1989), whereas repeat 15 of β-spectrin has been found to be responsible for interaction with ankyrin (Kennedy et al., 1991). The two most C-terminal spectrin repeats of α-spectrin (21 and 22) and the first two of β-spectrin (1 and 2) once again show differences in sequence and structure from a typical spectrin repeat. This particular section of α-spectrin shows homology with the C-terminus of α-actinin whereas repeats 1 and 2 of β-spectrin share homology with the N-terminus. It has been found that these repeats are responsible for the dimerisation of α- and β-spectrin in a manner analogous to the four spectrin repeats of the α-actinin rod domain. (reviewed in Winkelmann, 1993). The rod domains of dystrophin and its close relative utrophin have not been found to mediate dimerisation (Winder *et al.*, 1996). It seems that the spectrin repeats of these two proteins function primarily to separate the N- and C-termini. However, it should be noted that the rod domains of dystrophin and utrophin are able to associate with filamentous actin although the manner of interaction differs for each protein (Amann et al., 1999; Rybakova et al., 2002).

The C-termini of spectrin family proteins also exhibit a variety of structural similarities including motifs involved in protein-protein interactions (Figure 1.1). EF-hands motifs are found in all but β-spectrin. The function of this domain is most notable in α-actinin where the binding of calcium is able to affect the interaction of the ABD with F-actin. This is only the case, though, for the non-muscle isoforms of α-actinin, as the muscle isoforms are calcium-insensitive (Blanchard et al., 1989). The C-terminus of α-spectrin has also been found to contain EF-hands similar to those of α-actinin. It is believed that these structures may play a role in modulating the functional conformation of the β-spectrin ABD when N- and C-termini are juxtaposed in the spectrin heterodimers. The EF-hands of dystrophin have been predicted to be unable to bind calcium although it is thought that they have an important structural role (Huang et al., 2000). Finally, a number of smaller motifs have been found at or within the C-termini of these proteins. The non-erythroid form of β-spectrin has been shown to possess a pleckstrin homology (PH) domain at its C-terminus. This fold is conserved in proteins that can interact with phospholipids and may allow direct interaction with the cell membrane. The remainder of the motifs are

found within the C-terminus of dystrophin and utrophin. These motifs consist of WW and ZZ domains that together with the EF-hand region form the cysteine-rich region. The WW domain is an example of a protein-protein interaction module that binds proline-rich sequences (Ilsley et al., 2002) whereas the ZZ domain is a zinc finger motif also involved in mediating protein-protein interactions (Ponting et al., 1996). At the extreme C-terminus of dystrophin and utrophin are two helices predicted to form dimeric coiled-coils (Blake et al., 1995) that mediate interaction with the dystrophin family proteins dystrobrevin and dystrophin-related protein 2 (DRP2).

1.2.4 *Function of spectrin superfamily proteins*

Spectrin is a common component of the sub-membranous cytoskeleton. It was first identified as a major constituent of the erythrocyte membrane cytoskeleton but has since been found in many other vertebrate tissues as well as in the non-vertebrates *Drosophila, Acanthamoeba, Dictyostelium* and echinoderms (Bennett and Condeelis, 1988; Byers et al., 1992; Dubreuil et al., 1989; Pollard, 1984; Wessel and Chen, 1993). The human erythrocyte possesses a characteristic bi-concave shape and remarkable viscoelastic properties. Electron microscopy studies performed on red blood cells (RBC), ghosts and skeletons revealed a two-dimensional lattice of cytoskeletal proteins. This meshwork of proteins was thought to determine the elastic properties of the RBC. This notion was supported further when it was found that detergent-extracted skeletons exhibited shape memory and since spectrin was the major constituent of these skeletons it was suggested that it was responsible for the elastic properties. The protein lattice that laminates the inner surface of the erythrocyte membrane is formed from interactions between actin, spectrin and integral membrane proteins (Bennett and Gilligan, 1993). The lattice is predominantly formed from α- and β-spectrin dimers which again dimerise to generate tetramers roughly 200 nm in length. Five or six of these tetramers bind through their tail ends to a junctional complex, consisting of filamentous actin and band 4.1 (reviewed in Winkelmann, 1993). The molecular function of the complete spectrin heterodimer relies on the inter- and intra-molecular interactions that occur at

two key points within the spectrin molecule. These associations take place at the head end where interchain binding between α- and β-spectrin gives rise to a heterodimer or the tetramer. The tail end of the molecule contains sites responsible for the interchain binding between spectrin chains integrating spectrin tetramers into a network via interactions with actin, protein 4.1 and other binding partners. Between the head and tail regions of the molecule much of the overall length of spectrin is attributed to the number of spectrin repeats, 20 for α-spectrin and 17 for β-spectrin. The spectrin tetramers associate with short actin oligomers to form a regular repeating polygonal lattice. This network is coupled to the membrane via a limited number of direct and indirect contacts between spectrin and integral membrane proteins. These attachments consist of interactions between ankyrin and band 3 protein, and between protein 4.1 and glycophorin C.

α-Actinin is the smallest member of the spectrin family of proteins (Pascual et al., 1997). It was first described as an actin cross-linker in skeletal muscle but has subsequently been found to be ubiquitously expressed (Otto, 1994). Additional family members have been found in smooth muscle and non-muscle cells (Blanchard et al., 1989) and are localised at the leading edge, cell adhesion sites, focal contacts and along actin-stress fibres in migrating cells (Knight et al., 2000). The functional unit of α-actinin is an antiparallel homodimer of polypeptide chain mass of 94-103 kDa (Blanchard et al., 1989) in which the amino-terminal CH domains together with the carboxy-terminal calmodulin (CaM) homology domain form the actin-binding heads of the molecule (Critchley, 2000). The connection between these two heads is composed of four spectrin repeats, which define the distance between the actin filaments that are cross-linked. α-Actinin has three main biological functions. It is the major thin filament cross-linking protein in the muscle Z-discs, where it holds the adjacent sarcomeres together (Masaki et al., 1967). α-Actinin is also found close to the plasma membrane where it crosslinks cortical actin to integrins (Otey et al., 1990) and serves as a linker between transmembrane receptors and the cytoskeleton. In non-muscle cells α-actinin is a major component of stress fibres, an analogous contractile structure to the more organised units found in striated muscle (Otey and Carpen, 2004). α-Actinin is also a constituent of dense bodies (Lazarides and

Burridge, 1975), which are believed to be structurally and functionally analogous to the sarcomere Z-disk.

Dystrophin is the product of the largest known gene within the human genome, spanning ~2.5Mb of genomic sequence and is composed of 79 exons (Coffey et al., 1992; Roberts, 1995). The protein product encoded by the transcript of this gene is known as dystrophin and the absence of this protein results in Duchenne muscular dystrophy (DMD) (Koenig et al., 1987). Dystrophin is predominantly expressed in skeletal and cardiac muscle but small amounts are found in the brain. These full-length isoforms are under the control of three independently regulated promoters referred to as brain, muscle and Purkinje, the names of which reflect the site at which dystrophin expression is driven. Additionally, four internal promoters give rise to truncated C-terminal isoforms and alternative splicing further increases the number of isoforms and variants. The spectrin repeats form the bulk of the protein (Figure 1.1) and are thought to allow flexibility and give the molecule a rod-like structure. Dystrophin can be found associated with the plasma membrane of cardiac and skeletal muscle, where it interacts with the integral membrane protein dystroglycan that binds to laminin on the extracellular face. The dystrophin-dystroglycan complex further interacts with the integral membrane sarcoglycan proteins and peripheral membrane proteins syntrophin and dystrobrevin, which together comprise the dystrophin glycoprotein complex (reviewed by (Winder et al., 1995). This complex of proteins can then interact with F-actin via the N-terminus of dystrophin to form a flexible link between the basal lamina of the extracellular matrix and the internal cytoskeletal network (Campbell and Kahl, 1989; Rando, 2001). It is believed that this complex serves to stabilise the sarcolemma and protect muscle fibres from contraction-induced damage. Indeed, the absence or mutation of dystrophin results in the X-linked myopathies Duchenne and Becker muscular dystrophies (DMD and BMD respectively; these are reviewed in (Blake et al., 2002).

Within the skeletal musculature dystrophin plays an important role in maintaining the integrity of the sarcolemmal membrane. Dystrophin is not able to perform this task alone and interacts with a number of other proteins that include dystroglycans, sarcoglycans, dystrobrevins, syntrophins and sarcospan (Straub and Campbell, 1997). Mutation of dystrophin or, indeed, other components of this

complex can result in a variety of disease pathologies. Most notable, though, is that of DMD, where a complete absence of dystrophin is observed resulting in progressive muscle wasting and eventual death of the affected individual. This complex of proteins is thought to provide a link between the cortical actin cytoskeletal network and laminin in the extracellular matrix (Ervasti and Campbell, 1993; Ervasti and Campbell, 1993). Hence, it is thought that dystrophin and the associated proteins provide a mechanically stabilising role that protects the sarcolemmal membrane from the shear stresses generated during eccentric contraction of muscle (Petrof et al., 1993). Dystrophin has been found to localise adjacent to the cytoplasmic face of the sarcolemmal membrane in regions known as costameres (Porter et al., 1992; Straub et al., 1992). These assemblies of cytoskeletal proteins are involved in linking the force-generating sarcomeric apparatus to the sarcolemmal membrane (Craig and Pardo, 1983; Pardo et al., 1983). Costameres transmit contractile forces laterally through the sarcolemmal membrane to the basal lamina (Danowski et al., 1992). It has been found that dystrophin is not required for the assembly of several of the proteins that comprise costamere-like structures but its absence does lead to an altered costameric lattice (Ehmer et al., 1997; Minetti et al., 1992; Porter et al., 1992; Williams and Bloch, 1999). These data suggest that dystrophin plays an important role in the organisation or stability of costameres perhaps via an interaction with actin filaments (Rybakova et al., 2000). Rybakova and colleagues (2000) showed that the dystrophin complex formed a mechanically strong link between the sarcolemma and the costameric cytoskeleton through interaction with γ-actin filaments (Rybakova et al., 2000).

Following the discovery of the dystrophin gene another cDNA was identified which showed considerable homology to that of dystrophin (Love et al., 1989). Initially this protein was referred to as dystrophin related protein (DRP), but once cloned and sequenced (Tinsley et al., 1992) it was subsequently renamed utrophin due to a ubiquitous expression pattern compared to that of dystrophin. Utrophin is found in many tissues but it does not exhibit a uniform distribution; for example, within muscle, utrophin localises to intramuscular nerves, blood vessels and myotendinous junctions. In muscle cells utrophin shares a high degree of functional similarity with dystrophin (Claudepierre et al., 1999; Earnest et al., 1995; Loh et al.,

2000; Matsumura et al., 1993; Nguyen et al., 1991; Pons et al., 1994; Raats et al., 2000) and within the myofibre, utrophin can be found at the neuromuscular junction where it binds to components of the dystrophin associated glycoprotein complex (DAGC) (Perkins and Davies, 2002). Given the overall similarities between utrophin and dystrophin it has been proposed that utrophin may function in a similar manner to dystrophin; for example, the extraocular muscles (EOM) within the the eyes of *mdx* mice do not exhibit myofibre degeneration and it has been proposed that endogenous upregulation of utrophin is responsible for the protection of extraocular muscle in dystrophinopathy (Porter *et al.*, 1998). This has led to the proposition of utrophin as a potential therapeutic replacement for dystrophin in the treatment of DMD (Matsumura et al., 1992; Pearce et al., 1993; Tinsley et al., 1992).

1.3 *Actin-binding domains*

Actin-binding domains generally consist of approximately 240 residues that comprise two functionally distinct but structurally equivalent domains (Gimona and Winder, 1998; Matsudaira, 1991). These domains have been named calponin homology or CH domains (Castresana and Saraste, 1995) based on the sequence similarity to the smooth muscle regulatory protein calponin (Winder and Walsh, 1990), where this domain is found only as a single copy. Compared to the single CH domain seen in calponin, the double domain found in the spectrin superfamily of proteins has been proposed to have arisen through a process of gene duplication (Castresana and Saraste, 1995; Matsudaira, 1991). Furthermore, phylogenetic analysis of CH domain-containing proteins has revealed that there is a greater similarity between the N-terminal CH domains (CH1) and the C-terminal CH domains (CH2) in any of the classes of actin-binding proteins than between the CH domains found within the same protein (Banuelos *et al.*, 1998; Keep *et al.*, 1999a; Korenbaum and Rivero, 2002; Stradal *et al.*, 1998). Some actin-binding proteins have been found to contain a single CH domain although the binding interaction requires additional elements as the isolated CH domains from these proteins do not exhibit analogous actin-binding when compared to the whole protein (Gimona and Mital, 1998). Functionally, it should be noted that characterisation of bacterially

expressed CH domains corresponding to the actin-binding domains of α-actinin, dystrophin and utrophin were found not to be equivalent (Way et al., 1992; Winder et al., 1995). When the two CH domains are separated and then used in actin-binding experiments it has been found that only CH1 has the ability to interact with F-actin although the affinity is reduced. CH2 has little or no intrinsic actin-binding activity but it is obvious that its presence is functionally important. It has been shown that both of the CH domains are required to achieve the greatest interaction with F-actin and hence, single CH domains are not regarded as actin-binding domains *per se* (Gimona and Winder, 1998).

The first crystal structures of CH domains were published in 1997. These were the CH2 domain of spectrin (Carugo et al., 1997) and the N-terminal ABD of fimbrin, comprising two CH domains (CH1.1 and CH2.1) (Goldsmith et al., 1997). The crystal structure of the second utrophin CH domain (CH2) was later published by (Keep *et al.*, 1999a). It was not long, however, before the complete actin-binding domain of utrophin was crystallised (Keep *et al.*, 1999b) followed closely by dystrophin (Norwood et al., 2000). The CH domain is a compact globular domain that appears to show a high degree of structural conservation. Overall, the domain comprises four main α-helices (A, C, E and G) that are approximately 11-18 residues in length and exhibit a roughly parallel orientation. Three shorter helices (B, D and F) are less regular and form lesser secondary structure elements. The structure can be considered to comprise a number of layers. The core of the domain is formed by a parallel arrangement of helices C and G, which are then sandwiched between helix E and the N-terminal helix A (Broderick and Winder, 2002).

The crystal structures of CH domains from α-actinin, dystrophin, utrophin, fimbrin, spectrin and plectin have been solved to date. These structures have given insight into certain aspects of CH domain function but have also raised many new questions regarding the interaction of these domains with actin. The dimeric organisation displayed by the crystallised utrophin and dystrophin ABDs contrasts strongly with that of the α-actinin and the related fimbrin actin-binding domain (Franzot et al., 2005; Goldsmith et al., 1997). When crystallised, fimbrin and α-actinin do so as compact monomers, where the two CH domains fold back on themselves to form a compact globular structure. These same interfaces are involved

in the dimerisation seen in utrophin, except it is the CH1 and CH2 domains from separate molecules that interact. The preservation of an interface between two domains of the same or related proteins when in monomeric or oligomeric forms is known as three-dimensional domain swapping (Schlunegger et al., 1997). Recent cryo-EM reconstructions of these domains with F-actin have not served to definitively resolve the mode of interaction of these proteins with F-actin. Reconstructions of fimbrin and bound to F-actin have been modelled on a compact conformation (Hanein et al., 1998) and the reconstruction of utrophin with F-actin on an extended conformation (Moores et al., 2000). Electron diffraction and modelling of the α-actinin molecule bound to F-actin showed that the ABD could be associating as an open bi-lobed structure (Tang et al., 2001; Taylor and Taylor, 1993). The cryo-EM reconstruction of α-actinin with F-actin (McGough et al., 1994), however, revealed a more globular difference density, suggesting that α-actinin might also associate with F-actin in a manner more analogous to the compact mode of interaction seen in the fimbrin crystal structure. The helical linkers between the two CH domains of these proteins may play an important role in determining the flexibility between the two CH domains and, subsequently, the manner they interact with F-actin. Gel-filtration studies of the utrophin ABD have shown it to be monomeric when in solution (Winder et al., 1995). Hence, the crystal structures of the ABDs from fimbrin and utrophin may represent two conformational extremes within this class of actin-binding proteins (Keep *et al.*, 1999b). Several modes of interaction with F-actin have been demonstrated in cryo-EM studies with the utrophin ABD (Galkin et al., 2002).

Within N-terminal actin-binding domains three actin-binding sites (ABS) have been delineated (ABS1, 2 and 3). The first and third ABS have been localised to the α1 helix in the first and second CH domains respectively. These sites were originally identified using synthetic peptides derived from dystrophin (Levine et al., 1990; Levine et al., 1992). The second ABS corresponding to helices α5 and α6 in the CH1 domain was first identified in the Dictyostelium actin-gelation factor ABP-120 (Bresnick et al., 1991; Bresnick et al., 1990). ABS2 was later identified in α-actinin using *in vitro* actin-binding studies with glutathione S-transferase (GST) fusion proteins (Kuhlman et al., 1992). It was later recognised that the ABS sequences were

not part of a fully folded globular protein and hence residues not normally involved in actin-binding may have been allowed to interact with actin. Structural approaches have begun to shed light on the mechanism by which the spectrin superfamily of proteins interact with the cytoskeleton. Biochemical work studying the actin-binding sites of α-actinin (Lebart et al., 1990; Lebart et al., 1993; McGough et al., 1994; Mimura and Asano, 1987) and dystrophin (Levine et al., 1992) have been successful in identifying actin subdomain 1 as an important binding site for this particular class of proteins. Electron microscope reconstructions of F-actin decorated with α-actinin (McGough et al., 1994; Tang et al., 2001) reveal that actin subdomain 1 forms the major site of interaction. Helical reconstruction also revealed that these two proteins interacted with adjacent actin monomers on the long pitch helix, a site apparently shared by most F-actin binding proteins (McGough, 1998). The crystal structure of the utrophin ABD suggested an alternate model to that of the association of fimbrin with actin (Keep *et al.*, 1999b). As utrophin crystallised as a head-to-tail dimer each of the monomers adopted an extended conformation. This arrangement placed the predicted ABSs on the surface of the protein clearly enabling interaction with actin. The dimerisation of utrophin seen in the crystal conserved the inter-CH domain interfaces suggesting that utrophin may adopt a more compact conformation when in solution. To date, there is no evidence to support anything other than a monomeric conformation of utrophin when in solution as the binding stoichiometry with actin is 1:1 (Keep *et al.*, 1999b; Winder *et al.*, 1996). However, the crystallisation of utrophin as a dimer suggested that the ABD of this protein may be flexible and allow actin-binding in an open conformation even when utrophin exists as a monomer in solution. Moores *et al.* (2000) developed this idea further by demonstrating a model of utrophin-actin binding which contrasted that of fimbrin bound to actin (Moores et al., 2000). A pseudo-atomic model of utrophin bound to F-actin in an open conformation was constructed, showing that all of the ABSs could be directly involved in the actin interaction. This mode of binding was found to create a different conformational change within actin compared with that caused by fimbrin, suggesting that an induced fit mechanism involving conformational flexibility of actin and utrophin may be crucial to their interaction (Moores et al., 2000). The validity of this model has recently been called into question (Galkin et al., 2003),

however, and alternative models have been proposed (Galkin et al., 2002). The comparison between the previously published model of fimbrin binding to actin and that of utrophin shows that both proteins possess a totally different mode of interaction even though their ABDs share sequence homology. Such a difference is likely to be related to the overall function of each protein but the utrophin model has identified an alternate means of actin association within a large family of proteins important to cellular organisation. It should be noted that Moores *et al.*, (2000) did not exclude the compact orientation in utrophin actin-binding (Moores et al., 2000). However, their model relies on inherent protein flexibility. Indeed, models of utrophin ABDs have been generated where association with F-actin is made in a closed compact conformation (Sutherland-Smith et al., 2003). Recent crystallographic and calorimetric studies of the plectin ABD demonstrated that while the two CH domains associate to form a closed conformation in the crystal structure binding to F-actin induces the open conformation (Garcia-Alvarez et al., 2003). Elucidation of spectrin's interaction with actin at the molecular level, however, has been hampered by an inability to express a functional spectrin ABD in isolation.

1.4 *Spectrin repeat region*

The rod domain of α-actinin is the shortest within this family of proteins and comprises just four spectrin-like repeats. Given the reduced length of this domain it is feasible to assume a greater degree of rigidity, especially as the functional unit of α-actinin is a dimer. The spectrin repeats of the rod domain are essential to the dimerisation of α-actinin. The fact that the rod domains of two monomers associate leads to a much more stable and less flexible domain overall (Djinovic-Carugo et al., 2002). Spectrin, dystrophin and utrophin all contain many more spectrin repeats that seem to play a more direct role in the cellular function of these proteins. Studies performed by Pasternak and colleagues show the sarcolemma of muscles from the mdx mouse is four times less stiff than in controls (Pasternak et al., 1995), demonstrating directly that dystrophin and its associated proteins reinforce the stability of the sarcomere. Spectrin forms roughly 5% of the total protein of the erythrocyte and is pivotal to the formation and function of the sub-membranous

skeleton in red blood cells. This erythrocyte plasma membrane possesses remarkable mechanical properties more like an elastic semi-solid (Evans and Hochmuth, 1977). This allows storage of energy during deformation, for example squeezing through a narrow capillary, but allows the erythrocyte to return to its normal shape once the deformation ceases (Bennett and Gilligan, 1993). The ability of erythrocytes to survive repeated deformation is essential to their physiological function and their prolonged life within the vasculature. Direct evidence has determined that spectrin is the major factor in providing the elastic properties exhibited by the erythrocyte. Studies of erythrocytes from patients suffering from hereditary spherocytosis clearly demonstrate this (Waugh and Agre, 1988) as reduced quantities of spectrin result in a greater extent of clinical severity and a reduction in the force required to deform the affected erythrocytes (Agre et al., 1986; Agre et al., 1985). This, perhaps, results from an overall effect of the structure of the sub-membranous lattice on the whole, but the properties of this mesh work of proteins can be linked to the properties of the spectrin repeats found within the rod domain. For many cytoskeletal and adhesion proteins the ability to survive extension and deformability is pivotal to their role in a cellular environment. Atomic force microscopy (AFM) has been employed to examine the extensibility of spectrin repeats (Rief et al., 1999). These studies have determined that the α-helical spectrin repeat can be forced to unfold in a stochastic one-domain-at-a-time fashion (Rief et al., 1999). The availability of tandem spectrin repeat structures from non-erythroid α-spectrin (Grum et al., 1999) and the four repeat rod domain of α-actinin (Ylanne *et al.*, 2001) have shown that individual spectrin repeats should not be considered as such and that the inter-spectrin repeat links are actually formed from contiguous helices rather than flexible linkers (Law et al., 2003). This has implications for the manner that spectrin repeats respond to mechanical stress inasmuch as the repeats within the rod domain do not unfold one at a time. Rather, they are subject to a cooperative manner of forced unfolding (Law et al., 2003). Helical linkers between spectrin repeats have been implicated to help explain the extensibility and elasticity observed within the erythrocyte cytoskeleton. The unfolding of spectrin repeats might explain thermal-softening (Waugh and Evans, 1979) and strain softening of the RBC sub-membranous network (Lee and Discher, 2001; Markle et al., 1983). Additionally, it has also been shown that tandem

spectrin repeats are thermodynamically more stable than individual repeats and that tandem repeats unfold in unison behaving similarly to an individual repeat (MacDonald and Pozharski, 2001).

The rod domains of spectrin family proteins are assumed to function solely as structural spacers that serve to separate the C-terminus from the N-terminal actin-binding domain. Whilst this is likely to be the case for α-actinin, and to a certain extent in spectrin, natural mutations and transgenic experiments would suggest otherwise for dystrophin. It was widely thought that the rod domain of dystrophin (and utrophin) served as flexible spacers or shock absorbers between the actin cytoskeleton and the sarcolemmal membrane (Winder et al., 1995). However, is the length of this 'shock absorber' crucial to the function of the protein? An individual with a large deletion in the dystrophin gene encompassing 46% of the entire protein and 73% of the rod region (repeats 4-19) presented with a very mild BMD phenotype (England et al., 1990). This would tend to suggest that rod domain length is not essential with regard to the proposed shock absorbing role of the protein. The fact that a dystrophic phenotype is observed, regardless of how mild, would suggest that there is functional importance regarding the length of the rod domain. However, dystrophin minigenes have been designed on the basis of this shortened dystrophin and have been used to correct the dystrophic phenotype in mdx mice (Phelps et al., 1995; Wells et al., 1995). Similarly, a minispectrin has also been generated that consists of the N-terminal ABD and the first two spectrin repeats of β-spectrin, and the C-terminus of α-spectrin consisting of the last two spectrin repeats and the calmodulin-like domain. This construct was still able to dimerise and retained the ability to bind F-actin and induce the formation of bundles but it is unlikely to be functional *in vivo* (Raae et al., 2003). The shock-absorbing role of the spectrin repeats found within these proteins is widely accepted, which leads on to the question of why there are so many coiled coils in dystrophin and utrophin. α-Actinin contains only four spectrin repeats, which mediate dimerisation and result in a rather inflexible link between the termini of the protein (Ylanne et al., 2001). In this case the length of the rod domain clearly defines the distance at which filamentous actin can be cross-linked. α-Actinin is localised to structures that require actin filaments to be cross-linked in either a parallel or antiparallel fashion. This requires the α-actinin

dimer to bind actin filaments in orientations separated by as much as 180°. Furthermore, α-actinin is able to accommodate a range of inter-actin filament cross-linking distances, from 15-40 nm (Liu et al., 2004; Luther, 2000; Taylor et al., 2000). The domain is essential to the formation of the functional dimer and for the separation of the C- and N-termini of the protein, but it would seem that the flexible hinge that separates the rod from the ABD and the ABD itself play an important role in determining the ultimate cross-linking distance.

1.5 *Other binding partners*

The repeating constituents of the rod domains of spectrin family proteins were generally regarded as modules for the construction of elongated molecules (Winder, 1997). However, this is not the only function of spectrin repeats. It is widely accepted that proteins containing spectrin repeats are localised to cellular sites that experience significant mechanical stress, and the properties of the spectrin repeat can be used to explain this functionality (see above, section 1.4). Additionally, some spectrin repeats have acquired functions with a purely structural role and these are able to interact with a variety of structural and signalling proteins (Djinovic-Carugo et al., 2002).

The function of spectrin superfamily proteins is particularly evident when taken in context of their cellular localisation. They often form flexible links or structures that allow interactions with the cellular cytoskeletal architecture and the membrane. In both spectrin and dystrophin such a function is performed but the spectrin repeats of these molecules are also able to interact with actin and contribute to binding. A portion of the dystrophin rod domain that spans residues 11-17 contains a number of basic repeats that allow a lateral interaction with filamentous actin (Rybakova et al., 1996). The homologous utrophin can also interact laterally with actin. This interaction is distinct from that of dystrophin as the utrophin rod domain lacks the basic repeat cluster and associates with actin via the first ten spectrin repeats (Rybakova et al., 2002). β-Spectrin also exhibits an extended contact with actin via the first spectrin repeat. In this situation it was found that the extended contact increased the association of the adjacent ABD with actin (Li and Bennett, 1996). In

conjunction with this interaction it has been found that the second repeat is also required for maximal interaction with adducin (Li and Bennett, 1996), a protein localised at the spectrin-actin junction, which is believed to contribute to the assembly of this structure in the membrane skeletal network (Gardner and Bennett, 1987). In the erythrocyte cytoskeletal lattice β-spectrin interacts with ankyrin, which in turn binds to the cytoplasmic domain of the membrane-associated anion exchanger. This indirect link to the cellular membrane occurs via repeat 15 of β-spectrin (Kennedy et al., 1991) and is largely responsible for the attachment of the spectrin-actin network to the erythrocyte membrane (Bennett and Baines, 2001). A much larger number of direct links to transmembrane proteins have been determined for the spectrin repeats of α-actinin (Djinovic-Carugo et al., 2002). The crystal structure of the α-actinin rod domain (Ylanne et al., 2001) has allowed the analysis of the surface features leading to predictions of possible protein-protein interaction sites. It was found that the most conserved surface residues were acidic in nature, which would correlate well with the relatively short basic sequences that can be found within the cytoplasmic domains of many transmembrane proteins (Ylanne et al., 2001). α-Actinin has been found to provide a direct link with a variety of transmembrane proteins including integrins, ICAMs, L-selectin, Ep-Cam, ADAM12 and NMDA receptor subunits (see Djinovic-Carugo *et al.*, 2002 for references). The α-actinin rod domain is also involved in a number of dynamic and regulatory interactions that involve interactions with titin (Young et al., 1998), myotilin (Salmikangas et al., 1999), ALP (Xia et al., 1997) and FATZ (Faulkner et al., 2000) at the Z-disk of striated muscle and interactions with Rho-kinase type protein kinase N (PKN) (Mukai et al., 1997). All of these interactions occur through the rod domain of α-actinin and demonstrate the multivarience of the rod domain as a binding site for the interactions with these proteins (Djinovic-Carugo et al., 2002). Spectrin and dystrophin rod domains have also been demonstrated to interact directly with lipid surfaces suggesting a lateral association with biological membranes (An et al., 2004; DeWolf et al., 1997; Le Rumeur et al., 2003; Maksymiw et al., 1987).

1.6 *Regulating interactions of spectrin superfamily proteins*

The spectrin family of proteins, depending on the particular function, has numerous smaller motifs and binding sites for interaction with other proteins. These regions are important as they are major protein-protein or protein-membrane interaction modules that bind to F-actin, proline-containing ligands and/or phospholipids. Spectrin and dystrophin/utrophin have all acquired copies of such domains since their evolution from α-actinin, presumably as a consequence of their more diverse roles in the cell.

1.6.1 *CH domains*

The calponin homology (CH) domain has been identified in many molecules of differing function. However, its presence usually signifies an interaction of some sort with the actin cytoskeleton via an association with F-actin. The domain was initially identified as a 100 residue motif found at the N-terminus of the smooth muscle regulatory protein calponin and, hence, was termed the CH domain (Castresana and Saraste, 1995). The refinement of algorithms for the identification of distinct protein motifs has allowed the identification of CH domains in proteins that range in function from cross-linking to signalling (Korenbaum and Rivero, 2002). Despite the functional variability of this domain the secondary structure is conserved remarkably well between proteins that contain it (Bramham et al., 2002).

Several mechanisms have been identified that seem to regulate the CH domains found in spectrin, dystrophin and α-actinin. These range from effects induced by calcium via EF-hand motifs, PIP_2 binding, phosphorylation and interactions with calmodulin. The actin-binding properties of the non-muscle isoforms of the F-actin crosslinker α-actinin can be regulated via the presence of EF-hands. Calcium does not directly regulate α-actinin's CH domains interaction with F-actin but it does bind to the EF-hand motif present in the molecule. As α-actinin dimerises this brings the CH domains and EF-hands in the antiparallel dimer in close association. The conformational changes induced in the EF-hand motif can then exert an effect on the CH domains to influence the interaction with F-actin (Noegel et al., 1987; Tang et

al., 2001). α-Actinin has also been found to bind phosphatidylinositol (4,5)-bisphosphate (PIP_2) at the muscle Z-line (Fukami et al., 1992). The PIP_2 binding site has been delineated to a region immediately C-terminal of the third ABS (Fukami et al., 1996) although the precise mechanism of control is not known for this region. It has been found, though, that in non-muscle cells where α-actinin is associated with actin this region contained bound PIP_2 whereas free α-actinin did not. This implicates a role for PIP_2 in the activation of α-actinin induced actin-bundling (Fukami et al., 1994).

Calmodulin has also been shown to regulate the interaction of the ABDs from dystrophin, utrophin and α-actinin by binding directly to the CH domains (Bonct-Kerrache et al., 1994; Jarrett and Foster, 1995; Winder et al., 1995) suggesting a potential role for modulating the attachment of these proteins to the cytoskeleton. Recently, it has been shown that α-actinin is phosphorylated by focal adhesion kinase (FAK) and that this phosphorylation reduces the ability of α-actinin to bind actin (Izaguirre et al., 2001). The site of tyrosine phosphorylation is N-terminal to the first CH domain in a region that is most conserved between spectrin family proteins.

1.6.2 *EF hands*

EF-hand regions are involved in the chelation of up to two divalent calcium cations (occasionally magnesium) via an interaction through a paired helix-loop-helix structure (Tufty and Kretsinger, 1975). Binding of calcium to this globular domain leads to a dramatic conformational change from "closed" to "open," exposing a hydrophobic surface that binds to a target peptide, often helical in nature. However, divergent evolution has led to a subset of EF-hands that no longer chelate calcium and possibly serve an alternate function (Nakayama and Kretsinger, 1994). This is exemplified in α-actinin non-muscle isoforms, where calcium is bound via the EF-hands thus allowing regulation of actin-binding. The muscle-specific isoforms of α-actinin have lost the ability to bind calcium through their EF-hands (Blanchard et al., 1989), possibly to protect the muscle architecture from the potential destabilising effect of calcium during calcium-induced contractions. Spectrin has also both retained and lost the ability to bind calcium. Calcium and calmodulin bind to human

non-erythroid spectrins (αIIβII) at sites that have either degenerated or are absent in erythroid spectrins (αIβI) (Lundberg et al., 1992). The roles of non-erythroid spectrins are far more diverse and, hence, calcium and calmodulin might participate in regulatory events not required in the erythrocyte (Buevich et al., 2004). The EF-hands of α-spectrin are brought in close opposition with the β-spectrin ABD once the proteins form the heterodimer. The EF-hand is then able to exert regulatory control over the actin-binding activity of the adjacent domain. The molecular details of how this is achieved are still to be determined, however. A similar interface is observed in α-actinin. It is thought that the EF-hand region could engage the actin-binding domain in a manner analogous to calmodulin binding a target peptide. Regulation of the interaction would be affected by the binding of calcium to the EF-hand, which would cause a conformational change resulting in altered interaction surfaces. The calcium-binding activity of non-erythroid spectrin has been located to the two EF-hands present in the C-terminus of the αII-spectrin (Lundberg et al., 1995; Trave et al., 1995). Buevich and colleagues (2004) found that the EF-hands in non erythroid spectrin exhibited a degree of co-operativity in their binding of calcium, suggesting that EF1 binds before EF2 and modulates the affinity of EF2 for calcium although overall, calcium binding to α-spectrin has been found to be much weaker than to other EF hand-containing proteins such as troponin C and calmodulin (Zhang et al., 1995).

Each of the three EF-hand structures solved from the spectrin family proteins exhibit unique structural and functional differences even though all are fundamentally similar. The α-spectrin (non-erythroid) EF-hands bind calcium and presumably perform some kind of regulatory role regarding the actin-binding function of spectrin (Zhang et al., 1995). Due to the low calcium affinity it is expected that calcium regulatory events involving spectrin would occur in areas of the cell that would experience a transient but significant fluctuation of calcium concentration (Buevich et al., 2004). It is possible that in the cell the calcium-bound form of spectrin would be stabilised by accessory proteins as non-erythroid spectrin interacts with many proteins that are involved in regulatory events and not just with the cytoskeleton. In muscle α-actinin (isoform 2) the third and fourth EF-hands can be referred to as 'empty' on the basis of a lack of key liganding residues and large

insertions in the helix-loop-helix motif. This muscle isoform of α-actinin is important in striated muscle Z-disk structure, where it interacts with F-actin and titin. The structure of this complex was solved and showed the titin Z-repeat peptide bound in a groove formed by the partially open lobes of the two EF-hands (Atkinson et al., 2001). The EF-hands of dystrophin were solved as part of a larger structure that also included the adjacent WW domain (Huang et al., 2000). These EF-hands had been predicted to be unable to bind calcium due to a lack of key liganding residues (Winder, 1997). The structure of the dystrophin WW-EF region indicated that the EF-hands may play a structural role and that they are not required to bind either calcium or a target peptide (Huang et al., 2000). It is still to be elucidated if this region of dystrophin interacts with other target peptides but as the EF-hands are oriented in a closed and compact manner it is difficult to see how these interactions would occur (Broderick and Winder, 2002). Indeed, studies with constructs spanning both the WW domains and EF-hand regions of dystrophin and utrophin have failed to show any calcium-induced regulation of binding to β-dystroglycan (James et al., 2000; Rentschler et al., 1999).

1.6.3 *Lipid binding*

Pleckstrin homology (PH) domains are motifs that are approximately 100 amino acids in length and which have been identified in over 100 different eukaryotic proteins. They are thought to participate in cell signalling and cytoskeletal regulation via interactions with phospholipids (Lemmon and Ferguson, 1998; Rebecchi and Scarlata, 1998). It has been suggested that these domains function as membrane anchors and tethers, as PH domains are often found within membrane-associated proteins (Ferguson et al., 1995). The domain was first recognised in 1993 (Haslam et al., 1993; Mayer et al., 1993; Musacchio et al., 1993) and was quickly followed by the determination of 3D structures.

The β-spectrin PH domain structure was solved in a lipid-free (Zhang et al., 1995) and lipid-bound form (Hyvonen et al., 1995). The role of the spectrin PH domain has been proposed to be part of the mechanism whereby spectrin associates directly with the membrane through binding phospholipids. The sub-membranous

framework formed by spectrin is linked to transmembrane polypeptides via peripheral proteins such as ankyrin and band 4.1 (Viel and Branton, 1996), and spectrin is essential to the integrity of this network. The PH domain of spectrin has been found to have a weak affinity and specificity for $PI(4,5)P_2$ (Harlan et al., 1994; Hyvonen et al., 1995). Lemmon and colleagues (2002) suggested that the β-spectrin/membrane interaction is driven by a delocalised electrostatic attraction between an anionic ligand and the positively charged face of the polarised PH domain (Lemmon et al., 2002). The PH domain of spectrin appears to falls into a class of PH domains which exhibit a moderate affinity for the phospohinositides. In cells this polarised domain may direct a few spectrin isoforms to $PI(4,5)P_2$ enriched sites such as caveoli or focal adhesions (Burridge and Chrzanowska-Wodnicka, 1996), where other determinants of membrane association are likely to play an equal or more dominant role in stabilizing attachment. Although membrane attachment is not necessarily dependent on this domain it has been shown that the PH domain of the human βIΣ2 spectrin isoform binds to protein-depleted membranes containing $PI(4,5)P_2$ and to $Ins(1,4,5)P_3$ in solution (Wang and Shaw, 1995). This domain localises to plasma membranes in COS7 cells (Wang et al., 1996). $Ins(1,4,5)P_3$ binding has been found to perturb residues located in or near loop 1 of the Drosophila spectrin PH domain as is the case for the N-terminal PH domain and the mouse form of β-spectrin (Zhou et al., 1995). The binding site of β-spectrin has no elaborate hydrogen bonding network and the inositol ring has no specific contacts with the protein, unlike the PH domain of PLC-δ_1 (Ferguson et al., 1995). Moreover, spectrin does not bind $Ins(1,4,5)P_3$ on the same face as PLC-δ_1, whose binding pocket is located on the other side of the protein.

The β-spectrin PH domain binds weakly to all phosphoinositides and is likely to associate with the negatively charged membrane surface via the positively charged face of the domain. Spectrin networks contain many spectrin molecules and it is likely that the individual weak association with phosphoinositides is facilitated by the overall collective interaction of many molecules. Such a mechanism of multivariant association allows only the assembled cytoskeletal components to interact strongly with cellular membranes such as in the RBC.

1.6.4 *Poly-proline binding domains*

The Src homology 3 (SH3) domain of α-spectrin was the first SH3 domain structure to be solved (Musacchio et al., 1992). The domain was initially identified as regions of similar sequence found within signalling proteins, such as the Src family of tyrosine kinases, the Crk adaptor protein, and phospholipase C-γ (Mayer et al., 1993). In the case of spectrin, the specific target ligand and function are still to be identified. The domain is approximately 60 residues in length and has been identified in many proteins (Bateman et al., 1999; Rubin et al., 2000). The SH3 domain continues to be identified within a variety of proteins and, subsequently, is regarded as one of the most common modular protein interaction domains found and is widespread in signalling, adaptor and cytoskeletal protein alike (Mayer, 2001). Due to the small size of this domain a search for a potential function focused on protein-protein interactions, with screening of expression libraries soon identifying seemingly specific binding partners (Cicchetti et al., 1992). Binding studies have indicated that the interaction sites of SH3 domains were proline-rich with PxxP being identified as a core conserved binding motif (Ren et al., 1993). It should also be noted that profilin and WW domains also make use of a similar mode of interaction with proline-rich helical ligands (Ilsley *et al.*, 2002; Kay *et al.*, 2000; Tanaka and Shibata, 1985; Zarrinpar and Lim, 2000).

As mentioned above the WW domain is another example of a protein-protein interaction module that binds proline-rich sequences (Kay et al., 2000). Dystrophin and utrophin WW domains interact predominantly with the extracellular matrix receptor dystroglycan, which contains a type 1 WW motif of consensus PPxY (Ilsley et al., 2002; Winder, 2001). A structure of a WW domain from dystrophin was solved recently as part of a structure including the EF-hand region, and also with and without a bound β-dystroglycan peptide (Huang et al., 2000).

Chung and Campanelli (1999) found that the interaction between utrophin and β-dystroglycan mirrored that of dystrophin (Chung and Campanelli, 1999). This is mainly mediated by the WW domain, which recognises the PPPY peptide at the carboxy terminus of β-dystroglycan. Adhesion-dependent tyrosine phosphorylation of β-dystroglycan within the WW domain binding motif has been found to be able to

regulate the WW domain-mediated interaction between utrophin and β-dystroglycan. This was the first demonstration of physiologically relevant tyrosine phosphorylation of a WW domain ligand and parallels the tyrosine phosphorylation of SH3 domain ligands regulating SH3 mediated interactions (James et al., 2000). Investigations performed by Rentschler and associates (1999) have also determined that the EF-hand regions following the WW domain are necessary for WW binding (Rentschler et al., 1999). It was later shown that the integrity of the utrophin WW-EF-ZZ region is essential for efficient binding to β-dystroglycan (Tommasi di Vignano et al., 2000). This binding activity can be abolished in utrophin if the ZZ domain is deleted, but only a reduction in binding is observed for dystrophin (Rentschler et al., 1999).

1.6.5 *ZZ domain*

Dystrophin and utrophin contain a putative zinc finger motif within their C-terminal cysteine-rich domains homologous to domains found in sequences of a wide variety of proteins (Ponting et al., 1996). The ZZ domains of dystrophin and utrophin have been shown to bind zinc (Michalak et al., 1996; Winder, 1997) and are believed to be involved in mediating protein-protein interactions although the precise function of the ZZ domain has not yet been elucidated. It has been found that the cysteine-rich domain of dystrophin is required for binding to β-dystroglycan and it has been shown that the ZZ domain strengthens the interaction between the dystrophin WW-EF region and β-dystroglycan (James et al., 2000; Jung et al., 1995; Rentschler et al., 1999). More recently, Ishikawa-Sakurai and colleagues identified the components of the C-terminal domain of dystrophin that are required for the full binding activity. They have detailed the extent of the C-terminal sequence (residues 3026-3345) that is required for effective binding and have identified cysteine 3340 within the ZZ domain as essential to the binding activity with β-dystroglycan (Ishikawa-Sakurai et al., 2004). The functional importance of the ZZ domain has been proven further by the identification of a rare mutation where C3340 has been mutated to a tyrosine resulting in the affected individual suffering from a form of DMD (Lenk et al., 1996). However, to date, no structure of any ZZ domain has been solved. C-terminal to the ZZ domain is a pair of highly conserved helices predicted to form dimeric

coiled-coils (Blake et al., 1995). These helices, which are restricted to dystrophin family proteins (dystrophin, utrophin, DRP2 and dystrobrevin), are involved in heterophilic-associations between family members and also members of the syntrophin family of proteins (Blake et al., 2002).

1.7 *Disease and spectrin superfamily proteins*

It has already been described how each of the spectrin superfamily members function within the cellular context and how these functions relate to the overall structure of each protein. These proteins each have specialised roles that are essential to the overall function to the specific cells and tissues in which they are found. Disruption of these proteins functionality via mutation may often result in undesirable pathologies that are detrimental to the overall health of the affected individual. For example, erythrocytes in the human blood stream have to squeeze repeatedly through narrow capillaries of diameters lesser in size than their own dimensions whilst resisting rupture. Spectrin forms an integral part of the erythrocyte cytoskeletal architecture and any defects that disrupt the association of the spectrin heterotetramer or the interaction with any of the other sub membranous proteins can result in red blood cell defects (Hassoun and Palek, 1996). Indeed, abnormalities of the β-spectrin N-terminus and the α-spectrin C-terminus affect the self-association site and result in hereditary elliptocytosis and hereditary pyropoikilocytosis (Delaunay, 1995; Delaunay and Dhermy, 1993; Palek and Jarolim, 1993) whereas defects outside the self-association site of spectrin are also associated with hereditary spherocytosis (HS) (Hassoun et al., 1997).

In humans, mutations in the ACTN4 gene result in α-actinin-4 mutations, which are believed to cause a form of familial focal segmental glomerulosclerosis (FSGS) (Kaplan et al., 2000). FSGS is a common non-specific renal lesion characterised by regions of sclerosis in some renal glomeruli often resulting in loss of kidney function and ultimately end-stage renal failure. Kaplan and colleagues (2000) have sequenced the coding region of ACTN4 from a number of families that present one form or another of FSGS. Three specific residues were characterised; K228E, T232I and S235P, all three of which can be found on the solvent-accessible surface in helix G of the second CH domain (Kaplan *et al.*, 2000). These mutations are not

expected to perturb the secondary structure of the actin-binding domain. However, they are all highly conserved amongst all of the four human isoforms of α-actinin as well as α-actinins of other species. The presence of these mutations has a marked affect on the functionality of the mutant protein when in the cellular environment and when binding to F-actin. Yao and colleagues (2004) have demonstrated that the mutant α-actinins exhibit altered structural characteristics, localise abnormally and are targeted for degradation (Yao et al., 2004). They suggest that the mutant α-actinin-4 is much less dynamic within the cellular environment and, due to its propensity to aggregate, loss of normal function becomes inevitable and contributes to progression of kidney disease.

Finally, mutations that affect dystrophin result in pathologies that are perhaps the most well known out of all the spectrin superfamily diseases, namely, the muscular dystrophies. Duchenne muscular dystrophy (DMD) is a severe X-linked recessive, progressive muscle wasting disease that affects approximately 1 in 3500 new-born males (Emery, 1991). An allelic variant of DMD is also known and this is referred to as Becker muscular dystrophy (BMD). The vast majority of DMD mutations result in the complete absence of dystrophin, whereas a truncated protein is often associated with the milder Becker form of the disease (Kingston et al., 1983). Mutations in the genes encoding other components of the dystrophin-associated protein complex cause other forms of dystrophy, such as limb-girdle and congenital dystrophies.

The cause of approximately 65% of DMD pathologies can be traced to large deletions or duplications within the dystrophin gene. The remainder of affected individuals are the result of small insertion/deletion mutations and point mutations (Koenig et al., 1989; Monaco et al., 1985; Roberts et al., 1994). In DMD, it has been found that point mutations nearly always result in a truncation of the open reading frame causing nonsense-mediated decay, but rare cases are known where a truncated non-functional protein is transcribed (Kerr et al., 2001). In BMD most point mutations disrupt splicing, which results in an intact but interstitially deleted open reading frame and a partially functional protein (Roberts et al., 1994). Mutations identified in all of the major domains of dystrophin result in disease phenotypes ranging from mild to severe. N-terminal mutations have been identified which stem

from mis-sense and in-frame mutations. In the ABD a mis-sense mutation resulting in an amino acid change of an arginine residue for leucine 54 results in a DMD phenotype with reduced levels of protein (Prior et al., 1995). DMD patients have also been described with in-frame deletions of exons 3-25 indirectly resulting in normal levels of truncated protein (Vainzof et al., 1993).

The rod domain of dystrophin has been found to accommodate large in-frame deletions. A case where a patient was found to missing exons 17-48 corresponding to a 73% deletion of the rod domain only exhibited a mild form of BMD (England et al., 1990). Other large deletions of the rod domain have also been observed in other BMD patients (Love et al., 1991; Winnard et al., 1993), the phenotypes of which are usually milder than those of DMD.

Few missense mutations have been described in DMD patients although two informative substitutions have been identified in the cysteine-rich domain. The cysteine-rich domain contains a number of motifs that are important for regulation and protein-protein interactions. The substitution of a conserved cysteine residue for a tyrosine at position 3340 results in reduced but detectable levels of dystrophin. This mutation alters one of the coordinating residues in the ZZ domain that is thought to interfere with the binding of the dystrophin-associated protein β-dystroglycan (Lenk et al., 1996). Another substitution involving an aspartate to a histidine at position 3335 is also thought to affect the β-dystroglycan binding site (Goldberg et al., 1998). Removal of a highly conserved glutamic acid (residue 3367) adjacent to the dystrophin ZZ domain results in a phenotype of DMD with substantial retention of a presumably functionally compromised dystrophin protein (Becker et al., 2003). Interestingly, the cysteine-rich domain is never deleted in BMD patients suggesting that this domain is critical for dystrophin function as the BMD phenotypes are less severe (Rafael et al., 1996).

A small number of cases have been identified in which there is a deletion of the carboxy-terminus of dystrophin. In these patients it is common for the mutant protein to localise to the sarcolemma (Bies et al., 1992; Helliwell et al., 1992; Hoffman et al., 1991). These cases are good examples of the importance of the cysteine-rich and C-terminal domains of dystrophin, presumably reflecting the importance of interactions with components of the dystrophin-associated glycoprotein complex.

1.8 *Summary and aims*

The spectrin superfamily is a group of cytoskeletal proteins that perform a variety of cellular functions. The role of each protein and the interactions that they are involved in within the cellular environment stem from the specific domains found within each protein and the manner in which they are organised. Of this group of proteins, utrophin has generated significant interest over recent years given the structural and functional similarities it shares with dystrophin. It has been proposed that utrophin may be of use to the treatment of muscular dystrophies where dystrophin is absent or disrupted. In order for utrophin to be developed as a functional replacement for dystrophin it is necessary to understand how the structure of the protein relates to the specific cellular functions that it exhibits and also what other proteins are interacted with and how these interactions are controlled and regulated. Much work has focussed on the up-regulation of utrophin to treat muscular dystrophy phenotypes; however, a large body of work has focused upon the interaction of the utrophin ABD with F-actin. Crystal structures are available for a small number of ABD containing proteins and it has been shown that these domains possess a certain degree of structural homology. It seems that the modelling of ABD association with F-actin has centred on the utrophin ABD however these studies have suggested a number of potential modes of interaction. The current research suggests that the utrophin ABD may associate with F-actin in either an open extended conformation or a closed and compact mode of interaction. There is much controversy over exactly which mode of interaction is correct; however, given the large degree of structural homology shared between CH domain containing ABDs, it is possible that the manner of interaction that the utrophin ABD exhibits when interacting with F-actin would be of importance when understanding the actin-binding interactions of related ABDs.

This study aims to further develop the current knowledge regarding the interaction of the utrophin ABD with F-actin via the manipulation of the domain conformation at varied solution pH and via the generation and characterisation of a number of utrophin ABD mutants.

Chapter 2:

Materials and Methods

Chapter 2
Materials and Methods

2.1. *Materials*

2.1.1 Molecular Biology Reagents

Restriction enzymes and their associated buffers were purchased from New England Biosciences (UK) Ltd. Pfu DNA polymerase was from Promega and dNTPs were obtained from Bioline. Mutagenesis was based around the QuikChange™ Site-directed mutagenesis kit, Stratagene Europe/Biocrest B.V. Small scale plasmid purification and agarose gel extraction of DNA were performed using QIAGEN QIAprep® Spin Miniprep and QIAquick® Gel Extraction Kits respectively.

Professor Steve Winder supplied the initial stock of pSJW1 expression vector (Winder and Kendrick-Jones, 1995) and provided an original stock of the vector containing the utrophin ABD construct (UTR261) (Winder et al., 1995). Oligonucleotides were purchased from MWG Biotech UK Ltd.

Protein expression and purification was performed using ampicillin and protease inhibitors obtained from Sigma. Protease inhibitors were bought as individual components which were then used to make the necessary inhibitor cocktail. IPTG was bought from Melford Laboratories.

Sephacryl™ S-200 HR, DEAE Sepharose™ and the Superose 12 HR analytical gel filtration column were purchased from Amersham Biosciences (UK) Ltd.

2.1.2 *SDS-PAGE and Western blotting*

Kaleidoscope pre-stained and unstained standards were obtained from Bio-Rad Laboratories Ltd. Nitrocellulose was purchased from Schleicher and Schuncll Biosciences and acrylamide:bisacrylamide was obtained from Severn Biotech Ltd..

Horse radish peroxidase (HRP) was purchased from Sigma and utrophin ABD antibody was supplied by Professor Winder.

2.1.3 *Miscellaneous*

Fluorescein-5-maleimide and tetramethylrhodamine-6-maleimide were obtained from Molecular Probes, Inc. All other chemicals used were of standard or AnalaR reagent grade and were purchased from Sigma-Aldrich Company Ltd. or Merck Ltd.

2.2 ***Methods***

2.2.1 *Restriction Digests*

Restriction digests were performed using Sal 1 and Nde I (New England Biosciences). Each digestion was performed as a double digest containing 1 unit of each enzyme and 1 µl of plasmid mini prep DNA made up to a total reaction volume of 10 µl. The double digestion was performed in Sal I buffer consisting of 50 mM Tris-HCl, 100 mM NaCl,10 mM $MgCl_2$ and1 mM (pH 7.9). Digestion was performed at 37 °C for 1 hour followed by enzyme deactivation at 65 °C for 20 minutes. Samples were then subjected to agarose gel electrophoresis.

2.2.2 *Agarose Gel electrophoresis*

DNA samples in DNA loading buffer were loaded onto 1 % (w/v) 40mM tris-acetate pH 8.2 1 mM EDTA (TAE) gels. Ethidium Bromide was added to the molten agarose prior to gel casting to allow visualisation of the DNA under UV light following electrophoresis. Electrophoresis was performed in TAE buffer at 60 V (constant voltage) for 1 hour. DNA markers in the range of 200-10,000 bp (HyperLadder I, Bioline) were run alongside the samples to allow molecular weight determination of the separated bands.

2.2.3 *DNA Purification from Agarose Gel*

After size separation by agarose gel electrophoresis, the required fragments of DNA were visualised under UV light and excised from the gel using a scalpel. The DNA was then purified from the gel slice using a QIAquick® gel extraction kit, according to the manufacturer's instructions.

2.2.4 *Ligation Reaction*

Ligation reactions were performed in 1 x ligation buffer in a final volume of 20 µl. Gel purified insert and cut vector were added in a 3:1 molar ratio in the presence of 1 unit of T4 DNA ligase. Ligations were incubated at room temperature for 5 minutes.

2.2.5 *Generation of Competent Cells*

An overnight culture of appropriate *E. coli* strain isolated from a single colony was used to inoculate 100 ml of 2 x YT broth. The culture was incubated at 37 °C, with shaking at approximately 200 rpm in a CERTOMAT® BS-1 incubator until an absorbance reading of 0.6 was obtained at 600 nm. After incubation the culture was chilled on ice for 30 minutes before the cells were harvested by centrifugation in sterile tubes at 1400 x g for 5 minutes at 4 °C. After removal of the supernatant the cell pellet was re-suspended in 50 ml of ice cold 100 mM $CaCl_2$ and left on ice for 30 minutes. Cells were again harvested by centrifugation at 1400 x g for 5 minutes at 4 °C before a final re-suspension of the cell pellet in 5 ml of 100 mM $CaCl_2$.

2.2.6 *Transformation of DNA into Competent Cells*

Competent *E. coli* cells (100 µl) were incubated on ice in sterile eppendorf tubes with 5 µl of plasmid DNA for 30 minutes. Cells were then subjected to a 2 minute heat shock at 42 °C before being briefly returned to ice. 2 x YT broth (900 µl) was subsequently added to the cells before culturing at 37 °C for 1 hour without shaking. After incubation the culture was spread onto sterile agar plates containing 100 µg/ml

ampicillin before incubation for 16 hours at 37 °C to select for those cells containing the transformed plasmid.

2.2.7 *Small Scale Plasmid Preparation*

A single colony of plasmid-containing *E. coli* DH5α was selected and grown overnight in 5 ml of 2 x YT containing 100 μg/ml ampicillin. 1 ml of the culture was then centrifuged at 12000 x g for 1 minute to pellet the bacterial cells. Following removal of the supernatant DNA was prepared using the QIAprep® Spin plasmid miniprep kit as described by the manufacturer's instructions.

2.2.8 *Polymerase Chain Reaction*

Polymerase Chain Reaction (PCR) was typically carried out with 1-10 ng of double stranded template DNA in a 50 μl reaction volume. The reaction contained 1 x buffer (as supplied by the manufacturer), 125 ng of forward and reverse primers, 200 μM dNTPs (from a 10 mM equimolar stock of each of the four bases) and 1 unit of Pfu DNA polymerase.

PCR cycling was carried out in a Biometra Personal Cycler. Typically, 35 cycles consisting of 3 steps were performed: 30 seconds at 95 °C (denaturation), 30 seconds at 45-65 °C (primer annealing) and 1 minute at 72 °C (elongation). Annealing temperature varied depending on the primers used, typically a temperature 5 °C below the lowest melting temperature of the two primers was chosen. Before the PCR cycles were allowed to commence an initial denaturation step of 2 minutes at 95 °C was performed. On completion of the PCR reaction all products were checked by agarose gel electrophoresis and sequencing.

2.2.9 *Mutagenesis*

Mutagenesis was carried out either by overlap extension or via use of the Stratagene QuickChange™ Site-directed mutagenesis kit. Primers, listed below (Table 2.1), were

designed to remove multiple amino acid residues or substitute selected amino acids with cysteine. Primer pairs were designed across the same section of sequence with the mutation in the centre of the sequence. The resulting primers were between 33-60 bases in length and complementary to each other. For optimal mutagenesis, the primers were designed such that the GC content was above 45 % and the melting temperatures above 75 °C.

Table 2.1 Mutagenesis primers

UTR Mutant	Forward Primer	Reverse Primer
UTR261	5′-GTGCGGATCCATATGGC CAAGTATGGAGAACAT-3′	5′-CTCCAGGTCGACCTAGT CTATGGTGACTTGCTGAGG-3′
$UTR^{fimbrin}$	5′-TGGCAGGTGAAAGATGT CATGAAGGATGAAGCTCTGG CTGCTCTGCTGCGTGATGGT GGA-3′	5′-CGTCTGCTGCAGGTCCG ACATGACTTCACCATCACGC AGCAGAGCAGCCAGAGCTTC -3′
$UTR^{\alpha\text{-actinin}}$	5′-ATCATTTTGCACTGGCA GGTGAAAGATGTCCTGCAGC AGACGAACAGTGAGAAGATC CTG-3′	5′-CAGGATCTTCTCACTGT TCGTCTGCTGCAGGCAATCT TTCACCTGCCAGTGCAAAAT GAT-3′
UTR^{T36C}	5′-GACGTACAGAAGAAATG TTTTACCAAATGGATA-3′	5′-TATCCATTTGGTAAAAC ATTTCTTCTGTACGTC-3′
$UTR^{T36C/S242C}$	5′-CTTCCTGACAAGAATT GTATAATTATGTATTTA-3′	5′-TAAATACATAATTATAC AATTCTTGTCAGGAAG-3′

2.2.10 *Bacterial Protein Expression*

The pSJW1 expression vector (Winder and Kendrick-Jones, 1995) (Appendix 1) containing the DNA encoding either wild type utrophin ABD or one of the ABD mutants was transformed into the BL21 (DE3) strain of *E. coli*. A fresh batch of competent cells was prepared each time protein expression was required. An overnight culture was used to inoculate 1 litre of 2 x YT broth containing 100 µg/ml ampicillin. This was shaken at 200 rpm in a 2 litre bevelled flask at 37 °C in a CERTOMAT® BS-1 shaking incubator until an A_{600} of approximately 0.6 was reached. IPTG was added to a final concentration of 0.5 mM and incubation continued with shaking for 2 hours to allow protein expression.

2.2.11 *Purification of Expressed Protein*

Following protein expression bacterial cultures were subjected to centrifugation at 5000 x g for 20 minutes and the bacterial cells that pelleted frozen. After thawing, the cells were then re-suspended in 25 % w/v sucrose, 1 mM EDTA and 50 mM Tris-HCl pH 8.0 (SET) (10 ml per litre of original culture) to which the required protease inhibitors had been added. Lysozyme was then added (5 mg per litre of original culture) and the cell lysate incubated at room temperature for 30 minutes. In some instances sonication was used to aid bacterial lysis. Prior to centrifugation $MgCl_2$ and $MnCl_2$ were added to the cell lysate to a final concentration of 10 mM and 1 mM respectively followed by addition of 10 µl of 10 mg/ml DNAase 1. The bacterial lysate was incubated for 10 minutes at room temperature before all insoluble material was pelleted by centrifugation at 30000 x g for 20 minutes. The supernatant was then applied directly to a Sepharose™ DEAE anion exchange column and after extensive washing of the column with 20 mM Tris-HCL, 1 mM EDTA and 1 mM DTT pH 8.0 (TED) the bound protein was eluted using a 0-0.5 M NaCl gradient. Fractions corresponding to protein peaks were subjected to sodium dodecyl sulphate polyacrylamide gel electrophoresis (SDS-PAGE) to identify the fractions containing the protein of interest. These fractions were then pooled, concentrated and gel purified using a Sephacry™ S-200 HR gel filtration column. Once again, eluted fractions corresponding to the protein of interest were pooled and concentrated before use.

2.2.12 *Recovery of Insoluble Protein from Inclusion Bodies*

In some instances bacterial expression resulted in the production of insoluble protein. In these circumstances the pellet formed after centrifugation of the lysed bacterial expression culture was re-suspended in 20 mM Tris-HCl, 200 mM NaCl, 1 mM EGTA and 0.25 % (w/v) deoxycholate (pH 8.0) (insoluble protein buffer I) (10 ml/L of original culture). The pellet was re-suspended with stirring and sonication to aid with the break-up of the sticky bacterial cell walls. The sample was then centrifuged

at 8000 x g for 5 minutes and the viscous supernatant discarded. The creamy white pellet was repeatedly re-suspended in 20 mM Tris-HCl, 1 mM EGTA and 0.25 (w/v) deoxycholate (pH 8.0) (insoluble protein buffer II) and centrifuged as above until the supernatant became clear and the pellet took on a granular texture and a grey colour. This pellet was then re-suspended in 20 mM Tris-HCl, and 1 mM EGTA (pH 8.0) (insoluble protein buffer III) and spun as above to remove traces of detergent. The final washed pellet was then re-suspended in 8M urea before dilution to 6M urea in buffer suitable for subsequent purification using a Sepharose™ DEAE anion exchange column and a Sephacry™ S-200 HR gel filtration column. Following collection of the eluted fractions corresponding to the protein of interest the urea was removed in a stepwise fashion by numerous rounds of dialysis. All solutions were made with TED pH 8.0 and urea was reduced from 6M to 4M, 2M, 1M, 0.5M, 0.25M, 0.1M then 500 mM NaCl and final dialysis into TED pH 8.0. The final protein solution was then concentrated before use.

2.2.13 *Determination of Protein Concentration*

Protein concentration was routinely determined using the Beer-Lambert law where the extinction coefficient of a protein and absorbance at 280 nm are used to determine the concentration of the protein in solution. The extinction coefficient of the utrophin ABD and the mutant proteins were calculated from the content of tryptophan, tyrosine and cysteine (Gill and von Hippel, 1989). The extinction coefficients ($cm^{-1}M^{-1}$) were determined to be as follows:

Wild type utrophin ABD = 39,160
$UTR^{fimbrin}$ = 39,160
$UTR^{\alpha\text{-actinin}}$ = 39,160
UTR^{136C} = 39,220
$UTR^{136C/S242C}$ = 39,280

2.2.14 *SDS-PAGE*

Sodium dodecyl sulphate polyacrylamide gel electrophoresis (SDS-PAGE) was performed essentially as described by Laemmli (1970) using the Matsudaira type gel system (Cambridge electrophoresis; (Laemmli, 1970)). Resolving gels were typically 15 % (except where stated) and stacking gels were always 5 %. Gels were prepared in batches of 10 using the following solutions:

Resolving Gel:

Acrylamide:bisacrylamide	25.2 ml
SDS-PAGE resolving buffer	12.5 ml
Water (dH_2O)	14.92 ml
10 % Ammonium Persulphate (freshly prepared)	150 µl
TEMED	25 µl

Stacking Gel:

Acrylamide:bisacrylamide	3.32 ml
SDS-PAGE stacking buffer	5 ml
Water (dH_2O)	11.52 ml
10 % Ammonium Persulphate (freshly prepared)	120 µl
TEMED	40 µl

Samples were prepared by boiling in 1 x sample buffer for 2 minutes. Pre-stained molecular weight markers were run for size comparison. Following electrophoresis in 1 x SDS-PAGE running buffer at a constant voltage of 400 V for between 40-60 minutes, proteins were detected by Coomassie Blue staining or transferred to nitrocellulose for western blot detection.

2.2.15 *SDS-PAGE Gel Staining*

Proteins were visualised directly on SDS-PAGE polyacrylamide gels following staining with Coomassie Blue consisting of 0.25 % (w/v) Coomassie Brilliant Blue

R250, 25 % (v/v) methanol and 10 % (v/v) acetic acid. Gels were incubated in Coomassie Blue stain for approximately 30 minutes before rinsing with dH_2O and destaining with a solution of 40 % (v/v) methanol and 10 % (v/v) acetic acid (destain) for either 30-60 minutes or over night.

2.2.16 *Western Blotting*

Protein transfer to nitrocellulose was performed using a BioRad mini Trans Blot kit® in blotting buffer consisting of 48 mM Tris-HCl, 39 mM glycine, 1.3 mM sodium dodecyl sulphate (SDS) and 20 % (v/v) methanol at 400 mA, 100 V for 1 hour. Following transfer, membranes were blocked in 2.5 % (w/v) semi-skimmed milk powder prepared in 10 mM Tris-HCl, 150 mM NaCl and 0.1 % (v/v) Tween-20 (pH 8.0) (TBST) for 1 hour. Incubation with utrophin 261 antibody (1/1000 dilution) in 2.5 % (w/v) semi-skimmed milk powder/TBST was performed for 1 hour at 4 °C. Following extensive washing in 2.5 % (w/v) semi-skimmed milk powder/TBST (5 x 5 minutes), blots were incubated with horse radish peroxidase (HRP) conjugated secondary antibody (1/500 dilution) prepared in 2.5 % (w/v) semi-skimmed milk powder/TBST for 1 hour at 4 °C. After subsequent washing in 2.5 % (w/v) semi-skimmed milk powder/TBST (5 x 5 minutes), immunoreactive bands were detected by enhanced chemiluminescence (ECL). Equal volumes of 100 mM Tris-HCl, 2.5 mM luminal, 396 µM *p*-coumaric acid (pH 8.5) (ECL solution I) and 100 mM Tris-HCl, 0.02 % (w/v) H_2O_2 (pH 8.5) (ECL solution II) were mixed and added to the membranes for 1 minute with minor agitation. Membranes were transferred to autoradiography cassettes and exposed to Konica Minolta medical X-ray film. Film was developed using a KODAK RP X-OMAT EX developer.

2.2.17 *High Speed Co-sedimentation Assay*

High speed co-sedimentation was performed essentially as described by Winder and Walsh, 1990 (Winder and Walsh, 1990). Each assay was performed in 1 x actin-binding buffer (ABB) pH 8.0 (usually prepared as a 10 x stock) consisting of 20 mM Tris-HCl, 100 mM NaCl, 2 mM $MgCl_2$, 1 mM DTT, 0.1 mM $CaCl_2$ and 1 mM ATP

in a reaction volume of 50 µl. A standard assay usually contained 5-10 µM F-actin and 0-400 µM of binding ligand. Where the pH of the experiment was required to be varied the 10 x ABB stock was made with either MES or CAPS and then the pH adjusted to either 6.0 or 10.0 respectively. Binding assays that required the removal of reducing agents were performed with buffer components lacking in DTT. Typically, an assay would involve the step-wise addition of 10 x ABB, TED buffer and then ligand to generate the required final ligand concentration in the 50 µl assay volume. This was briefly vortexed before addition of F-actin followed by a final mixing. It is essential that all reagents have been clarified by centrifugation at 100000 g prior to use to remove suspended particulates and insoluble protein. Each assay was then incubated at room temperature for 5 minutes before centrifugation at 100000 x g for 15 minutes at 4 °C in a TLA-100 rotor using an Optima™ Benchtop Ultracentrifuge (Beckman Coulter). After centrifugation an aliquot of supernatant from each assay tube was taken and mixed with an equal volume of 2 x sample buffer. The excess supernatant was then carefully removed and the pelleted F-actin and bound ligand re-suspended with 2 x sample buffer. It is important to retain an equivalent proportion of pellet and supernatant fraction. These fractions were then run on 15 % SDS-PAGE gels in equivalent amounts ensuring sufficient loading separation between samples so that protein bands of the higher ligand concentrations would not merge. Gels were then stained with Coomassie Blue and thoroughly destained until background staining was minimal or absent. Gels were then transferred to water and scanned using an Epson Expression 1680 Pro set to transmissive mode. The densities of the protein bands were calculated and corrected for background using NIH Image 1.63. These densities were used to determine the proportion of ligand that remained soluble and that which was recovered in the pellet bound to F-actin. An actin-binding curve was then generated to show the relationship between ligand concentration and that which bound to F-actin.

2.2.18 *Preparation of rabbit muscle acetone powder*

Rabbit muscle acetone powder was prepared essentially as described by (Perry, 1955). The hind leg muscle was quickly excised from two freshly killed rabbits and

immediately placed into ice to preserve endogenous ATP. After cooling for 30 minutes all fat and connective tissue was removed before mincing the tissue twice. The tissue was then mixed with three volumes of 300 mM NaCl, 100 mM NaH_2PO_4, 50 mM Na_2HPO_4, 1 mM sodium azide, 0.05 mM PMSF, 2 mM ATP 1 mM $MgCl_2$ and 1 mM $Na_4P_2O_7$ (pH 6.5) (Guba Straub buffer) with stirring at 4 °C for 15 minutes. After extraction the residual muscle tissue was centrifuged at 40000 x g for 20 minutes before re-suspension in ten volumes of 5 mM $NaHCO_3$ and 0.01 mM $CaCl_2$ (extraction buffer I) with stirring at 4 °C for 15 minutes. The residue was then filtered through cheese cloth to allow removal of the salt and the pH adjusted to 9.0 before re-suspension in one volume of 10 mM $NaHCO_3$, 10 mM Na_2CO_3 and 0.1 mM $CaCl_2$ (extraction buffer II) with stirring at 4 °C for 10 minutes. Once again, the residue is filtered through cheese cloth before re-suspension in ten volumes of chilled distilled H_2O. The distilled H_2O must be removed quickly, again using cheese cloth, to prevent the excessive swelling of the muscle tissue and to prevent loss of actin as F-actin will rapidly convert to monomer. The remaining residue was then re-suspended in 2.5 litres of cold acetone and allowed to stand at room temperature for 15 minutes before filtering through cheese cloth. The acetone washing and filtering was repeated until the supernatant became clear before the muscle residue was spread out on filter paper and allowed to dry over night in a fume hood.

2.2.19 *Actin extraction from acetone powder*

G-actin was prepared as described by Winder et al., (1995) essentially a modified version of the method described by Spudich and Watt (Spudich and Watt, 1971). 20 ml of 2 mM Tris-HCl pH 8.0, 0.2 mM ATP, 0.5 mM DTT, 1 mM $CaCl_2$ and 1 mM NaN_3 (G buffer) was mixed with each gram of acetone powder and stirred on ice for 30 minutes. Following re-hydration the muscle tissue was pelleted by centrifugation at approximately 40000 x g and the supernatant retained. The supernatant was then filtered through glass wool, 8 µm, 1.2 µm, 0.45 µm and finally, 0.22 µm filters. The polymerisation of actin was induced by the addition of $MgCl_2$ to 2 mM and KCl to 0.8 M followed by stirring at room temperature for 30 minutes and then at 4 °C for another 30 minutes. The polymerised F-actin was then pelleted by centrifugation at

100000 x g in a Ti45 rotor at 4 °C for 2 hours. The pellet was then re-suspended in approximately 10 ml of G buffer using a glass Teflon homogeniser before dialysis in G buffer for 2 days with at least two changes of dialysate. Following dialysis, the actin solution was again pelleted (as described above) and the top 2/3 of each tube retained before running on a Sephacryl S200 column in G buffer. The peak and training fractions containing monomeric actin were collected and pooled. The concentration of G-actin was then calculated using the absorbance at 290 nm (0.0264 μM/cm or 0.63 mg/cm).

2.2.20 *Analytical Gel Filtration*

Analytical gel filtration was performed using a calibrated Superose™ 12 HR column (Amersham Biosciences) under control of a BioCad 700E Perfusion Chromatography system or an ÄKTA FPLC system (Amersham Biosciences). Prior to gel filtration, the column was equilibrated by washing with at least two column volumes of appropriate buffer at the required pH. All solutions were 0.22 micron filtered to remove particulates and 200 mM NaCl was present to minimise electrostatic interactions with the column matrix. Protein samples were loaded onto the column using a 100 μl sample loop and the point of injection marked on the chart recorder to allow the elution volume of the protein peak to be determined. Each run was performed at a flow rate of 0.4 ml/min and the elution of the loaded protein monitored using absorbance at 280 nm. The elution volume was then used to calculate the apparent molecular weight of the protein. This was achieved by using a calibration curve determined by running a set of protein standards of known molecular weight. The elution volumes of these proteins were used to calculate the K_{av} for each protein using the following equation:

$$K_{av} = \frac{Ve - Vo}{Vc - Vo}$$

Where: Ve = Protein elution volume.
Vc = Column volume.
Vo = Column void volume.

K_{av} was then plotted against the Log MW of the protein standards to generate the calibration curve. The calibration curve was then used to determine the relative molecular weight of an eluted protein using a K_{av} calculated from the elution data.

2.2.21 *Analytical Ultracentrifugation*

Sedimentation velocity and equilibration analyses were performed with the utrophin ABD at pH 6, 8 and 10 in the presence of 100 mM NaCl. All experimental runs were performed using a Beckman Optima XL-I analytical ultracentrifuge equipped with interference optics.

2.2.21.1 *Sedimentation Equilibrium*

Utrophin ABD was subjected to sedimentation equilibrium analysis at 20000, 25000 and 30000 rpm. A serial dilution of the utrophin stocks at pH 6, 8 and 10 were prepared to give nine samples ranging in concentration between 0.1 and 0.5 au at 280 nm. 100 µl of each concentration was prepared using the buffer dialysate at each pH consisting of 100 mM NaCl, 1 mM EDTA and either 20 mM Tris at pH 8 or 10 or MES at pH 6. 20 µl of each sample concentration was loaded into two 8 channel centrepieces along with a 20 µl reference buffer sample. An initial scan was recorded at 3000 rpm to check for cell leakage before running the samples at 18000, 25000 and 30000 rpm at 4 °C. Scans of sample distribution were recorded at each of these speeds and were used to calculate whole-cell apparent weight molecular masses for the utrophin ABD at each pH. The biophysical data required to determine the apparent molecular weight (buffer density, viscosity and v-bar) were calculated using the program *sednterp* (Laue, 1992).

2.2.21.2 *Sedimentation Velocity*

Sedimentation velocity experiments were performed following dilution of the protein stocks, with the respective buffers, to give a range of concentrations covering several orders of magnitude at each pH. 360 µl of each sample concentration was loaded into

a two channel centrepiece along with 360 µl of buffer to serve as a reference. Once again, an initial scan was recorded at 3000 rpm to check for cell leakage. Once thermal equilibrium was attained (20 °C) the centrifuge was accelerated to 50000 rpm and 240 scans of sample distribution were recorded at 2 minute intervals. Data from the sedimentation velocity runs was analysed using the program *sedfit* (Schuck, 1998).

2.2.22 *Proteolytic Digestion*

2.2.22.1 *Trypsin Digestion*

Trypsin was made as a 1 mg/ml stock in TED pH 8.0 100 mM NaCl and diluted to a working concentration of 0.01 mg/ml in the final reaction volume. Reactions were performed in 100 µl TED pH 8.0 with 100 mM NaCl. Wild type utrophin ABD and $UTR^{fimbrin}$ were diluted to 20 µM and incubated for 1 hour at room temperature. The digestion and degradation products formed were visualised using SDS-PAGE and Coomassie Blue staining.

2.2.22.2 *Papain and Proteinase K Digestion*

A 200 µl solution comprising 25 µM utrophin, 100 mM NaCl, 1 mM EDTA, 1 mM DTT and 20 mM Tris pH 10 or MES pH 6 was subjected to proteolytic degradation by either papain or proteinase K. Proteinase K or papain were added to a final concentration of 0.01 mg/ml and 0.001 mg/ml respectively. These concentrations were determined to give a reasonable degree of protein degradation. The complete assay solution was incubated at room temperature for a total of 60 minutes. Samples of digested utrophin ABD were removed after 5, 10, 20, 40 and 60 minutes and the degradation reaction halted by boiling in SDS-PAGE sample buffer for 2 minutes. A 1 mg/ml solution of BSA was also digested by each enzyme at both pH values to help assess the activity of both enzymes over the range of pH used in the experiment. All samples were subjected to gel electrophoresis and non-digested utrophin and BSA samples were run as a comparison.

2.2.22.3 *Digestion of Utrophin ABD Bound to F-actin*

200 µl reactions containing either 25 µM utrophin, 10 µM F-actin, papain (0.01 mg/ml) or a mixture of protease and utrophin or F-actin were prepared in TED pH 8 and 1 x ABB. These samples were incubated at room temperature for 30 minutes before centrifugation at 100000 x g for 15 minutes. Supernatant and pellet fractions were then separated to give samples corresponding to all species in the presence and absence of protease. All components were then combined in one reaction and incubated at room temperature for 30 minutes, aliquots were removed at 5, 10, 15, 20 and 30 minute time points and the remaining sample was then centrifuged as described before to show the protein distribution between supernatant and pellet fractions. All samples were then subjected to SDS-PAGE analysis so that the extent of protein degradation could be compared.

2.2.23 Circular Dichroism

Near and far UV circular dichroism (CD) and thermal denaturation analyses of the utrophin ABD and the $UTR^{fimbrin}$ linker mutant were performed at the University of Glasgow with the help of Dr Sharon Kelly. Near and far UV CD and thermal denaturation analyses of the $UTR^{\alpha\text{-actinin}}$ linker mutant were performed at the University of Sheffield along with repeats of utrophin ABD near and far UV CD. Thermal denaturation of utrophin ABD was not repeated. The Glasgow work encompassed the thermal denaturation of the wild type utrophin ABD and the $UTR^{fimbrin}$ mutant along with analysis of the utrophin ABD at pH 6, 8 and 10. These studies were performed using a Jasco J-600 spectropolarimeter. Utrophin ABD and $UTR^{fimbrin}$ were prepared in 10 mM phosphate buffer at the required pH at a concentration of 0.5 mg/ml. Near and far UV measurements were made between 320-260 and 260-190 nm respectively. Protein samples were scanned in either 0.5 or 0.02 cm quartz cuvettes depending on whether data were collected in the near or far UV regions. Thermal denaturation of the utrophin ABD and $UTR^{fimbrin}$ was monitored in the far UV region between 20 and 80°C. One final scan was made after heating to 80°C after the sample was allowed to cool to 20°C to allow protein

refolding. All scans were performed with a data pitch of 0.2 nm, a band width of 1 nm, a detector response time of 2 seconds and a scanning speed of 100 nm/minute. Three accumulations were collected for each protein sample. Secondary structure prediction was performed by Dr Kelly using SELCON (Sreerama and Woody, 1993).

Analysis of the $UTR^{\alpha\text{-actinin}}$ mutant was performed at the University of Sheffield using a J-810 CD spectropolarimeter equipped with a PFD 425S Peltier temperature controller. Near and far UV CD spectra were performed using 1 or 0.2 cm quartz cuvettes scanned between 320-260 nm and 260-190 nm respectively. Protein samples were prepared in 10 mM phosphate buffer at concentrations of 1 and 0.4 mg/ml corresponding to near and far UV measurements respectively. Thermal denaturation of $UTR^{\alpha\text{-actinin}}$ was performed over the same range of temperature as described previously. CD spectra were collected using a data pitch of 0.1 nm, band width of 1 nm, detector response time of 4 seconds and at a scanning speed of 100 nm/minute. Once again, three scans were performed for each protein sample. As with the Glasgow work, Dr Kelly kindly provided help analysing the data using SELCON.

2.2.24 *Tryptophan Fluorescence*

The fluorescence of the intrinsic tryptophans present within the utrophin ABD were measured using a Shimadzu RF-5301PC spectrofluorophotometer. Protein samples were held within a 1 cm quartz cuvette and excited at 296 nm. Fluorescence emission data were recorded between 300-450 nm using a slow scanning speed with excitation and emission slits set to 1.5 nm. Protein samples were prepared in 20 mM Tris-HCl pH 8.0 and 1 mM EDTA (TE) to a final concentration of 30 μM. All solutions and samples were 0.22 micron filtered to remove all particulates and extensive dialysis was used to ensure that no reducing agents were present. All buffers solutions were scanned prior to use to ensure that there was no fluorescence after excitation at 296 nm. Experiments involving F-actin were performed in the presence of 5 μM F-actin and 1 x ABB. Where this was the case, all other buffering solutions within the experiment (for example utrophin ABD in the absence of F-actin) also contained 1 x

ABB to ensure that any fluorescence attributable to the 1 x ABB remained constant throughout all experimental samples.

2.2.25 *NTCB Digestion*

Specific cleavage of peptide backbone at cysteine residues was performed in the presence of 2-Nitro-5-thiocyanobenzoate (NTCB) (Jacobson et al., 1973). The protein to be digested was diluted to 20 μM in a total reaction volume of 100 μl using 6M urea prepared with TED pH 8.0. NTCB was then added to the reaction in a 10-fold molar excess compared to the protein and then incubated for 1 hour at room temperature. After incubation the pH of the solution was adjusted to 9.0 by the addition of 5 μl of 1M NaOH/1M Tris-HCl solution before incubation at 30 °C for 3 hours. After incubation a molar excess of β-mercaptoethanol was added to halt the reaction and the samples then run on 15 % SDS-PAGE gels to visualise the size of peptide fragments generated compared to a molecular weight standard.

2.2.26 *Disulphide Bond Formation in the Double Cysteine Mutant*

$UTR^{T36C/S242C}$ was dialysed into TE pH 8.0 to remove the reducing affects of DTT. To this solution *o*-phenanthroline and $CuSO_4$ were added in a drop-wise fashion with vigorous stirring to final concentrations of 4 mM and 1 mM respectively. The protein solution was incubated overnight at 4 °C to allow oxidation and disulphide bond formation. Oxidation was also performed by dialysis of the protein sample into a solution of TE pH 8.0 containing 4 mM *o*-phenanthroline and 1 mM $CuSO_4$ overnight at 4°C. Following oxidation, *o*-phenanthroline and $CuSO_4$ were removed via extensive dialysis with TE pH 8.0 and then samples of reduced and oxidised $UTR^{T36C/S242C}$ run on 15 % SDS-PAGE gels to assess the success of disulphide bond formation. It is important to allow sufficient separation between reduced and non-reduced samples when running on a gel so that the oxidised sample will not be partially reduced by diffusion of β-mercaptoethanol from the reduced sample lane.

2.2.27 *Generation and Purification of Fluorescently Labelled Protein*

$UTR^{T36C/S242C}$ was singly labelled with either fluorescein-5-maleimide or tetramethylrhodamine-5-maleimide (single isomer) or double labelled with both. The labelling reaction was performed essentially as described by the Molecular Probes Handbook and generally involved reaction of a 100 μM solution of $UTR^{T36C/S242C}$ prepared in TE pH 7.0 with the fluorescent dyes. It is important that the reaction solution remains around pH 7.0 to ensure that protein thiol groups are sufficiently nucleophilic and hydrolysis of the maleimide to an unreactive product can compete significantly with thiol modification, particularly above pH 8. A 10-fold molar excess of Tris(2-carboxyethyl)phosphine hydrochloride (TCEP) was added prior to labelling to reduce any disulphide bonds that may form. Each of the reactive dyes was prepared as a 10 mM stock made up in dimethyl sulphoxide (DMSO). The dyes were then added to the reduced $UTR^{T36C/S242C}$ in a drop-wise manner with vigorous stirring until a 20-fold molar excess was attained. The reaction was allowed to proceed for 16 hours at 4 °C. Upon completion of the reaction a molar excess of β-mercaptoethanol was added to consume the excess thiol-reactive reagent. The labelled $UTR^{T36C/S242C}$ was then extensively dialysed using TE pH 7.0 to remove any un-conjugated fluorescent dye and then gel purified. At all stages during the reaction and purification procedures reagents and protein solutions were protected from light as much as possible due to reagent sensitivity to light.

The degree of labelling was calculated as follows:

$$\frac{A\chi}{\varepsilon} \times \frac{\text{MW of protein}}{\text{mg protein/mL}} = \frac{\text{moles of dye}}{\text{moles of protein}}$$

Where:
$A\chi$ = the absorbance value of the dye at the absorbance maximum wavelength.
ε = molar extinction coefficient of the dye or reagent at the absorption maximum wavelength.

2.2.28 *Utrophin ABD Inter-Domain FRET*

Following fluorescent labelling of $UTR^{T36C/S242C}$ with rhodamine, fluorescein or both, excitation and emission scans were collected at the specific excitation and emission wavelengths of the two fluors. Rhodamine can be excited at 555 nm producing an emission at 580 nm whilst fluorescein can be excited at 494 nm and produces an emission at 518 nm. Scans of fluorescence excitation and emission were performed using a 1 cm quartz cuvette and a Shimadzu RF-5301PC spectrofluorophotometer. Scans were collected at a slow scanning speed between 480 and 700 nm with excitation and emission slit widths set to 1.5 nm. An emission scan involves the stimulation of the protein sample at a specific excitation wavelength recording the wavelength of any fluorescent emission. An excitation scan involves recording the fluorescence produced after excitation of the sample with radiation that covers a specific range, in this case between 480 and 700 nm. Protein samples were prepared in TE pH 7.0 with labelled $UTR^{T36C/S242C}$ present to a final concentration of 10 µM. 1 x ABB was also added where samples of labelled $UTR^{T36C/S242C}$ were to be compared with samples in the presence of F-actin. In these instances F-actin was added to a final concentration of 5 µM. Initially, samples of $UTR^{T36C/S242C}$ individually labelled with fluorescein or rhodamine were subjected to excitation and emission scans at the wavelengths of both fluors to test if one fluor could be stimulated by the others excitation or emission parameters. This was then repeated for a mixture of $UTR^{T36C/S242C}$ individually labelled with either rhodamine or fluorescein before the final experiment was attempted with double labelled $UTR^{T36C/S242C}$. Fluorescein and rhodamine form a donor/acceptor pair that may allow FRET to occur within doubly labelled $UTR^{T36C/S242C}$. A FRET signal would present itself as a rhodamine emission at 580 nm following stimulation of the doubly labelled $UTR^{T36C/S242C}$ sample at 494 nm (fluorescein excitation wavelength). The affect of binding to F-actin on the FRET signal was also assessed by the addition of F-actin to the final concentration stated above. Fluorescent emission and excitation spectra of an F-actin solution were also collected at rhodamine and fluorescein wavelengths prior to the addition of labelled $UTR^{T36C/S242C}$ to determine if actin alone could be stimulated at any of the wavelengths used in the experiment.

2.2.29 *Differential Scanning Calorimetry*

Differential scanning calorimetry (DSC) experiments were kindly performed by Dr Andrey Bobkov at the Burnham Institute, La Jolla, CA. DSC experiments were performed using a N-DSC II differential scanning calorimeter from Calorimetry Sciences Corp (Provo, UT), at scanning rate of 1 K/min under 3.0 atm pressure. DSC samples contained 10 μM utrophin ABD (wild type or mutants), 20 mM PIPES (pH 7.0), 50 mM NaCl, 1.0 mM $MgCl_2$, 0.2 mM ATP and, when stated, 10μM F-actin or 20μM F-actin + 20μM phalloidin (Sigma, St Louis, MO). Utrophin ABD, $UTR^{T36C/S242C}$ and UTR^{T36C} samples under reducing conditions were kept with 1.0 mM DTT at all times and diluted 10 fold with DTT-free buffer immediately before loading into the calorimeter.

2.3 ***Solution Compositions***

1 x Actin Binding Buffer

Tris-HCl pH 8.0	20 mM
NaCl	100 mM
$MgCl_2$	2 mM
DTT	1 mM
$CaCl_2$	0.1 mM
ATP	1 mM

Blotting Buffer

Tris-HCl	48 mM
Glycine	39 mM
SDS	1.3 mM
Methanol	20 % (v/v)

Coomassie Blue Stain

Coomassie Brilliant Blue R250	0.25 % (w/v)
Methanol	25 % (v/v)
Acetic acid	10 % (v/v)

Destain

Methanol	40 % (v/v)
Acetic acid	10 % (v/v)

DNA Loading Buffer

Ficoll	30 % (w/v)
EDTA pH 8.0	100 mM
Orange G to colour	

ECL Solution I

Tris-HCl pH 8.5	100 mM
Luminol	2.5 mM
p-coumaric acid	396 μM

ECL Solution II

Tris-HCl pH 8.5	100 mM
H_2O_2	0.02 % (w/v)

Extraction Buffer I

$NaHCO_3$	5 mM
$CaCl_2$	0.01 mM

Extraction Buffer II

$NaHCO_3$	10 mM
Na_2CO_3	10 mM
$CaCl_2$	0.1 mM

G - Buffer

Tris-HCl pH 8.0	2 mM
ATP	0.2 mM
DTT	0.5 mM
$CaCl_2$	1 mM
NaN_3	1 mM

Guba Straub Buffer

NaCl	0.3 M
NaH_2PO_4	0.1 M
Na_2HPO_4	0.05 M
Sodium Azide	1 mM
PMSF	0.05 mM
ATP	2 mM
$MgCl_2$	1 mM
$Na_4P_2O_7$	1 mM
dH_2O to 4 litres pH to 6.5	

Insoluble Protein Buffer 1

Tris-HCl pH 8.0	20 mM
NaCl	200 mM
EGTA	1 mM
Deoxycholate	0.25 % (w/v)

Insoluble Protein Buffer 2

Tris-HCl pH 8.0	20 mM
EGTA	1 mM
Deoxycholate	0.25 % (w/v)

Insuluble Protein Buffer 3

Tris-HCl pH 8.0	20 mM
EGTA	1mM

10 x KME

Tris-HCl pH 8.0	100 mM
KCl	500 mM
$MgSO_4$	10 mM
EGTA	10 mM

2 x Sample Buffer

Tris-HCl pH 6.8	50 mM
SDS	1 % (w/v)
Glycerol	30 % (v/v)
Bromophenol Blue	0.01 % (w/v)
β-Mercaptoethanol	20 µl/ml before use

2 x YT Broth

Yeast Extract	10 g/L
NaCl	5 g/L
Tryptone	16 g/L

2 x TY Agar

Yeast Extract	10 g/L
NaCl	5 g/L
Tryptone	16 g/L
Agar	20 g/L

SDS-PAGE Resolving Buffer

SDS	0.4 % (w/v)
Tris-HCl pH 8.8	1.5 M

SDS-PAGE Stacking Buffer

SDS	0.4 % (w/v)
Tris-HCl pH 6.8	0.5 M

SDS-PAGE Running Buffer

Tris-HCl	3 g/L
Glycine	14.4 g/L
SDS	0.1 % (w/v)

SET

Sucrose	25 % (w/v)
Tris-HCl pH 8.0	50 mM
EDTA	1 mM

TAE

Tris acetate pH 8.2	40 mM
EDTA	1 mM

TBST

Tris-HCl pH 8.0	10 mM
NaCl	150 mM
Tween-20	0.1 % (v/v)

TED

Tris-HCl pH 8.0	20 mM
EDTA	1 mM
DTT	1 mM

Chapter 3:

pH Induced Conformational Change of the Utrophin ABD

Chapter 3
pH Induced Conformational Change of the Utrophin ABD

3.1 *Introduction*

The amino terminal utrophin actin-binding domain (ABD) was first crystallised by Keep et al, 1999. This structure revealed that two utrophin monomers interact in an antiparallel manner to form a crystallographic dimer where the first and second CH domains of the adjacent monomers are in close association (Keep *et al.*, 1999b). Analysis of the utrophin ABD when in solution indicates that the protein behaves as a monomer and hence, the dimerisation observed in the crystal is probably an artefact of the crystallisation process (Moores and Kendrick-Jones, 2000). The ABD of the highly homologous dystrophin also crystallised as an anti-parallel homodimer (Norwood et al., 2000); however, the ABD from the actin bundling protein fimbrin, was found to crystallise as a monomer with the two CH domains in close association with one another (Goldsmith et al., 1997). It was apparent, from the crystal structures of utrophin and fimbrin that the interface observed between the two CH domains in the fimbrin crystal was preserved in the interface between opposing CH domains in the utrophin dimer. This kind of structural similarity between related proteins can be described by a phenomenon referred to as three-dimensional domain swapping (Schlunegger et al., 1997). Modelling of the utrophin ABD binding to F-actin using cryo-electron microscopy (cryo-EM) reconstruction suggested that utrophin was binding in a conformation similar to that observed in the utrophin crystal structure (Moores et al., 2000); however, fimbrin has been modelled to bind F-actin in a compact conformation similar to that observed in the fimbrin crystal structure (Hanein et al., 1998). Recent modelling of utrophin binding to F-actin has suggested a number of possible modes of interaction, including both extended and compact binding interactions (Galkin et al., 2002; Lehman et al., 2004; Sutherland-Smith et al., 2003)

It is apparent from this previous work that the binding of the utrophin ABD to F-actin is highly dynamic. Biochemical analyses of the utrophin ABD in solution indicate that the protein is monomeric (Winder et al., 1995), potentially adopting a conformation more akin to that of the fimbrin crystal structure. This conformation is

then induced to 'open' upon binding with F-actin to become more similar to the structure observed in the utrophin crystal dimer. This 'opening' of the molecule requires a loss of association between the two CH domains to switch from one conformation to the other.

Preliminary work performed by Professor Winder suggested that the conformation of the utrophin ABD (open or closed) could be influenced by the pH of the buffering solution. It appeared that at lower pH the ABD behaved as if a more compact conformation were adopted compared to a more 'open' or extended conformation at higher pH. It is possible that at different pH the electrostatic interactions that occur between the two CH domains are altered allowing the degree of 'openness' to be affected. Many proteins undergo a shift in their conformation or an alteration in activity resulting from a change in the pH of their environment (Blondin et al., 2002; Lagarrigue et al., 2003; Lamb et al., 1993; Schmidt et al., 1993; Stoeckelhuber et al., 1996) and hence, it is feasible that similar effects could contribute to a change in conformation of the utrophin ABD over a range of pH.

To test these hypotheses the utrophin ABD was subjected to a number of analyses that would investigate the potential structural and conformational changes induced by varying pH and how these potential changes would affect the interaction with F-actin.

3.2 ***Results***

3.2.1 *pH dependent conformational change of the utrophin ABD*

The amino terminal ABD of utrophin was purified as described previously ((Winder and Kendrick-Jones, 1995); section 2.2.11; Appendix 2). Preliminary gel filtration studies suggested that the utrophin ABD was experiencing a size dependent shift when eluted from an analytical gel filtration column at varying pH. It appeared that the utrophin ABD was increasing in relative size as the pH of the buffering solution was elevated suggesting a separation of the two CH domains and the protein adopting a more 'open' conformation. In order to replicate this experiment gel purified samples of utrophin ABD were dialysed into suitable buffer to give a series

of pH ranging from 5 to 9. 100 µl samples of utrophin ABD at each pH were loaded onto a Superose™ 12 HR analytical gel filtration column equilibrated with buffer at equivalent pH to the samples. The exact point of loading was recorded and the protein elution followed via absorbance at 280 nm (Section 2.2.20). Figure 3.4 represents an overlay of the utrophin ABD elution at each pH. From the curves it is evident that as the pH of the buffer solution decreased from 9 down to 5 there was an increase in the elution volume of the utrophin ABD. This increase in elution volume suggested that at lower pH the utrophin ABD was interacting with the column matrix to a greater extent hindering passage through the column. The increased elution would be consistent with a relative reduction in size of the protein. It is also evident from Figure 3.1 that the protein peaks are not of an equivalent size. This is attributable to difference in protein concentration of each sample that was loaded onto the column.

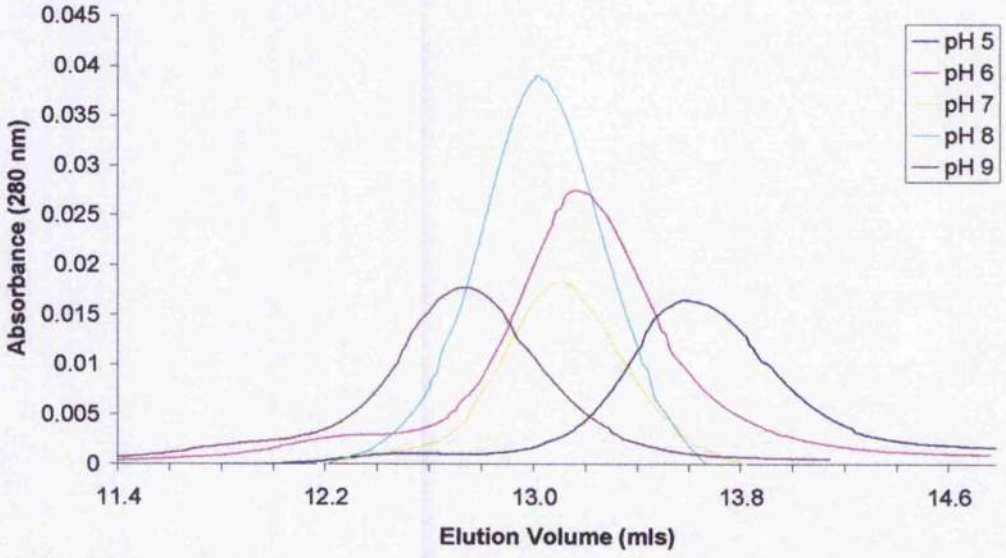

Figure 3.1: Preliminary gel filtration data of the utrophin ABD at varying pH. Samples of utrophin ABD ranging in pH from 5 to 9 were subjected to gel filtration analysis using a Superose™ 12 HR analytical gel filtration column. The column was run at 0.4 ml/min and the elution volume of utrophin ABD was monitored using protein absorbance at 280 nm.

In order to estimate the change in size of the utrophin ABD a calibration curve produced for the column at pH 8 was used. Previous experiments have determined the MW of the utrophin ABD to be approximately 30 kDa (Winder et al.,

1995). The calculated relative MW at each pH (Table 3.1) indicated a size shift ranging from 31 kDa at pH 5 up to 40 kDa at pH 9. This was a large change in the apparent size of the protein in solution however; the calculated MW at pH 8 was very different to previously determined values and hence, it was necessary to repeat the experiment using more stringent conditions.

pH	5	6	7	8	9
Elution Volume (ml)	13.6	13.2	13.1	13.0	12.7
Relative MW (kDa)	31	34	35	37	40

Table 3.1: Preliminary determination of the utrophin ABD apparent MW at varying pH. The preliminary gel filtration data (protein elution volume) was used to determine the relative MW of the utrophin ABD at each pH when compared to the elution volumes of a set of protein standards of known MW (Section 2.2.20).

The pH range of the above experiment was subsequently modified to span the pH range 6 to 10. This range was chosen to centre the maximum and minimum pH values on pH 8, a value at which much utrophin ABD biochemistry has been performed (Moores and Kendrick-Jones, 2000; Morris et al., 1999; Winder et al., 1995; Winder et al., 1995; Winder and Kendrick-Jones, 1995). This served to generate an equal change in the pH above and below pH 8 whilst maximising the potential to visualise a pH induced effect. At each pH (6, 8 and 10) multiple runs were performed and the average elution volume at each pH was plotted (Figure 3.5). In these instances 100 µl samples of 20 µM utrophin ABD were loaded onto a Superose™ 12 HR column. The samples were run at 0.4 ml/min and all buffers contained 200 mM NaCl to prevent electrostatic interactions with the column matrix. Once again a pH dependent shift in the elution was observed potentially attributable to a shift in size of the protein when in solution. Indeed these data suggested that the relative MW of the utrophin ABD was increasing in size from pH 6 to 10. However, during equilibration and sample runs at pH 6 and 10 it was noticed that the volume of gel bed was changing slightly from that of pH 8. In order to calibrate the column for the calculation of MW the gel bed volume must be known accurately or this would affect the MW ultimately determined.

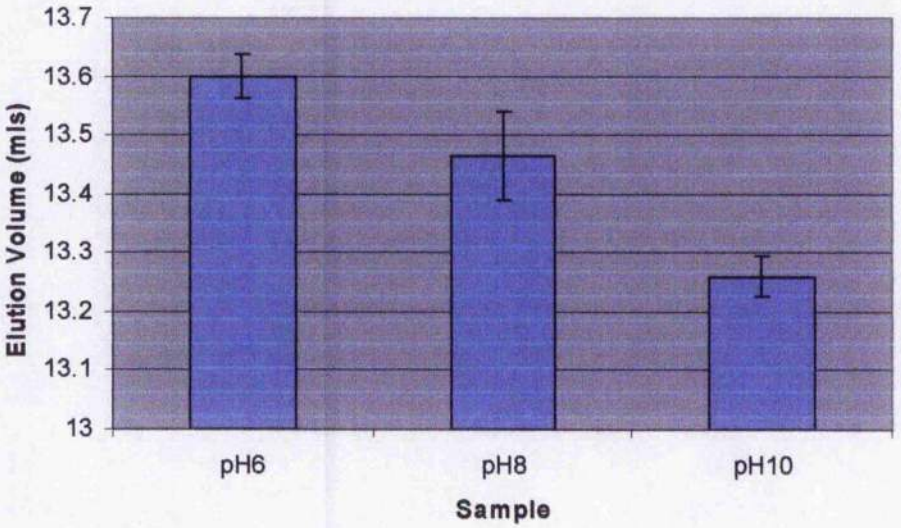

Figure 3.2: Gel filtration elution volume of the utrophin ABD at varying pH. Utrophin ABD samples were subjected to gel filtration analysis at pH 6, 8 and 10. All experiments were run at 0.4 ml/min and 200 mM NaCl was present to prevent electrostatic interactions with the column matrix. Elution of the utrophin ABD was monitored via absorbance at 280 nm and each experiment was repeated in triplicate to obtain an average elution volume at each pH. Error bars represent standard deviation.

So that the relative MW of the utrophin ABD at each pH could be calculated accurately the Superose™ 12 HR column was calibrated at each pH with a set of protein standards of known molecular weight. This would remove any potential effects that the buffering pH would exhibit on the final calculated MW. The standards consisted of blue dextran, ribonuclease A (13.7 kDa), chymotrypsinogen (25 kDa), ovalbumin (43 kDa) and albumin (67 kDa). Blue dextran is a large protein and was used to calculate the column void volume as it effectively passes through the column with very little interaction with the gel matrix. From these data a calibration curve could be generated for the column at each pH (Appendix 3) which could be used to determine the relative MW of the utrophin ABD at each pH

Following calibration of the gel filtration column at each pH the relative MW of the utrophin ABD could be calculated (Figure 3.3). From the data the relative MW calculated at each pH was 30.6, 29.8, and 30.7 kDa corresponding to pH 6, 8 and 10 respectively. These values of MW are in agreement with literature values (Moores

and Kendrick-Jones, 2000; Winder et al., 1995) and those determined in Figure 3.1. However, it is clear that there is no appreciable size change over this range of pH.

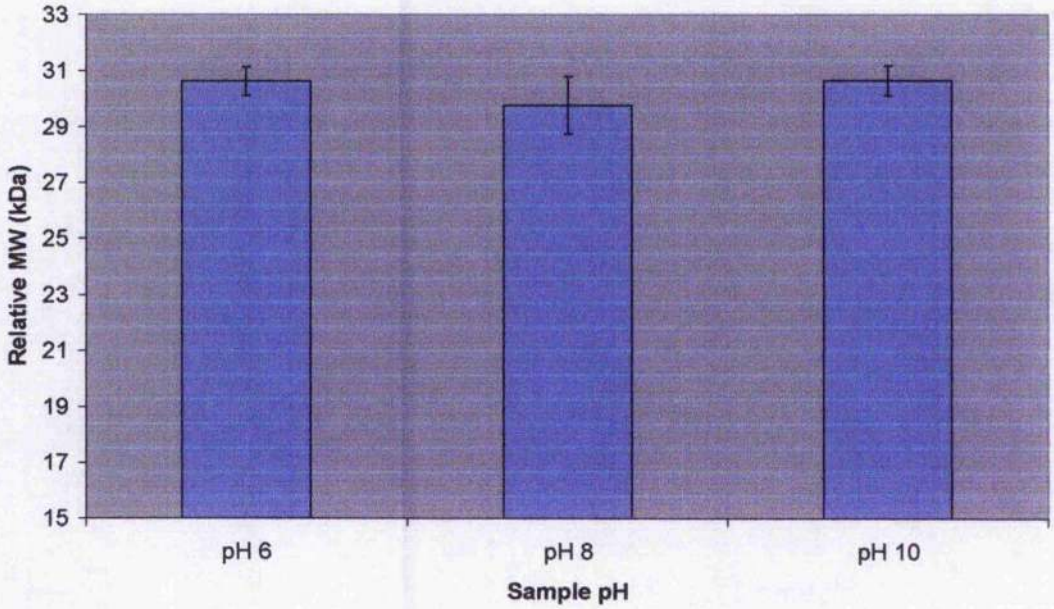

Figure 3.3: Relative MW of the utrophin ABD at pH 6, 8 and 10. Utrophin ABD at pH 6, 8 and 10 was run through a calibrated Superose 12 HR column at each pH. The elution volumes of the domain were used to calculate the relative MW of the protein at each pH when compared to a set of protein standards. Each experiment was performed in triplicate and the error bars represent standard deviation.

3.2.2 *pH dependent effects of the utrophin ABD binding to F-actin.*

Utrophin is an actin-binding protein that interacts with F-actin via its N-terminal ABD (Banuelos et al., 1998; Broderick and Winder, 2002; Gimona et al., 2002; Stradal et al., 1998; Winder, 2003; Winder et al., 1995). This interaction has previously been characterised via the use of high speed co-sedimentation assay (Moores and Kendrick-Jones, 2000; Winder et al., 1995). An example of a utrophin ABD actin-binding assay is shown in Figure 3.4. This figure clearly demonstrates the pelleting of F-actin and associated utrophin ABD following centrifugation.

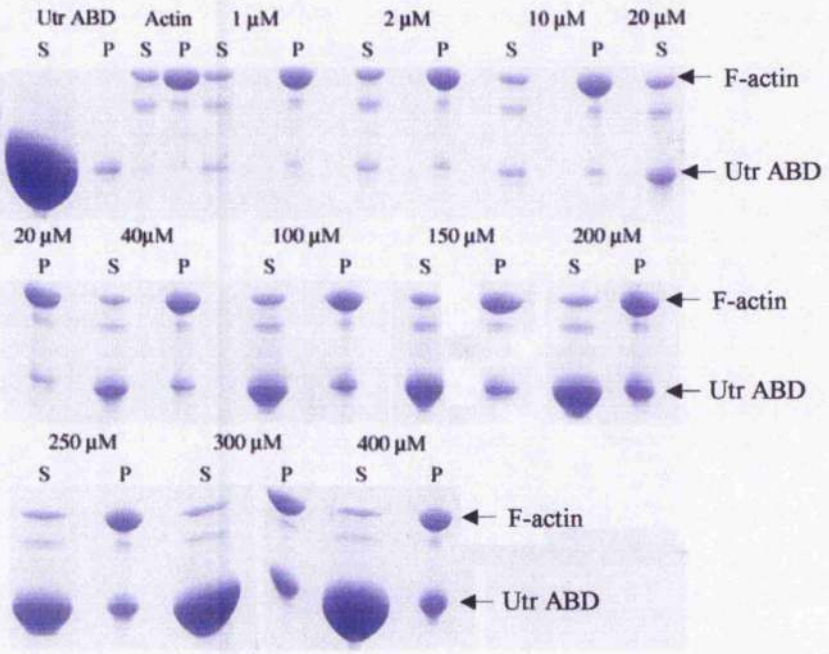

Figure 3.4: Example of a utrophin ABD high speed co-sedimentation assay. High speed co-sedimentation involves the titration of a range of utrophin ABD with F-actin. Typically, this involves utrophin ABD over a concentration range of 1-400 μM, F-actin is typically added to 5 μM. Utrophin ABD and F-actin are incubated in the presence of 1 x ABB typically at pH 8 although the exact pH of the experiment can be varied. F-actin and bound utrophin ABD are pelleted at 100,000 x g to produce samples that correspond to soluble (S) and insoluble (P) protein fractions. These fractions are prepared using 1 x sample buffer and are then run out on a SDS-PAGE gel. Following separation, the gel is stained with Coomassie to visualise the protein bands, these bands are then quantified to determine the proportion of protein present which can then be used to determine the stoichiometry and binding affinity of utrophin ABD for F-actin. Each experiment is typically performed in triplicate.

Previous experiments have determined that the utrophin ABD binds to F-actin with a 1:1 ratio and K_d of approximately 20 μM (Winder et al., 1995). The conformation of a protein is of particular importance in an interaction with another as the affinity or mode of interaction may be affected (Creighton, 1996). Current models of utrophin ABD binding to F-actin in the open conformation rely of the assumption of utrophin 'opening' from a monomeric state in solution to present the actin-binding surfaces towards F-actin. The analytical gel filtration data suggest little difference in the apparent size of the protein in solution at differing pH; however, there may be a structural effect not detectable by analytical gel filtration that might be more apparent when the utrophin ABD binds F-actin. If the association between

the two CH domains within the solution monomer can be reduced, by altering the pH of the surrounding solution, it might be possible that the association of the utrophin ABD with F-actin would be more favourable, potentially resulting in an increased binding affinity.

The binding of the utrophin ABD to F-actin was characterised using co-sedimentation assays ranging in pH from 6 to 10. Polymerised actin was titrated with a range of utrophin ABD concentrations in TED and 1 x ABB buffer at the appropriate pH. These data were used to produce actin-binding curves (Figure 3.5) at pH 6, 8, and 10, from which the binding affinity and stoichiometry could be determined (Table 3.2).

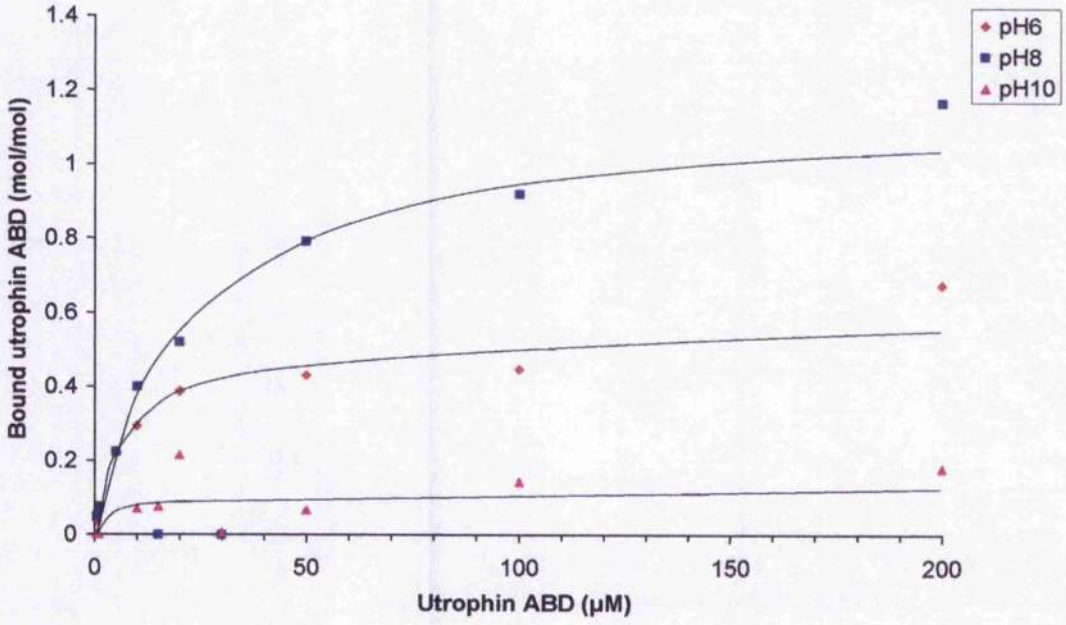

Figure 3.5: Utrophin ABD F-actin binding curves at pH 6, 8 and 10. Actin-binding curves were generated for utrophin ABD interacting with rabbit skeletal actin at pH 6, 8 and 10. The binding curves were generated essentially as described by Winder et al., 1995 (Section 2.2.17). The data were subjected to a Michaelis-Menten-type fitting to determine the affinity and the stoichiometry of the binding reaction. At each pH standard error was calculated (n=3) however, the error bars have been omitted for clarity of the figure.

pH	Stoichiometry	+/-	K_d (μM)	+/-
6	0.6	0.05	10.6	3.8
8	1.2	0.06	25.7	4.1
10	0.2	0.07	11.3	20.7

Table 3.2: Stoichiometry and binding affinity of the utrophin ABD at pH 6, 8 and 10. The table presents the calculated utrophin ABD/F-actin binding affinities and stoichiometries determined using a Michaelis-Menten-type fitting of the co-sedimentation data. In each case the standard error has been displayed adjacent to the stoichiometry and affinity (K_d) data (n=3).

From binding data it is apparent that the interaction of utrophin ABD with F-actin varies considerably depending on the pH at which binding occurs. The binding affinity (25.7 μM ± 4.1) and stoichiometry (1.2:1) determined at pH 8 are very similar to the literature values determined by Winder et al., 1995 however, the pH 6 and 10 values differ greatly. At pH 6 the ratio of binding has reduced to 0.6:1 and the binding affinity has increased to 10.6 μM ± 3.8. This reduced stoichiometry may be explained by the half binding model of association proposed by Galkin and colleagues where the utrophin ABD binds in an extended conformation spanning two actin monomers within the filament (Galkin et al., 2002).The data at pH 10 cannot be considered reliable but may suggest a much lower stoichiometry of 0.2:1 and an increase in affinity to 11.3 μM ± 20.7. This data is not realistic and does not conform to any of known utrophin ABD biochemistry or binding models. The binding affinity calculated at pH 10 is much greater than normal and it is associated with a considerable error whereas the stoichiometry suggests the association of approximately eight utrophin ABDs to each actin monomer in the filament. In this instance, the lack of reliability of the pH 10 binding data may result from the decreased stability of F-actin at elevated pH. It was observed during the analysis of the data at pH 10 that the proportion of F-actin recovered in the pellet was particularly low and varied greatly. This fluctuation in the pelleting F-actin would have significant consequences on the stoichiometries and affinities calculated from the data. The F-actin that pelleted at pH 6 and 8 was very consistent, if anything, the proportion of G-actin at pH 6 was much less than at pH 8 suggesting greater stability.

This increased stability may help to explain the increased affinity of the utrophin ABD at this pH.

3.2.3 *Investigation of utrophin ABD structure using circular dichroism.*

In order to assess the effects of varied pH on the structure and conformation of the utrophin ABD protein samples at pH 6, 8 and 10 was subjected to near and far UV CD analysis. Any differences in the structure or conformation of the protein over the pH range could result in differences in the CD spectra. Figure 3.6 represents the near and far UV spectra of the three utrophin samples. From these data the secondary structure content of the protein was predicted using SELCON (Table 3.3).

Figure 3.6A demonstrates that the utrophin samples show very little difference in their secondary structures. There appears to be a slight variation in the molar ellipticity at pH 10 however, this is most likely to be attributable to a slight difference in sample concentration. The SELCON analyses determined that the utrophin ABD consisted of approximately 60 % α-helix, which would be expected when compared to the known crystal structure of the utrophin ABD (Keep *et al.*, 1999a; Keep *et al.*, 1999b).

It is evident that there is little difference in the secondary structure of the protein over the pH range. The near UV spectra (Figure 3.6B) demonstrate that there is no major change in the near UV region and hence, no change in the overall conformation of the utrophin ABD over the range of pH tested.

	Helix	A	P	Turn	Other
pH 6	60%	5%	2%	17%	17%
pH 8	61%	5%	1%	16%	18%
pH 10	60%	4%	1%	17%	19%

Table 3.3: Predicted secondary structure elements of the utrophin ABD at varying pH. The proportion of each secondary structure element that contributes to the utrophin CD spectra as predicted using SELCON analysis (Sreerama and Woody, 1993). Secondary structural elements predicted consist of α-helix (helix), anti-parallel β-sheet (A), parallel β-sheet (P), turn and other.

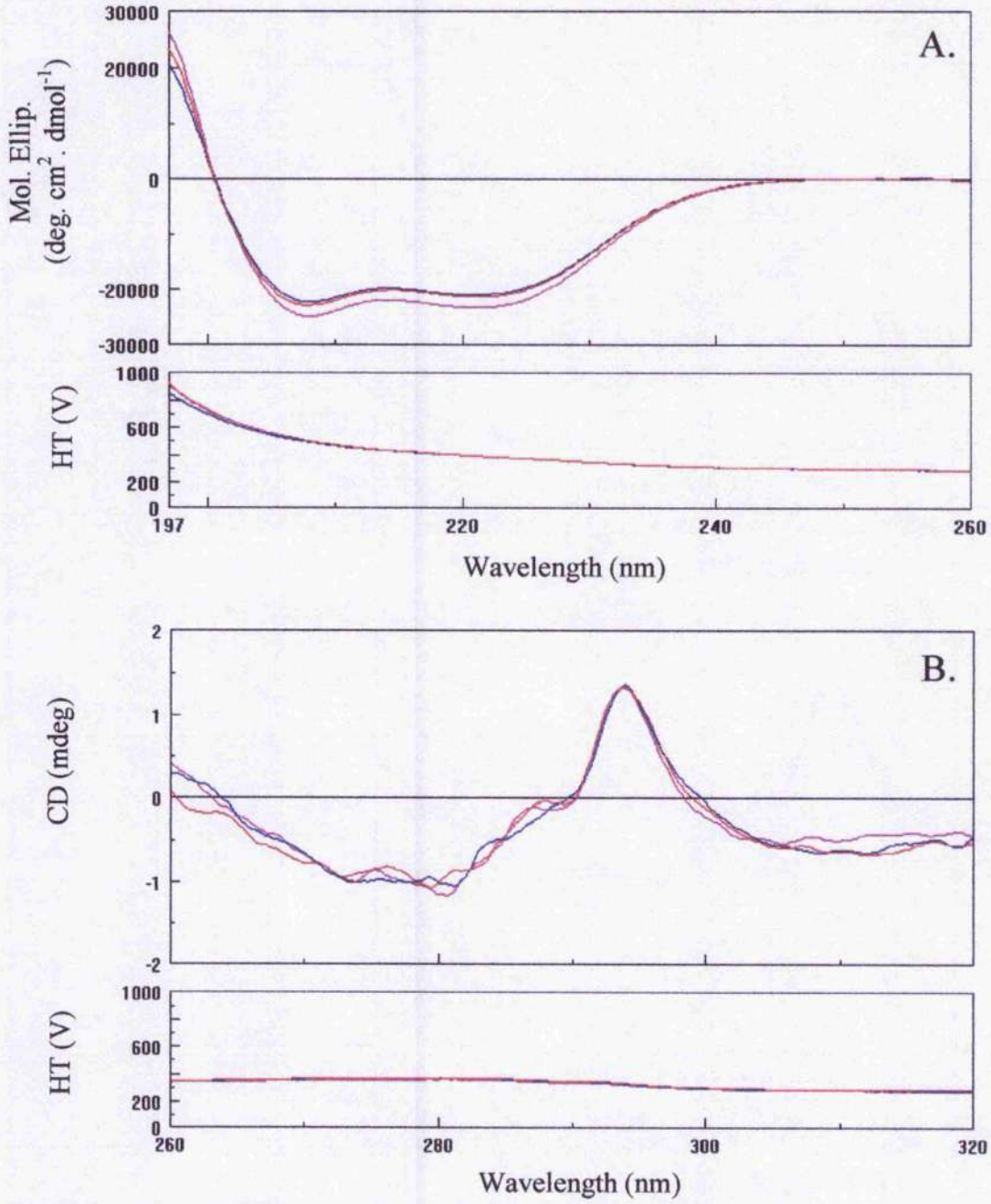

Figure 3.6: Near and far UV CD spectra of the utrophin ABD at varying pH. Samples of utrophin ABD (0.5 mg/ml) prepared in 10 mM phosphate buffer at pH 6, 8 and 10 were subjected to near and far UV CD analysis. Far UV CD spectra of utrophin ABD are presented in panel A whereas near UV CD spectra are displayed in panel B. Utrophin ABD samples at pH 6, 8 and 10 are represented in magenta, blue and red respectively. In panel A the data has been converted into mean residue molar ellipticity whereas panel B presents the near UV CD data in terms of the raw ellipticity of the data measured in millidegrees (mdeg).

3.2.4 *Investigation of utrophin ABD structure using tryptophan fluorescence.*

Proteins can be stimulated to produce an intrinsic fluorescence that may be of use when investigating conformational transitions, substrate binding or association and denaturation (Chen and Barkley, 1998). Within a polypeptide the aromatic amino acids tryptophan, phenylalanine and tyrosine are responsible for fluorescence however tryptophan is usually the dominant intrinsic fluorophore (Lakowicz, 1999). The utrophin ABD contains six tryptophan residues, three in each CH domain (Figure 3.7), that could be useful to investigate any structural changes or differences in conformation that might occur over a varied pH range.

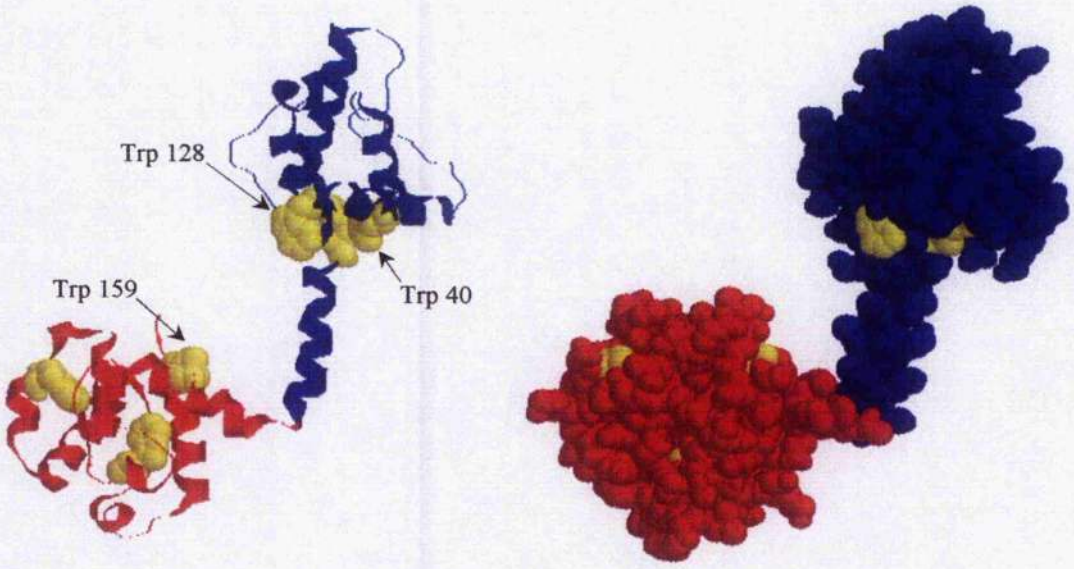

Figure 3.7: Location of tryptophan residues within the utrophin ABD. Ribbon and spacefill diagrams of the utrophin ABD highlighted to show the location of the six tryptophan residues (yellow) found within the utrophin ABD. The three tryptophan residues that may be affected by a conformational change are indicated. The first and second CH domains are shown in blue and red respectively.

In this instance, the presence of multiple fluorescent residues complicates the analysis of utrophin ABD tryptophan fluorescence; however, three of the six tryptophan residues 40, 128 and 159 may be useful. These three residues could be located at the potential interface between the two CH domains when the utrophin ABD is in solution. If the ABD adopts a closed conformation in solution, similar to the CH1/CH2 interface of opposing monomers in the crystal dimer (Keep *et al.*,

1999b), then inducing a change in protein conformation by varying the pH might alter the environment of these residues allowing detection of the conformational change via altered tryptophan fluorescence. Analysis of the tryptophan fluorescence would also complement the near UV data collected in the previous experiment.

To test this hypothesis 0.5 mg/ml samples of utrophin ABD at pH 6, 8 and 10 were excited at a wavelength of 296 nm and the resulting fluorescence recorded between 300 and 400 nm (Figure 3.8). From the data plot it is evident that there has been a reduction in the fluorescent intensity recorded at pH 10 when compared to that at pH 6 and 8. This reduction could be due, in part, to fluorescence quenching of one or more tryptophan residues upon increased exposure to the solvent (Lakowicz, 1999). However, if this were the case then a red shifting of the fluorescence peak would also occur (Vivian and Callis, 2001).

It is more likely that this sample is of slightly lower concentration than that of the pH 6 and 8 samples (as stated in 3.2.4) and this reduced concentration would serve to give a slightly lower fluorescence upon stimulation. The fluorescence of the utrophin ABD samples at pH 6 and 10 are maximal at approximately 339 nm whereas the peak at pH 8 corresponds to roughly 337 nm. The difference in the fluorescence maxima of these three samples is not particularly great and hence, there is very little difference in the tryptophan environments over the range of pH.

It is apparent that the tryptophan fluorescence of the utrophin ABD is invariant over the range of pH. The actin nucleation and severing protein gelsolin experiences a marked change in activity as pH is varied (Lagarrigue et al., 2003). Tryptophan fluorescence of gelsolin changes considerably over a much narrower pH range than used in this investigation. Hence, if utrophin was to exhibit a pH dependent conformational change an alteration in tryptophan fluorescence should be detectable. The lack of any variance of tryptophan fluorescence agrees with the near UV CD data which demonstrates no overall change in the tertiary structure of the protein (Figure 3.6).

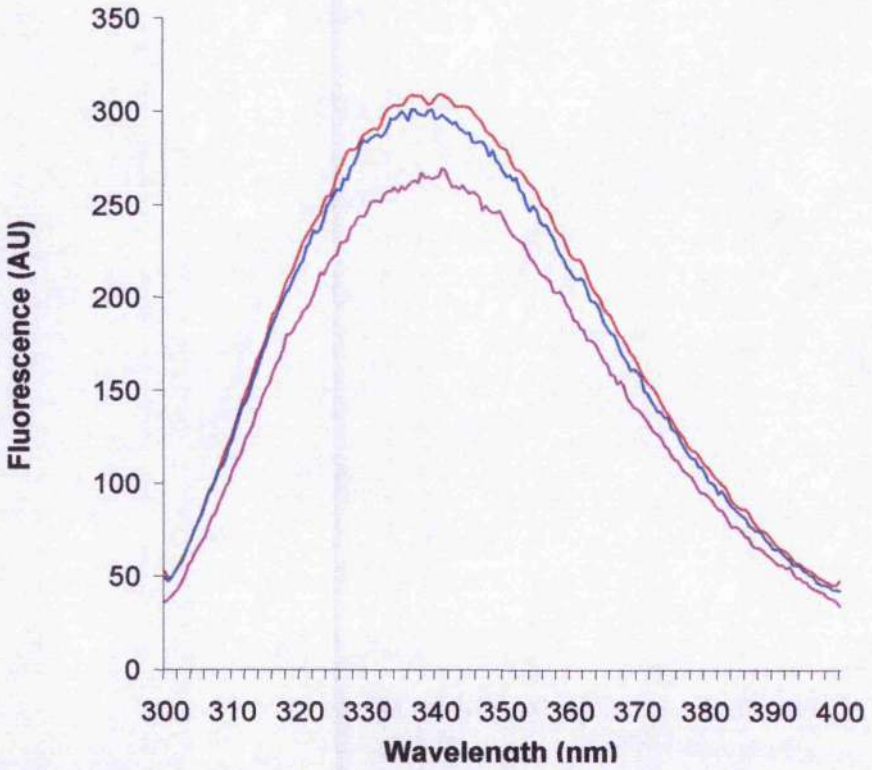

Figure 3.8: Tryptophan fluorescence of the utrophin ABD at varying pH. Samples of utrophin ABD (0.5 mg/ml) at pH 6 (red), 8 (blue) and 10 (magenta) were stimulated at 296 nm and the fluorescent emission between 300 and 400 nm recorded at a slow scanning rate. Excitation and emission slit widths were set at 1.5 nm and fluorescence is represented in arbitrary units (AU).

3.2.5 *Analytical ultracentrifugation analysis of the utrophin ABD at varying pH.*

The analysis of the secondary and tertiary structure of the utrophin ABD over a range of pH revealed little difference in the overall conformation of the protein although is apparent that the binding of the utrophin ABD to F-actin varies considerably over the range of experimental pH (section 3.2.3). This variability in binding may result from structural changes experienced by F-actin and not the utrophin ABD over the range of experimental pH. For completeness of the structural and conformational analysis of the utrophin ABD at pH 6, 8 and 10 analytical ultracentrifugation was performed. These analyses were performed with the help of Dr Olwyn Byron and her technician Gordon Campbell at the University of Glasgow. This technique provided a means of characterising the hydrodynamic and solution behaviour of the utrophin ABD when in solution.

3.2.5.1 *Sedimentation equilibrium analysis of the utrophin ABD at varying pH.*

Sedimentation equilibrium (SE) is particularly useful in determining molar mass and the study of self-association and heterogeneous interactions of proteins in solution. When multiple SE experiments are performed at varying speeds of centrifugation an accurate determination of monomer molecular weight can be determined along with the stoichiometry of any oligomeric state occurring through self-interaction. Utrophin ABD at pH 6, 8 and 10 was subjected to sedimentation equilibrium analysis at 20000, 25000 and 30000 rpm. The resultant whole-cell apparent molecular weight (MW, app; kDa) are shown in Figure 3.9 (data tables are shown in Appendix 4).

These data demonstrate how the apparent MW of the utrophin ABD varies when compared to the protein concentration of the sedimenting samples. When the utrophin ABD was sedimented at 25000 rpm the data suggest that the molecular weight of the protein changes quite considerably as the concentration of the sample increases. It is known that the utrophin ABD is monomeric when in solution and has a MW of approximately 30 kDa (Moores and Kendrick-Jones, 2000; Winder et al., 1995). The data at 25000 rpm suggest a stoichiometry that ranges from a dimer at pH 6 and 8 up to an octamer at two data points at pH 10. This is an unlikely stoichiometry however; the pH 10 data seems to suggest a self association of the utrophin ABD that is not apparent at pH 6 and 8. The 25000 and 30000 rpm experiments both suggest a higher molecular weight of utrophin at pH 10, a tetramer at 25000 rpm and a dimer at 30000 rpm. Overall, the mass of the utrophin ABD at pH 10 appears to be reducing as the centrifugal speed used in the experiment increases. The pH 6 and 8 data suggest that that the molecular mass of the utrophin ABD at 25000 rpm corresponds to a dimer whereas, at 25000 and 30000 rpm the molecular mass is representative of a monomer. This value, approximately 30 kDa is similar to the known MW of the utrophin ABD and the MW determined from gel filtration and gel electrophoresis (Appendix 2). The pH 10 data suggested a higher MW potentially resulting from oligomerisation, a second set of data at 25000 and 30000 rpm was collected using the same the utrophin ABD samples and experimental parameters.

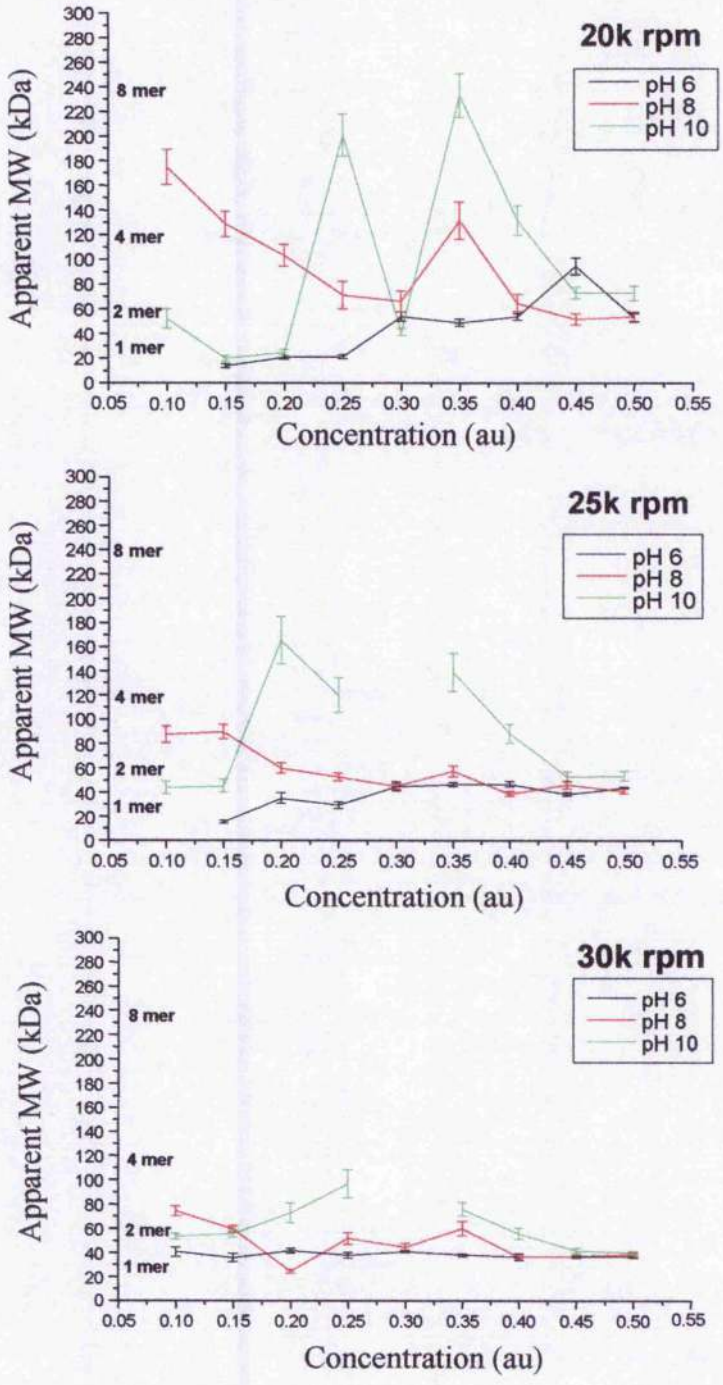

Figure 3.9: Apparent MW of the utrophin ABD versus protein concentration at varying pH. Sedimentation equilibration data of the utrophin ABD collected at pH 6, 8 and 10 and at sedimentation speeds of 20000, 25000 and 30000 rpm. Each experiment depicts the oligomeric state of the utrophin ABD at each pH and at each centrifugation speed. The discontinuity of the pH 10 data results from the failure of the pH 10 sample cell. The raw data for this figure can be found in Appendix 4. Protein concentration is represented by arbitrary units (au).

From these data (Figure 3.10, Appendix 5) it is evident that at pH 10, once again, the mass of utrophin appears to increase dramatically to almost 10 times the known value. The pH 6 and 8 samples do not exhibit a similar effect. At the higher protein concentration (above 0.4 au) the pH 10 samples behave as if they were monomeric and over lay closely with the pH 6 and 8 samples at both centrifugation speeds. Hence, these sedimentation equilibrium data generally indicate that the utrophin ABD is monomeric at pH 6 and 8 however at pH 10 the protein appears to self associate.

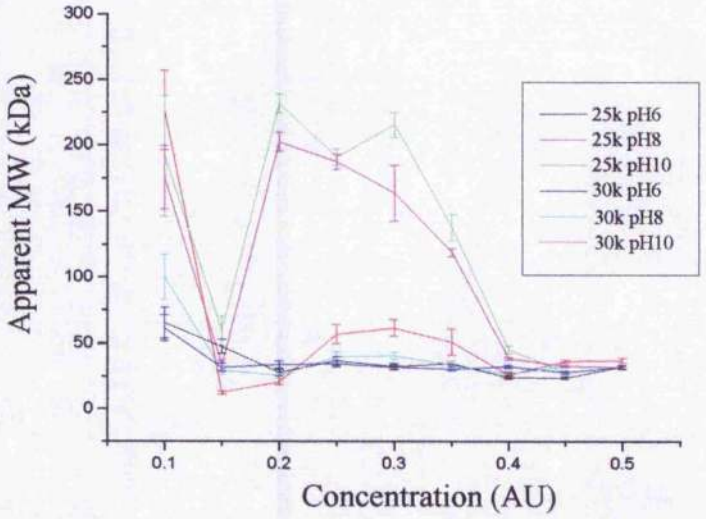

Figure 3.10: Apparent MW of the utrophin ABD versus protein concentration at varying pH (repeated experiment). Sedimentation equilibration experiments of the utrophin ABD were repeated at 25000 and 30000 rpm using samples at pH 6, 8 and 10. The data used to generate the figure can be found in Appendix 5.

3.2.5.2 Sedimentation velocity analysis of the utrophin ABD at varying pH.

The SE experiments determined that the utrophin ABD was monomeric at pH 6 and 8 although there did appear to be oligomerisation at pH 10. Sedimentation velocity (SV) experiments can be used to determine the sedimentation coefficient, S, which is extremely valuable in characterising changes in size or shape of a molecule over varying experimental conditions, in this instance, change in pH.

Before the SV experiment was performed hydrodynamic bead modelling was used to assess the potential difference in the hydrodynamic properties of the utrophin

ABD in 'open' and 'closed' conformations (Byron, 2000; Garcia De La Torre et al., 2000). The crystal structures of utrophin and fimbrin (Goldsmith *et al.*, 1997; Keep *et al.*, 1999b) were used to calculate the sedimentation coefficient and radius of gyration of the molecules in solution. The fimbrin structure was used to generate modelled data attributable to the 'closed' utrophin conformation whilst the utrophin crystal monomer was used to represent the 'open' conformation. The utrophin crystal dimer was also modelled for comparison.

The modelling determined that the extended and compact conformations could, in theory, be differentiated hydrodynamically. The closed conformation generated a radius of gyration of 19.6 Å and a sedimentation coefficient of 2.72 S. The extended conformation generated a radius of gyration of 26.6 Å and 2.33 S and the utrophin crystal dimer a radius of gyration of 27.6 Å and 3.74 S respectively.

The utrophin ABD was subjected to sedimentation velocity analysis at pH 6, 8 and 10. The SV data (Appendix 6) are presented in Figure 3.11 as plots of sedimentation coefficient distribution (c(s)) versus sedimentation coefficient corrected for temperature and buffer density (s20w). The data were analysed using direct boundary modelling with a distribution of Lamm equation solutions (Schuck, 2000).

At low protein concentration (approximately 0.5 mg/ml) the utrophin ABD does not appear to exhibit any detectable difference in sedimentation coefficient however, at higher concentrations it appears that the molecule does display a slight difference over the range of pH. The sedimentation coefficients calculated at the highest utrophin ABD concentrations were determined as 2.55 S, 2.48 S and 2.47 S corresponding to pH 6, 8 and 10 respectively. This difference is small however, it suggests that at pH 6 the domain behaves as if it were more compact than at pH 8 and the pH 10 data suggests that the domain is more open. The modelled hydrodynamic properties of the compact and open conformations of utrophin ABD demonstrate that a difference in conformation could be detected in solution however it is evident, from the SV analysis, that pH only affects the hydrodynamic properties of the utrophin ABD to a small degree.

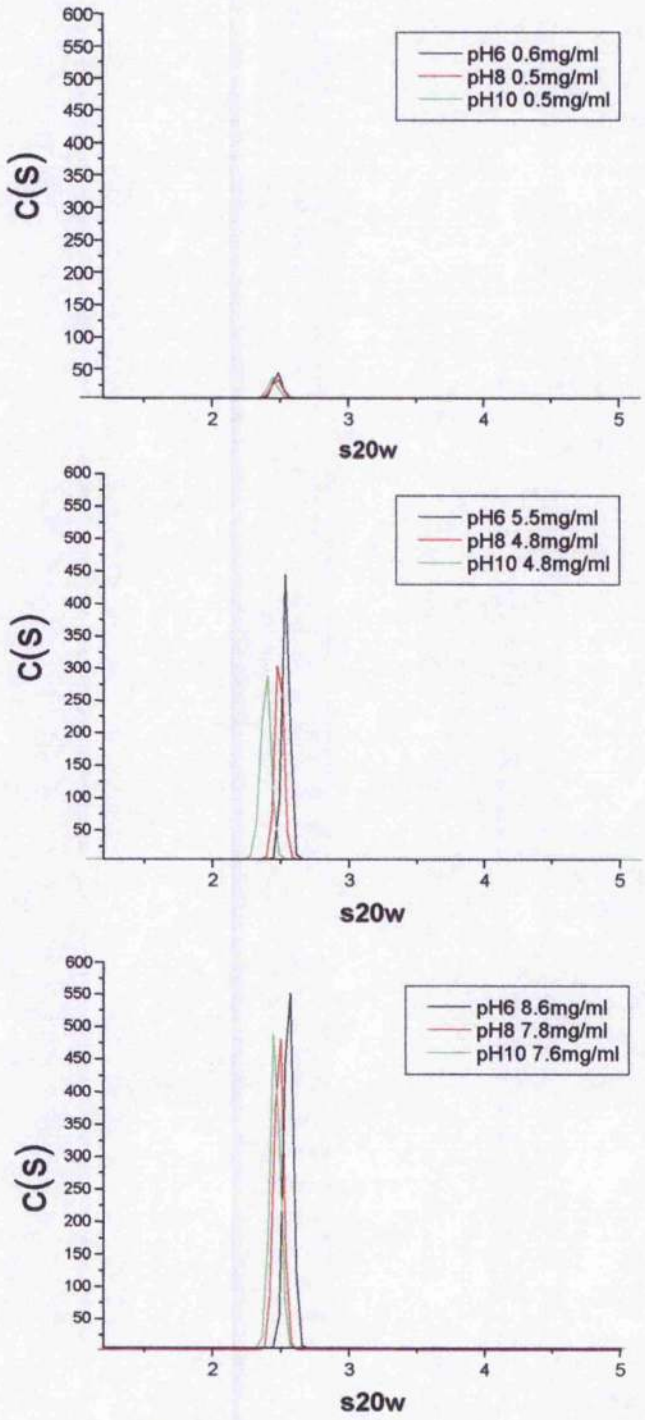

Figure 3.11: Sedimentation coefficient distribution plots of the utrophin ABD at approximately similar concentration, varying pH. Sedimentation coefficient distribution (c(s)) plots of the utrophin ABD at each pH and approximately similar concentration after deconvolution of diffusion effects based on direct boundary modelling with a distribution of Lamm equation solutions. The sedimentation coefficients calculated have been corrected for temperature and buffer density (s20w).

3.2.6 *Resistance of the utrophin ABD to proteolytic degradation at varying pH by papain and proteinase K.*

The sedimentation velocity data suggest that there is only a slight pH dependant change in the overall shape of the molecule when in solution (section 3.2.5.2). From these data it is possible that the varied pH is responsible for the change in the hydrodynamic properties of the protein and hence a slight change in the tertiary structure of the protein. The utrophin ABD is monomeric in solution, potentially adopting a compact globular structure; however, models exist where the utrophin ABD binds F-actin in an open conformation. If the degree of compactness is affected across the range of experimental pH then it is possible that the protein may display an altered susceptibility to proteolytic degradation. Therefore, it is possible that at higher pH, when the protein was predicted to be more 'open', a protease may be able to degrade the utrophin ABD to a greater extent than at lower pH when a more compact conformation might be adopted.

Papain and proteinase K are two proteases that display activity over a wide range of pH. Any difference in the overall structure of the utrophin ABD resulting from a pH induced conformational change may be detectable by a change in the pattern of peptide fragments produced by digestion with these two proteases at different pH.

Papain and proteinase K were found to readily digest utrophin ABD at pH 8. Utrophin ABD was subjected to digestion by papain and proteinase K for 5, 10, 20, 40 and 60 minutes at pH 6 and 10 (Section 2.2.22.2). A 1 mg/ml solution of BSA was also digested by each enzyme at both pH values to help assess the activity of both enzymes over the range of pH used in the experiment. All samples were subjected to gel electrophoresis and non-digested utrophin and BSA samples were run as a comparison (Figure 3.12).

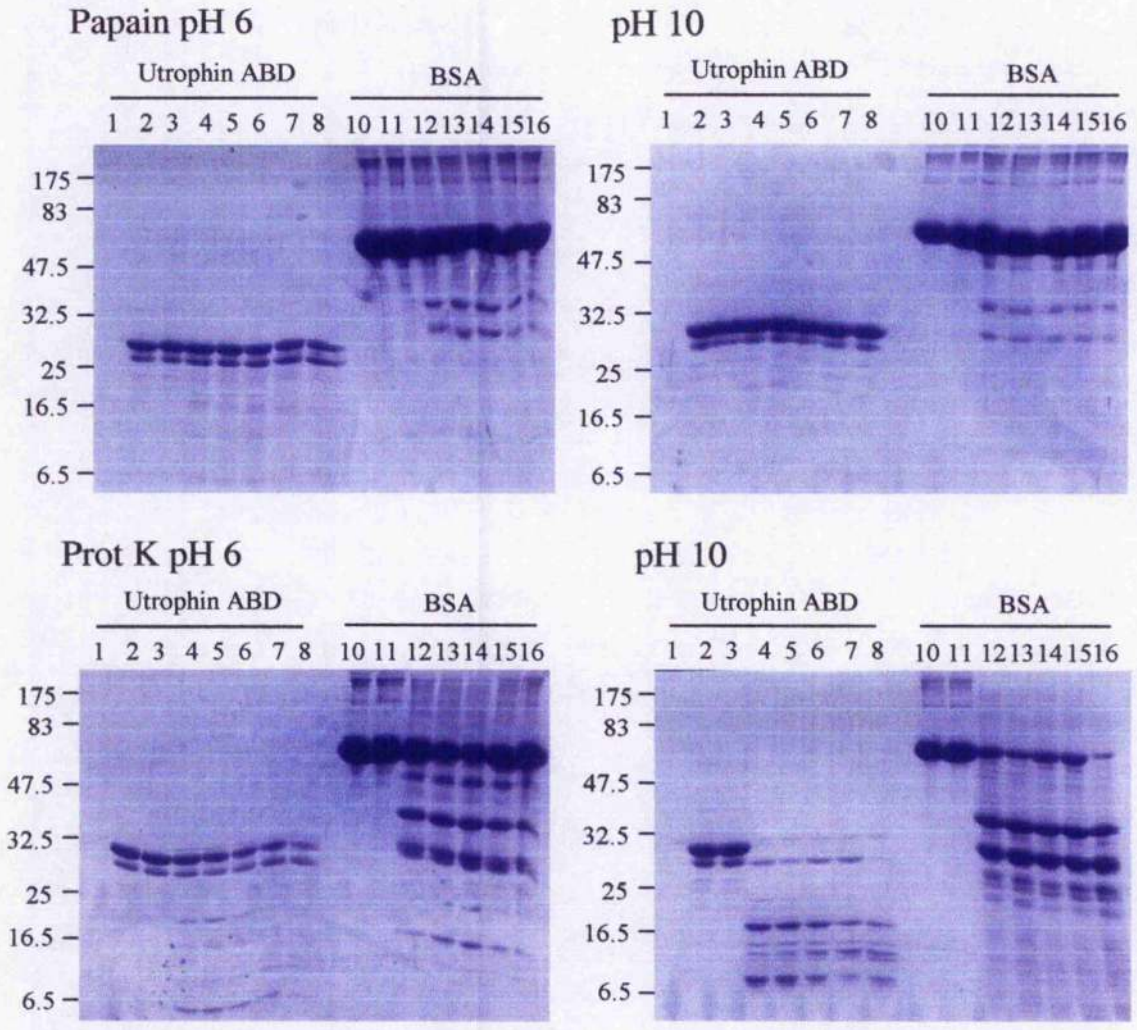

Figure 3.12: Resistance of the utrophin ABD to proteolytic degradation at varying pH. 25 μM samples of the utrophin ABD were subjected to proteolytic degradation by papain and proteinase K at pH 6 and 10. Lane 1 of each gel corresponds to a sample of protease alone. Lane 2 and 3 represent the utrophin ABD alone before and after 60 minutes of incubation at room temperature. Lanes 4 to 8 represent utrophin degradation at 5, 10, 20, 40 and 60 minutes after addition of protease and incubation at room temperature. A 1 mg/ml sample of BSA was also subjected to degradation. Lanes 10 and 11 represent BSA alone before and after 60 minutes of incubation and lanes 12 to 16 show degradation at 5, 10, 20, 40 and 60 minutes after addition of protease. Digestion was performed in 100 mM NaCl, 1 mM EDTA, 1 mM DTT and 20 mM Tris pH 10 or MES pH 6 and papain or proteinase K were present at final working concentrations of 0.01 mg/ml and 0.001 mg/ml respectively. Molecular weight markers are shown to the left of each gel (kDa).

Figure 3.12 demonstrates the degradation of utrophin ABD by papain and protease K. It is apparent that digestion by papain does not seem to have progressed

to a great extent; however, the degradation of utrophin ABD at pH 6 by this enzyme seems to have generated a number of peptide fragments that are not visible in the undigested sample of utrophin ABD. Much of the full length utrophin ABD remains un-degraded by the end of the time course. The BSA control also shows little degradation at pH 6. When the digestion was performed at pH 10 there appeared to be less degradation of utrophin ABD and the pattern of products formed was different to that of pH 6. The BSA control also showed little degradation; however, a similar pattern of fragments was generated compared to those formed at pH 6 and the degradation resulted in fewer peptide fragments.

The digestion of the utrophin ABD with proteinase K was much more successful. At pH 6 much of the full-length the utrophin ABD remains after 60 minutes but a number of fragments have been produced. The degradation that occurred at pH 10 was much more substantial. Almost all full-length utrophin ABD was degraded after 5 minutes; the band that remains at approximately 30 kDa corresponds to proteinase K. The fragments are similar to the fragments produced by digestion at pH 6 however they are produced in much greater quantities. It is clear form these digestions that the activity of the enzyme has, once again, varied considerably. Comparison of the BSA degradation mirrors this, demonstrating that almost all BSA is degraded over the course of the 60 minute assay.

Both proteinase K and papain clearly degrade the utrophin ABD at pH 6 and 10; however they do so with a large variability in their activities. Even though both enzymes are stable over a broad pH range the large difference in their activities would make comparison of utrophin degradation between papain and proteinase K experiments difficult. The experiment aimed to identify any potential differences in the extent of cleavage and the cleavage products formed by digestion of the utrophin ABD by these two proteases at varied pH. From these data it is evident that these two enzymes are not suitable to compare the resistance of the utrophin ABD to proteolytic degradation at pH 6 and 10.

The utrophin ABD has been modelled to bind to F-actin in a variety of different conformations (Galkin et al., 2002; Moores et al., 2000). If different modes of interaction can be induced by varying the pH then it is possible that the difference in association of the utrophin ABD with F-actin could protect actin from proteolytic

degradation to differing extents. Before this hypothesis could be tested a preliminary experiment was performed to assess the resistance of F-actin to proteolytic degradation when the utrophin ABD was bound. Papain was chosen to perform the digestion as the number of peptide fragments generated by digestion with this enzyme were less than those produced by proteinase K however, the protease concentration was increased to 0.01 mg/ml to increase the extent of degradation. The preliminary experiment involved the digestion of a 25 μM sample of utrophin ABD in the presence of 10 μM F-actin and 0.01 mg/ml of papain prepared in TED pH 8 and 1 x ABB (section 2.2.22.3). All samples were subjected to proteolytic degradation and SDS-PAGE analysis so that the extent of protein degradation could be assessed (Figure 3.13).

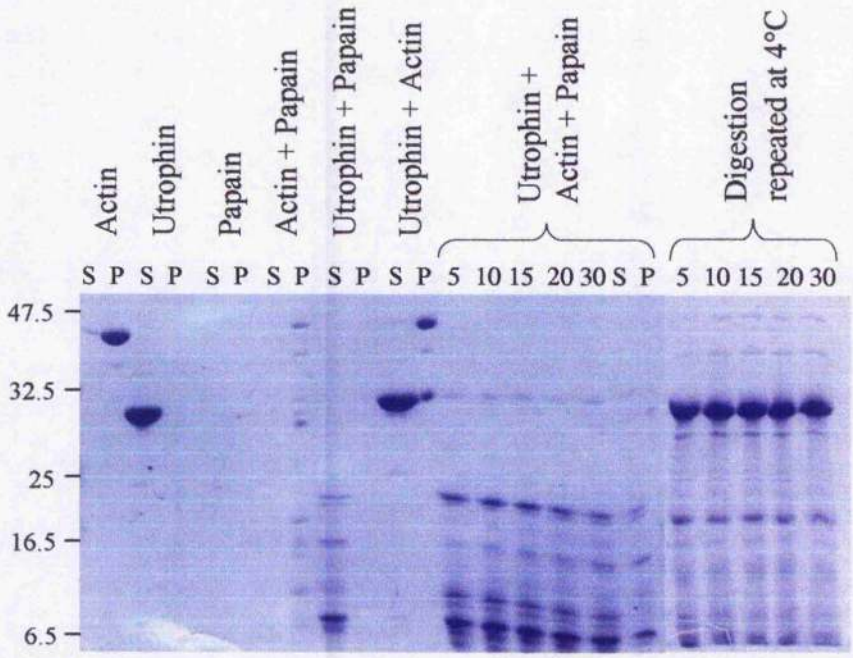

Figure 3.13: Protection of F-actin from proteolysis by binding of the utrophin ABD. Samples of the utrophin ABD (25 μM) and F-actin (10 μM) at pH 8 were subjected to proteolysis by papain (0.01 mg/ml) at room temperature. These samples are compared to undigested protein samples. In all cases, samples were subjected to high-speed sedimentation to separate soluble and insoluble protein fractions. F-actin degradation in the presence of the utrophin ABD was followed for 30 minutes. Samples were removed at 5, 10, 15, 20 and 30 minute time intervals. The remaining sample was then centrifuged at high speed to pellet any remaining insoluble protein. The limited proteolysis of F-actin in the presence of the utrophin ABD was repeated at 4°C. Samples were removed from the proteolytic reaction at equivalent time points as those taken at room temperature.

Figure 3.13 demonstrates the size of the utrophin ABD, F-actin, papain and the combinations of these species before and after proteolytic degradation. The utrophin ABD is soluble and remains in the supernatant fraction whilst F-actin is readily pelleted. Combination of these two proteins clearly shows the utrophin ABD associating with F-actin in the pellet fraction. Addition of protease to utrophin ABD and F-actin alone produces complete digestion of full-length utrophin; however, F-actin is not completely degraded but the fragments that are generated still localise to the pellet fraction. The F-actin/utrophin sample shows complete degradation of full-length F-actin after only 5 minutes and almost complete degradation of the utrophin ABD. This indicates that the activity of the enzyme is too high and/or that binding of the utrophin ABD to F-actin is affording little protection from proteolysis. A small amount of full-length utrophin ABD seems to perpetuate throughout the time course.

These data combined with the varied enzyme activity at different pH make any differences in digestion difficult to interpret. It is evident that F-actin was not protected from proteolysis by the binding of the utrophin ABD and hence, the experiment was not developed further.

3.3 *Discussion*

Based upon preliminary data and the proposed models of the utrophin ABD interacting with F-actin, we have investigated the structural and conformational effects that varied solution pH has on the utrophin ABD structure. To achieve this, the utrophin ABD at pH 6, 8 and 10 was subjected to a number of biochemical and biophysical analyses.

Preliminary gel filtration data suggested that the apparent size of the utrophin ABD may be induced to change by varying the solution pH. This apparent pH dependant change in molecular weight suggested that the conformation of the utrophin ABD was changing from a more 'compact' configuration at lower pH to a more 'open' configuration at higher pH. It has been assumed that the utrophin ABD adopts a closed and compact state when in solution. It was possible that the interactions between the two CH domains of the utrophin ABD when in the monomeric solution state were disrupted at higher pH allowing separation of the CH

domains. Analytical gel filtration analysis determined that there was no difference in the MW of the utrophin ABD over the range of pH used (section 3.2.1) although, the calculated MW (29.8 kDa) matched closely with previously determined values of the utrophin ABD MW (Winder and Kendrick-Jones, 1995a). It was evident that the original pH dependant size shift determined for the utrophin ABD was a result of a difference in the gel bed volume of the gel filtration column. Calibration of the column at each pH resulted in a loss of the apparent pH induced size shift originally determined for the protein.

Although there was no detectable change in the MW of utrophin using gel filtration, the surface charge, and hence, the degree of association of the two CH domains could still be altered as the extent of protonation varies depending on pH. This led on to the investigation of the utrophin ABD binding to F-actin at varied pH. If the electrostatic association between the CH domains could be disrupted or the overall structure of the domain altered in any way then binding to F-actin in an 'open' conformation may become more favourable and conversely, if the CH domain association was increased, then binding in a more 'closed' conformation may also occur. The binding affinity and stoichiometry of binding of the utrophin ABD to F-actin was determined at pH 6, 8 and 10 (section 3.2.3). From these data it was apparent that at a reduced pH the affinity of the utrophin ABD for F-actin was increased to 10.6 μM compared to 25.7 μM at pH 8. The stoichiometry of the interaction also changed significantly from 1:1 to 0.6:1, suggesting binding of one molecule of utrophin molecule to two molecules of actin or a possible half-binding interaction (Galkin et al., 2002). The pH 10 data were not sufficiently reliable to rationally explain, the binding affinity was unreliable due to the large degree of associated error whilst the binding stoichiometry suggests that one molecule of utrophin ABD was associating with six molecules of actin. Full length utrophin has been shown to bind laterally to F-actin with a stoichiometry of 1:14 but this interaction requires association of the ABD and a number of the spectrin repeats that form the rod domain of the complete molecule (Rybakova et al., 2002). Reduction of the number of spectrin repeats following the utrophin ABD appears to reduce the binding stoichiometry (Zuellig et al., 2000) to a value intermediate to that of full length utrophin and the ABD alone. These studies indicate that the binding

stoichiometry of 1:6 determined at pH 10 would not be possible for the isolated utrophin ABD.

During determination of the binding data it was noticed that the proportion of F-actin that pelleted during the co-sedimentation assay was not consistent at pH 10. It appeared that the proportion of F-actin compared to G-actin was greatly reduced at pH 10 when compared to pH 6 and 8. A destabilisation of F-actin at pH 10 would help explain the error associated with the pH 10 binding data which would contribute to the determined stoichiometry. Indeed, this was found to be the problem. The structure and stability of F-actin is affected significantly by the pH of the surrounding solution. Polymerisation of G-actin to form F-actin, requires nucleation and then elongation of the actin filaments, a process referred to as the nucleation-elongation reaction (Oosawa and Kasai, 1962). The polymerisation of actin is influenced strongly by pH. At lower pH, proton binding increases and induces a conformational change causing a large increase in the stability of actin dimers (Zimmerle and Frieden, 1988). This increased stability, in turn, generates a faster rate of polymerisation (Zimmerle and Frieden, 1988). It has also been found that the critical concentration required for filament formation also increases significantly at higher pH (Zimmerle and Frieden, 1988). From these studies it is evident that the stability of F-actin at pH 10 would be significantly lower that at pH 6 and hence, any data collected at the elevated pH could be unreliable. Indeed, comparison of the pH 6 and 10 data would also be difficult as the structure of the actin filament is also affected by varying pH. Oda, et al., 2001 demonstrated that the helical pitch of F-actin is slightly larger at lower pH (Oda et al., 2001). This would potentially affect the utrophin ABD/F-actin binding interaction producing another variable that would need to be taken into account when interpreting the data.

From these data it is evident that the analysis of the utrophin ABD binding to F-actin at pH 6 and 10 would be very difficult and would require the structural effects experienced by F-actin to be taken into consideration. However, the utrophin ABD does bind F-actin with a higher affinity at pH 6 than at pH 8 and a stoichiometry that suggests half binding. It is unlikely that the utrophin ABD has a bundling ability, an effect that could explain the 1:2 stoichiometry, as this would require binding of CH1 and 2 to adjacent actin filaments. In light of current

knowledge this is not possible as the utrophin ABD CH domains are not equivalent with regard their actin-binding ability (Gimona and Winder, 1998). Separation of the two CH domains has shown that only CH1 can bind F-actin, although this association is greatly reduced and hence, the utrophin ABD would be required to dimerise so that actin filaments could be cross-linked. It is clear from the gel filtration data (section 3.2.2) and analytical ultracentrifugation data (section 3.2.6.1) that the utrophin ABD is monomeric at pH 6 indicating that the 1:2 stoichiometry at this pH can not be explained via utrophin dimerisation. However, it should be noted that the CH2 does play a significant role in the actin-binding interaction of the utrophin ABD. The binding affinity of CH1 alone is much reduced when compared to that of the complete ABD although CH2 does have an important role to play in the interaction of the complete domain with F-actin. Solutions of separated CH1 and CH2 domains found that only CH1 associated with F-actin (Winder et al., 1995). In this instance the connection of the two CH domains by the utrophin helical linker is required to aid in the association of CH2 with F-actin and the realisation of the ABD full binding potential.

It is possible however, that the utrophin ABD at pH 6 is binding to F-actin in a half decorated manner, a model proposed by Galkin et al., 2002. This model describes utrophin interacting with F-actin in an extended conformation where one molecule of utrophin binds two molecules of actin in the filament. A number of proteins that bind F-actin exhibit a conformational change or an alteration in their activity in a pH dependent manner. For example, members of the actin depolymerising factor (ADF)/ cofilin family bind F-actin at low pH but to G-actin at higher pH values (Blondin et al., 2002) whereas low values of pH activate the actin nucleation and severing protein gelsolin (Lagarrigue et al., 2003). In these two instances the change in activity of the proteins in question stems from either a conformational change in F-actin or within the binding protein itself. However, it is clear that the binding of the utrophin ABD to F-actin over the experimental range of pH is more dependent on the conformation and structure of F-actin rather than a detectable structural or conformational change induced in the utrophin ABD. The proposed half binding of the utrophin ABD at lower pH may be caused by the

increased filament pitch of F-actin at lower pH and may result in the determined stoichiometry and increased affinity.

It has proven complicated to differentiate any pH dependant structural or conformational changes in the utrophin ABD when interacting with F-actin. Altering the concentration of hydrogen ions in solution would affect amino acid protonation and hence, there may still be a detectable structural or conformational alteration. The actin-binding protein hisactophilin from *Dictyostelium discoideum* demonstrates a pH dependent actin-binding seemingly based around the p*K*a of histidine - an amino acid found in abundance within the protein (Scheel et al., 1989; Stoeckelhuber et al., 1996); however, the utrophin ABD only contains nine histidine residues (compared to 31 for hisactophilin) so it would be unlikely that a gross conformational change could be induced by so few residues. To continue the structural and conformational analysis of the utrophin ABD, circular dichroism was used to investigate the secondary and tertiary structure of the protein. The far UV spectra of the utrophin ABD at pH 6, 8 and 10 (Figure 3.6) showed little difference in the secondary structures of the utrophin ABD over the range of pH. SELCON analysis determined that the utrophin ABD was approximately 60 % α-helix at all pH values whereas the content of the other secondary structure elements varied little over the range of pH although there appeared to be a slight increase in the proportion of anti-parallel and parallel β-sheet as pH decreased from 10 to 6. It is odd that the secondary structure prediction suggests the presence of β-sheet as the utrophin ABD has been shown to contain no such structures and is comprised primarily of α-helix (Keep *et al.*, 1999b). The near and far UV analysis of the utrophin ABD structure at each pH demonstrated that there was no change in the structure of the protein. The activation of gelsolin at low pH is generated by the movement of a number of protein domains; this activation occurs over a narrower range of pH than used here but it is evident that varied pH does not alter the structure of the utrophin ABD.

The tryptophan fluorescence of the utrophin ABD at pH 6, 8 and 10 was measured to detect any alteration in the environment of the tryptophan residues present within the protein. This analysis would be purely qualitative, as utrophin contains six tryptophan residues and distinguishing between the contribution of each to the overall fluorescence would be impossible. However, if one or more of the

tryptophans became more or less solvent exposed due to a conformational change in the utrophin ABD a shift in the fluorescent maxima would be observed (Lakowicz, 1999; Vivian and Callis, 2001). The structural change exhibited by gelsolin resulted in increased tryptophan fluorescence and a red shifting of the fluorescence maxima as pH was elevated (Lagarrigue et al., 2003); no such increase or shifting of the utrophin ABD fluorescence intensities was observed. From these analyses it is clear that the tryptophan environments are not altered across the range of pH and hence, the conformation of the utrophin ABD does not appear to alter as pH is varied.

The utrophin ABD has been modelled to bind to actin in both open and closed conformations and much controversy exists over the exact manner of association (Lehman et al., 2004). Binding of the utrophin ABD to F-actin in an extended manner would require the opening of the molecule, from the proposed closed solution state, to an extended conformation (Galkin et al., 2002; Moores et al., 2000). Hydrodynamic bead modelling was used to determine if there could be a detectable difference in the hydrodynamic properties of the utrophin ABD if a more open or closed conformation was occurring in solution. The crystal structure of fimbrin was used to represent the closed solution conformation (Goldsmith et al., 1997) whilst the utrophin crystal structure was used to represent the open conformation (Keep *et al.*, 1999b). The modelling demonstrated that the radius of gyration and sedimentation coefficient of the two conformations were quite different and could be detected by sedimentation velocity analysis. Sedimentation equilibrium analysis of the utrophin ABD demonstrated variability in the apparent oligomeric state of the domain in solution. Generally, at pH 6 and 8, the protein was a monomer however at pH 10 the data were confusing suggesting a variety of oligomeric states. This does not fit with the known utrophin ABD biochemistry as the protein has been found to be monomeric when in solution (Moores and Kendrick-Jones, 2000; Winder et al., 1995). The highly homologous domain from dystrophin has been shown to dimerise (Norwood et al., 2000) but other studies dispute this (Chan and Kunkel, 1997) however, no larger oligomers have been reported. The fact that no utrophin dimerisation was occurring at pH 6 suggests that the F-actin binding stoichiometry determined in section 3.2.3 was not a result of the utrophin ABD self associating. The sedimentation velocity data (section 3.2.6.2) demonstrated that the utrophin

ABD was experiencing a slight pH dependent variation in sedimentation coefficient. This variation could be consistent with the modelling of the open and closed states of the utrophin ABD. At pH 6 the sedimentation coefficient was slightly higher than at pH 10 suggesting a more compact globular conformation potentially attributable to an increased interaction between the two CH domains. The slightly lower sedimentation coefficient at pH 10 could therefore represent a slightly extended conformation where the CH domain association has been reduced. A pH induced increase in hydrodynamic size has been reported for gelsolin however, the 'opening up' of gelsolin was caused by a decreased pH (Lamb et al., 1993), an opposite effect to that exhibited by the utrophin ABD. From these data it is apparent that utrophin might exhibit a slight pH dependent change in conformation although a disassociation of the CH domains would be expected to generate a larger difference in sedimentation coefficient. For example binding of ATP to the alpha subunit of the *E. coli* F_1 ATPase causes a conformational change that increases the sedimentation coefficient from 3.52 to 4.00 (Dunn, 1980); this is quite a large difference when compared to the pH induced change in the utrophin ABD.

The slight difference in conformation determined via ultracentrifugation might also be detectable by a differing resistance to proteolytic degradation. A preliminary experiment was performed to assess the resistance of the utrophin ABD to degradation by two proteases that were stable over a broad range of pH. These two enzymes, papain and proteinase K are stable over a pH range of 4 – 10 and 4 – 12.5 respectively (Zucker et al., 1985) and therefore, would be ideally suited to bring about proteolysis over the experimental range of pH. Utrophin ABD and BSA were subjected to degradation by both enzyme but, unfortunately, the optimum activity of both enzymes was not maintained over their complete pH stable range. Proteinase K was found to be much more active at higher pH, whereas, papain was much more active at lower pH. The peptide fragments produced by both enzymes also varied with pH and hence, comparison between high and low pH would be difficult and complicated. As a result of these findings the experiment was not carried further. Interestingly, the sedimentation velocity data suggest a more compact conformation of the utrophin ABD at pH 6, which is opposite to the actin-binding data, which suggests greater affinity for F-actin at lower pH and a more 'open' conformation of

binding. The actin-binding data is heavily influenced by the structure of F-actin at each pH but the sedimentation velocity data suggested a potential change in the conformation of the utrophin ABD when in solution. It was therefore possible that pH induced changes in actin-binding were a combination of pH effects on both the utrophin ABD and F-actin. Altering pH has many effects on actin and the proteins that bind to it. For example, low pH allows ADF/cofilin and talin to bind F-actin and gelsolin to be activated whereas higher pH allows binding of ADF/cofilin to G-actin (Blondin et al., 2002; Hawkins et al., 1993; Lagarrigue et al., 2003; Schmidt et al., 1993). If the binding conformation of the utrophin ABD to F-actin at each pH differed, then it was possible that a slightly different binding surface would be bound on actin at each pH. The differences in binding surface may protect F-actin from proteolytic degradation to differing extents at each pH. A preliminary investigation of the resistance of F-actin with bound utrophin at pH 8 found that there was little protection from degradation by papain even when the experiment was repeated at lower temperature.

Previous studies have utilised limited proteolysis of utrophin ABD and F-actin to probe the interaction of these two species (Moores and Kendrick-Jones, 2000; Winder et al., 1995). In these instances chymotrypsin and trypsin were used; however, both of these enzymes display a more restricted and distinct range of pH activity than both papain and proteinase K and hence, would be unsuitable in this experiment. From this preliminary work it was evident that neither papain or proteinase K were suitable for the investigation of pH dependent differences in degradation of utrophin bound to F-actin at varying pH and hence, the experiment was not developed further.

In summary, the data presented here suggest that the actin-binding domain of human utrophin can not be induced to undergo a pH dependent induced change in conformation. It is apparent that the original hypothesis predicting a pH induced conformational change of the domain was flawed. Even though the sedimentation velocity data do suggest a slight pH dependent conformational change the near UV and fluorescence data suggest no change in the structure of the protein. From these data it is clear that the utrophin ABD conformation is independent of pH and that the

proposed conformational change observed upon binding to F-actin cannot be induced in solution by altering the electrostatic environment of the protein.

Chapter 4:

Utrophin ABD Linker Mutants

Chapter 4

Utrophin ABD Linker Mutants

4.1 *Introduction*

Studies investigating the interaction of the utrophin ABD and F-actin have identified a number of possible modes of interaction ranging from a 'closed' compact conformation to an 'open' extended conformation (Galkin et al., 2003; Galkin et al., 2002; Moores et al., 2000; Sutherland-Smith et al., 2003). The interaction of utrophin with F-actin in these various ways requires the protein to possess a certain degree of structural flexibility. Indeed, orienting the utrophin ABD crystal structure into the cryo-EM electron densities generated by utrophin ABD bound to F-actin required an induced fitting of the protein (Moores et al., 2000). The utrophin ABD has been shown to be monomeric when in solution, presumably adopting a compact globular conformation (Winder et al., 1995). This conformation contrasts with the extended arrangement exhibited by the utrophin ABD crystal structure which was found to be open and extended (Keep *et al.*, 1999b). The dimeric organisation of this crystal structure contrasts with that of the fimbrin ABD structure which was shown to be a compact monomer (Goldsmith et al., 1997). The two CH domains in the fimbrin crystal fold back on themselves to generate a similar inter-CH domain interface that is seen in the anti-parallel CH domain interface of the utrophin ABD crystal structure, a phenomenon described as three dimensional domain swapping (section 3.1). This phenomenon describes the structures that link swapped domains to be of particularly importance in facilitating this kind of dimer formation (Schlunegger et al., 1997). The formation of the utrophin ABD solution monomer requires the linker region separating the two CH domains to be sufficiently long to allow the linker to fold back on itself (Keep *et al.*, 1999b). Sequence alignment has shown that the fimbrin ABD linker region is longer than that of the utrophin ABD ((Goldsmith et al., 1997); section 4.2.1) and that this extra length may allow greater flexibility assisting in the crystallisation of the fimbrin ABD as a monomer and the association of the molecule with F-actin in a closed and compact conformation (Hanein et al., 1998).

The ABD of the actin cross-linking protein α-actinin has also been modelled when bound to F-actin. These models have demonstrated either an open, bi-lobed manner of interaction or a compact globular interaction as seen with the fimbrin ABD (McGough et al., 1994; Tang et al., 2001; Taylor and Taylor, 1993). The linker residues that separate the CH domains in this protein are fewer in number than in the utrophin ABD (section 4.2.6) and may influence the way in which the α-actinin ABD crystallises and interacts with F-actin.

It is possible that the number of residues that separate CH domains may be of particular importance in determining the manner of interaction of an actin-binding protein with F-actin. A larger number of residues would render the linker more flexible and may favour adoption of a compact ABD conformation upon interaction with F-actin. Conversely, shortening of the linker may increase rigidity, lessening interaction of the CH domains and favouring a more open conformation when interacting with F-actin. In order to test these hypotheses two linker mutants of the utrophin ABD were generated. The first involved extension of the utrophin inter-CH domain linker to model the longer linker seen in the fimbrin ABD and the second involved shortening of the utrophin ABD linker to model the reduced length of the α-actinin linker region.

4.2 ***Results***

4.2.1.1 Design of the utrophin ABD fimbrin linker mutant

Alignment of the utrophin and fimbrin ABD amino acid sequences revealed a stretch of sequence separating the two CH domains that was present in fimbrin but not utrophin ABD (Figure 4.1). The extra residues present in the fimbrin sequence corresponded to 11 amino acids and it was these amino acids that were chosen to be inserted into the utrophin ABD linker region. Primers were designed using the utrophin and fimbrin sequences and overlap extension PCR was used to introduce the 11 amino acids into the utrophin ABD sequence. This construct was then inserted into the pSJW1 expression vector (section 2.2.10). The presence of the correct

mutation was confirmed via sequencing before expression of the mutant construct was attempted.

```
Utr 134 WQVKDVMKD----------VMSDLQQTNSEKILLSW 159
Fim 140 FADIELSRNEALAALLRDGETLEELMKLSPEELLLRW 136
          :   :: :             .:.:* : ..*::** *
Mut 134 WQVKDVMKDEALAALLRDGEVMSDLQQTNSEKILLSW 159
```

Figure 4.1: Sequence alignments of the utrophin and fimbrin actin-binding domain linker regions. Clustal W alignment of utrophin (Utr) and fimbrin (Fim) ABD linker regions demonstrating the stretch of extra linker residues found in the fimbrin ABD that are not seen in the utrophin ABD. The 11 extra residues that were inserted into the utrophin ABD linker to form $UTR^{fimbrin}$ (Mut) are highlighted in red. The consensus symbols and residue colours are defined as follows: "*", ":" and "." represent identical residues, conserved substitutions and semi-conserved substitutions respectively whilst red, blue, magenta and green represent small/hydrophobic, acidic, basic and hydroxyl/amine/basic residues respectively.

4.2.1.2 Expression and purification of $UTR^{fimbrin}$.

pSJW1 vector containing the mutated utrophin ABD was transformed into competent *E. coli* strain BL21 (DE3); expression of the mutant protein was performed as described previously (Winder et al., 1995; section 2.2.10). The fimbrin linker mutant ($UTR^{fimbrin}$) seemed to express well showing a large induction after addition of IPTG (Figure 4.2) however, separation of the insoluble and soluble protein fractions revealed that $UTR^{fimbrin}$ was completely insoluble. This required the mutant protein to be recovered from its insoluble form within bacterial inclusion bodies before purification (section 2.2.11). This was performed via an inclusion body preparation and solubilisation with urea. At this point the protein was subjected to anion exchange and gel filtration chromatography before step wise refolding of the protein via gradual removal of the denaturant (section 2.2.12); a method used successfully for other utrophin ABD constructs (Winder et al., 1995). A sample of soluble refolded $UTR^{fimbrin}$ is shown in lane 5 of Figure 4.2.

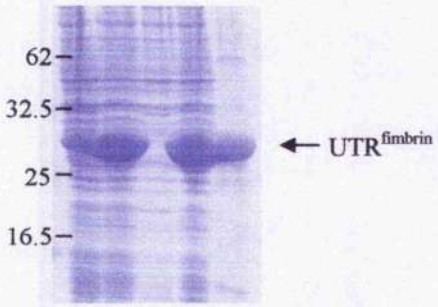

Figure 4.2: Expression, solubility and purification of the UTR^{fimbrin} linker mutant. Freshly competent BL21 (DE3) *E. coli* were transformed with the pSJW1 UTR^{fimbrin} construct. The bacteria were grown to a cell density of 0.6 at 600 nm before induction of protein expression via addition of IPTG. The protein present at pre and post induction are shown in lanes 1 and 2 respectively. After bacterial harvesting and lysis insoluble and soluble protein fractions are presented in lanes 3 and 4. Lane 5 represents a fraction of purified UTR^{fimbrin}. MW markers (kDa) are shown on the left.

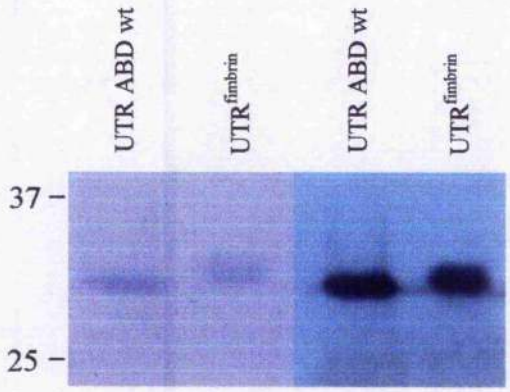

Figure 4.3: SDS PAGE and western analysis of the utrophin ABD and the UTR^{fimbrin} linker mutant. 1 μM samples of utrophin ABD and UTR^{fimbrin} were prepared. 2 x sample buffer was added to these samples and 10 μl was loaded onto a 15 % acrylamide gel. Following separation the proteins were transferred to nitrocellulose ready for western blotting using the utrophin antibody (right hand panel). The acrylamide gel was then treated with Coomassie Blue to detect any protein not transferred to the nitrocellulose (left hand panel). MW markers (kDa) are shown on the left.

UTR^{fimbrin} appeared to refold from a denatured state; however, there was protein precipitation during this process. Comparison of the mutant with utrophin ABD indicated that UTR^{fimbrin} was slightly larger than the wild type protein (Figure 4.3) which was to be expected given the insertion of 11 amino acid residues. Western

analysis of the wild type and mutant proteins demonstrated reactivity with an antibody raised to the wild type utrophin ABD sequence indicating that the mutant protein was sufficiently similar to the wild type protein (Figure 4.3).

4.2.1.3 Circular dichroism analysis of the UTR^{fimbrin} linker mutant.

Before biochemical analyses were performed with the UTR^{fimbrin} mutant it was necessary to check that the insertion of the fimbrin linker sequence into the utrophin ABD linker had not disrupted the overall structure of the protein. CD and the analysis of the collected utrophin ABD and UTR^{fimbrin} data was performed with the help of Dr Sharon Kelly at the Scottish Circular Dichroism facility situated at The University of Glasgow. Far UV CD was used to compare the secondary structure of the mutant with the wild type protein (Figure 4.4). The utrophin ABD is a mostly helical protein (Keep *et al.*, 1999b) and the far UV CD spectra demonstrates this producing a trace indicative of a protein with high α-helix content (Kelly and Price, 2000). The utrophin ABD spectra demonstrates characteristic intensities at approximately 209 and 222 nm commonly associated with α-helix; however, the UTR^{fimbrin} mutant does not display a characteristic α-helical intensity at 209 nm. Overall the intensity of the UTR^{fimbrin} spectra is reduced compared to that of the utrophin ABD although the mutant protein does appear to have some secondary structure even though the spectrum is more indicative of a protein comprised of β-sheet.

The near UV CD spectra of UTR^{fimbrin} were also dissimilar to those of the utrophin ABD. These data give an indication of the similarities of the proteins tertiary structures based on the environments of aromatic residues present within the protein (Kelly and Price, 2000). Utrophin ABD displays a pronounced intensity at 296 nm attributable to the tryptophan residues that it contains. The UTR^{fimbrin} mutant should display a similar trace as the lengthened linker does not contain any extra aromatics. This was found not to be the case; the UTR^{fimbrin} spectrum is completely dissimilar to the utrophin ABD and does not appear to suggest a tertiary structure comparable to the wild type protein. From these data is probable that the UTR^{fimbrin}

possesses little tertiary structure and that the overall folding of the protein is not equivalent to that of the utrophin ABD.

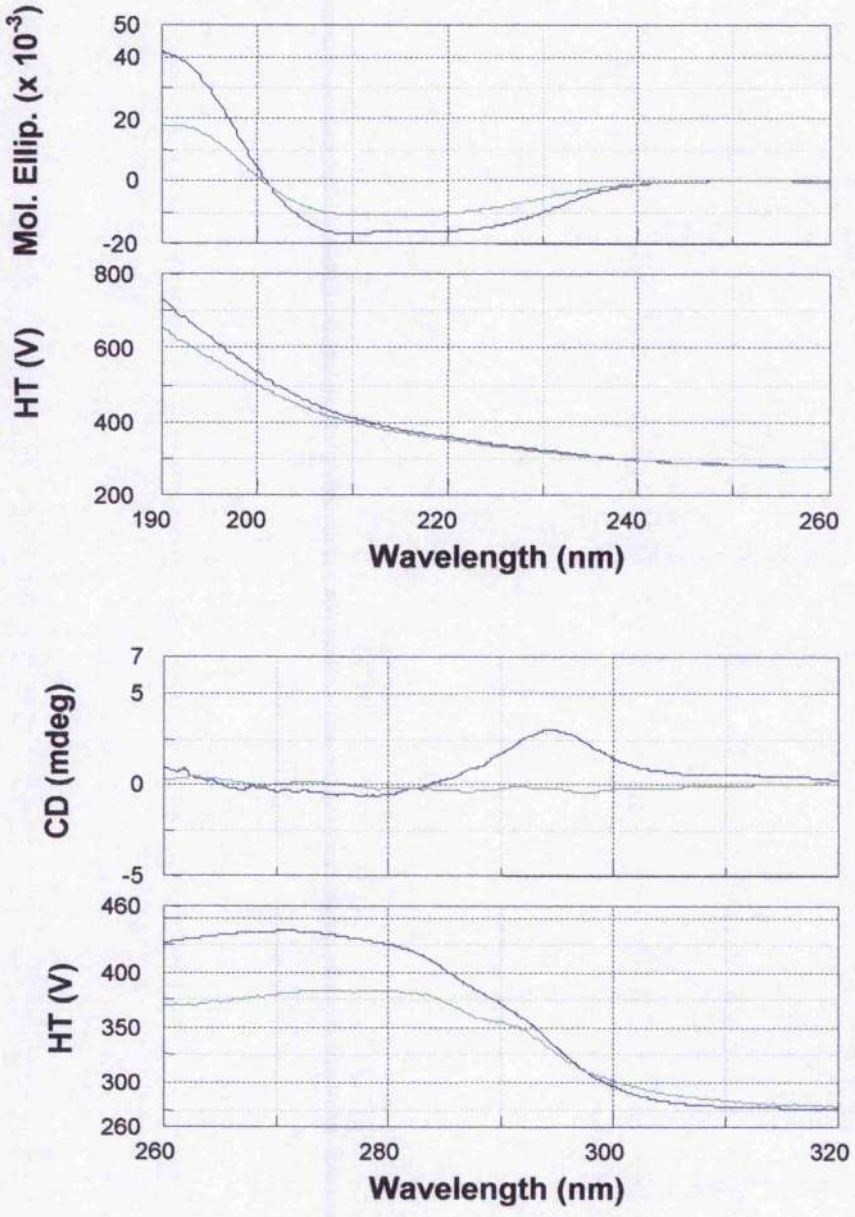

Figure 4.4: Near and far UV CD spectra of the utrophin ABD and the UTR^{fimbrin} linker mutant. Samples of the utrophin ABD (blue spectra) and UTR^{fimbrin} (green spectra) were subjected to near (1 mg/ml) and far (0.4 mg/ml) UV CD analysis using 10 and 0.2 mm quartz cells respectively. Protein samples were prepared in 10 mM phosphate buffer (pH 8.0). Each spectrum was an average of 3 scans recorded with a data pitch of 0.2 and a detector response time of 2 seconds. Near UV data are shown in terms of normalised CD millidegrees whereas far UV data are expressed as molar ellipticity (degrees cm^2 dmol^{-1}).

To further investigate the structure of the utrophin ABD and $UTR^{fimbrin}$ SELCON 3 analysis was performed for both proteins to give an estimation of the secondary structure content of the two proteins (Sreerama and Woody, 2000). The utrophin ABD analysis estimated that the protein was approximately 50 % α-helix with much of the remaining structure attributable to unordered elements. This estimation would be expected given that the utrophin ABD is composed of a CH domain pair, formed almost exclusively, from α-helices and their interconnecting loops (Banuelos et al., 1998). CD analysis of $UTR^{fimbrin}$ has suggested that the addition of a section of the fimbrin linker sequence has disrupted the structure of the mutant protein. The SELCON 3 analysis seems to agree with this. The proportions of each secondary structure element within the mutant protein are very different compared to the wild type. Most noticeably, the α-helical content has diminished from nearly 50 % to approximately 29 %. Importantly, the percentage of regular α-helix has halved which would severely affect the overall structure of the CH domains. The proportion of turn and β-strand has also risen dramatically (even though this element is not present within the utrophin ABD) as has the percentage of unordered structure. It appears that insertion of the fimbrin linker sequence has severely disrupted the secondary structure of the mutant protein. If this were to be the case then it is unlikely that $UTR^{fimbrin}$ would be functional.

	α_R	α_D	β_R	β_D	Turn	Unordered
Utrophin ABD	32 %	16%	7 %	5 %	13 %	26 %
$UTR^{fimbrin}$	16 %	13 %	11 %	9 %	22 %	30 %

Table 4.1: SELCON analysis of the secondary structure content of utrophin and $UTR^{fimbrin}$ ABDs. SELCON 3 was used to analyse the utrophin ABD and $UTR^{fimbrin}$ far UV CD spectra to give an estimation of the proportions of secondary structure elements present within the proteins. The α-helical and β-sheet structures were split into regular and distorted classes as described by (Sreerama and Woody, 2000) to give the six secondary structure classes: regular α-helix, α_R; distorted α-helix, α_D; regular β-strand, β_R; distorted β-strand, β_D; turn and unordered.

SELCON 3 analysis of $UTR^{fimbrin}$ suggests that the linker mutation has severely altered the secondary structure of the protein. To further analyse the possibility of this occurrence a thermal denaturation of $UTR^{fimbrin}$ was undertaken so that the melting of the protein could be compared with the utrophin ABD in order to assess the overall stability of the proteins. Samples of the utrophin ABD and $UTR^{fimbrin}$ were subjected to thermal denaturation over the temperature range 20-77°C and 20-89°C respectively. The effect of elevated temperature on the secondary structure of the proteins was monitored using far UV CD. The $UTR^{fimbrin}$ mutant was taken to a higher maximum temperature as it was evident, during the course of the experiment, that increasing temperature was producing little effect on the observed spectra. Figure 4.5 demonstrates the melting profiles of both proteins between the temperatures stated previously.

Thermal denaturation of the utrophin ABD resulted in changes in the CD spectra indicating an alteration of the secondary structure of the protein as the temperature was elevated. Figure 4.5 illustrates the alteration of the CD spectra occurring during thermal denaturation of the utrophin ABD and $UTR^{fimbrin}$. As the temperature increases, the intensity of the utrophin ABD CD spectra decreases and the peak maxima shift to shorter wavelengths. The peak initially found at 209 nm gradually shifts to approximately 204 nm with the largest shift occurring between 37 and 77°C. A similar shift in peak maxima and intensity were not observed for $UTR^{fimbrin}$. There appeared to be a slight decrease in the spectral intensity of the $UTR^{fimbrin}$ sample at 30°C; however, the intensities present in the utrophin ABD at 209 and 220 nm were not observable.

After completion of the initial melt, the utrophin ABD and $UTR^{fimbrin}$ were allowed to cool back to 20°C, to verify if the denaturation was reversible. Figure 4.6 shows the CD spectra of the initial the utrophin ABD and $UTR^{fimbrin}$ scans at 20°C compared to the spectra produced after cooling of the sample back to 20°C from 77 and 89°C respectively. It is apparent that the utrophin ABD spectra are very similar however, the intensity of the refolded protein is slightly reduced and the peak found initially at 209 nm has shifted to approximately 207 nm. The spectra of the refolded $UTR^{fimbrin}$ linker mutant was almost identical to the initial scan at 20°C although there is a slight decrease in intensity.

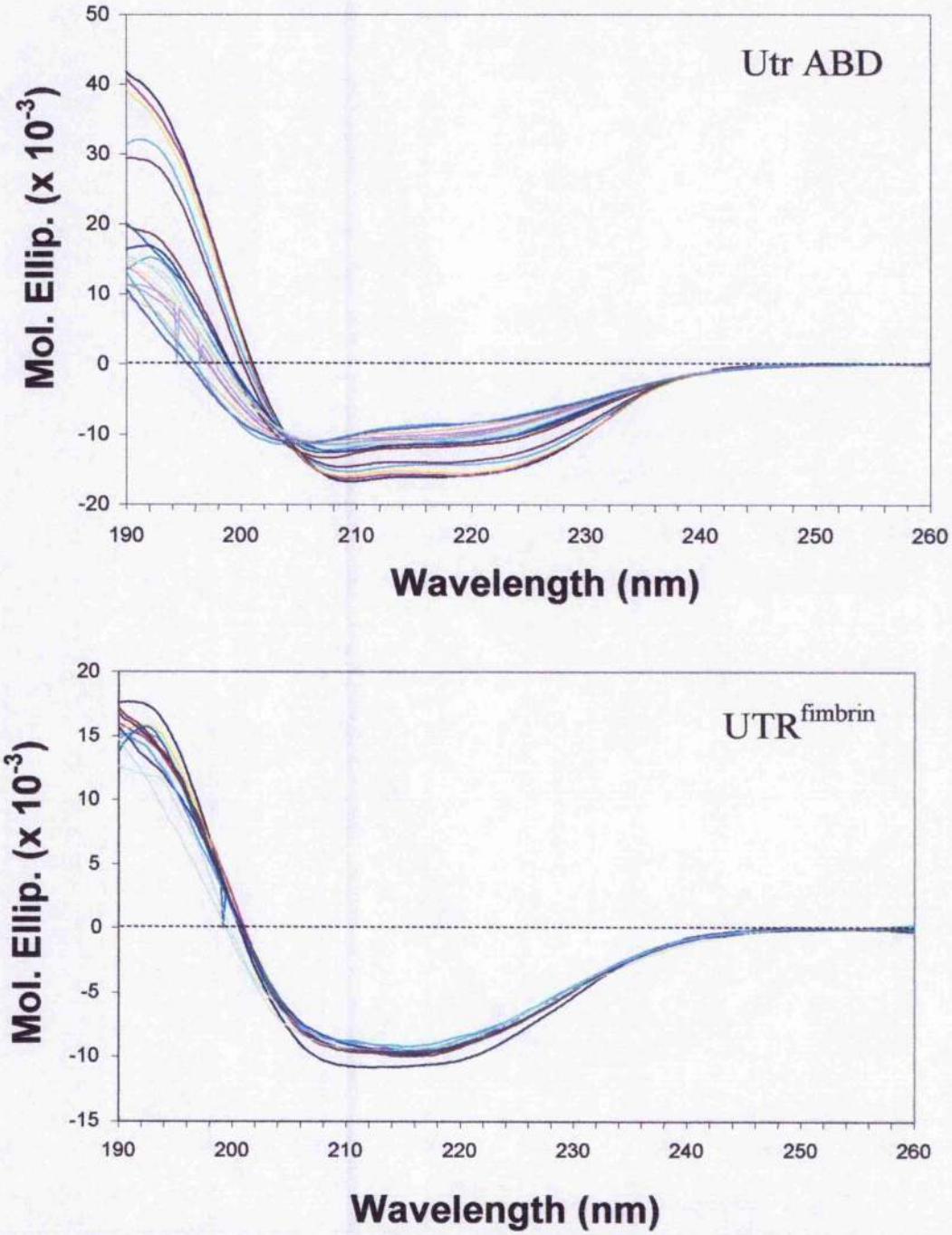

Figure 4.5: Far UV CD spectra demonstrating the thermal denaturation of the utrophin ABD and UTR^{fimbrin} linker mutant. The secondary structure changes exhibited by the utrophin ABD and UTR^{fimbrin} were monitored using far UV CD. 0.4 mg/ml samples of each protein were scanned between 190 and 260 nm over a temperature range of 20 - 77°C for the utrophin ABD and 20 - 89°C for UTR^{fimbrin}. The spectra at each temperature are the result of three accumulations. Molar ellipticity is represented in degrees cm^2 dmol^{-1}.

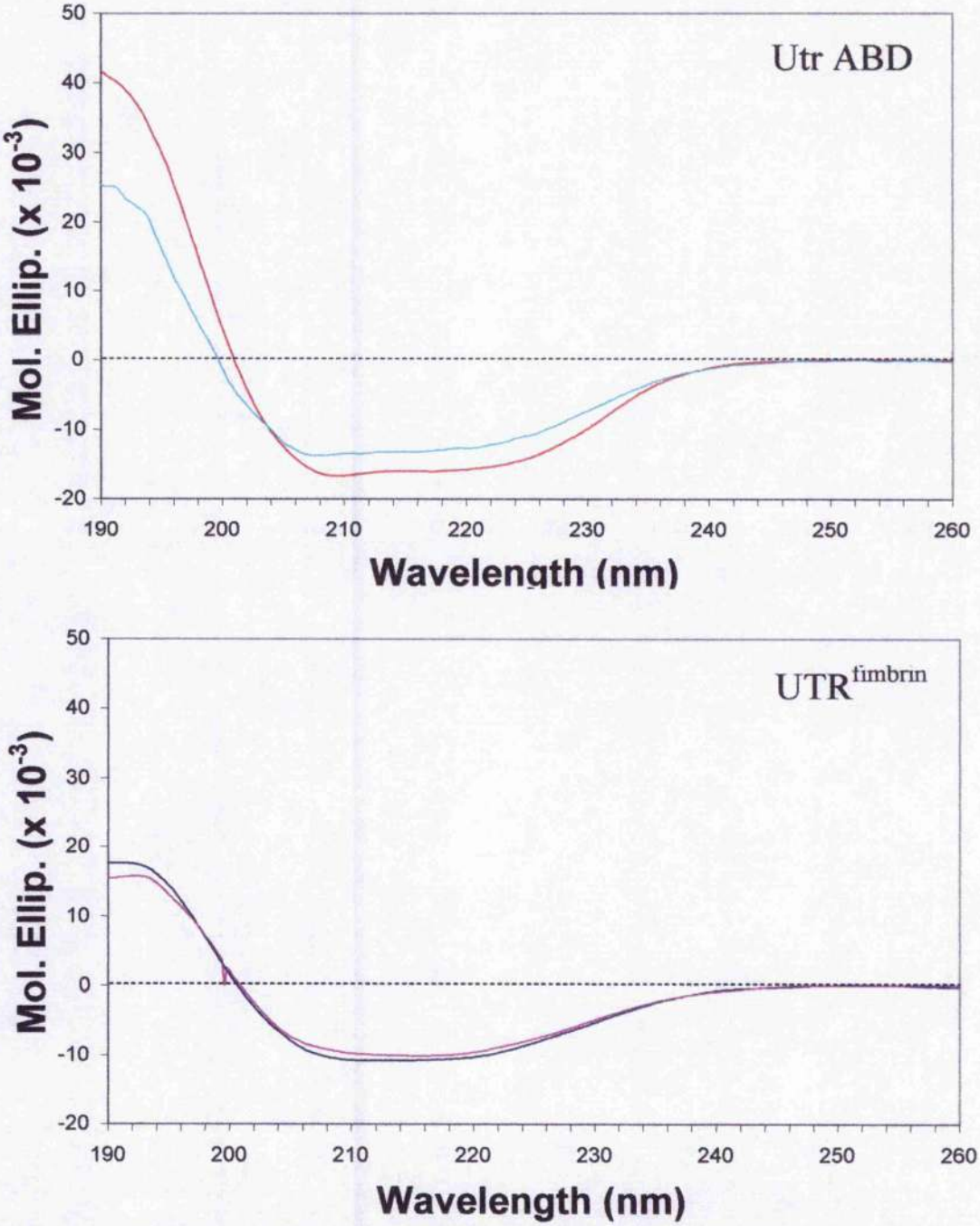

Figure 4.6: CD spectra demonstrating the refolding of the utrophin ABD and UTR^{fimbrin} following thermal denaturation. Samples of utrophin ABD and UTR^{fimbrin} were heated from 20°C up to maximum temperatures of 77 and 89°C respectively. After scanning of these samples both proteins were allowed to cool back to 20°C before a final scan in the far UV region was made. The utrophin ABD spectra at 20°C before and after denaturation are represented in red and cyan whereas UTR^{fimbrin} spectra before and after denaturation are represented in blue and magenta. The spectra at each temperature are the result of three accumulations. Molar ellipticity is represented in degrees cm^2 dmol^{-1}.

These data indicate that the wild type protein does refold after cooling but not completely whilst the $UTR^{fimbrin}$ mutant reverts back to a structural state almost identical to that observed in the initial scan at 20°C. The lack of complete refolding by the utrophin ABD may result from taking the protein so close to complete denaturation. It is evident that the secondary structures present within $UTR^{fimbrin}$ have not been damaged or disrupted by denaturation of the protein even though the maximal denaturation temperature was much higher for the mutant protein.

4.2.1.4 Tryptophan fluorescence analysis of $UTR^{fimbrin}$.

The fluorescence of aromatic residues is sensitive to the environment in which they are located (Lakowicz, 1999). The tryptophan fluorescence of the utrophin ABD and $UTR^{fimbrin}$ were compared in order to investigate the similarities between the two proteins. The addition of the fimbrin residues to the utrophin ABD did not involve any aromatics hence the fluorescent spectra should be identical for the mutant and wild type proteins. 1 mg/ml samples of the utrophin ABD and $UTR^{fimbrin}$ were excited at 296 nm and an emission spectrum recorded between 300 and 450 nm (Figure 4.7).

It was apparent that the fluorescent emission of $UTR^{fimbrin}$ was slightly larger than the utrophin ABD. In light of the CD data, which suggests that the mutant protein is most likely not folded correctly, disruption of the structure of the protein would alter the environment of the aromatics potentially exposing then to the solvent. Exposure to solvent is suggested by the $UTR^{fimbrin}$ spectra given that the fluorescence intensity has red shifted from 334 nm to 338 nm. The utrophin ABD displays emission maxima similar to proteins that contain partially exposed tryptophan residues, for example, staphylococcal nuclease (Lakowicz, 1999). The addition of the fimbrin linker sequence has altered the structure of the protein suggesting that the tryptophan residues are now more exposed to the solvent (Vivian and Callis, 2001). Once again, these data suggest that the structure of $UTR^{fimbrin}$ has been disrupted by the mutation.

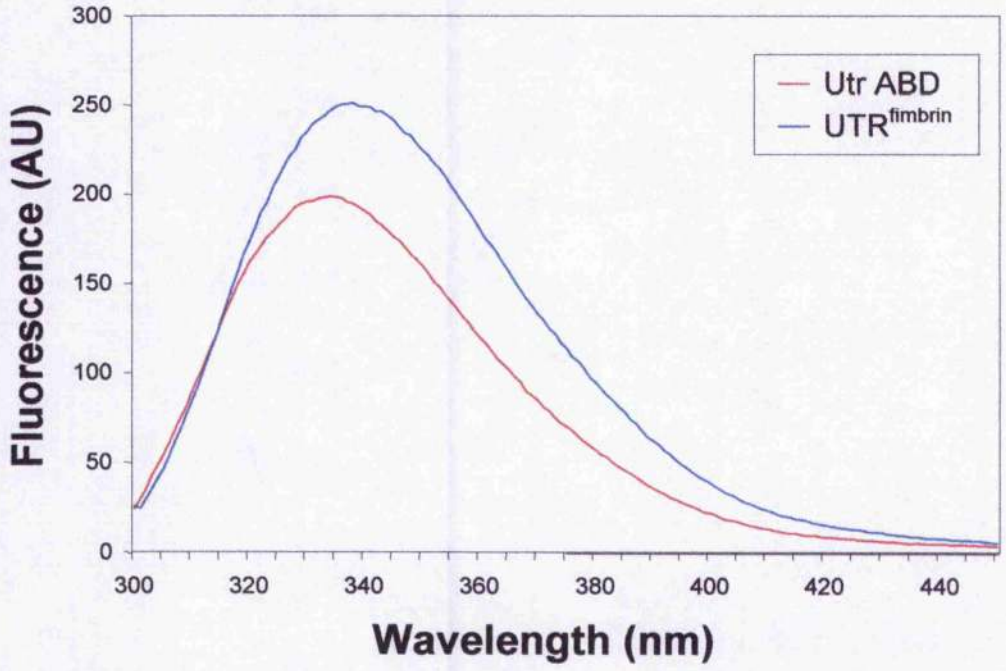

Figure 4.7: Tryptophan fluorescence spectra of the utrophin ABD and UTR^{fimbrin} linker mutant. Samples of utrophin ABD and UTR^{fimbrin}, each at 30 μM, were excited at 296 nm and emission spectra recorded between 300 and 450 nm. Scans were performed at slow speed with emission and excitation slit widths of 1 nm. The utrophin ABD is represented in red whilst UTR^{fimbrin} is represented in blue. Fluorescence is represented by arbitrary units (AU).

4.2.1.5 Proteolytic resistance of UTR^{fimbrin}.

The CD analysis of the UTR^{fimbrin} mutant suggests that the protein is not refolding correctly from the urea denatured state. Soluble UTR^{fimbrin} can be produced but it is unlikely that the protein would be functionally comparable with the biochemical characteristics of the wild type protein and hence, the true effect of the fimbrin linker sequence could not be determined. One final experiment was performed to assess the structural integrity of UTR^{fimbrin}. This involved the investigation of the mutant protein's ability to resist degradation by trypsin. A pair of CH domains form the ABD of utrophin; this particular domain fold is quite compact and would be relatively resistant to proteolysis. Previous studies of the utrophin ABD involving limited proteolysis demonstrate the resistance of this domain to proteolytic

cleavage (Moores and Kendrick-Jones, 2000). If the structure of the $UTR^{fimbrin}$ mutant is dissimilar to that of the utrophin ABD then the digestion pattern of the two proteins would differ. Also, if the mutant protein was folded incorrectly then it would exhibit a reduced resistance to the actions of the protease.

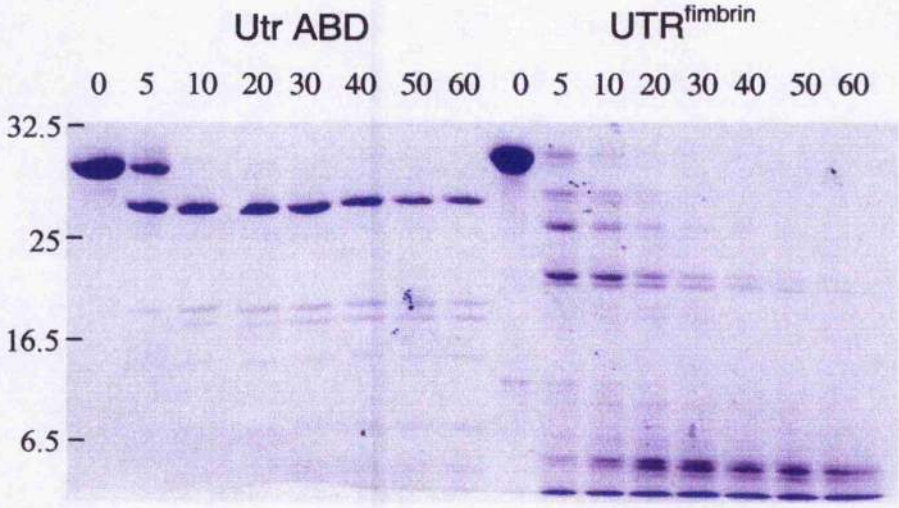

Figure 4.8: Proteolytic resistance of utrophin ABD and $UTR^{fimbrin}$. 20 μM samples of utrophin ABD and $UTR^{fimbrin}$ were subjected to proteolytic degradation by trypsin. Time 0 represents an undigested sample of each protein whereas the remaining lanes represent protein samples that have been digested with trypsin for 5, 10, 20, 30, 40, 50, and 60 minutes. At each time point during the course of the digestion samples were removed from the main reaction; proteolysis was halted by boiling of sample in 2 x sample buffer. 10 μl of each time point sample were loaded and run on a 15 % acrylamide gel. Protein bands were visualised using Coomassie Blue staining. MW markers (kDa) are shown on the left.

A sample of utrophin ABD and $UTR^{fimbrin}$ was subjected to degradation by trypsin. At various time points degraded samples were removed from the main reactions and the digestion halted by boiling (section 2.2.22.1). SDS PAGE was used to visualise the digestion patterns of both proteins (Figure 4.8). Figure 4.8 demonstrates that the utrophin ABD is relatively resistant to degradation by trypsin under these assay conditions; however, it is apparent that $UTR^{fimbrin}$ is not. The utrophin ABD shows complete degradation from the full length form after ten minutes. A species of approximately 27 kDa persists throughout the course of the assay although it is apparent that this species is also degrading and protein bands of

roughly 18, 17, 15 and 6.5 kDa are beginning to increase in quantity as the digestion progresses. A completely different digestion product is formed for the $UTR^{fimbrin}$ mutant. The full length protein is almost completely degraded after 5 minutes and no 27 kDa species persist after 20 minutes of digestion. The protein fragments that are generated do not persist and are rapidly degraded. By the end of the time course only low MW fragments can be seen.

4.2.2.1 Design of the utrophin ABD α-actinin linker mutant

α-Actinin is an F-actin cross-linking protein and a member of the spectrin superfamily of proteins. The ABD of α-actinin is formed from a pair of CH domains and the binding of this domain to F-actin has been proposed to occur in either an extended (Tang et al., 2001; Taylor and Taylor, 1993) or a compact conformation (Liu et al., 2004; McGough et al., 1994). Sequence comparisons between the utrophin ABD and α-actinin revealed that the linker region separating the two CH domains is shorter than that of the utrophin ABD (Figure 4.9). It is possible that the reduced length may favour a more extended conformation owing to reduced flexibility within the linker.

To test this hypothesis a mutant utrophin ABD was designed that possesses a linker shortened by seven residues. The α-actinin linker sequence is only six residues shorter than that of the utrophin ABD; however, removal of seven residues would allow nearly two complete turns of α-helix to be removed. This would hopefully prevent disruption to the orientation of the two CH domains with regard to each other as removal of incomplete helical turns might force twisting along the long axis of the protein. It was intended that by reducing the length of the helical linker then the flexibility of the interconnecting helix would be reduced. If the linker was less flexible then it would be more difficult for the CH domains to associate to form a compact conformation when in solution or when interacting with F-actin. This would potentially favour the mutated ABD to adopt a more 'open' conformation perhaps forcing association with F-actin in an open and extended conformation as proposed by Moores and colleagues (Moores et al., 2000).

The utrophin ABD sequence was used to design primers that would facilitate removal of the target sequence using site directed mutagenesis (section 2.2.9). The success of the mutation was validated by sequencing before the mutated pSJW1 construct could be used to express the mutant protein. $UTR^{\alpha\text{-actinin}}$ was generated after the production and analysis of the $UTR^{fimbrin}$ mutant with the intention that the removal of sequence from the ABD would be less disruptive to the structure of the ABD.

```
Utrophin    134 WQVKDVMKDVMSDLQQTNSEKGLLSW 159
α-Actinin   125 FAIQDIS------VEETSAKEGLLLW 144
                : ::*:        :::*.:::*** *
Mutant      134 WQVKDV-------LQQTNSEKILLSW 159
```

Figure 4.9: Sequence alignment of the utrophin and α-actinin ABD linker regions. Clustal W alignment of utrophin and α-actinin ABD linker regions demonstrating the stretch of residues found in the utrophin ABD that are not seen in the α-actinin ABD. The 7 residues that are to be removed from the utrophin ABD linker are highlighted in grey. The consensus symbols and residue colours are defined as follows: "*", ":" and "." represent identical residues, conserved substitutions and semi-conserved substitutions respectively whilst red, blue, magenta and green represent small/hydrophobic, acidic, basic and hydroxyl/amine/basic residues respectively.

4.2.2.2 Expression and purification of the $UTR^{\alpha\text{-actinin}}$.

The $UTR^{\alpha\text{-actinin}}$ linker mutant pSJW1 construct was used to transform freshly competent BL21 (DE3) *E. coli* before expression and purification was attempted as described previously (Winder et al., 1995; section 2.2.11). The mutant protein expressed successfully as demonstrated by lanes 1 and 2 of Figure 4.10. Unlike the $UTR^{fimbrin}$ mutant there was a small portion of the expressed protein that was soluble (Figure 4.8 lane 3); however a large portion of the protein did appear to be localised to the insoluble bacterial fraction (Figure 4.8 lane 4). Once again the mutation of the linker appeared to be seriously affecting the production and processing of the protein within the bacteria. Fortunately, some protein was soluble and present in sufficient

quantity to be purified in an analogous manner to the wild type protein. A sample of purified $UTR^{\alpha\text{-actinin}}$ is shown in lane 5 of Figure 4.10.

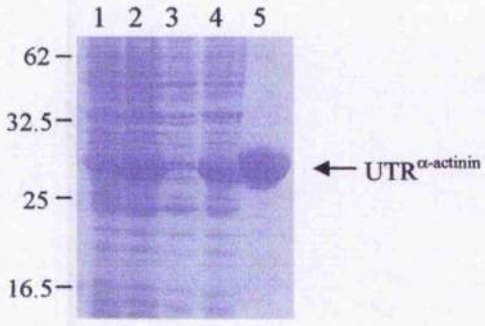

Figure 4.10: Expression, solubility and purification of the $UTR^{\alpha\text{-actinin}}$ linker mutant. Freshly competent BL21 (DE3) *E. coli* were transformed with the pSJW1 $UTR^{\alpha\text{-actinin}}$ construct. The bacteria were grown to a cell density of 0.6 at 600 nm before induction of protein expression via addition of IPTG. The protein present at pre and post induction are shown in lanes 1 and 2 respectively. After bacterial harvesting and lysis soluble and insoluble protein fractions are presented in lanes 3 and 4. Lane 5 represents a fraction of purified $UTR^{\alpha\text{-actinin}}$. MW markers (kDa) are shown to the left.

The purified $UTR^{\alpha\text{-actinin}}$ mutant appeared to be approximately 30 kDa in size however it was possible that the protein represented in lane 3 of Figure 4.10 was not the $UTR^{\alpha\text{-actinin}}$ mutant. Most of the expressed protein appeared to be insoluble and therefore, it was necessary to confirm that the protein band selected for purification was indeed a utrophin ABD mutant. To test this, a sample of $UTR^{\alpha\text{-actinin}}$ mutant and utrophin ABD was subjected to SDS-PAGE and the resultant gel either Coomassie Blue stained or subjected to western analysis (Figure 4.11).

Figure 4.11 demonstrates that the $UTR^{\alpha\text{-actinin}}$ mutant is slightly smaller than the utrophin ABD. This may be expected given that seven linker residues have been removed from the protein. The western analysis confirms that $UTR^{\alpha\text{-actinin}}$ is indeed a mutant of the utrophin ABD given the reactivity with the utrophin antibody. It does appear however, that the $UTR^{\alpha\text{-actinin}}$ band is not as dense as that of the wild type utrophin ABD. From these data it appeared that the $UTR^{\alpha\text{-actinin}}$ mutant had been successfully expressed and purified. Before any biochemistry was attempted CD and

fluorescence spectroscopy were employed to investigate the structure of the mutant compared to the wild type protein. Lengthening of the ABD linker appeared to disrupt the overall structure of the $UTR^{fimbrin}$ ABD; it is possible that a similar effect may result from a shortening of the linker.

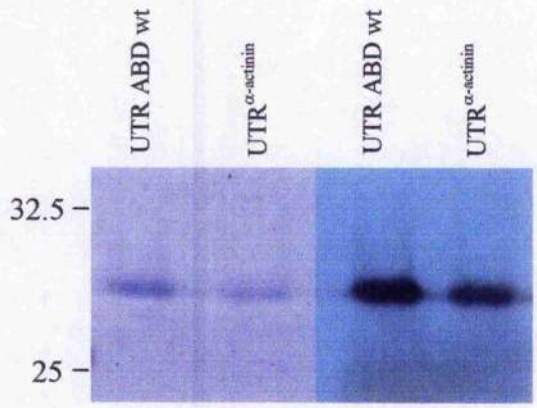

Figure 4.11: SDS PAGE and western analysis of the utrophin ABD and $UTR^{\alpha\text{-actinin}}$ linker mutant. 1 μM samples of utrophin ABD and $UTR^{\alpha\text{-actinin}}$ were prepared. 2 x sample buffer was added to these samples and 10 μl was loaded onto a 15 % acrylamide gel. Following separation the proteins were transferred to nitrocellulose ready for western blotting using the utrophin antibody (right hand panel). The acrylamide gel was then treated with Coomassie Blue to detect any protein not transferred to nitrocellulose (left hand panel). MW markers (kDa) are shown to the left.

4.2.2.3 Circular dichroism analysis of $UTR^{\alpha\text{-actinin}}$.

As with the $UTR^{fimbrin}$ mutant, the $UTR^{\alpha\text{-actinin}}$ mutant was subjected to near and far UV CD analysis and thermal denaturation. The $UTR^{\alpha\text{-actinin}}$ mutant CD data were collected at the University of Sheffield however help with the data analysis was sought from Dr Sharon Kelly at the Scottish Circular Dichroism Facility situated at the University of Glasgow. Once again, these analyses demonstrated that mutation of the linker region within the ABD severely affects the structure of the protein.

Near and far UV CD spectra of $UTR^{\alpha\text{-actinin}}$ were compared to spectra of the utrophin ABD (Figure 4.12). The far UV spectra of the utrophin ABD show negative deflections at 222 and 209 nm that are not visible in the $UTR^{\alpha\text{-actinin}}$ spectra (Figure

4.12). These deflections are indicative of a protein formed from α-helix; therefore, it is apparent that $UTR^{\alpha\text{-actinin}}$ is not formed from α-helix or it has a greatly reduced content of this structural element when compared to wild type utrophin ABD. The $UTR^{\alpha\text{-actinin}}$ far UV spectra also appear very similar to those collected for the $UTR^{fimbrin}$ mutant (section 4.2.3) so it would seem that the secondary structure of the mutant differs from that of the utrophin ABD.

The near UV CD spectra of $UTR^{\alpha\text{-actinin}}$ are again, very different to that of the wild type protein. The utrophin ABD shows a pronounced intensity at 296 nm generated by the tryptophan residues present within the protein; however, $UTR^{\alpha\text{-actinin}}$ does not display a peak at this wavelength and instead, pronounced peaks can be seen at approximately 270 and 280 nm. It is apparent that the removal of the short stretch of linker has disrupted the tertiary structure of the protein in some way. The fact that there is a signal indicates the presence of some tertiary structure; however the tertiary structure of the mutant is significantly different to that of the utrophin ABD.

Far and near UV CD indicates that the secondary and tertiary structures of $UTR^{\alpha\text{-actinin}}$ are not comparable to those of the utrophin ABD. In order to give an indication of the secondary structure elements present SELCON analysis was performed using the mutant and wild type far UV CD spectra. The proportions of each type of structural element are displayed in Table 4.2. It is apparent that $UTR^{\alpha\text{-actinin}}$ does contain a significant proportion of secondary structure but the amount of each element does differ from that of the utrophin ABD. The utrophin ABD is essentially an α-helical protein: the utrophin ABD crystal structure has been determined and clearly demonstrates the helical nature of the secondary structure elements present within the protein (Keep *et al.*, 1999b). The SELCON analysis echoes this although a small proportion of β-sheet has been determined to be present. Analysis of $UTR^{\alpha\text{-actinin}}$ demonstrates that the protein does contain a significant proportion of α-helix although the amount of regular and distorted helix has dropped by 5 % and 1 % respectively. The proportion of β-sheet has also increased in the mutant protein and the proportion of turn and unordered structure has risen to 17 % and 29 % respectively. Overall the $UTR^{\alpha\text{-actinin}}$ mutant displays a reduced helical content which does help to explain the differences in the far UV CD spectra. The presence of increased proportions of the other elements also indicates that the

mutation has caused the overall structure of the protein to be disrupted greatly affecting the environments of the aromatic residues detected in the near UV region.

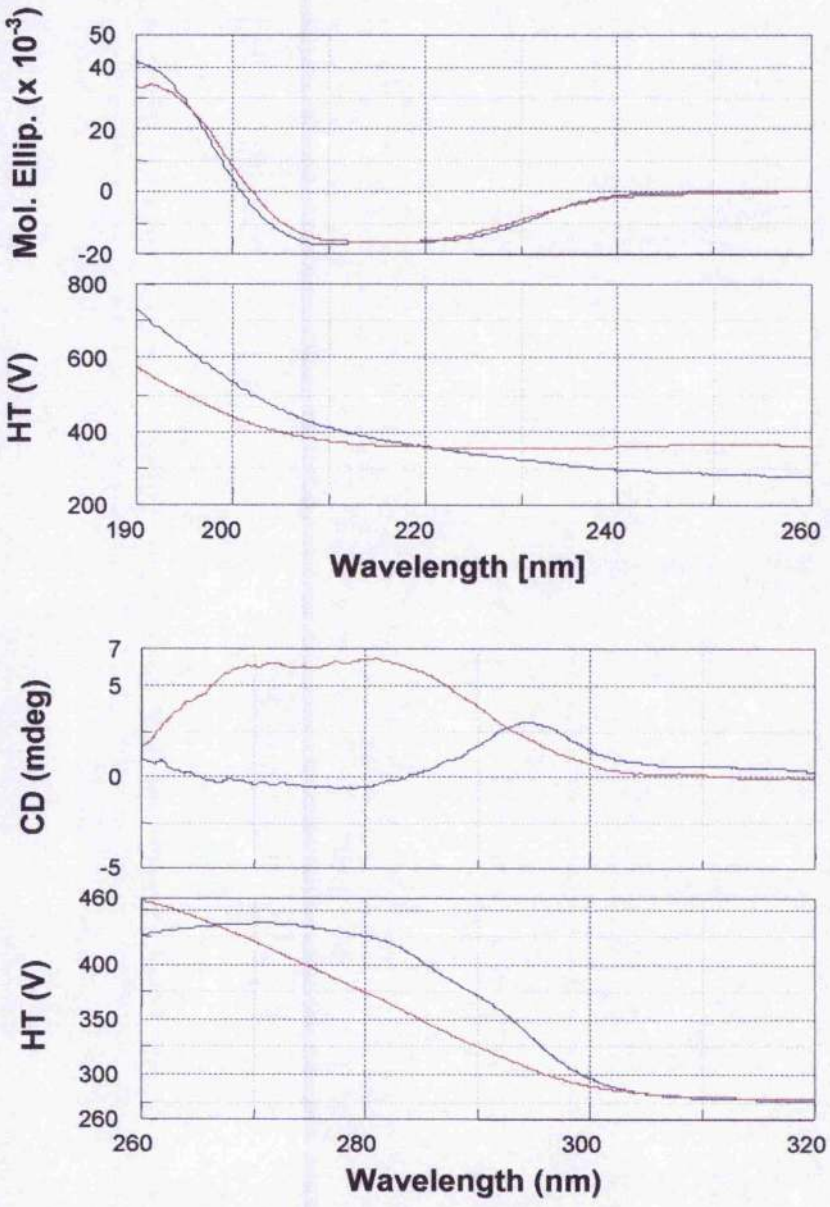

Figure 4.12: Near and far UV CD spectra of the utrophin ABD and UTR$^{\alpha\text{-actinin}}$ linker mutant. Samples of utrophin ABD (blue spectra) and UTR$^{\alpha\text{-actinin}}$ (red spectra) were subjected to near (1 mg/ml) and far (0.4 mg/ml) UV CD analysis using 10 and 0.2 mm quartz cells respectively. Protein samples were prepared in 10 mM phosphate buffer (pH 8.0). Each spectrum was an average of 3 scans recorded between 260-320 nm and 190-260 nm corresponding to near and far UV CD regions. Near UV data are shown in terms of normalised CD millidegrees whereas far UV data are expressed as molar ellipticity (degrees cm^2 dmol^{-1}).

	α_R	α_D	β_R	β_D	Turn	Unordered
Utrophin ABD	32 %	16 %	7 %	5 %	13 %	26 %
$UTR^{\alpha\text{-actinin}}$	27 %	15 %	7 %	7 %	17%	29 %

Table 4.2: SELCON analysis of the secondary structure content of the utrophin ABD and $UTR^{\alpha\text{-actinin}}$ linker mutant. Utrophin ABD and $UTR^{\alpha\text{-actinin}}$ spectra were analysed using SELCON 3 to estimate the proportions of secondary structure elements present within the proteins. The α-helical and β-sheet structures were split into regular and distorted classes as described by Sreerama and Woody (2000) to give the six secondary structure classes: regular α-helix, α_R; distorted α-helix, α_D; regular β-strand, β_R; distorted β-strand, β_D; turn and unordered.

The final set of CD experiments involved investigation of the structural changes induced by the thermal denaturation of $UTR^{\alpha\text{-actinin}}$. Samples of utrophin ABD and $UTR^{\alpha\text{-actinin}}$ were subjected to thermal denaturation over the temperature range 20-77°C and 20-80°C respectively (Figure 4.13). The effect of elevated temperature on the secondary structure of the proteins was monitored using far UV CD. A similar set of experiments performed with $UTR^{fimbrin}$ demonstrated the mutant structure changing little during the course of denaturation. If the removal of the linker sequence to generate the $UTR^{\alpha\text{-actinin}}$ mutant had disrupted the overall structure of the protein (as seen with $UTR^{fimbrin}$) it was likely that there would be little change in the spectra during thermal denaturation.

Figure 4.13 demonstrates the change in structure of the wild type utrophin ABD as it is heated from 20 to 77°C. It is apparent that the α-helical signatures at 222 and 209 nm reduce in intensity and experience a blue shifting, the most noticeable of which, is the movement of the 209 nm intensity to approximately 204 nm. Thermal denaturation of chicken gizzard calponin shows a similar reduction in deflection and shifting in intensities when heated from 20 to 80°C (Czurylo et al., 2000). The $UTR^{\alpha\text{-actinin}}$ mutant does not demonstrate a similar shift in peak intensities (Figure 4.13) instead the only noticeable difference during the course of the thermal denaturation is a reduction in the intensity of the spectra at 210 nm from approximately -16000 to -13000 degrees cm^2 $dmol^{-1}$.

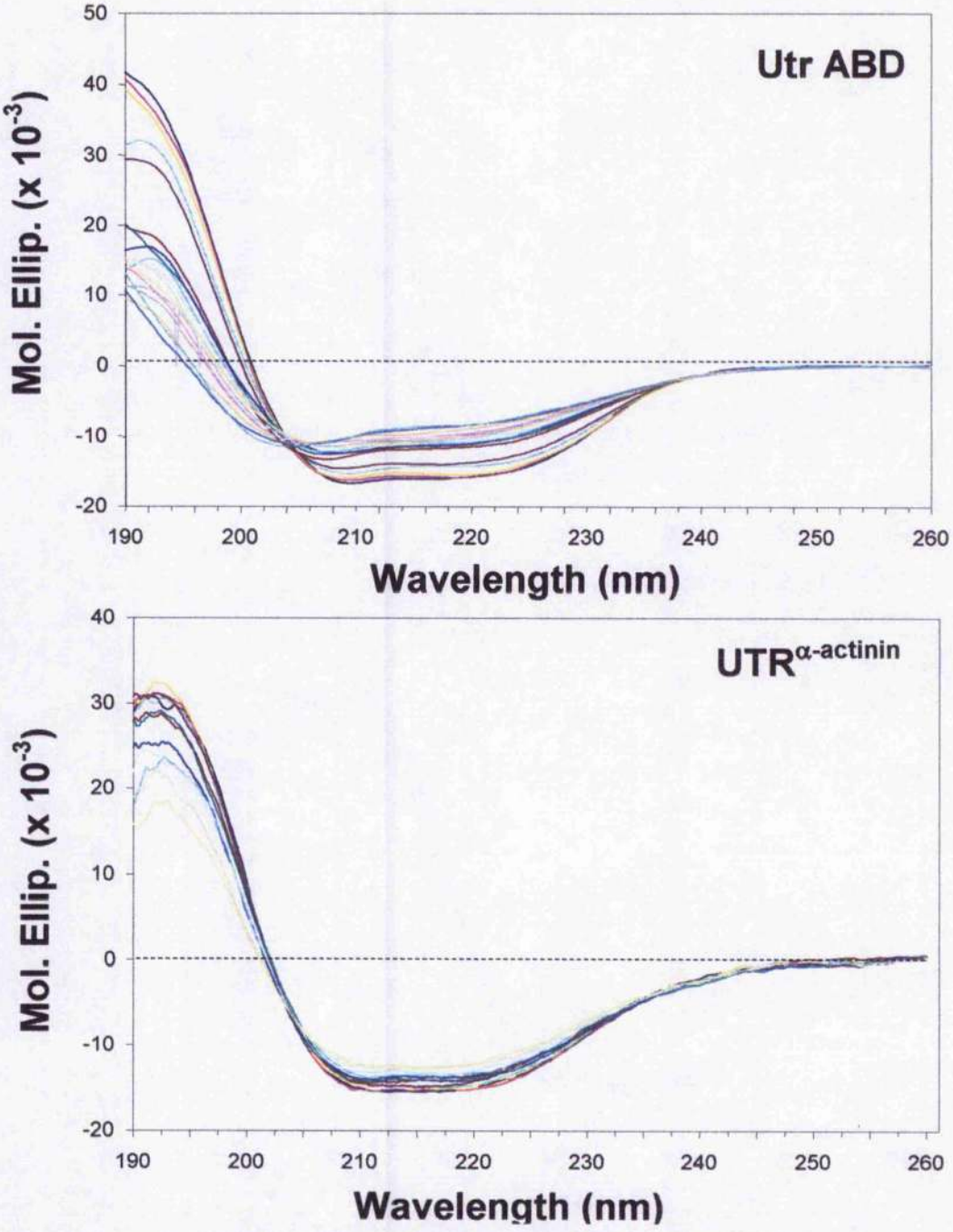

Figure 4.13: Far UV CD spectra demonstrating the thermal denaturation of the utrophin ABD and UTR$^{\alpha\text{-actinin}}$ linker mutant. The secondary structure changes exhibited by the utrophin ABD and UTR$^{\alpha\text{-actinin}}$ were monitored using far UV CD. 0.4 mg/ml samples of each protein were scanned between 190 and 260 nm over a temperature range of 20 - 77°C for the utrophin ABD and 20 - 80°C for UTR$^{\alpha\text{-actinin}}$. Each trace results from three accumulations with molar ellipticity represented in degrees cm^2 dmol^{-1}.

After completion of the initial melt, the utrophin ABD and $UTR^{\alpha\text{-actinin}}$ were allowed to cool back to 20°C, to verify if the denaturation was reversible. Figure 4.14 shows the CD spectra of the initial utrophin ABD and $UTR^{\alpha\text{-actinin}}$ scans at 20°C compared to the spectra produced after cooling of the samples back to 20°C from 77 and 80°C respectively. The utrophin ABD spectra were described previously in section 4.2.3 Figure 4.6; however, it is apparent that the $UTR^{\alpha\text{-actinin}}$ mutant does not behave like the wild type protein. Before denaturation, $UTR^{\alpha\text{-actinin}}$ did not display the peak intensities at 222 or 209 nm like the wild type protein. After cooling, the utrophin ABD does not refold completely as the spectrum shows a loss of intensity and the 209 nm peak remains slightly blue shifted at approximately 208 nm. Interestingly, after refolding, $UTR^{\alpha\text{-actinin}}$ displays intensity at approximately 211 nm not present before denaturation. It appears that cooling of the mutant protein sample after denaturation has allowed a slight adjustment to the secondary structure of the protein resulting in an improved α-helical CD signal. The fact that the wild type protein does not return to the structural state prior to denaturation probably results from bringing the protein close to the point of complete denaturation although the $UTR^{\alpha\text{-actinin}}$ mutant appears to have benefited from this process. Overall, $UTR^{\alpha\text{-actinin}}$ does not appear to have a similar secondary or tertiary structure when compared to the utrophin ABD and it does not behave in an analogous manner when subjected to thermal denaturation.

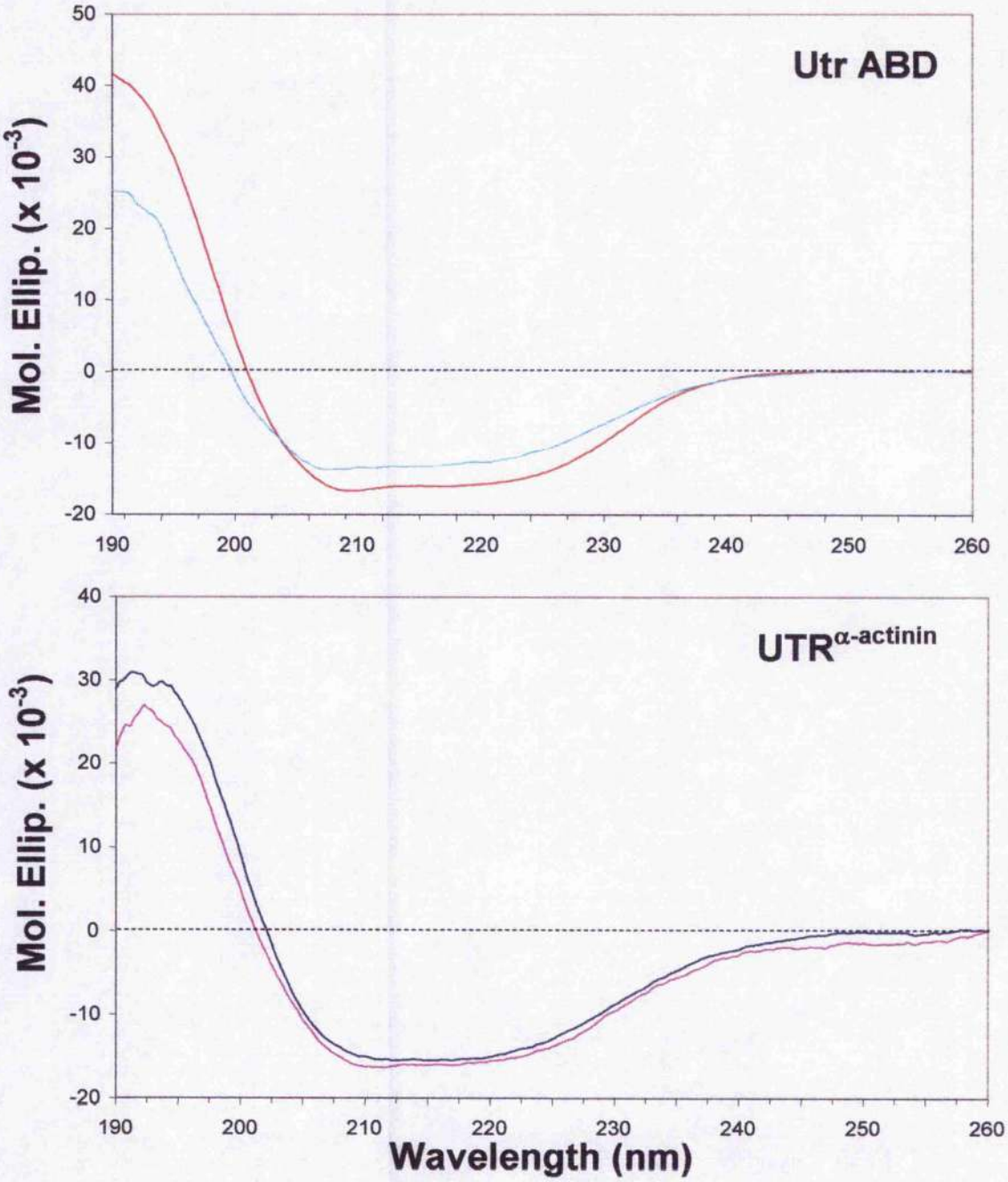

Figure 4.14: Far UV CD spectra of the utrophin ABD and UTR$^{\alpha\text{-actinin}}$ before and after thermal denaturation. The structural affects of thermal denaturation on the utrophin ABD and UTR$^{\alpha\text{-actinin}}$ were monitored using far UV CD. Samples of utrophin ABD and UTR$^{\alpha\text{-actinin}}$ (1 mg/ml) were gradually heated from 20°C to a maximum temperature of 77 and 80°C respectively. The samples were allowed to cool back to 20°C allowing refolding of the denatured proteins. Utrophin ABD spectra before and after cooling are represented by red and cyan traces, whereas UTR$^{\alpha\text{-actinin}}$ before and after refolding are represented in blue and magenta. Each trace results from three accumulations with molar ellipticity represented in degrees cm^2 dmol^{-1}. Utrophin ABD and UTR$^{\alpha\text{-actinin}}$ traces have been separated for clarity.

4.2.2.4 *Tryptophan fluorescence analysis of UTR$^{\alpha\text{-actinin}}$.*

The removal of the seven residues from the utrophin ABD linker region did not involve any aromatic amino acids and hence, the fluorescent spectra should be identical for the mutant and wild type proteins. 1 mg/ml samples of utrophin ABD and UTR$^{\alpha\text{-actinin}}$ were excited at 296 nm and an emission spectrum recorded between 300 and 450 nm (Figure 4.15).

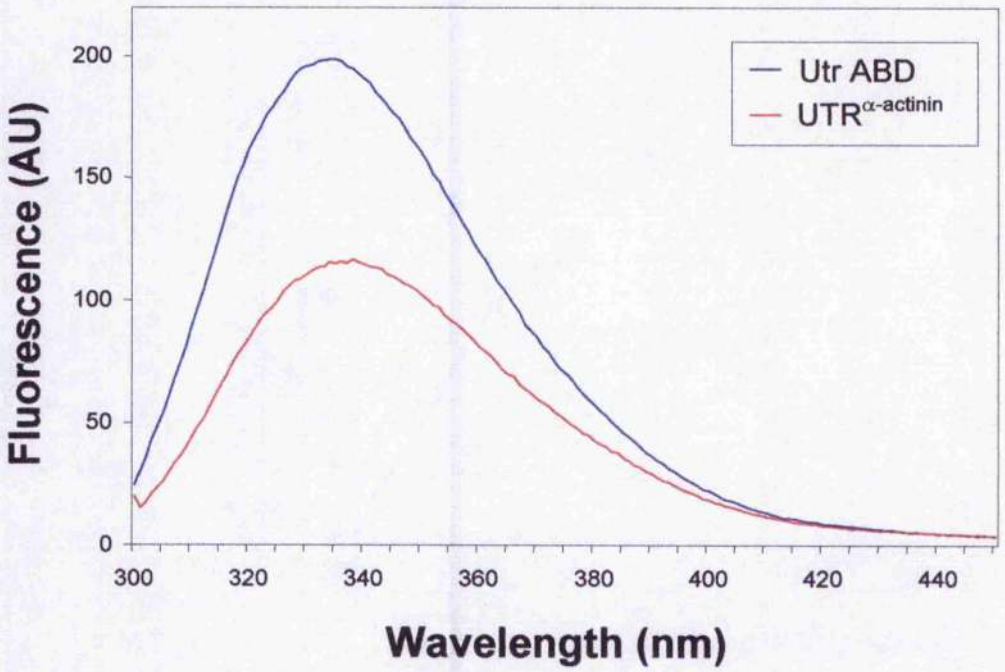

Figure 4.15: Tryptophan fluorescence of the utrophin ABD and UTR$^{\alpha\text{-actinin}}$ linker mutant. Samples of utrophin ABD and UTR$^{\alpha\text{-actinin}}$, each at 30 μM, were excited at 296 nm and emission spectra recorded between 300 and 450 nm. Scans were performed at slow speed with emission and excitation slit widths set to 1.5 nm. The utrophin ABD is represented in blue whilst UTR$^{\alpha\text{-actinin}}$ is represented in red. Fluorescence is represented in arbitrary units (AU).

It is apparent that the fluorescence of UTR$^{\alpha\text{-actinin}}$ is reduced compared to the utrophin ABD. This would be consistent with an exposure of tryptophan residues to the aqueous solvent allowing quenching to occur (Vivian and Callis, 2001). The CD data suggests that the structure of UTR$^{\alpha\text{-actinin}}$ has been disrupted as a result of the mutation. As with the UTR$^{\text{fimbrin}}$ tryptophan fluorescence spectra, the UTR$^{\alpha\text{-actinin}}$ spectra suggest an exposure of the tryptophan residues to the solvent as the

fluorescent intensity recorded for the wild type protein is red shifted from 334 nm to 338 nm in the mutant. Once again, these data suggest that the structure of $UTR^{\alpha\text{-actinin}}$ has been disrupted by the mutation.

4.3 *Discussion*

Comparison of the amino acid sequence of fimbrin and α-actinin ABDs with the utrophin ABD revealed a respective extension or reduction in the length of the inter-CH domain linker. These three proteins exhibit very different functions and have been modelled to have differing modes of interaction with F-actin (reviewed in (Winder, 2003). It has been proposed that the length of the linker that separates the CH domains of these proteins may have relevance to the manner in which they interact with F-actin. In order to test this hypothesis two mutants of the utrophin ABD were designed, one containing an extended linker region modelling the fimbrin linker and one with a shortened linker modelling the α-actinin linker. Before a comparison could be made between the mutant proteins and wild type utrophin ABD it was necessary to express and purify the mutant proteins.

The first mutant generated was the fimbrin linker mutant, $UTR^{fimbrin}$. Generation of the mutation was straightforward using overlap extension PCR however the expression and purification of the protein was a little more problematic. Unfortunately, the protein was not soluble when expressed in BL21 (DE3) *E. coli* (Figure 4.2); however recovery of the mis-folded protein from the insoluble bacterial lysate was attempted. Refolding of the protein was not perceived to be problematic as other studies involving expressed CH domain containing proteins (Bramham et al., 2002; Winder et al., 1995; Winder et al., 2003) utilised protein refolded from urea. It appeared that refolding of $UTR^{fimbrin}$ from urea was also successful based on its solubility (section 4.2.2). The mutant protein appeared to be slightly larger than the wild type; this would be expected given the extra residues present in the mutant protein and it was also reactive with a utrophin ABD polyclonal antibody. $UTR^{\alpha\text{-actinin}}$ was generated using site directed mutagenesis and expression of the protein in BL21 (DE3) *E. coli* was less problematic than that of $UTR^{fimbrin}$. A sufficient quantity of $UTR^{\alpha\text{-actinin}}$ was purified from the soluble fraction allowing initial

analyses of the protein. Once again, there was a size shift when compared to the wild type and the mutant was detectable using the utrophin ABD antibody (section 4.2.7).

Following purification of the two mutant proteins it was necessary to determine that the structure of each protein had not been adversely affected by the introduction or removal of linker residues. CD was chosen to initially assess the structural similarities between the utrophin ABD and the linker mutants. It was expected that the near and far UV CD spectra of the mutants would almost be identical to the wild type protein given that the mutations was not made within either of the CH domains and no extra aromatic residues were inserted. The mutant proteins would still, essentially, be wild type utrophin ABD but this was not found to be the case. The utrophin ABD is largely formed from α-helix and the far UV CD spectra demonstrated typical α-helical features very similar to polylysine in the all helical conformation (Greenfield and Fasman, 1969) and the smooth muscle regulatory protein calponin (that contains a single CH domain) (Czurylo et al., 2000; Stafford et al., 1995). The spectrum of $UTR^{fimbrin}$ did not display the characteristic α-helical intensities at 209 and 222nm instead the mutant spectrum appeared to be more β-sheet like in nature. It was apparent that the secondary structure of $UTR^{fimbrin}$ was not similar to that of the utrophin ABD. It is evident that $UTR^{fimbrin}$ contains significantly less α-helix than the utrophin ABD, SELCON analysis identifies a shift in secondary structure content demonstrating a significant increase in turn and unordered structures but also the β-sheet content. The near UV CD of $UTR^{fimbrin}$ indicated that the tertiary structure of the protein had been disrupted. The utrophin ABD gave a strong tryptophan signal that was not visible in $UTR^{fimbrin}$ indeed, it was apparent that $UTR^{fimbrin}$ did not exhibit any tertiary structure. The structural analysis continued via thermal denaturation of both utrophin ABD and $UTR^{fimbrin}$. This demonstrated that the utrophin ABD was denatured as temperature increased and that most of the secondary structure elements were recovered after cooling. $UTR^{fimbrin}$ did not display any loss of structure as the sample was heated. The fact that there was no significant near UV signal and that there was no change in the far UV signal suggests that the protein was incorrectly folded. The tryptophan fluorescence data demonstrated a red shifting in intensity which would be expected if tryptophan residues were exposed to the polar environment of the solvent (Vivian and Callis, 2001). The lack of correctly

folded structure was finally demonstrated via the investigation of $UTR^{fimbrin}$ resistance to proteolysis. The utrophin ABD appeared to be resistant to proteolysis by trypsin. Previous studies involving the limited digestion of the utrophin ABD with trypsin (Moores and Kendrick-Jones, 2000) demonstrated similar digestion patterns to those presented here (2.2.22.1). They determined that the resistance of the utrophin ABD to trypsin degradation was attributable to the compact nature of the utrophin ABD in solution. The $UTR^{fimbrin}$ mutant evidently does not possess this compact structure as it displayed no resistance to degradation by trypsin. Overall, it was assumed that $UTR^{fimbrin}$ was not folded correctly and hence was not suitable for further analysis; however, it was hoped that the $UTR^{\alpha\text{-actinin}}$ mutant would prove more successful.

Initial far UV CD data suggested that $UTR^{\alpha\text{-actinin}}$ did possess secondary structure but once again the spectra were not comparable to the wild type protein. As with $UTR^{fimbrin}$, none of the CH domain secondary structure had been targeted for mutation so it was expected that the CD spectra of $UTR^{\alpha\text{-actinin}}$ and wild type protein would be very similar. In fact, $UTR^{\alpha\text{-actinin}}$ spectra appeared to be more similar to the $UTR^{fimbrin}$ spectra. Thermal denaturation demonstrated that the mutant protein was very resistant to thermal denaturation. $UTR^{\alpha\text{-actinin}}$ could be heated to higher temperatures than the utrophin ABD and did not show a change in secondary structure that was observed with utrophin ABD denaturation. Interestingly, after cooling of $UTR^{\alpha\text{-actinin}}$ back to 20°C, the spectra suggested that the protein was now more α-helical in nature as there was a definite intensity present at 211 nm that was not observable prior to heating. Near UV CD of $UTR^{\alpha\text{-actinin}}$ demonstrated that there was some tertiary structure; however it was not at all comparable to the utrophin ABD. The tryptophan fluorescence of the wild type utrophin ABD was taken to be a signature for the correctly folded conformation of the ABD and $UTR^{\alpha\text{-actinin}}$ spectra should have been similar given that no aromatic residues were removed in the mutation. Tryptophan fluorescence confirmed that the environment of the aromatics had indeed changed. The fluorescence intensity of $UTR^{\alpha\text{-actinin}}$ had shifted from 334 to 338 nm and the intensity of the fluorescence had reduced by approximately 40 % compared to the wild type. This would be consistent with the tryptophan residues

becoming more solvent exposed and would indicate disruption of the CH domain structures as this is where these residues are located in the ABD.

Unfortunately the differences in the spectra suggest that, once again, the mutation of the linker region has caused the disruption of the overall structure of the mutant protein. It was hoped that the removal of residues would not be as disruptive to the overall structure of the ABD as addition of residues but it was apparent that this was not the case. No further analyses of the $UTR^{\alpha\text{-actinin}}$ mutant were performed and as neither of the mutant proteins were perceived to be folded correctly no actin binding experiments were attempted.

Unfortunately, it appears that the insertion of the extra residues into the inter-CH domain linker has disrupted the overall structure of the mutant proteins. The extension of the utrophin ABD linker to generate $UTR^{fimbrin}$ involved the addition of 11 residues inserted between residues 142 and 143 based on the utrophin crystal structure of Keep et al., 1999. This particular section of the protein is α-helical in nature and has been denoted the α6A helix. This particular helix is not directly part of either CH domain although it does follow the sixth α-helix of CH1. Referral to the fimbrin crystal structure (1AOA) determined by Hanein et al., indicated that the section of linker chosen for insertion into the utrophin ABD does not have any defined structure (Hanein et al., 1998). It appears that this section of the protein is formed by an extended loop of residues. Binding of the utrophin ABD to F-actin has been modelled to occur in a number of different open and extended conformations but also closed and compact conformations (Lehman et al., 2004) similar to the proposed binding to F-actin by the fimbrin ABD (Figure 4.1). The CH domain interface present in the fimbrin crystal structure is very similar to an interface generated within the utrophin ABD crystal dimer (Figure 4.1). This similarity has led to the idea that the utrophin ABD may open from a closed fimbrin like state in solution to bind F-actin in an extended manner although binding in a closed compact conformation may also occur.

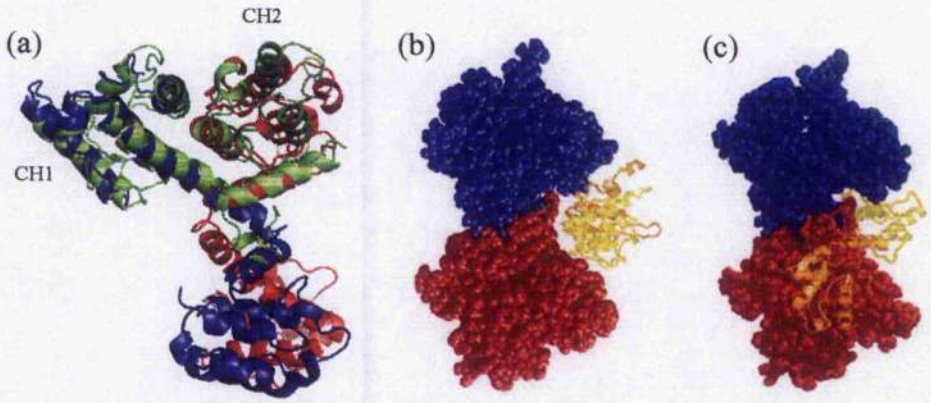

Figure 4.16: Structural superposition of fimbrin and utrophin ABDs and models of proposed actin-binding by these domains. (a) PyMol was used to superimpose the utrophin (Keep *et al.*, 1999b) and fimbrin (Goldsmith et al., 1997) crystal structures. The utrophin crystal monomers are represented in blue and red whereas fimbrin is represented in green. (b) Reconstruction of fimbrin ABD, comprising two CH domains, bound to F-actin (Hanein et al., 1998). (c) Reconstruction of utrophin ABD bound to F-actin in an open conformation at a density of 1:1 with actin (Moores et al., 2000). Both of these reconstructions were taken from Winder, 2003 (Winder, 2003) with actin monomers represented in blue and red whilst CH1 and CH2 of the ABDs are represented by yellow and orange respectively.

It was the similarity in the CH domain interface and the difference in the linker length that led to the production of the fimbrin linker mutant. It has become apparent though that the insertion of the fimbrin linker region into the utrophin ABD disrupts the structure of the inter-CH domain linker to such an extent that the overall structures of the CH domains that flank the mutation have been perturbed. This was not expected to occur but it is known that mis-sense mutations within the ABD of dystrophin can have dramatic affects on the structure and overall function of the domain. In these instances, for example, mutation of Leu54 to an arginine results in the destabilisation of the CH domain fold by the presence of a large charged side chain in an essentially hydrophobic environment (Prior et al., 1993). Another three mis-sense mutations are known that occur in BMD patients, all of which induce a destabilisation of a protein fold or the overall structure of the CH domain (Muntoni et al., 1994; Roberts et al., 1994). The position of the mutations suggests that the mutations affect the structure as none of the residues affected are directly involved in actin-binding (Norwood et al., 2000). The presence of a single point mutation within the utrophin ABD has also been found to have a dramatic effect on the function of

the whole domain. In this instance the domain was found to possess a substitution where a threonine was exchanged for a threonine at residue 113 (Winder et al., 1995). This caused the domain to bind actin in a 2:1 ratio however correction of the mutation back to wild type restored the normal stoichiometry (1:1). In hind sight, it may have been more favourable to insert a duplicated section of the utrophin ABD α6A helix which would maintain the helical nature of the linker and may have prevented the overall disruption of the domain. However, the existence of dystrophin ABD mutations resulting from relatively small mis-sense mutations and the large functional affects that a single point mutation can generate point towards the relative sensitivity of the ABD to mutation.

The utrophin ABD α-actinin linker mutant was generated following the investigation of $UTR^{fimbrin}$. It was hoped that the removal of the residues from the utrophin ABD would be less disruptive to the overall structure of the domain than addition. The inter-CH domain linker of the utrophin ABD was found to be 6 residues longer compared to the α-actinin linker. Seven residues were removed from the utrophin ABD (almost two complete helical turns) to form $UTR^{\alpha\text{-actinin}}$. These residues encompass amino acids 140 - 146 of the utrophin ABD structure (1QAG) (Keep *et al.*, 1999b). These residues form part of the α6A helix; essentially, the mutation would have shortened this helix by approximately two turns preventing any relative twisting of the CH domains with respect to one another. This would result in a reduction of the length of the α6A helix by approximately 10.8 Å (Creighton, 1996). The shortening of the utrophin linker was intended to model the manner of association that the α-actinin ABD may adopt when binding to F-actin. Interaction of α-actinin with actin has been proposed to occur in either open or closed conformations (Liu et al., 2004; Tang et al., 2001; Taylor and Taylor, 1993)but it was proposed that shortening of the utrophin ABD linker would reduce flexibility and disrupt CH domain association. This, in turn, may force the mutant utrophin ABD to adopt a more 'open' conformation in solution resulting in binding with F-actin in this manner. Figure 4.2 demonstrates the different conformations of smooth muscle α-actinin ABD within a 2D array of the protein and clearly depicts the different conformations that the domain may adopt when binding to F-actin.

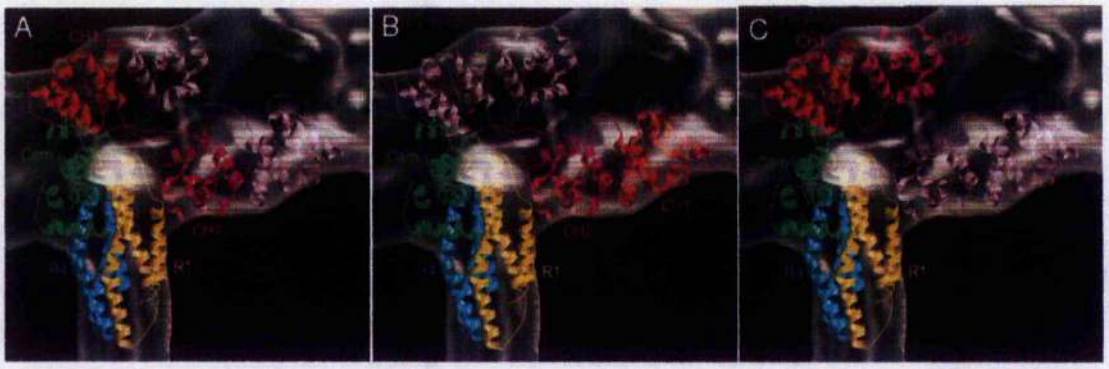

Figure 4.17: Cryo-Em reconstruction of the ABD of smooth muscle α-actinin. 2D arrays of smooth muscle α-actinin were used by Liu and colleagues to generate 3D images of α-actinin within the array lattice. Three possible interpretations of how the ABD may fit into the N-terminal densities are presented. A, depicts an open conformation involving domain swapping whereas B and C depict closed conformations without domain swapping. In each reconstruction the various domains present within α-actinin have been labelled accordingly (Liu et al., 2004).

Unfortunately, following expression and initial analysis of $UTR^{\alpha\text{-actinin}}$ it was determined that the overall structure of the protein was dissimilar to that of wild type protein. Removal of the linker residues had, once again, disrupted the structure of the mutant proteins ABD and rendered the protein unsuitable for any further biochemistry. It was believed that the removal of a relatively small number of residues within the ABD linker region would not affect the structure of the CH domains themselves but this was not found to be the case. Deletions of much larger regions of the dystrophin ABD can result in muscular dystrophy pathologies of varying severity. In frame deletions of exons 3 (residues 32-62) and 5 (residues 89-119) of the dystrophin gene have been characterised (Muntoni et al., 1994) and found to cause large scale affects on the structure and function of the protein (Norwood et al., 2000). In any case, recent crystal structures of the α-actinin ABD have been determined and depict the domain in a closed and compact fimbrin like conformation (Franzot et al., 2005). Superposition of the crystal structure in this conformation indicates that the overall CH domain architecture matches well (Figure 4.3); however, the shortened linker region does not adopt a helical conformation instead being formed from an extended loop. It is now clear that comparison of a shortened utrophin linker with the actual linker depicted in the α-actinin crystal structure would

not be correct although it is possible that the reduced number of residues may still restrict CH domain motion in manner relevant to the function and regulation of binding of α-actinin to F-actin.

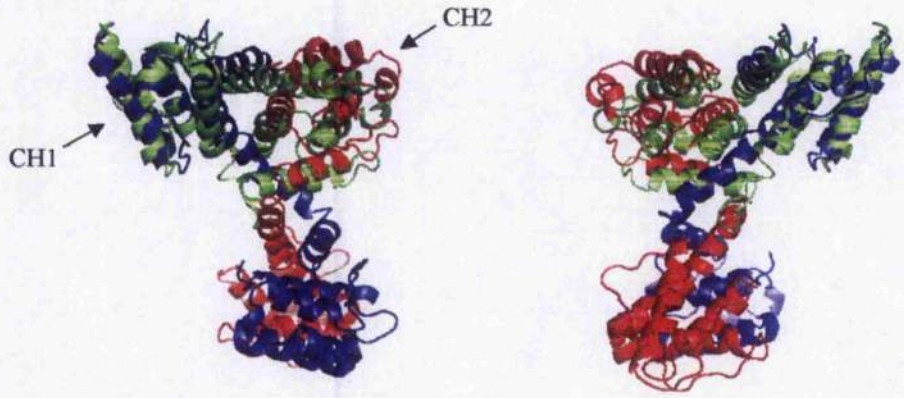

Figure 4.18: Structural superposition of the utrophin and α-actinin ABDs. PyMol was used to prepare a superposition of utrophin (Keep *et al.*, 1999b) and α-actinin (Franzot et al., 2005) ABD crystal structures. Two views are presented so that it is clear to identify the structural similarities exhibited by both proteins CH domains. The α-actinin crystal structure is represented in green whilst the two utrophin monomers are represented in blue and red. The CH domains have been labelled accordingly.

It is apparent that the linker region of the utrophin ABD is particularly sensitive to mutation. Both utrophin ABD linker mutants appeared to be structurally dissimilar to the wild type protein; this was not expected given the lack of mutation to the CH domains and the general stability of the protein domain fold. The structure of the CH domains is pivotal to the correct presentation of the actin-binding surfaces towards F-actin and any disruption to the domain fold would be detrimental to the overall function of the ABD (as proven by pathogenic mutation of the dystrophin ABD). It is clear that the linker region of the utrophin ABD is important not only for the connection of the CH domains but also has a significant relevance for the overall structure and function of the ABD.

Chapter 5:

Utrophin ABD Cysteine Mutants

Chapter 5

Utrophin ABD Cysteine Mutants

5.1 Introduction

The utrophin ABD appears to possess a certain degree of inherent flexibility. The isolated ABD is monomeric in solution and does not exhibit the dimeric organisation observed in the crystal structure. It is much more likely that the solution monomer is more similar to the fimbrin ABD crystal structure. Three dimensional domain swapping helps to describe how the interface between the CH domains of these two proteins is so similar but also suggests a significant importance to the linkers that join the domain swapped regions of the proteins (Schlunegger et al., 1997). Modelling the utrophin ABD when interacting with F-actin has relied upon a degree of assumed flexibility; it is apparent that the helical linker that connects the two CH domains is indeed flexible, given that the crystallised protein forms an anti-parallel dimer with the ABD of the two crystal monomers, adopting an open extended conformation. Conversely, the solution monomer may be more closed and compact perhaps adopting a conformation more akin to the crystal structure of fimbrin. In any case, the utrophin ABD has been modelled bound to F-actin in both an open and a closed conformation (Galkin et al., 2003; Moores et al., 2000; Sutherland-Smith et al., 2003). These studies have shown that interactions in these two modes do present the actin-binding sites of the protein towards the surface of F-actin. It is becoming increasingly clear that CH domain-containing-ABDs are required to be particularly dynamic upon interaction with F-actin. Recent work investigating the interaction of plectin with F-actin suggests a conformational change of the plectin ABD upon interaction with F-actin (Garcia-Alvarez et al., 2003). It is known that the CH domains that form ABDs are not equivalent in their ability to bind actin. Indeed, only the first CH domain of the utrophin ABD has the ability to bind F-actin, albeit weakly, the second CH domain does not (Gimona et al., 2002; Winder et al., 1995). The full binding of the domain is not achieved unless both CH1 and CH2 are present so it is clear that the second CH domain has an important role in either locating the domain on the surface of F-actin or the enhancement of the binding interaction. The modelling of the utrophin ABD when bound to F-actin in an

open conformation requires an induced fitting of the utrophin ABD crystal structure within the bound protein's electron density (Moores et al., 2000). This fitting requires the solution monomer to 'open' to allow association with F-actin. This conformational change must occur upon interaction with F-actin but will the utrophin ABD still associate with F-actin if the opening of the two CH domains can be restricted?

To test this hypothesis a double cysteine mutant of the utrophin ABD was designed that would allow the formation of a disulphide bond between CH1 and CH2, effectively locking the domain in the closed conformation. The mutant protein was subjected to a number of biochemical and biophysical analyses that would help to determine the effects of locking the ABD in the closed conformation. These data would provide further information on the manner in which the utrophin ABD interacts with F-actin.

5.2 Results

5.2.1 *Design of the utrophin ABD cysteine mutants.*

The utrophin ABD has been shown to be monomeric in solution (Moores and Kendrick-Jones, 2000), presumably adopting a compact configuration, but upon interaction with F-actin the molecule opens to associate in an extended conformation (Moores et al., 2000). In order to probe the necessity of this 'opening' for the actin interaction a double cysteine mutant of the utrophin ABD was designed that would allow covalent linkage of the two CH domains and prevent opening of the molecule. The location for the mutations was determined using the utrophin ABD crystal structure. The utrophin ABD was proposed to adopt a similar configuration to the fimbrin crystal when in solution; the utrophin ABD crystal is formed from an anti-parallel dimer; however, the CH1 and CH2 domains from the two different molecules form a similar interface to that observed in the fimbrin crystal (Keep *et al.*, 1999b). The utrophin ABD crystal structure was viewed using Rasmol and two residues were chosen that appeared to be orientated so that a disulphide bond could be formed if these residues were mutated to cysteines (Figure 5.1). Primers were then designed (Table 2.1) to allow the site directed mutation of these residues using the UTR261 pSJW1 construct. Initially, the T36C mutation was generated and

sequenced to confirm the correct substitution of the amino acid before being used to generate the double mutation by further site directed mutagenesis at S242. Following sequencing to confirm the presence of the correct mutations, the constructs were used to generate utrophin ABD containing both the single and double cysteine mutations denoted UTR^{T36C} and $UTR^{T36C/S242C}$ respectively.

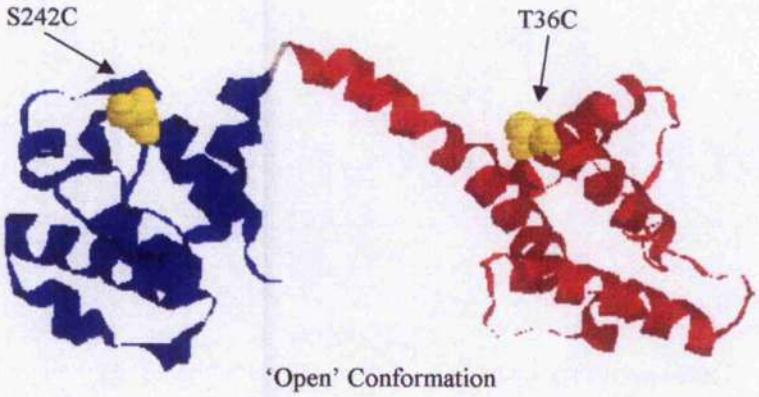

'Open' Conformation

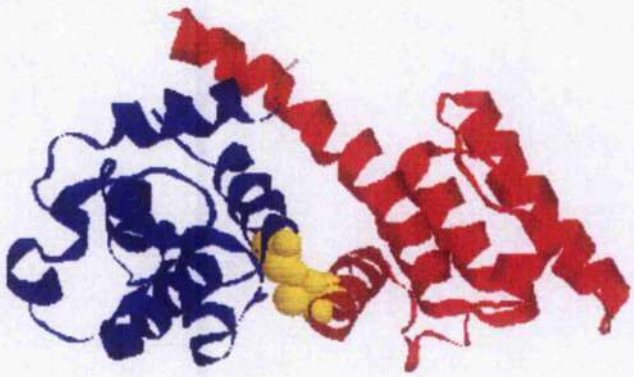

'Closed' Conformation

Figure 5.1: Location of the cysteine mutations within the utrophin ABD. Site directed mutagenesis was used to mutate threonine 36 and serine 242 to cysteine residues (yellow space-fill). CH1 and CH2 of the utrophin ABD are highlighted in red and blue respectively. The utrophin ABD is shown in the 'open' and 'closed' conformations based on the crystal structure of Keep and Winder et al., 1999.

5.2.2 *Expression of UTR^{T36C} and $UTR^{T36C/S242C}$ mutants*

UTR^{T36C} and $UTR^{T36C/S242C}$ pSJW1 constructs were transformed into freshly competent BL21 (DE3) *E. coli*. These bacteria were then grown and used to express the UTR261 cysteine mutants. Figure 5.2 demonstrates the expression of both UTR^{T36C} and $UTR^{T36C/S242C}$. Lane 1 and 2 of both panels represent pre and post induction sample after addition of IPTG. Both of the mutant proteins demonstrate a clear induction of protein generated. Lanes 3 and 4 demonstrate the soluble and insoluble protein fractions following bacterial lysis. Both UTR^{T36C} and $UTR^{T36C/S242C}$ are soluble although there does appear to be a proportion of both proteins that localises in the insoluble fraction. It is likely that the cellular debris generated by lysis was trapping a proportion of soluble protein within the pellet matrix. Following anion exchange and gel filtration chromatography a purified portion of both mutants is displayed in lane 5 of Figure 5.2. The UTR^{T36C} and $UTR^{T36C/S242C}$ mutants appear to be similar in size to the other mutants expressed in this study and the wild type utrophin ABD.

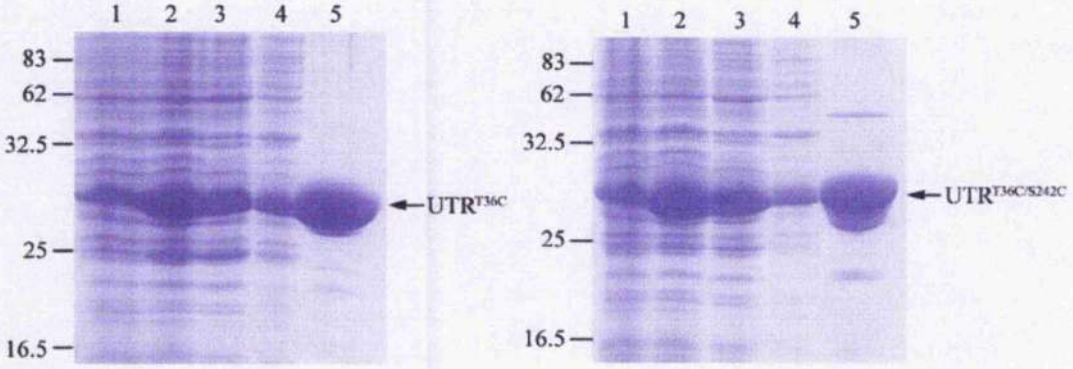

Figure 5.2: Expression, solubility and purification of UTR^{T36C} and $UTR^{T36C/S242C}$. Freshly competent BL21 (DE3) *E. coli* were transformed with the pSJW1 UTR^{T36C} and $UTR^{T36C/S242C}$ constructs. The bacteria were grown to a cell density of 0.6 at 600 nm before induction of protein expression via addition of IPTG. Protein present at pre and post induction are shown in lanes 1 and 2 respectively. After bacterial harvesting and lysis insoluble and soluble protein fractions are presented in lanes 3 and 4. Lane 5 represents a fraction of the purified mutant proteins. Molecular weight markers (kDa) are shown to the left of each gel and the protein band representative of each mutant is indicated.

5.2.3 *SDS PAGE and western analysis of UTR^{T36C} and UTR$^{T36C/S242C}$ mutants*

Following expression and purification of the UTR^{T36C} and UTR$^{T36C/S242C}$ mutants SDS PAGE and western analysis was used to compare the mutants with wild type utrophin ABD (UTR261) (Figure 5.3). SDS PAGE analysis of the mutants indicates that they are identical in size to wild type utrophin ABD; approximately 30 kDa (Moores and Kendrick-Jones, 2000; Winder and Kendrick-Jones, 1995). This would be expected given that only one or two amino acids (depending on the mutant) have been substituted for cysteines. The change in MW generated by these substitutions would not be sufficient to cause a size shift identifiable by SDS PAGE. Western analysis (Figure 5.3, right hand panel) indicates that the UTR^{T36C} and UTR$^{T36C/S242C}$ mutants are detectable using the utrophin antibody raised against the wild type ABD.

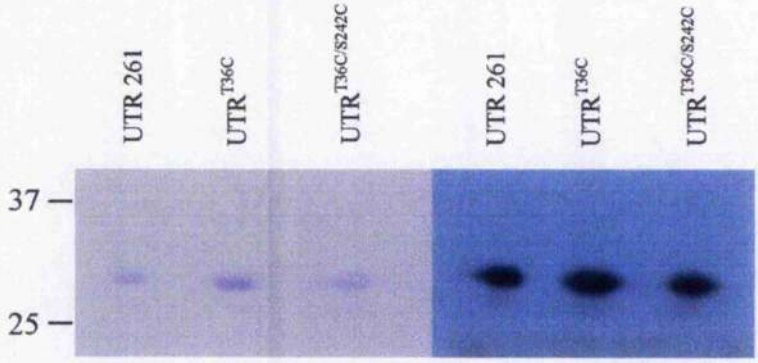

Figure 5.3: SDS PAGE and western analysis of UTR^{T36C} and UTR$^{T36C/S242C}$. 1 µM samples of UTR261, UTR^{T36C} and UTR$^{T36C/S242C}$ were prepared. 2 x sample buffer was added to these samples and 10 µl was loaded onto a 15 % acrylamide gel. Following separation the proteins were transferred to nitrocellulose ready for western blotting with the utrophin antibody (right hand panel). An identical acrylamide gel was run to allow comparison of the mutant proteins via Coomassie Blue staining (left hand panel). Molecular weight markers (kDa) are shown to the left.

5.2.4 *NTCB digestion of UTR$^{T36C/S242C}$*

Sequencing of UTR^{T36C} and UTR$^{T36C/S242C}$ confirmed the presence of the cysteine mutations but NTCB digestion was also used to demonstrate the presence of cysteines in the purified proteins. NTCB cleaves specifically at cysteine residues (Jacobson et al., 1973) and the presence of the amino acid within the peptide chain of

the cysteine mutants will allow peptide fragments to be generated that would not occur in UTR261 which, contains no cysteine (Jacobson et al., 1973). Figure 5.4 demonstrates the NTCB cleavage of UTR261 and $UTR^{T36C/S242C}$. It is clear that the digestion of utrophin ABD has not been possible as there was no appreciable reduction of full length utrophin ABD when in the presence of NTCB. The $UTR^{T36C/S242C}$ sample in the absence of NTCB shows no appreciable digestion; however, addition of NTCB has almost completely digested full length $UTR^{T36C/S242C}$ resulting in the formation of two peptide fragments that are approximately 26 and 27 kDa in size. This experiment clearly demonstrates the presence of the cysteines within the $UTR^{T36C/S242C}$ mutant.

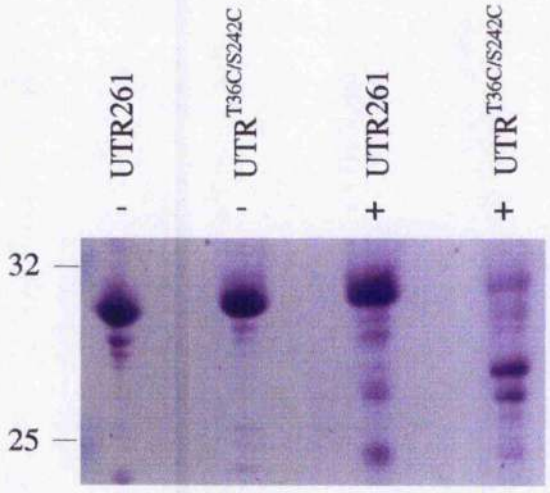

Figure 5.4: NTCB digestion of utrophin ABD and $UTR^{T36C/S242C}$. A 20 μM sample of UTR261 and $UTR^{T36C/S242C}$ denatured in 6M urea in TE pH 8.0 was incubated with a ten-fold excess of NTCB for 1 at room temperature. Following adjustment to pH 9.0 the samples were incubated at 30°C for three hours. Following digestion samples were subjected to SDS PAGE and the cleavage products visualised using Coomassie Blue staining. Samples of UTR261 and $UTR^{T36C/S242C}$ are indicated in the presence (+) and absence (-) of NTCB. Molecular weight markers (kDa) are shown to the left of the figure.

5.2.5 *Formation of the disulphide bond within $UTR^{T36C/S242C}$*

Sequencing and NTCB digestion have clearly demonstrated that $UTR^{T36C/S242C}$ contained two cysteine residues in the correct positions. It was necessary to demonstrate that these cysteines were capable of forming a disulphide bond, thus locking the mutant protein in a closed conformation. To allow the formation of the

disulphide all reducing agents were removed from the protein solution via extensive dialysis. To promote oxidation and formation of the disulphide bond copper sulphate and phenanthroline were used as described in section 2.2.26. Two oxidation methods were attempted; one involving a drop-wise addition of the reagents and one involving overnight dialysis. The dialysis method was found to be the least likely to cause protein aggregation. Figure 5.5 demonstrates two separate sets of protein samples that have been subjected to oxidation. The figure clearly demonstrates that UTR261 and UTR^{T36C} do not experience a size shift after oxidation. There was the potential for the single and double cysteine mutants to form disulphides with other protein molecules; however, SDS PAGE and gel filtration analysis (Section 5.2.6) did not find this to occur. The $UTR^{T36C/S242C}$ samples that were subjected to oxidation demonstrate a clear shift in size when compared to UTR261 and UTR^{T36C}. This shift appears to suggest that the disulphide does form in $UTR^{T36C/S242C}$ as the oxidised protein samples run slightly faster when subjected to SDS PAGE (Figure 5.5).

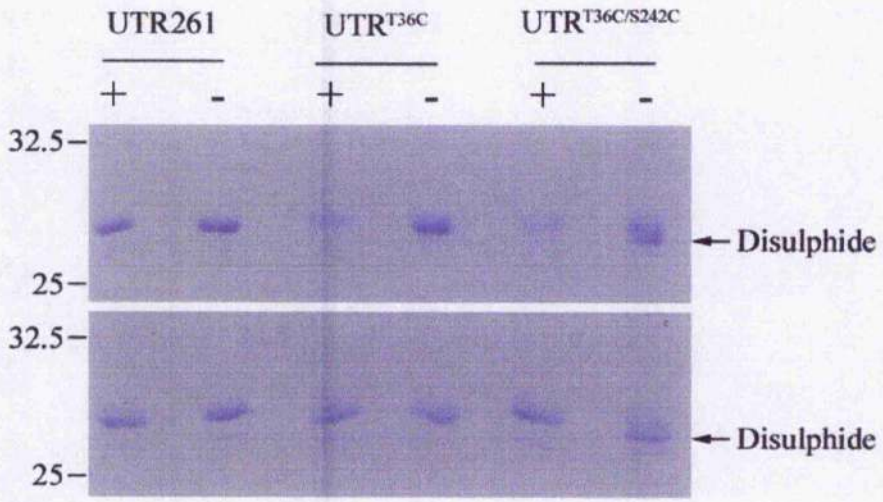

Figure 5.5: Oxidation of $UTR^{T36C/S242C}$ to form the disulphide bond. Solutions of UTR261, UTR^{T36C} and $UTR^{T36C/S242C}$ were oxidised by dialysis with a solution containing 1 mM $CuSO_4$ and 4 mM phenanthroline. All solutions were prepared in TE pH 8.0 and no DTT was present. After overnight oxidation samples of each protein were prepared for SDS PAGE by addition of reducing (+) and non-reducing (-) sample buffer. Samples were run on a non-reducing gel for comparison. Protein bands were visualised using Coomassie Blue staining. The experiment was duplicated and the position of the disulphide linked protein has been indicated. Molecular weight markers (kDa) are shown to the left.

Figure 5.6 demonstrates a $UTR^{T36C/S242C}$ sample at higher concentration that has been oxidised. It is clear that there was a size shift in the oxidised protein although it is apparent that not all of $UTR^{T36C/S242C}$ remains in the oxidised form. It is possible that the close proximity of the reduced sample lane has allowed partial reduction of the oxidised sample. In the presence of the oxidising agents all of the $UTR^{T36C/S242C}$ sample were observed to form the disulphide however, removal of oxidant does allow some protein to remain in a none cross-linked state (data not shown) and therefore, it is feasible that the $UTR^{T36C/S242C}$ sample contains a proportion of protein that does not form the disulphide.

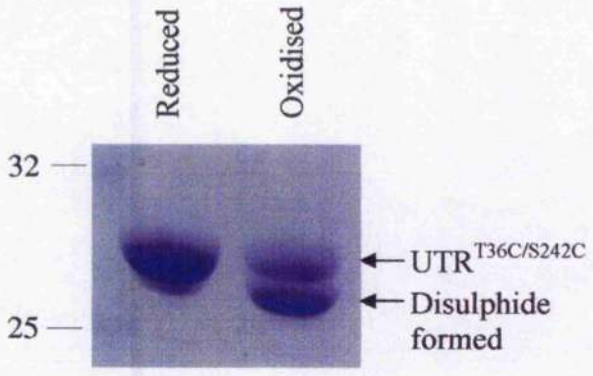

Figure 5.6: Oxidised and reduced samples of $UTR^{T36C/S242C}$. Oxidised and reduced samples of $UTR^{T36C/S242C}$ are shown following SDS PAGE using a non-reducing gel. The position of $UTR^{T36C/S242C}$ after disulphide formation is indicated and molecular weight markers (kDa) are shown to the left.

5.2.6 *Gel filtration analysis of utrophin ABD and the UTR^{T36C} and $UTR^{T36C/S242C}$ mutants.*

The utrophin ABD is known to behave as a monomer when in solution however, the introduction of cysteines into the domain generates the potential for oligomerisation. The double cysteine mutant was designed to allow the formation of a disulphide between the two CH domains of the ABD. It is possible, if the ABD does not adopt a closed and compact conformation when in solution, that a disulphide may form with another molecule of utrophin ABD. To investigate if this was possible analytical gel filtration was utilised to determine if oligomers of the cysteine mutants were occurring in solution. Samples of utrophin ABD, UTR^{T36C} and

$UTR^{T36C/S242C}$ in the reduced and oxidised conformations (disulphide formed) were run through a calibrated analytical gel filtration column (Section 2.2.20). The relative MW of each protein was calculated to evaluate the relative size of the proteins when in solution (Table 5.1).

The relative MW of each protein was comparable to literature values and those previously determined in section 3.2.1. It appears that utrophin ABD and UTR^{T36C} are slightly larger than $UTR^{T36C/S242C}$ in either the oxidised or reduced form. This may suggest that the solution monomer was less compact than $UTR^{T36C/S242C}$ although, the introduction of the disulphide does not seem to result in the $UTR^{T36C/S242C}$ mutant becoming more compact than the reduced form. Most importantly, all proteins eluted as a single species, with no visibly larger peaks present on the gel filtration elution profiles. Hence, the presence of cysteine residues within the mutated ABDs does not result in protein oligomerisation.

	UTR ABD	UTR^{T36C}	$UTR^{T36C/S242C}$	$UTR^{T36C/S242C}$ ox
MW (kDa)	29.4 ± 0.03	29.5 ± 0.06	28.0 ± 0.14	28.2 ± 0.14

Table 5.1: Relative MW of the utrophin ABD, UTR^{T36C} and $UTR^{T36C/S242C}$ mutants following gel filtration analysis. Samples of utrophin ABD, UTR^{T36C} and $UTR^{T36C/S242C}$ were subjected to gel filtration analysis using a calibrated Superose 12 HR gel filtration column under control of an Akta FPLC system. Two sets of samples were run for $UTR^{T36C/S242C}$: one set was not oxidised prior to the run whereas the other contained $UTR^{T36C/S242C}$ with the disulphide formed (ox). The elution volume of each protein after loading was used to determine the relative molecular weight of each protein. Protein samples were ran at 0.4 ml/min in TE pH 8.0 and 200 mM NaCl. Standard error was calculated (n = 3).

5.2.7 *Actin-binding analysis of $UTR^{T36C/S242C}$*

The utrophin ABD has been shown to associate with F-actin with a moderate affinity (K_d approximately 20 μM) and a binding stoichiometry of 1:1 (Keep *et al.*, 1999a; Winder *et al.*, 1995). Models of the utrophin ABD when associated with F-actin favour an open mode of association where the molecule appears to bind across actin subdomain 1 with CH1 lying between two actin monomers (Moores et al.,

2000). The opening of the ABD to present the actin-binding sites towards F-actin would be prevented in the oxidised $UTR^{T36C/S242C}$ mutant. The disulphide bond would prevent the dissociation of CH1 and CH2 forcing the molecule to bind F-actin in a closed conformation or possibly not at all. High speed co-sedimentation assays were performed with the $UTR^{T36C/S242C}$ mutant in the oxidised or reduced form to assess the affect the disulphide may have upon actin binding. The actin-binding data generated are presented in Figure 5.7.

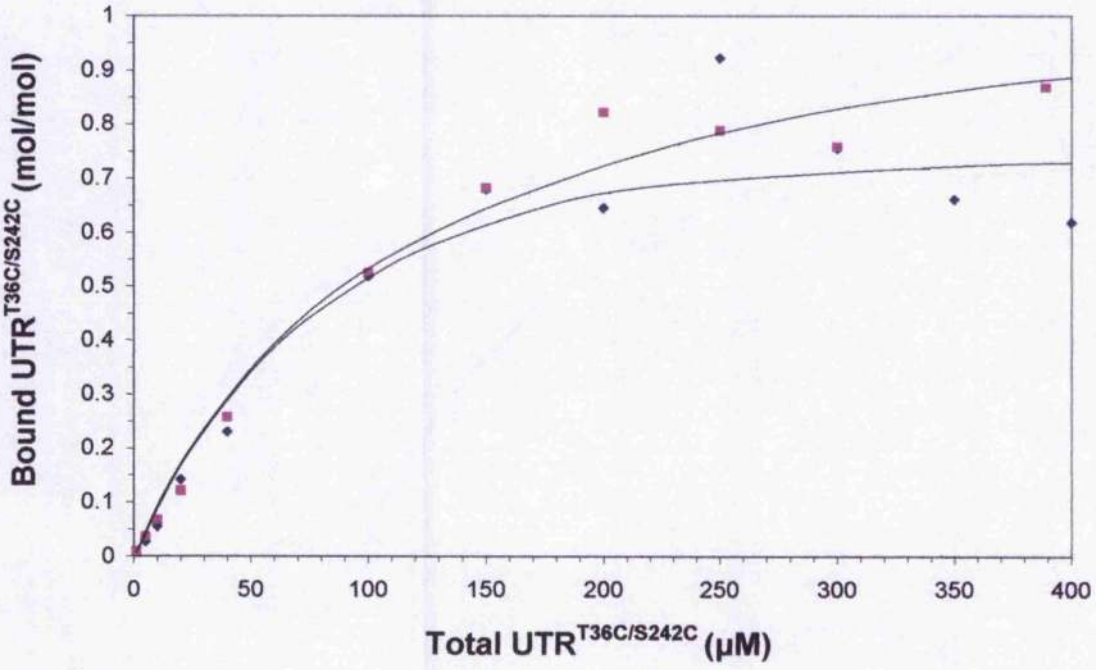

Figure 5.7: $UTR^{T36C/S242C}$ actin-binding curves determined with oxidised and reduced forms of the protein. $UTR^{T36C/S242C}$ in the disulphide formed (oxidised; magenta) and reduced (blue) state was subjected to high speed co-sedimentation assay (n = 3). A range of $UTR^{T36C/S242C}$ concentration (1 - 400 μM) was titrated with 5 μM F-actin (Winder et al., 1995). Soluble and insoluble protein fractions were separated and subjected to SDS PAGE; Coomassie Blue staining was used to visualise the separated protein. The proportion of $UTR^{T36C/S242C}$ that bound F-actin was calculated from gel densitometry measurements of the Coomassie stained gels (NIH Image). Binding affinities and stoichiometries were determined using a Michaelis-Menten-type fitting. Error bars are omitted for clarity.

The co-sedimentation data suggest that the oxidised $UTR^{T36C/S242C}$ mutant does retain the ability to bind to F-actin. This is surprising although not unlikely as the ABD of fimbrin and α-actinin has been modelled to associate with F-actin in a closed conformation (Hanein et al., 1998; McGough et al., 1994). Cryo-EM

reconstructions of the utrophin ABD bound to F-actin have determined that it is possible to fit a structure of the proposed utrophin ABD solution monomer into the electron densities associated with F-actin (Moores et al., 2000; Sutherland-Smith et al., 2003). The positioning of the compact model appeared to fit reasonably well however, the orientation of the molecule was significantly different to the proposed orientation that fimbrin would adopt when associating with F-actin (Moores et al., 2000). It has also been found that the ABD of plectin also retains the ability to associate with F-actin when the CH domains are linked by a disulphide (Garcia-Alvarez et al., 2003).

The binding affinities and stoichiometries of the oxidised and reduced forms of $UTR^{T36C/S242C}$ also differ from that of the wild type protein (Table 5.2). The binding stoichiometry of the reduced form is identical to the wild type protein however; the oxidised form of the mutant displays a slightly higher value of approximately 1.2:1 (Table 5.2). This value is not greatly dissimilar but the increase may be significant when considering that the association with F-actin occurs when the utrophin ABD is in a closed conformation. Interestingly, binding of a utrophin ABD construct that lacked the first 27 N-terminal residues also displayed a similar stoichiometry (1.29 ± 0.08) but essentially, the stoichiometry was 1:1 (Keep *et al.*, 1999a). Garcia-Alvarez and colleagues did not determine a binding stoichiometry of the plectin ABD when binding F-actin however; the binding affinities are significantly different between the reduced and oxidised forms of the protein (Garcia-Alvarez et al., 2003).

	UTR ABD	$UTR^{T36C/S242C}$ red.	$UTR^{T36C/S242C}$ ox.
K_d (μM)	19.2 ± 2.2 μM	74.8 ± 19.2 μM	123 ± 14.1 μM
Stoichiometry	1:1 ± 0.06	1:1 ± 0.06	1.2:1 ± 0.06

Table 5.2: Binding affinity and stoichiometry of reduced and oxidised $UTR^{T36C/S242C}$ compared with wild type utrophin ABD. The calculated stoichiometries and binding affinities of the $UTR^{T36C/S242C}$ mutant when in the reduced and oxidised form are compared to literature values of utrophin ABD determined by Winder and colleagues (Winder *et al.*, 1996). Michaelis-Menten-type fitting was used to determine the respective affinities and stoichiometries. Standard error is shown (n = 3).

This was found to be the case with the oxidised and reduced forms of $UTR^{T36C/S242C}$. In the reduced form $UTR^{T36C/S242C}$ bound F-actin with a lower affinity than the wild type protein (K_d = 74.8 ± 19.2 μM) suggesting that the cysteine

mutations were disrupting binding to F-actin. The affinity of the oxidised mutant was significantly lower than the reduced form (K_d = 123 ± 14.1 μM) suggesting that the formation of the disulphide made association with F-actin less favourable. A similar reduction in the binding affinity was also observed when the plectin ABD was locked in the closed conformation by a disulphide bond. In this situation the affinity of the plectin ABD reduced by a factor of two although the initial affinity of the ABD for F-actin was identical to that of the wild type protein (Garcia-Alvarez et al., 2003).

It is apparent that the utrophin ABD retains the ability to bind to F-actin even when the domain is prevented form opening by locking the two CH domains together using a disulphide bond. This is interesting given that it is clear that F-actin bound utrophin ABD demonstrates clear electron density attributable to either extended or compact modes of association (Moores et al., 2000; Sutherland-Smith et al., 2003).

5.2.8 *Labelling $UTR^{T36C/S242C}$ with fluorescein and rhodamine*

Generation of the utrophin ABD double cysteine mutant has allowed the investigation of the constraints a disulphide bond imposes upon the F-actin interaction. Wild type utrophin ABD does not contain cysteine but the generation of the double cysteine mutant allows further analysis of the utrophin ABD conformation via the conjugation of fluorescent labels to the cysteine residues in the mutant proteins.

The utrophin ABD has been shown to be monomeric in solution. If the domain adopts a compact conformation in solution where the two CH domains are in close association then it should be possible for fluorescence resonance energy transfer (FRET) to occur between a donor and an acceptor chromophore conjugated to the cysteine residues of $UTR^{T36C/S242C}$. The two fluorophores were chosen that exhibit a suitable spectral overlap that would allow FRET to occur. These two fluors were fluorescein-5-maleimide and tetramethylrhodamine-6-maleimide (rhodamine). These two fluors form a donor/acceptor pair that achieves maximal energy transfer over a Förster radius (R_o) of approximately 55 Å (Molecular probes handbook). The labelling of $UTR^{T36C/S242C}$ with both fluors was achieved by the selective reduction of the cysteine thiol groups using TCEP. The maleimide conjugated fluors react in a

thiol-selective manner allowing specific labelling only at the cysteine residues. Once conjugation was complete excess un-conjugated fluor was removed via extensive dialysis before the extent of labelling could be determined (Section 2.2.28).

Figure 5.8 demonstrates that the conjugation of both fluors to $UTR^{T36C/S242C}$ either individually, or as a mix, was possible. A solution of purified $UTR^{T36C/S242C}$ either singly labelled with fluorescein, rhodamine or a mix of both can be seen after the samples were subjected to SDS PAGE. The Coomassie Blue stained gel demonstrates that the protein-dye conjugates are all loaded equally and the labelled protein was of the expected size (approximately 30 kDa). The lower panel of Figure 5.8 shows the SDS PAGE gel prior to Coomassie Blue staining viewed when placed over a UV light box. It is clear that $UTR^{T36C/S242C}$ conjugated to fluorescein of rhodamine emits a green or red fluorescence respectively, whereas the double labelled protein emits a yellow fluorescence (combination of green and red). The extent of labelling for all protein samples was then determined (Section 2.2.27). It was calculated that $UTR^{T36C/S242C}$ was labelled with rhodamine at a ratio of 1:0.81 whereas fluorescein labelling was approximately 1:2. The doubly labelled protein was labelled with rhodamine and fluorescein at ratios of 0.48:1 and 0.78:1 respectively.

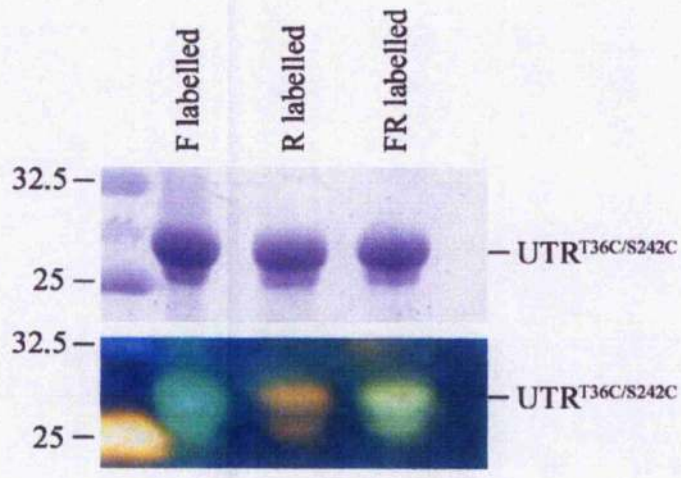

Figure 5.8: Successful labelling of $UTR^{T36C/S242C}$ with rhodamine and fluorescein. $UTR^{T36C/S242C}$ was labelled with either rhodamine (red), fluorescein (green) or a mixture of both (yellow). Samples of $UTR^{T36C/S242C}$ labelled with each fluor were subjected to SDS PAGE. A UV light box was used to demonstrate successful conjugation of the fluors to $UTR^{T36C/S242C}$ (lower panel) before Coomassie Blue staining of the gel was performed to visualise the protein present. Molecular weight markers (kDa) are shown to the left.

5.2.9 *Fluorescence Resonance Energy Transfer between fluorescein and rhodamine conjugated to $UTR^{T36C/S242C}$.*

Before the actual FRET experiment was attempted it was necessary to check that the conjugated chromophores were detectable spectroscopically and that the fluorescent signal generated from the samples was attributable to the fluors and not $UTR^{T36C/S242C}$ or a buffer component. Appendix 7 demonstrates excitation and emission spectra of $UTR^{T36C/S242C}$ that have been labelled with either rhodamine or fluorescein. In both instances, neither fluor emitted a significant fluorescence signal after collection of excitation and emission spectra at the wavelengths of the opposite fluor. Once this was established, a mix of the two $UTR^{T36C/S242C}$ samples labelled with either rhodamine or fluorescein was prepared. The known extent of labelling was then used to adjust the quantity of each labelled protein that was added so that equivalent proportions of each fluor were present within the final sample of labelled $UTR^{T36C/S242C}$. Excitation and emission spectra of this sample were collected to determine if there was any FRET between the $UTR^{T36C/S242C}$ solution monomers labelled with either fluorescein or rhodamine (Figure 5.9).

It is apparent that the fluorescence of the rhodamine excitation and emission spectra are much larger than those of fluorescein. This indicated that the proportion of fluorescein labelled protein was less than expected even though it was attempted to add an equivalent amount of fluor when preparing the $UTR^{T36C/S242C}$ mixture. In any case, it does not appear that there was any FRET between the singly labelled $UTR^{T36C/S242C}$. FRET would be expected when the sample was excited at 494 nm. This would excite fluorescein allowing FRET to rhodamine which should generate a rhodamine emission intensity at approximately 580 nm (Lakowicz, 1999). This does not appear to occur although there is a fluorescence intensity produced at approximately 565 nm after excitation at 494 nm.

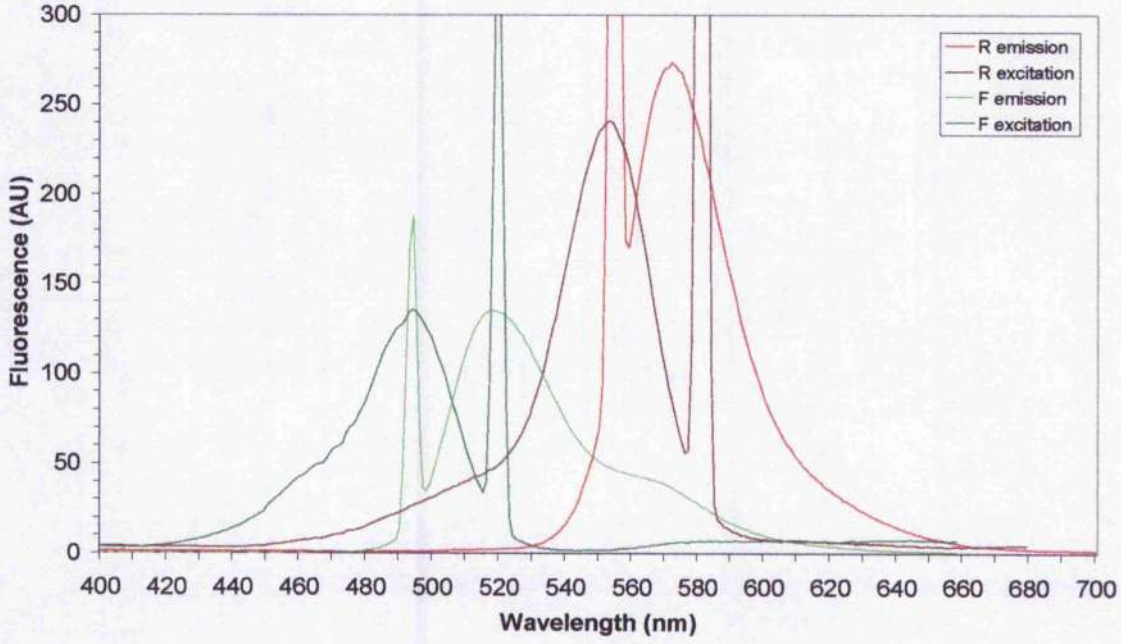

Figure 5.9: Fluorescence spectra of a mixture of UTR$^{T36C/S242C}$ labelled with either fluorescein or rhodamine. 30 μM samples containing both fluorescein (F) and rhodamine (R) labelled UTR$^{T36C/S242C}$ were examined for fluorescence at the emission and excitation wavelengths of both fluorescent conjugates. Spectra were collected at a slow scanning speed with excitation and emission slit widths of 1.5 nm. Excitation and emission wavelengths are as follows: fluorescein, 494 and 518 nm respectively; rhodamine, 555 and 580 nm respectively. Fluorescence is shown in arbitrary units (AU).

It was clear that there was no FRET between a mixture of singly labelled protein. If there was to be FRET intra-molecularly then the two fluors would need to be close enough and orientated correctly to allow energy transfer (Berney and Danuser, 2003). Figure 5.10 demonstrates a sample of doubly labelled UTR$^{T36C/S242C}$ that has been scanned at the fluorescein and rhodamine emission wavelengths. A FRET signal would be expected at 580 nm after excitation at 494 nm. There is a fluorescent intensity at approximately 570 nm but this is not attributable to FRET. Comparison of the relative fluorescence of this shoulder peak with the similar peak visible in the mix of singly labelled proteins (Figure 5.9) indicated that, proportionally, the peaks were of equivalent size when compared to the larger fluorescein excitation peak at 518 nm. Therefore, it is apparent that there is no significant FRET between the two fluors. Fluorescein and rhodamine have been used previously to determine molecular distances and to determine protein interactions

over much larger distances that were attempted here (Johnson et al., 1984; Kosk-Kosicka et al., 1989). The effects of cAMP and kinase inhibitor on the association of the catalytic subunits of cAMP-dependant protein kinase demonstrated that fluorescein and rhodamine were suitable candidates for the study of protein subunit interaction (Lakowicz, 1999). Essentially, CH1 and CH2 are protein subunits that interact with each other therefore; it should have been possible to demonstrate FRET if the fluors were suitably positioned (Wu and Brand, 1994). It is apparent that the fluors are not able to interact and hence, it is likely that the positioning of the fluors within $UTR^{T36C/S242C}$ do not permit FRET to occur.

The utrophin ABD is an actin-binding protein: F-actin was added to the double labelled protein in an attempt to determine the affects of actin binding on the fluorescence of the fluors. Initially, it was hoped that a FRET signal would be generated when the labelled $UTR^{T36C/S242C}$ was in solution and that this signal would be altered upon interaction with F-actin. As FRET can be used to determine inter-atomic distances the technique has many uses for the investigation of structural and conformational change in proteins (Heyduk, 2002). However, there was no FRET signal when $UTR^{T36C/S242C}$ was in solution and this continued to be the case when F-actin was added. The lower panel of Figure 5.10 demonstrates the spectra collected at fluorescein and rhodamine excitation and emission wavelengths. A sample of F-actin was scanned previously at the emission and excitation wavelengths of the fluors to determine if there was any auto-fluorescence of the sample; none was found (Appendix 8).

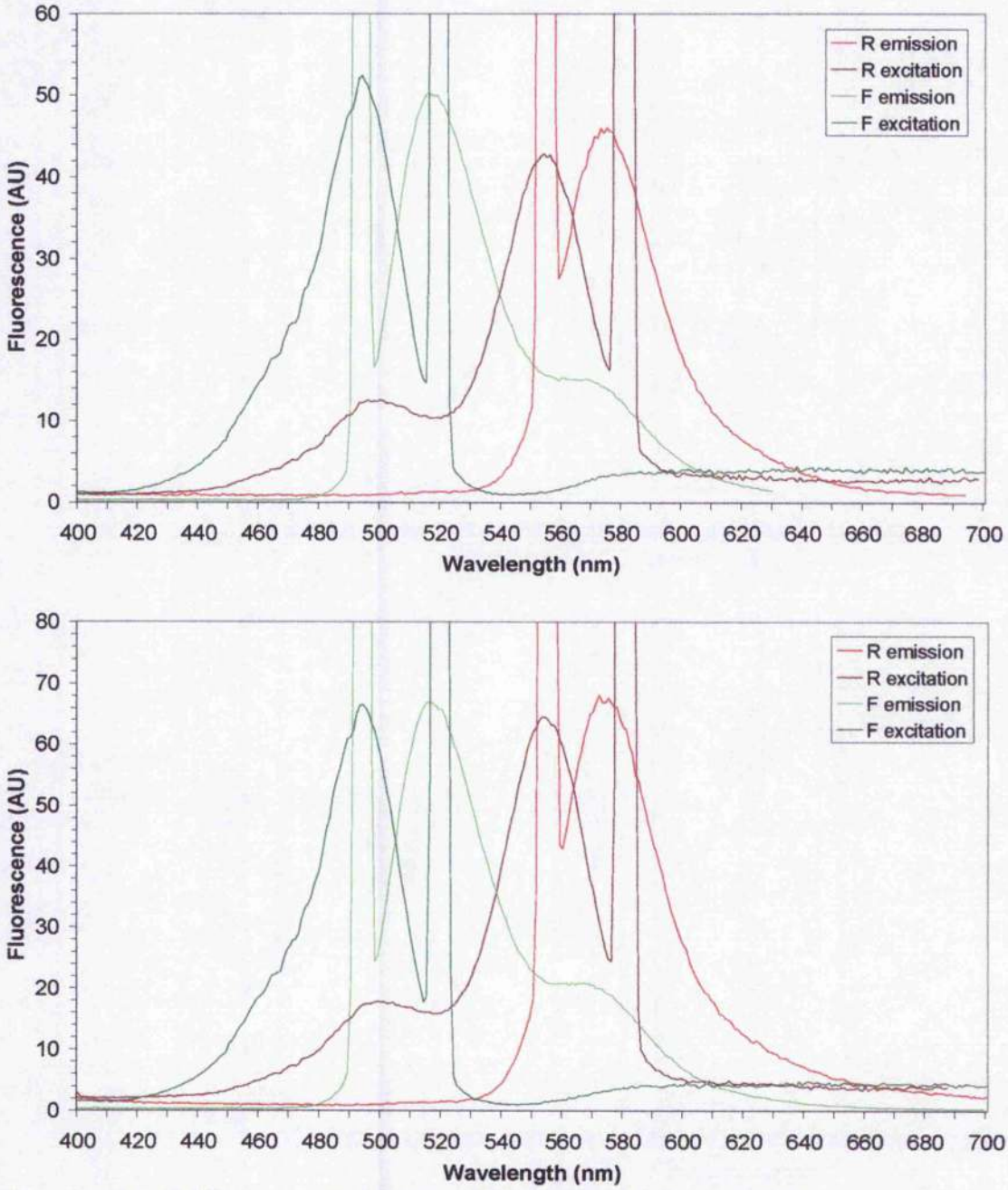

Figure 5.10: Fluorescence spectra of $UTR^{T36C/S242C}$ labelled with fluorescein and rhodamine. 30 μM samples of $UTR^{T36C/S242C}$ labelled with equal proportions of rhodamine and fluorescein were scanned at the excitation and emission wavelengths for both fluorescent conjugates (fluorescein: 404 and 518 nm; Rhodamine: 555 and 580 nm). All scans were performed at a slow speed and emission and excitation slit widths were 1.5 nm. The data demonstrates spectra collected in the absence of F-actin (top panel) and after addition of F-actin to a final concentration of 5 μM (bottom panel). All experiments were performed in TE pH 7.0 and 1 x ABB.

5.2.10 *Comparison of tryptophan fluorescence between UTR^{T36C}, $UTR^{T36C/S242C}$ and wild type utrophin ABD*

The intrinsic fluorophores of a protein may be of use when determining a conformational change or the effects of a mutation (Chen and Barkley, 1998; Vivian and Callis, 2001). The utrophin ABD contains six tryptophan residues that could be useful in determining the affects of the cysteine mutations introduced into the utrophin ABD and may yield information regarding the interaction of the domain with F-actin. To allow comparison of the tryptophan fluorescence of wild type protein with that of the oxidised and reduced forms of $UTR^{T36C/S242C}$ initial fluorescent scans were performed with the wild type protein in the presence and absence of F-actin (Figure 5.11). These scans demonstrate that the fluorescence associated with individual samples of the utrophin ABD and F-actin and a mixture of the two where the utrophin ABD would be expected to bind to F-actin. The fluorescent maxima of F-actin (332 nm) was slightly blue shifted compared to that of utrophin (334 nm); however, the combined sample displayed a maximum identical to the utrophin ABD alone (334 nm). The sample where utrophin ABD was bound to F-actin was found to exhibit a tryptophan fluorescence that was less than the sum of the two proteins alone. This probably results from a degree of tryptophan fluorescence quenching occurring upon interaction of the two proteins. It is difficult to determine what proportion of the total fluorescence would result from either of the proteins given the multiple number of chromophores present within the structure of each but it may provide a method for comparing the association of the cysteine mutants with F-actin and the wild-type protein binding. A similar method was used by Garcia-Alvarez and colleagues to monitor the binding of the plectin ABD to F-actin (Garcia-Alvarez et al., 2003).

Samples of each cysteine mutant and the wild type utrophin ABD were scanned for tryptophan fluorescence in the presence and absence of F-actin (Figure 5.12). The spectra demonstrated that the presence of cysteine and the formation of absence of the disulphide bond resulted in a marked difference in the fluorescent intensity generated by the tryptophan residues. The fluorescent maxima were also found to vary slightly from the value obtained from the wild type ABD signifying an alteration in the local environment of some of the tryptophan residues. Cysteine has

been shown to be an efficient quencher of tryptophan fluorescence (Gonnelli and Strambini, 1995).

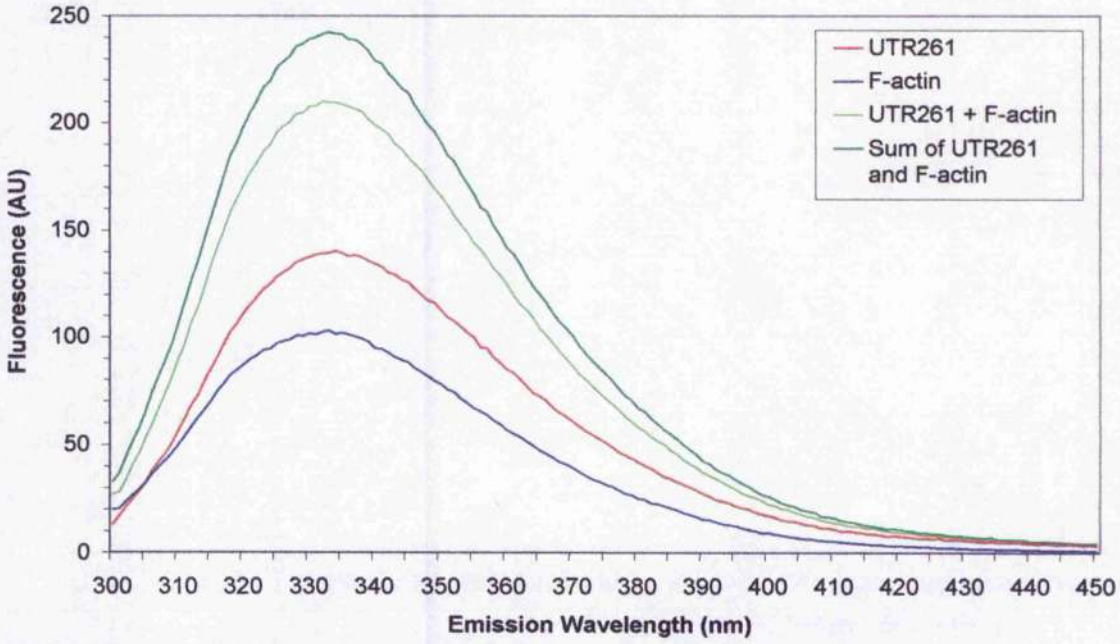

Figure 5.11: Intrinsic tryptophan fluorescence of the utrophin ABD in the presence and absence of F-actin. 30 μM samples of utrophin ABD were excited at 296 nm and the resultant tryptophan fluorescence recorded between 300 and 450 nm. All scans were performed at a slow scanning speed with excitation and emission sit widths set to 1 nm. All samples were prepared in TE pH 8.0 in the presence of 1 x ABB. F-actin was added to a final concentration of 5 μM. Spectra of utrophin ABD and F-actin are demonstrated alongside a solution of utrophin ABD/F-actin and the sum of fluorescent spectra of the individual proteins. Tryptophan fluorescence is represented in arbitrary units (AU).

The proximity of this amino acid to tryptophan produces a quenching affect that has been used to measure the formation of specific intra-molecular contacts (Buscaglia et al., 2003). In this study it is apparent that the cysteine present in the UTR^{T36C} and $UTR^{T36C/S242C}$ mutants has produced a quenching effect towards the tryptophan fluorescence of these proteins. The utrophin ABD contains six tryptophans located at the positions highlighted in Figure 5.13. The cysteine mutations are located at residues 36 and 242 of the utrophin ABD. The utrophin ABD is displayed in the open crystal conformation; it is apparent that tryptophan residues 40 and 128 are particularly close to the cysteine mutation at S36; and may be amenable to cysteine quenching of the fluorescence they produce.

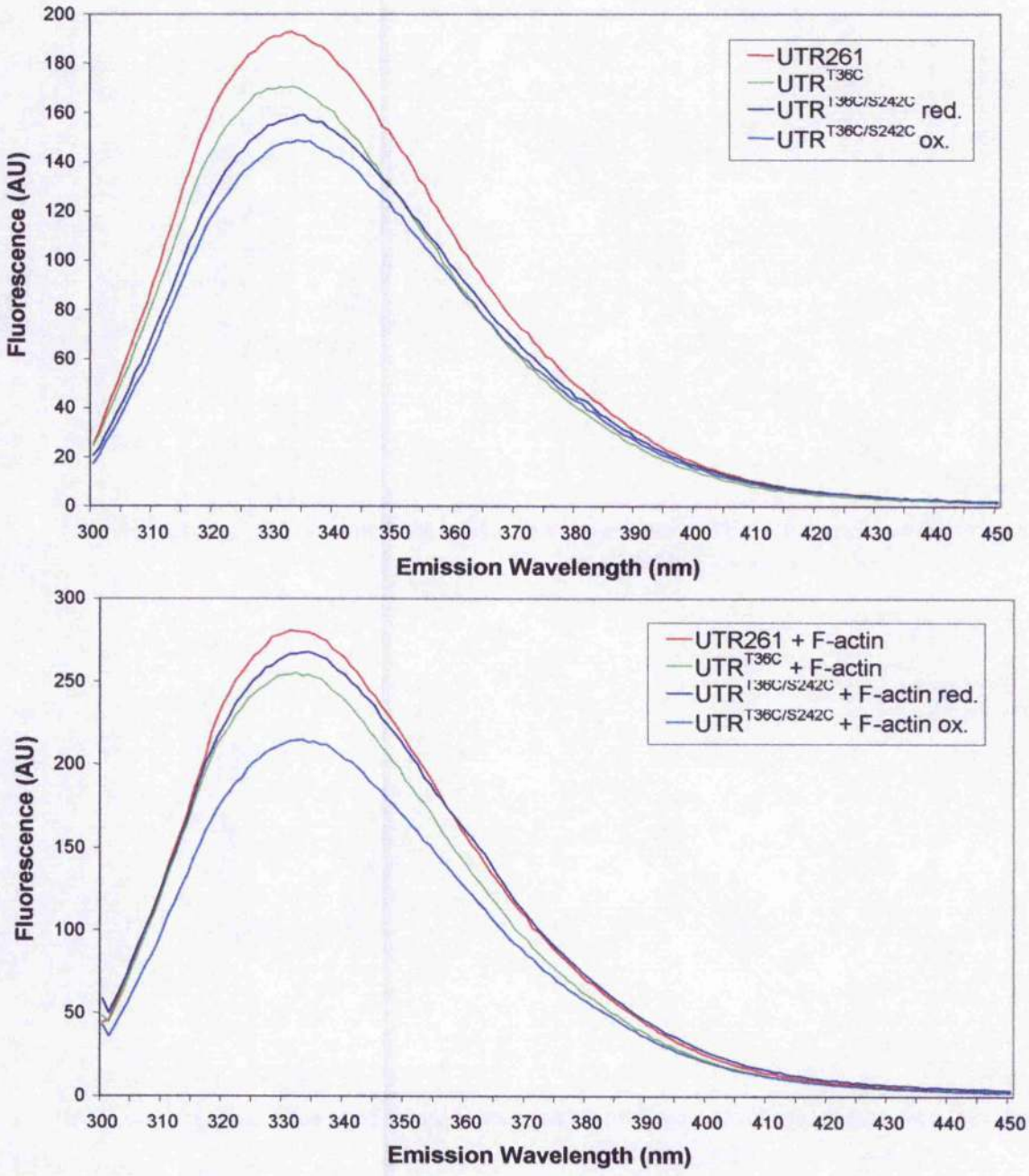

Figure 5.12: Comparison between the sum of the intrinsic tryptophan fluorescences of the utrophin ABD, UTR^{T36C} and UTR$^{T36C/S242C}$. 30 μM samples of utrophin ABD, F-actin and the cysteine mutants were excited at 296 nm and the resultant tryptophan fluorescence recorded between 300 and 450 nm. All scans were performed at a slow scanning speed with excitation and emission sit widths set to 1 nm. All samples were prepared in TE pH 8.0 in the presence of 1 x ABB. F-actin was added to a final concentration of 5 μM. Spectra of each protein alone and in the presence of F-actin are shown. Tryptophan fluorescence is represented in arbitrary units (AU).

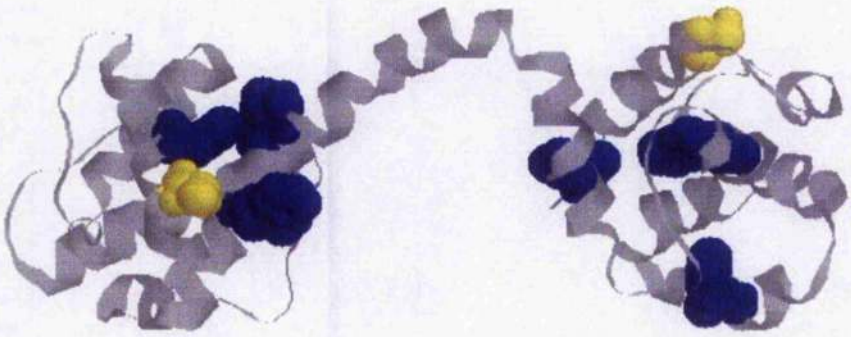

Figure 5.13: Position of the two cysteine mutations within UTR$^{T36C/S242C}$ in relation to the tryptophan residues present within the ABD. The two cysteine residues of UTR$^{T36C/S242C}$ are represented by yellow spacefill to identify their location and proximity to the six tryptophan residues present within the utrophin ABD (blue spacefill).

Figure 5.12 demonstrates that the fluorescent intensity of the UTR^{T36C} was lower than that of wild type utrophin ABD probably as a result of a quenching effect. The reduced form of UTR$^{T36C/S242C}$ demonstrated a further reduction of fluorescence with the oxidised form exhibiting the greatest decrease in intensity. The peak maxima of the UTR$^{T36C/S242C}$ mutants also appear to be slightly red shifted when compared to wild type utrophin ABD (333 nm), demonstrating maxima at 335 and 334 nm for the reduced and oxidised forms respectively; this may represent a slight change in tryptophan environment caused by the presence of both cysteine residues.

Following addition of F-actin, all of the cysteine mutants display a similar pattern of fluorescence when compared to the intensities generated in the absence of actin. However, it appears that the fluorescent intensity of the oxidised mutant is much lower than wild type utrophin ABD, UTR^{T36C} or UTR$^{T36C/S242C}$ in the reduced form. In the oxidised state the protein displays a fluorescent intensity slightly lower than that of the protein sample when in the absence of F-actin (Figure 5.12). In this form, UTR$^{T36C/S242C}$ may be interacting with F-actin in a manner that is distinct to that of the reduced form resulting in a marked difference in the combined protein fluorescence. Given that in the oxidised form of UTR$^{T36C/S242C}$ where the CH

domains of the utrophin ABD are locked together it is not unreasonable to assume that the domain is interacting with F-actin in a manner distinct to that of the reduced form of the protein.

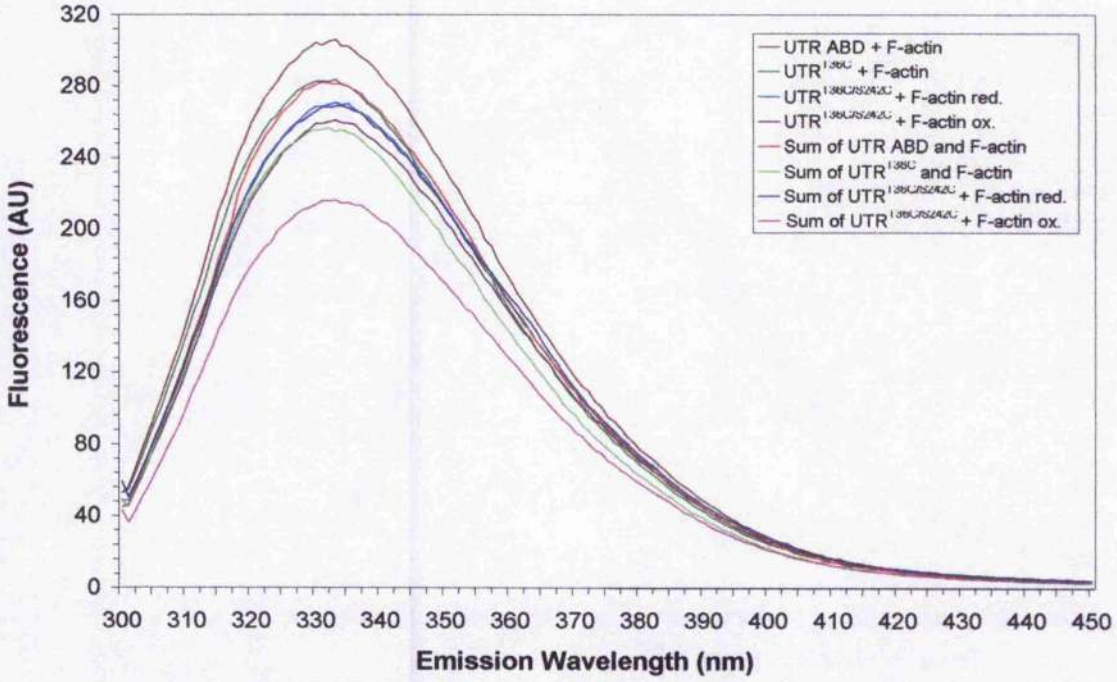

Figure 5.14: Comparison between the tryptophan fluorescence of the utrophin ABD, UTR^{T36C} and UTR$^{T36C/S242C}$ when bound to F-actin with the sum of the individual fluorescences of each protein. The fluorescence spectra of each ligand when in the presence of F-actin was recorded; these spectra were then compared to a sum of each ligands spectra and F-actin alone. Fluorescence is represented in arbitrary units (AU).

In an attempt to clarify the differences in fluorescence, the intensities of each protein in the presence of F-actin were compared to the sum of the individual proteins and F-actin (Figure 5.14). In each case the sum of the fluorescence were greater than the actual fluorescence of the ligand in the presence of F-actin. The difference between the fluorescent intensities between samples of ligand and F-actin and the sum of the individual intensities was used as a measure of the difference in fluorescence resulting from the interaction of the ligand with F-actin (Figure 5.15).

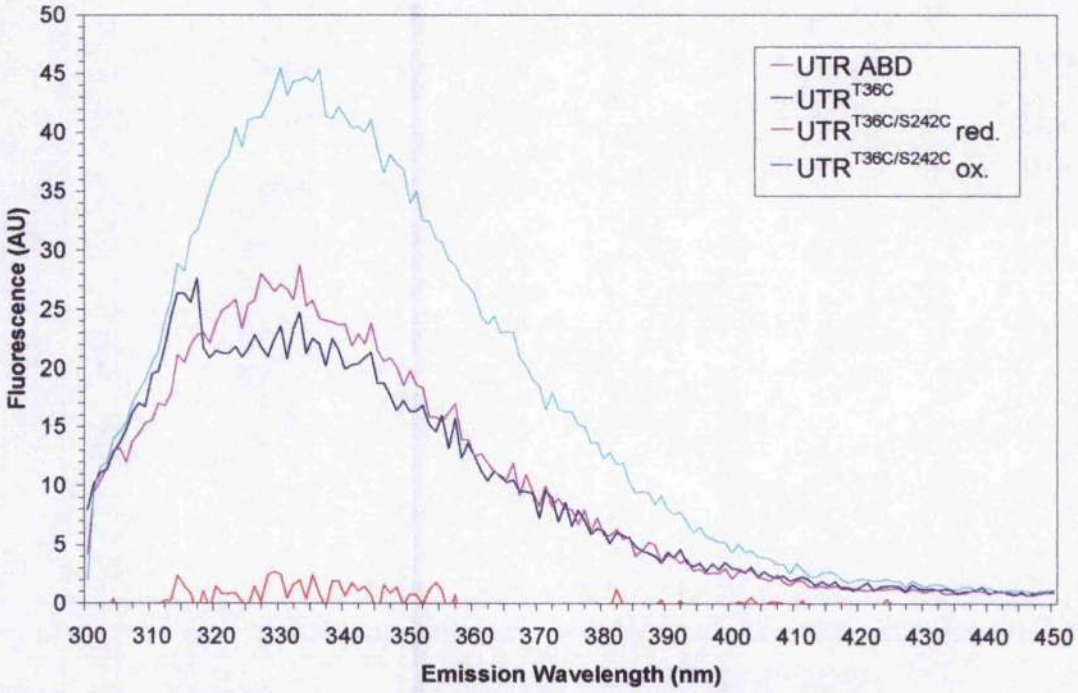

Figure 5.15: Difference between the fluorescence of ligand in the presence of F-actin and the arithmetic sum of ligand and F-actin fluorescence. The arithmetic sum of the individual proteins fluorescences when compared to the actual fluorescence of ligand and F-actin was found to be slightly larger. Subtraction of the combined fluorescence from the arithmetic sum allows a comparison between the extent of quenching caused by the presence of the cysteine residues within the utrophin ABD mutants and/or quenching caused by interaction with F-actin. Fluorescence intensity is represented by arbitrary units (AU).

Figure 5.15 demonstrates that the single cysteine mutation results in slightly less fluorescence; this is attributable to a greater extent of quenching when UTR^{T36C} interacts with F-actin when compared to the wild type protein interaction with F-actin. The reduced form of the double cysteine mutant (UTR$^{T36C/S242C}$) appears to generate a larger fluorescence than would be expected as the additional cysteine residue should result in greater quenching. It appears that in this form the double mutant displays little difference in fluorescence of the sum of the individual intensities when compared to the sample where both F-actin and ligand were present. The oxidised double cysteine mutant demonstrates a larger degree of quenching signified by the larger difference in fluorescence.

It is apparent that the introduction of a single cysteine residue into the utrophin ABD generates a significant degree of tryptophan quenching when compared with the wild type fluorescence. When the second cysteine mutation was introduced this

increased the fluorescent quenching; however, there appeared to be a relative loss of quenching of the double cysteine mutant when interacting with F-actin, possible resulting from the cysteine residues separating as the molecule interacts with F-actin. The $UTR^{T36C/S242C}$ mutant with the disulphide formed displayed a greater extent of quenching than the reduced form and the single cysteine mutant except that this quenching affect was not lost upon interaction with F-actin. This suggests that the utrophin ABD may still interact with F-actin in the closed conformation although the large proportional difference between the sum of the individual components and the ligand/F-actin mixture may hint at a different manner of interaction of the utrophin ABD in this form.

5.2.11 *Differential Scanning Calorimetry of the utrophin ABD*

Differential scanning calorimetry has been used previously to demonstrate that the plectin ABD exists in a closed state when in solution but preferentially binds to F-actin in an open conformation (Garcia-Alvarez et al., 2003). This study also identified that the plectin ABD was also able to interact to F-actin if the domain was locked closed by the formation of an engineered disulphide bond between the two CH domains of the protein (Garcia-Alvarez et al., 2003).

It was apparent that the cysteine mutants generated during this study would be amenable to similar analysis; samples of the wild type utrophin ABD, UTR^{T36C} and $UTR^{T36C/S242C}$ were subjected to DSC with the help of Dr Andrey Bobkov at the Burnham Institute, La Jolla. It was thought that these analyses would help to provide insight into the conformational state of the utrophin ABD when in solution and upon interaction with F-actin.

The utrophin ABD (UTR261) was found to denature as a single peak with a transition midpoint (T_m) of 53.3 °C (Figure 5.16, Table 5.3). This T_m was much lower than the T_m of 63.9 °C recorded for the plectin ABD in solution and was similar to the T_m of 59.1 °C recorded for the plectin ABD in complex with F-actin (Garcia-Alvarez et al., 2003). Comparison with the data of Garcia-Alvarez et al. implies that the utrophin ABD adopts an open conformation when in solution similar to the conformation determined from plectin (Garcia-Alvarez et al., 2003). These

data oppose other studies that propose that the utrophin ABD adopts a closed compact structure in solution only opening upon interaction with F-actin. Gel filtration and SDS PAGE analysis have confirmed that the oxidised $UTR^{T36C/S242C}$ mutant remains monomeric in solution (Section 5.2.5; 5.2.6) but the formation of the disulphide should lock the protein in a closed state. DSC determined that oxidised $UTR^{T36C/S242C}$ denatured at a much higher temperature than UTR261 (Figure 5.17, Table 5.3). The T_m of 68.1 °C was very close to the oxidised plectin ABD mutant in the locked closed conformation (Garcia-Alvarez et al., 2003) suggesting that the production of the disulphide bond was successful and that $UTR^{T36C/S242C}$ was locked in a closed conformation.

It was necessary to verify that the increased T_m resulted from the formation of a disulphide and not from the presence of the two cysteine mutations within the utrophin ABD. To test this, DSC was performed on a sample of UTR^{T36C}, containing a single cysteine mutation at T36, and a sample of $UTR^{T36C/S242C}$ when in the reduced form (no disulphide formation). The determined melting profile and T_m of UTR^{T36C} were very close to that of UTR261 (Figure 5.17, Table 5.3) indicating that the single cysteine mutation had no significant effect on the conformation of the utrophin ABD in solution. The melting profile of reduced $UTR^{T36C/S242C}$ demonstrated two peaks (Figure 5.17, Table 5.3); indicating the presence of two populations of utrophin ABD with differing conformations. The larger population of reduced $UTR^{T36C/S242C}$ melted with a T_m of 56.3 °C, very close to that of wild type utrophin ABD. The smaller population of reduced $UTR^{T36C/S242C}$ melted with a T_m of 68.6 °C very close to that of oxidised $UTR^{T36C/S242C}$. Based on the similarity to the oxidised form it is likely that this proportion of reduced $UTR^{T36C/S242C}$ exists in the closed conformation when in solution whereas the larger population of reduced $UTR^{T36C/S242C}$ adopts the open conformation. It is apparent that the formation of the disulphide between the CH domains of the utrophin ABD results in a shift of the solution equilibrium of $UTR^{T36C/S242C}$ from the open state towards that of the closed conformation.

In the presence of F-actin the utrophin ABD demonstrates an increase in T_m to 55.5 °C (Figure 5.16, Table 5.3); this indicates binding of the domain to F-actin although the relatively small increase in T_m (2.2 °C) suggests no major change in the conformation of the protein upon interaction with F-actin. Thus, the utrophin ABD

binds F-actin in the open conformation which is in agreement with Moores et al., but also the unmodified plectin ABD also associated with F-actin in the open state (Garcia-Alvarez et al., 2003; Moores et al., 2000). The single cysteine mutant, UTR^{T36C}, also behaved in a similar manner to the wild type protein indicating the lack of disulphide formation and any effects on the structure of the domain overall (Figure 5.16 B).

The DSC profile of oxidised $UTR^{T36C/S242C}$ bound to F-actin (Figure 5.17 B) displayed a main peak with a T_m of 69.7 °C and a shoulder at approximately 67 °C. The main peak represents the melting of F-actin and it is likely that the shoulder can be attributed to the melting of $UTR^{T36C/S242C}$. To resolve these peaks the experiment was repeated in the presence of phalloidin, which serves to increase the melting temperature of F-actin by approximately 10 °C (Figure 5.16 and 5.17) resulting from a stabilisation effect between the inter-subunit contacts of F-actin (Levitsky et al., 1998). The actin samples where phalloidin was present were also doubled in concentration to investigate if the actin effect on the utrophin ABD was saturated. It was apparent that the melting profiles of oxidised $UTR^{T36C/S242C}$ in the presence and absence of phalloidin-F-actin are very similar (Figure 5.17B, Table 5.3); thus oxidised $UTR^{T36C/S242C}$ associates with phalloidin-F-actin in the closed conformation. It was possible that the presence of phalloidin was altering the manner of interaction of the utrophin ABD with actin. To verify that phalloidin does not alter the interaction, DSC was performed with the wild type utrophin ABD in the presence of Phalloidin-F-actin (Figure 5.16A, Table 5.3). The data demonstrate that the effects of F-actin and phalloidin-F-actin on the conformation of the wild type protein are similar.

The melting profile of reduced $UTR^{T36C/S242C}$ in the presence of F-actin was very similar to that of the oxidised form of the protein (Figure 5.17 A and B respectively). Once again, phalloidin-F-actin was used to allow resolution of the T_m peaks. Reduced $UTR^{T36C/S242C}$ was found to melt with a single peak of Tm 68 °C (Figure 5.17 A, Table 5.2) thus, the majority of reduced $UTR^{T36C/S242C}$ adopts a closed conformation when F-actin is present; however, in the absence of F-actin reduced $UTR^{T36C/S242C}$ approximately 60 % of the protein molecules adopt an open conformational state (Figure 5.17 A).

The results indicate that $UTR^{T36C/S242C}$ favours the closed conformational state but interestingly, UTR^{T36C} displays a reduced intensity of the peak at 56.5 °C and an appearance of a shoulder at 69 °C in the presence of phalloidin-F-actin (Figure 5.16 B). These data imply that a small proportion of UTR^{T36C} molecules adopt a closed conformation upon interaction with F-actin. The wild type utrophin ABD also displays a small shoulder at 68 °C in the presence of phalloidin-F-actin (Figure 5.16.A); thus although the vast majority of wild type utrophin ABD associates with F-actin in the open conformation, the potential for association of a small population of molecules in the closed conformation does exist.

Proteins	T_{m1} (°C)	T_{m2} (°C)	T_{m3} (°C)
UTR261	53.3	--	--
UTR^{T36C}	52.6	--	--
$UTR^{T36C/S242C}$ reduced	56.3	68.6	--
$UTR^{T36C/S242C}$ oxidized	--	68.1	--
F-actin	--	--	69.1
UTR261 + F-actin	55.5	--	69.8
UTR^{T36C} + F-actin	55.0	--	68.7
$UTR^{T36C/S242C}$ reduced + F-actin	--	shoulder at ~67	69.7
$UTR^{T36C/S242C}$ oxidized + F-actin	--	shoulder at ~67	69.6
F-actin-phalloidin	--	--	80.0
UTR261 + F-actin-phall.	56.2	--	79.8
UTR^{T36C} + F-actin-phall.	56.5	shoulder at ~69	80.6
$UTR^{T36C/S242C}$ reduced + F-actin-phall.	--	68.5	80.8
$UTR^{T36C/S242C}$ oxidized + F-actin-phall.	--	68.2	79.4

Table 5.3: Denaturation temperatures for DSC scans shown in Figure 5.16 and 5.17. DSC data of the wild type utrophin ABD and the UTR^{T36C} and $UTR^{T36C/S242C}$ mutants. The transition peaks (T_m) recorded during each scan are denoted T_m 1-3 and the absolute errors in T_m values did not exceed 0.2°C.

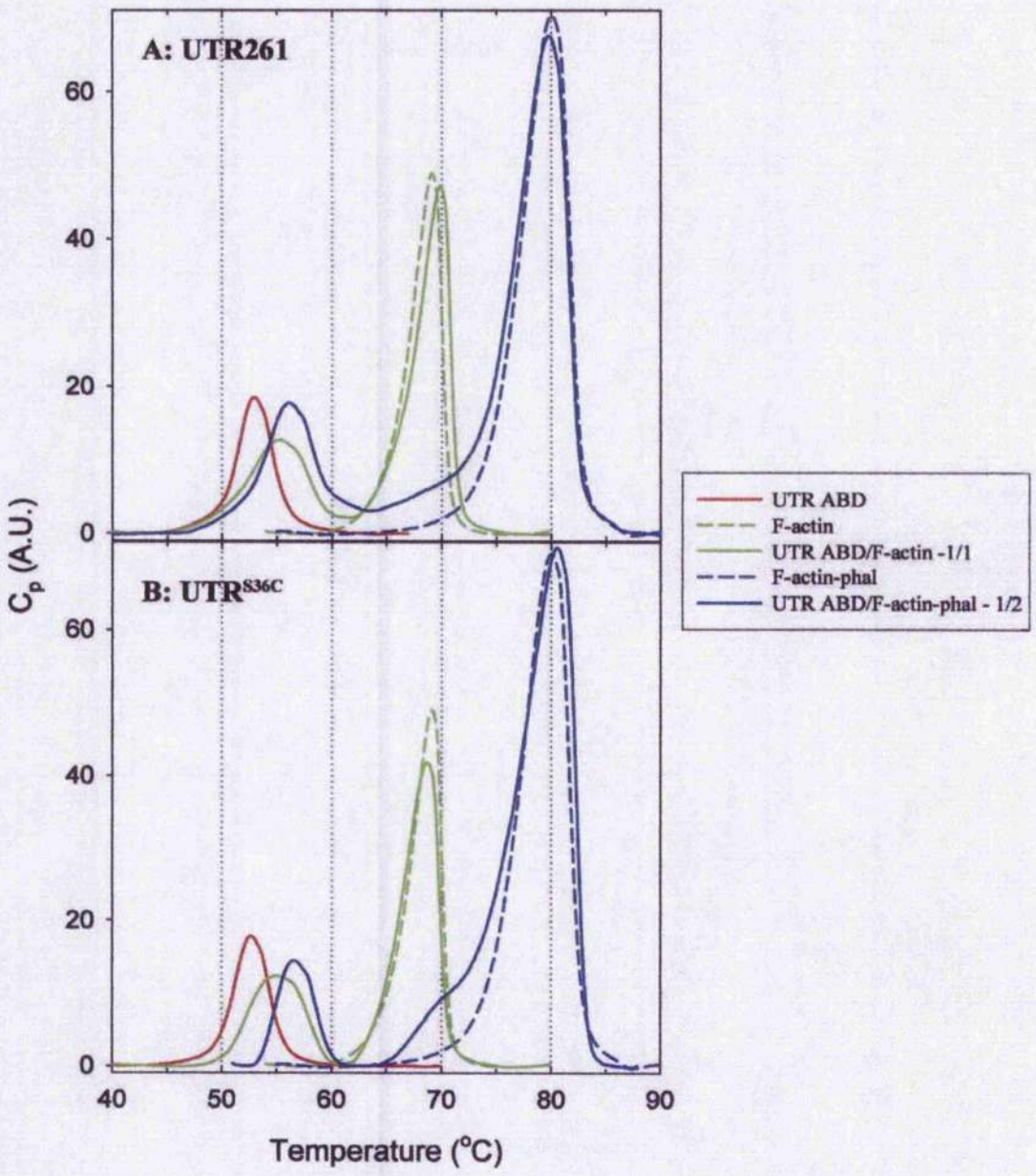

Figure 5.16: Differential Scanning Calorimetry data for the utrophin ABD and the UTR^{T36C} mutant. DSC melting profiles of the wild type utrophin ABD (A) and the single cysteine UTR^{T36C} mutant (B). 10 μM samples of each protein were scanned at a rate of 1K/min under 3 atmospheres of pressure in 20 mM PIPES pH 7.0, 50 mM NaCl, 1 mM $MgCl_2$, 0.2 mM ATP and where necessary, 10 μM F-actin or 20 μM F-actin + 20 μM phalloidin. Protein samples under reducing conditions were kept with 1 mM DTT at all times and diluted 10 fold with DTT-free buffer immediately before analysis. C_P represents the heat energy uptake during the unfolding transition expressed in arbitrary units (A.U.).

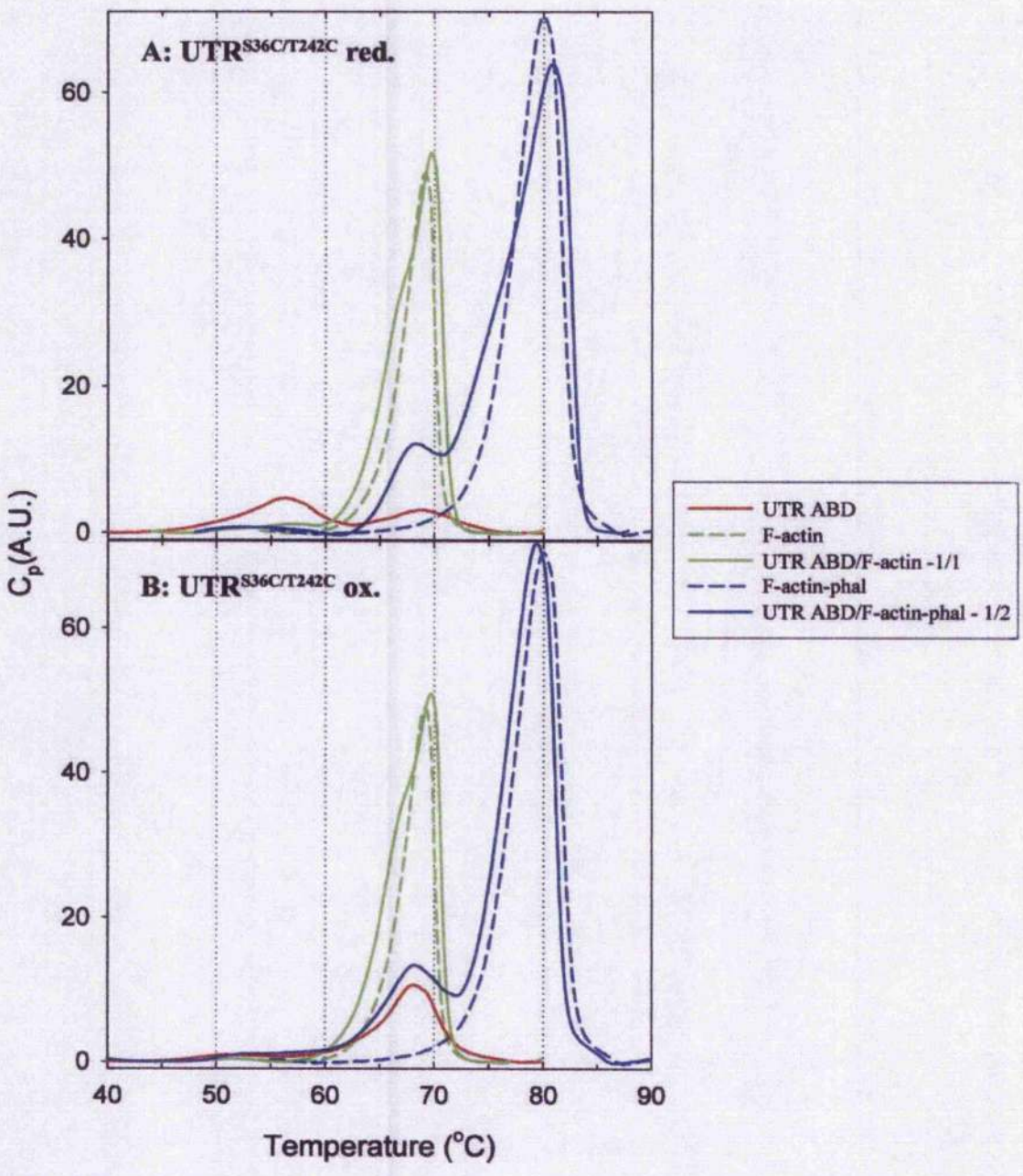

Figure 5.17: Differential scanning calorimetry data for the utrophin ABD and the UTR$^{T36C/S242C}$ mutant in the oxidised and reduced form. DSC melting profiles of the UTR$^{T36C/S242C}$ mutant when analysed in the reduced (A) and oxidised (B) form. 10 μM samples of the protein were scanned at a rate of 1K/min under 3 atmospheres of pressure in 20 mM PIPES pH 7.0, 50 mM NaCl, 1 mM $MgCl_2$, 0.2 mM ATP and where necessary, 10 μM F-actin or 20 μM F-actin + 20 μM phalloidin. Protein samples under reducing conditions were kept with 1 mM DTT at all times and diluted 10 fold with DTT-free buffer immediately before analysis. C_P represents the heat energy uptake during the unfolding transition expressed in arbitrary units (A.U.).

5.3 Discussion

The utrophin ABD comprises a tandem pair of CH domains separated by a helical linker that is believed to permit the CH domains a certain degree of flexibility (Broderick and Winder, 2005). The utrophin ABD is one of a handful of CH domain containing ABDs that have been crystallised (Garcia-Alvarez *et al.*, 2003; Goldsmith *et al.*, 1997; Keep *et al.*, 1999b; Klein *et al.*, 2004; Norwood *et al.*, 2000), most notable however, is the similarity that exists between the CH1 and CH2 domains of the utrophin crystallographic dimer and the fimbrin crystal structure (Keep *et al.*, 1999b). The CH domain interface that exists between CH1 and CH2 domains of the opposed utrophin crystal monomers, forming the utrophin crystal dimer, is very similar in orientation and interface to the CH domain arrangement exhibited by the fimbrin crystal structure. This phenomenon can be described as three dimensional domain swapping but it has been proposed that the utrophin ABD may exist as a closed compact monomer when in solution similar in conformation to the fimbrin crystal structure (Keep *et al.*, 1999b); binding of the domain to F-actin causes a rearrangement of the CH domains allowing interaction in an open conformation more analogous to the extended arrangement of the utrophin crystal dimer (Galkin et al., 2002; Moores et al., 2000). The work of this chapter has served to further investigate the apparent flexibility of the utrophin ABD by the generation of a double cysteine mutant that permits the two CH domains to be covalently linked thus, preventing disassociation of the domains in solution or upon interaction with F-actin.

Initially, it was necessary to generate and purify the double cysteine mutation. The double cysteine mutation was generated via two rounds of site directed mutagenesis, firstly via the generation of a single cysteine mutation at T36 followed by addition of a second cysteine mutation at position S242 of the utrophin ABD. This served to generate two mutant proteins containing either a single or double cysteine mutation. The single cysteine mutant, UTR^{T36C}, was deemed to be useful towards the characterisation of the double mutant, $UTR^{T36C/S242C}$ so this form of utrophin ABD was also expressed.

Initial analysis of the cysteine mutants proved the presence of the correct mutations within the utrophin ABD and that the disulphide bond could be induced to

form between the CH domains of the $UTR^{T36C/S242C}$ mutant. A similar cross-linking of the plectin ABD demonstrated that a disulphide bond could be successfully generated between the CH domains of this protein (Garcia-Alvarez et al., 2003). The introduction of cysteine residues into the utrophin ABD generated the potential for cross-linking to occur inter-molecularly; gel filtration analysis and SDS PAGE were used to prove that this was not the case. After formation of the disulphide within $UTR^{T36C/S242C}$ it was found that the mobility of the protein on a gel was increased indicating that the disulphide had formed successfully. The disulphide did not result in the generation of any larger molecular weight species indicating that the mutant protein was still behaving as a monomer in solution. Previous analyses of the utrophin ABD have indicated that it does not exist in an oligomeric state when bound to F-actin or when in solution (Moores and Kendrick-Jones, 2000); the only known instance of utrophin interacting with itself is within the crystal dimer. In this instance it is apparent that the extreme conditions that are required for crystal formation could result in this molecular arrangement (Liu and Eisenberg, 2002) although it is interesting that the homologous dystrophin ABD also crystallised as an antiparallel dimer (Norwood et al., 2000). The large degree of sequence identity between these two proteins may explain why they crystallise in a similar manner although it has been shown previously that the dystrophin ABD can dimerise in solution and bind to F-actin in this conformation (Norwood et al., 2000); these are abilities not shared by the utrophin ABD or the double cysteine mutant.

The covalent linkage of the CH domains within the utrophin ABD allowed the effect of the disulphide upon actin binding to be assessed. It was found that the presence of the disulphide did not prevent the utrophin ABD from interacting with F-actin. Interaction with F-actin in this state indicated that binding must occur when the utrophin ABD is in the closed conformation. This manner of association would be in agreement with models proposed by Sutherland-Smith et al., and Lehman et al., in which the utrophin ABD was shown to associate with F-actin in a closed conformation (Lehman et al., 2004; Sutherland-Smith et al., 2003). These models are in sharp contrast to the open and extended models of association proposed by Galkin et al., and Moores et al., (Galkin et al., 2002; Moores et al., 2000). It is unlikely that all of the current models of the utrophin ABD bound to F-actin are correct when

describing the interaction of the wild type protein with F-actin and this matter was recently discussed by Lehman and colleagues (Lehman et al., 2004).

The models where the utrophin ABD associates with F-actin in an open and extended conformation assume that the domain opens from a relatively compact solution monomer (Galkin et al., 2002; Moores et al., 2000). This assumption was based on the structural similarities that exist between the CH domain interface of the utrophin ABD and fimbrin ABD crystal (Keep *et al.*, 1999b) and the fact that the domain is strictly mono-disperse in solution. The models where actin-binding occurs in an open conformation are all very different; Moores et al., and Galkin et al., both propose models where CH1 and CH2 of the utrophin ABD are associated with F-actin; however, the Galkin model depicts utrophin spanning two actin monomers generating a binding stoichiometry of 1:2 (known as the 'half decorated'). Biochemical evidence presented here, and determined previously, suggest that utrophin binding with F-actin occurs in a 1:1 ratio so it seems unlikely that this model describes the actual mode of interaction with actin. An alternate model proposed by Galkin and colleagues suggests binding of the utrophin ABD to F-actin via CH1 only with CH2 remaining free from the actin filament ('singly decorated' model) (Galkin et al., 2002). This latter model fits well with the known biochemistry of the individual CH domains but it does seem unlikely overall as the presence of the second CH domain has been shown to strengthen the binding activity of the complete domain.

The model proposed by Moores et al., was generated after an induced fitting of the utrophin crystal structure within the electron densities generated by bound utrophin ABD (Moores et al., 2000). Modelling in this study also identified density attributable to the helical linker that separates the CH domains but the necessity for an induced fit of the utrophin crystal structure suggests that this is not the exact mode of interaction that the domain adopts when binding actin (Moores et al., 2000). The work presented here proposes that the utrophin ABD may bind F-actin in a closed conformation. The formation of the disulphide prevents the opening of the domain upon association with F-actin and hence the interaction must occur in a closed conformation. The 1:1 stoichiometry of the interaction is identical to previously determined ratios for the wild type protein (Moores and Kendrick-Jones, 2000). The

binding affinities of the $UTR^{T36C/S242C}$ mutant in the reduced (K_d = 74.8 ± 19.2 μM) and oxidised (K_d = 123.2 ± 14.1 μM) forms are not too dissimilar to the documented wild type protein affinity (K_d = 20 μM) (Moores and Kendrick-Jones, 2000; Winder et al., 1995). These binding affinities indicate that the presence of the cysteine residues do not affect the binding interaction to any great extent when the protein is in the reduced form but also that the disulphide does not prevent association with F-actin. It is apparent that the presence of the disulphide does compromise the actin-binding reaction to some extent as the cross-linked ABD exhibits a slightly lower actin-binding affinity. The overall structure of the CH domains that form the ABD of many actin binding proteins are very similar, so it would seem feasible to assume a similar mode of interaction, although the large difference in sequence homology may allow some variation in the exact manner of interaction.

The ABD of α-actinin has been modelled to bind in both 'open' and 'closed' conformations (Liu et al., 2004; Tang et al., 2001; Taylor and Taylor, 1993) whilst the ABD of fimbrin has been found to associate with F-actin in a closed conformation (Hanein et al., 1998). The locations of the cysteine mutations in the utrophin ABD were selected based on their proximity to one another using the utrophin ABD crystal structure. The utrophin and fimbrin crystal structures can be overlaid to demonstrate the similarities between the CH domain interface exhibited by each protein; this led to the proposition that the utrophin ABD may adopt a closed fimbrin like conformation when in solution (Keep *et al.*, 1999a).

The ability to cross-link the utrophin ABD CH domains via use of a disulphide demonstrates that these residues are sufficiently close to allow formation of the bond. It was thought that labelling of the two cysteine residues of $UTR^{T36C/S242C}$ with rhodamine and fluorescein would allow FRET to occur between this donor/acceptor pair. FRET can occur between rhodamine and fluorescein over a distance of approximately 56 angstroms; however, the efficiency of energy transfer could be significantly affected by the relative orientation of the two fluors with regard to one another (Berney and Danuser, 2003; Ha et al., 1996) and the distance that separates them. FRET analysis of $UTR^{T36C/S242C}$ indicated that there was no energy transfer between the fluors. It is possible that the labelling of the cysteines was at fault given that double labelling with rhodamine and fluorescein could generate a number of

different species within the population of labelled $UTR^{T36C/S242C}$. The proportion of the two dyes was adjusted to try and ensure equal labelling of the protein; however, labelling may not be complete and the double labelled protein sample would contain a number of differently labelled species comprising protein singly and double labelled, at either the first or second cysteine mutation, but also species that are not completely labelled at one or the other of the cysteine residues, or not at all. In any case the FRET experiment was not successful. The fact that a disulphide could be formed between the two cysteines of $UTR^{T36C/S242C}$ indicates that these resides are sufficiently close, at least transiently, for the bond to form. However, it is possible that the fluors were not oriented correctly or were not close enough to allow a FRET signal to be generated.

The disulphide linkage formed between the CH domains of the plectin ABD was induced in almost 100 % of the protein sample (Garcia-Alvarez et al., 2003). SDS PAGE analysis indicates that not all the oxidised $UTR^{T36C/S242C}$ sample forms the disulphide. DSC analysis confirms this, demonstrating that the oxidised $UTR^{T36C/S242C}$ melting profile contains two peaks, one with a higher T_m similar to the disulphide linker plectin ABD and the other with a lower T_m at a value similar to the wild type protein that contains no cysteine residues. Referral to the utrophin ABD crystal structure also highlights another potential reason for a lack of complete oxidation of the sample (Keep *et al.*, 1999b). The inter-CH domain α-helix is believed to be flexible allowing the ABD to shift from a closed solution monomer structure to an open extended conformation upon F-actin binding (Keep *et al.*, 1999b; Moores *et al.*, 2000). This linker may not be as flexible as initially thought. Figure 5.1 demonstrates the proposed structure of the cross-linked utrophin ABD; in this configuration the helical linker would be required to bend back over upon itself quite significantly. It is apparent that this can occur as a disulphide can be formed; however, a degree of strain may be imparted upon the disulphide bond due to the un-natural flexing of the linker that may result in the disulphide formation being less favourable. Garcia-Alvarez and colleagues used a program, SSBOND, when designing their double cysteine mutant (Garcia-Alvarez et al., 2003); this program uses the crystal structure of the protein to choose the most optimal residues to mutate based on the crystal co-ordinates (Hazes and Dijkstra, 1988). In this instance the use

of this program may have allowed a more favourable cysteine configuration to be devised but if the actual solution structure of utrophin is very different to that proposed by comparison to the fimbrin crystal then it is possible that design of the mutant in this way would still not allow favourable bond formation. Keep and colleagues proposed that a modest level of structural unwinding may allow formation of the utrophin ABD solution monomer whilst Moores and colleagues describe the interconnecting α-helix to have a hydrophobic surface (Keep *et al.*, 1999b; Moores *et al.*, 2000). These two studies give credence to the formation of a closed and compact solution monomer similar to the fimbrin crystal structure; however it has become evident that the CH domains of the utrophin ABD are not as closely associated when in solution as previously thought.

The DSC analyses of the utrophin ABD demonstrate that the domain does bind to F-actin in an open conformation, which agrees with previous data; however, the relatively small increase in the amplitude of the T_m upon actin binding is not indicative of a conformational change. The plectin ABD was determined to experience a conformational change upon association with F-actin rationalised by a two step mechanism of association (Garcia-Alvarez et al., 2003). The utrophin ABD does not exhibit a conformational change which suggests that the domain adopts an open conformation when in solution. It is likely that the species that exists in solution is not as 'open' as can be seen in the crystallographic dimer (Keep *et al.*, 1999b) but utrophin does not adopt a closed and compact conformation similar to the fimbrin crystal structure (Goldsmith et al., 1997). The inability to generate a RET signal and completely oxidise 100 % of $UTR^{T36C/S242C}$ supports the notion that the actual utrophin solution monomer is not represented by a closed compact conformation. It is more likely that the utrophin ABD is dynamic in solution adopting a more 'open' configuration than previously thought. Interestingly, it was proposed by Keep et al., that the molecular interface of the utrophin CH domains may be more dynamic than the similar interface observed in the fimbrin crystal based upon analysis of the gap/volume index (Keep *et al.*, 1999b). It has become clear that the utrophin ABD is indeed more dynamic when in solution.

Analyses of numerous ABDs have allowed the determination of a series of sites deemed to be responsible for the association of an ABD with F-actin (Bresnick

et al., 1991; Bresnick et al., 1990; Corrado et al., 1994; Fabbrizio et al., 1993; Kuhlman et al., 1992; Levine et al., 1990; Levine et al., 1992; Morris et al., 1999). These actin-binding sites (ABS) are believed to be presented towards F-actin in order to facilitate binding. The generation of the disulphide bond within the utrophin ABD effectively prevents ABS1 from interacting with F-actin. The first cysteine mutation is located within ABS1 (Figure 5.18), which spans residues 34-43 (Moores et al., 2000); it is interesting that the domain can still associate and bind to F-actin when the disulphide bond is formed. Cross-linking the two CH domains effectively places ABS1 at the CH domain interface and would prevent association with F-actin. The fimbrin ABD has been modelled to bind F-actin in a closed conformation (Hanein et al., 1998); during interaction with F-actin the fimbrin ABD present all three ABSs towards actin. This manner of interaction would require a modest amount of CH domain movement from the CH domain interface visible in the crystal structure (Hanein et al., 1998). The formation of the disulphide bond in the utrophin ABD would not allow this to occur but it is apparent that ABS 2 and 3 can still participate in the F-actin interaction.

The CH domains that form ABDs are not equal in their ability to bind F-actin (Gimona et al., 2002; Way et al., 1992; Winder et al., 1995); when separated only CH1 can bind to F-actin, whereas CH2 has no appreciable affinity. It is interesting that the removal of ABS1 still allows association of the utrophin ABD with F-actin. The cross-linked plectin ABD (Garcia-Alvarez et al., 2003) was also able to retain its ability to bind F-actin so it is possible that utrophin may interact with F-actin in a manner analogous to the proposed interaction of the plectin ABD. If this were to occur then the utrophin ABD would initially associate with F-actin with a closed conformation similar to the proposed binding of fimbrin where ABS2 and ABS3 and the inter-domain linker form the initial interaction surface (Garcia-Alvarez et al., 2003; Hanein et al., 1998). The second step of the binding interaction may then involve a structural change in the ABD potentially caused by actin allowing the final presentation of the actin binding surfaces towards the filament. However, it has been shown here that the utrophin ABD exhibits a more open conformation when in solution. It may therefore be more feasible to assume an initial association by CH1, as this domain possesses an inherent actin-binding affinity not exhibited by CH2

(Gimona and Winder, 1998; Way et al., 1992; Winder et al., 1995), which then allows the correct location of CH2 upon the actin filament to achieve the full actin-binding capability of the overall ABD.

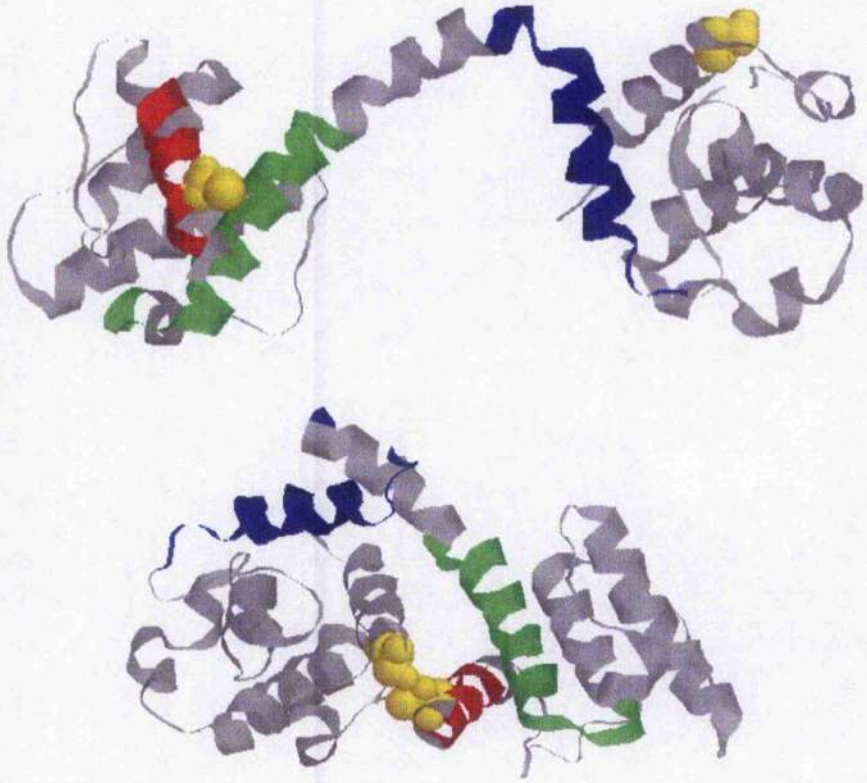

Figure 5.18: Location of the three actin-binding sites within the utrophin ABD when the domain is in an open or closed configuration. The three ABS of the utrophin ABD have been highlighted to show their relative positions when the molecule is in the open and closed conformation. The location of the two cysteine residues that were inserted into the ABD to generate the $UTR^{T36C/S242C}$ mutant are indicated in yellow. ABS1, 2 and 3 are highlighted based on information taken from Moores *et al.* (2000) and are represented in red, green and blue respectively.

Overall, the work presented here demonstrates that the utrophin ABD can adopt two conformations, closed and open. Previous studies have led to the assumption that the utrophin ABD adopted a closed and compact configuration in solution more analogous to the fimbrin crystal structure but this has been found not

to be the case. It appears that the utrophin ABD is in fact more open in solution and does not appear to undergo a vast conformational change upon interaction with F-actin. These analyses have interesting implications regarding the interpretation of current models of the utrophin ABD and other related ABDs when interacting with F-actin.

Chapter 6:

Final Discussion

Chapter 6

Final Discussion

Utrophin is the autosomal homologue of the cytoskeletal protein, dystrophin. Much research has focused upon the potential use of utrophin as a therapeutic replacement for dystrophin in the treatment of muscular dystrophy. However, a considerable body of work has focused upon the N-terminal ABD of this protein and specifically, the modelling of how this domain interacts with F-actin during binding. The exact manner in which the utrophin ABD interacts with F-actin has been the subject of much controversy over recent years. Currently, four models exist that depict binding of the domain to F-actin in either closed or compact conformations (Galkin et al., 2003; Galkin et al., 2002; Lehman et al., 2004; Moores et al., 2000; Sutherland-Smith et al., 2003). The utrophin ABD crystal structure has provided an invaluable tool for the generation of these models; however, the dimeric state of the domain within the crystal structure does not correlate with the known behaviour of the domain in solution or when binding to F-actin; in these situations binding normally occurs in a 1:1 ratio and the protein is exclusively monomeric (Moores and Kendrick-Jones, 2000; Winder et al., 1995). The interface generated within the utrophin ABD crystal between the CH1 and CH2 domains of opposing crystal monomers was very similar to the interface exhibited within the fimbrin ABD crystal structure formed from a single molecule (Goldsmith *et al.*, 1997; Keep *et al.*, 1999b). It was postulated that the utrophin ABD adopted a closed state in solution (which would fit the known biochemistry) and could then associate with F-actin in an open conformation (Keep *et al.*, 1999b). Indeed, this was modelled to occur by Moores and colleagues (Moores et al., 2000); however later research has suggested that binding may also occur in a closed conformation (Sutherland-Smith et al., 2003). It was apparent that the utrophin ABD possesses a certain degree of structural flexibility attributable to the extended helical linkage that separated the two CH domains. The initial work presented herein aimed to investigate the effects that a varied solution pH would produce regarding the solution state and the effects upon actin-binding. Many proteins exhibit a pH-dependent conformational change and activity; however it was found that the utrophin ABD did not. Varying the solution

pH only served to generate a slight pH-dependent shift in the sedimentation coefficient of the domain. This shift, however, did correlate with hydrodynamic models generated from the closed fimbrin crystal structure and the open structure of the utrophin ABD crystal so it would appear that altering the electrostatic environment of the utrophin ABD does slightly affect the structure of the protein but this is not to any great extent. Binding of the domain to F-actin at varied pH generated a marked difference in both stoichiometry and binding affinity. Unfortunately, the structure of F-actin is particularly sensitive to varied pH and hence, it was impossible to differentiate between effects caused by the varied pH upon the utrophin ABD and those resulting from an altered F-actin structure. It became apparent that the original hypothesis was flawed and that altered pH could not be used to induce a conformational change within the utrophin ABD.

The utrophin, and many other ABDs, are formed from a pair of CH domains separated by a linker (Stradal et al., 1998; Winder, 2003). This linker has been found to be of differing length and conformation; continued analysis of the utrophin ABD focused upon the flexibility of this region within the domain. Two utrophin ABD mutants were designed that would allow modelling of the linker regions of the F-actin cross-linking protein α-actinin and the bundling protein fimbrin. These two proteins possess linkers that are either shorter (α-actinin) or longer (fimbrin) than the equivalent portion of the utrophin ABD. It was proposed that the length of the inter-CH domain linker may be relevant to the manner in which the ABDs of these proteins interact with F-actin. The fimbrin ABD has been modelled to bind F-actin in a closed conformation (Hanein et al., 1998) whereas the α-actinin domain has been modelled to bind in both open and closed conformations (McGough et al., 1994; Tang et al., 2001; Taylor and Taylor, 1993). It was assumed that shortening the inter-helical linker would force the domain to adopt a more open conformation whereas increasing the linker length would result in greater flexibility and CH domain association. Unfortunately, neither of the two linker mutants were found to be folded correctly; the secondary and tertiary structures of the two mutants differed greatly from the wild type utrophin ABD and as a result no biochemistry was performed.

CH domains are found within a large number of proteins and generally the overall structure of these domains is well conserved even though at a sequence level

they can be quite different (Korenbaum and Rivero, 2002). The differences in protein sequence potentially allow for unique interaction sites that facilitate binding with F-actin but it seems that the linker region that separates the CH domains is also of particular importance. The disruption of this region to produce the utrophin ABD linker mutants resulted in mis-folding of the mutant proteins. CH domains are particularly stable and it seems that the mutations have caused destabilisation of CH domain structure in both mutants even though soluble protein was produced. The linker region that separates the CH domains of the utrophin ABD is principally α-helical in nature however the equivalent stretch of sequence in the fimbrin domain exhibits no defined structure. This introduction of this stretch of sequence has obviously perturbed the structure of the CH domain helices that flank the mutation in the utrophin fimbrin linker mutant. Removal of a stretch of the utrophin ABD linker to generate the α-actinin linker mutant was hoped to be less disruptive to the overall structure of the ABD; however this mutation was also unsuccessful. Reference to the recently published crystal structure of the α-actinin ABD suggests that the inter-CH domain linker is formed principally from helix although there is a stretch of sequence predicted to form turn (Franzot et al., 2005). In the case of the utrophin ABD, it appears that the helical nature of the utrophin ABD linker region is of particular importance to the overall structure of the domain. The α-actinin linker mutant was expressed as a soluble protein whereas the fimbrin linker mutant required solubilisation and recovery from urea. It may be possible to express both of these mutants and generate soluble protein if expression was performed at a lower temperature or a strain of bacteria was used that would assist with protein folding. In any case, it is interesting that there is such a contrast in the structure of the linker domains between ABD-containing proteins given that utrophin and dystrophin linkers are almost exclusively helical in nature (Keep *et al.*, 1999b; Norwood *et al.*, 2000); α-actinin and plectin contain some helix but a large amount of turn (Franzot et al., 2005; Garcia-Alvarez et al., 2003) and fimbrin has no defined structure (Goldsmith et al., 1997). It should be noted, however, that the crystallisation of these protein domains may result in a linker structure that is not representative of the native protein in solution. It is quite possible that the association of the CH domains

to generate the compact crystal structures of plectin, α-actinin and fimbrin may result in a certain degree of helical disruption and unwinding of the linker region.

If future studies of the importance of linker domain structure and function are undertaken it may be more useful to manipulate the linker sequence as little as possible to minimise potential disruption to the surrounding CH domains. For instance, duplication of a portion of the utrophin linker sequence that is α-helical in nature would serve to lengthen the linker without the introduction of foreign sequence and this may be less disruptive. It is odd that removal of sequence to generate the α-actinin linker mutant was problematic, especially as the mutant was designed to remove almost two complete helical turns, but it is likely that the stretch of sequence that flanked the removed portion was not compatible once joined. If this were the case then a larger region of the linker may need to be mutated to ensure that the helical nature of the linker is maintained and disruption to the structure of the flanking CH domains does not occur. In any case, it is apparent that the design of the linker mutants would have benefited from a more stringent experimental design focussing upon the maintenance of the secondary structure of the linker rather than the simple insertion or removal of sequence to lengthen or shorten the linker respectively.

It was apparent that the conformation of the utrophin ABD could not be easily investigated by simply altering solution pH or by mutating the linker region. However, it would be possible to prevent the proposed opening of the molecule upon F-actin binding by introducing a disulphide bond into the domain. The presence of a disulphide bond effectively forces the utrophin ABD to remain in a closed conformation when in solution and when associating with F-actin. The location of the cysteine residues that would form the disulphide were chosen based upon two residues that opposed one another in the CH domain interface of the utrophin ABD crystal dimer. This interface was very similar to the interface generated within the fimbrin crystal dimer and this structure has been used to model the association of the utrophin ABD with F-actin in the closed conformation (Lehman et al., 2004; Sutherland-Smith et al., 2003). The mutant protein was expressed well and was soluble. The initial characterisation confirmed the presence of the cysteines within the mutant protein and that the presence of these residues did not cause any

oligomerisation in solution. Following these analyses the disulphide bond was successfully induced to form via oxidation but it was clear that not all of the protein sample could be induced to form the disulphide. A small portion of the sample remained in the non-cross-linked state when the oxidants were removed potentially suggesting that the disulphide was under strain. This was interesting as it implied that the CH domain interface generated in the crystal was not the interface adopted when in solution and given the extreme conditions employed during crystal formation this was not surprising. It was possible, however, that the position of the disulphide could be altered to give a more favourable alignment of the two cysteine residues. A similar disulphide was engineered into the plectin ABD using a program called SSBOND (Garcia-Alvarez et al., 2003). If this program were used to predict the residues to mutate it may be possible to generate a disulphide that would form more favourably. However, this program bases its predictions upon the crystal structure of the protein in question so it may not improve upon the locations of the cysteines that are chosen manually. The formation of the disulphide within the plectin ABD resulted in complete oxidation of the protein indicating that the cysteine residues were favourably aligned and/or that the plectin ABD crystal structure was very similar to the structure of the protein in solution (Garcia-Alvarez et al., 2003). It may be possible that the plectin inter-CH domain linker allows much more freedom to the positioning of the CH domains than the utrophin ABD linker. The fact that the utrophin ABD linker is mostly helical in nature may limit the free rotation of the CH domains with regard to one another and this may be relevant to the mode of binding with F-actin.

The presence of cysteines within the utrophin ABD also allowed the fluorescent labelling of the mutant ABD. It was hoped that the conjugation of fluors to the cysteine residues could be used to indicate the conformation of the domain when in solution via use of FRET. Following the successful labelling of the double cysteine mutant with fluorescein and rhodmaine FRET was attempted. No energy transfer was detected suggesting that the two fluors were not aligned and/or close enough to allow FRET. It was clear, in conjunction with a failure to completely oxidise the protein sample, that the utrophin ABD solution state is not represented by the CH domain interface observed in the crystal structure.

Initial analyses confirmed that a disulphide was formed within the utrophin ABD effectively locking the domain in a closed conformation. It was shown that the oxidised (locked closed) utrophin ABD retained an ability to bind F-actin with a 1:1 stoichiometry and a binding affinity similar to the reduced (no disulphide) protein sample. The binding affinity of the double cysteine mutant in both oxidised and reduced forms was found to be less than that of the wild type protein with the oxidised mutant exhibiting an affinity that was lower than that of the reduced mutant. This demonstrates that it is not essential for the utrophin ABD to open upon binding and presumably, this manner of association could be described by the closed model of binding proposed by Sutherland-Smith and colleagues (Sutherland-Smith et al., 2003). The DSC analysis demonstrates that the utrophin ABD does interact with F-actin in the locked closed conformation but interestingly the data for the wild type protein suggests that binding occurs in an open manner with no obvious conformational change upon association. The tryptophan fluorescence data also suggests that the oxidised double cysteine mutant is associating with F-actin in a different manner to the wild type protein but the question remains as to how this relates to the known models of the utrophin ABD binding to F-actin. The fact that the utrophin ABD binds in an open conformation is in agreement with the binding models of Moores and colleagues (Moores et al., 2000) but the ability to bind in a locked closed conformation could be described by the Sutherland-Smith model (Sutherland-Smith et al., 2003). The data presented here suggest that the utrophin ABD does not experience a large change in conformation upon association with F-actin as previously thought. The DSC analysis suggests that the domain adopts a more open conformation in solution which is also supported by the inability to generate a FRET signal and to completely oxidise the double cysteine mutant. A recent review presented by Lehman and colleagues attempted to evaluate the different models of utrophin ABD association with F-actin (Lehman et al., 2004). Lehman et al., (2004) proposed that the different methodologies used to produce the molecular reconstructions of the utrophin ABD/F-actin interaction could potentially be where problems have arisen in the generation of a number of seemingly exclusive models. It was proposed that the relatively low affinity of the utrophin ABD towards F-actin required a high molar excess to be used to ensure saturation of actin filaments

(Lehman et al., 2004). This large excess poses the danger of generating spurious binding and may contribute towards generating binding models where interaction with F-actin was partial and varied considerably. In any case, Lehman and colleagues re-analysed some of their earlier data using iterative helical real space refinement (IHRSR) and could find no differences when compared to earlier data generated using helical reconstruction (Lehman et al., 2004). They maintain that the utrophin ABD associates with F-actin in a closed and compact configuration similar to the models generated for the fimbrin and α-actinin ABDs (Hanein et al., 1998; Tang et al., 2001). Given the similarity of the overall structure of these domains it would not be surprising for actin-binding to occur in a similar manner. However, during the construction of the utrophin binding models it is often required to fit the ABD crystal structure into the density envelope attributed to bound protein. Models of the utrophin ABD binding actin in the closed state often employ a CH domain arrangement that is similar to the closed and compact fimbrin crystal structure (Lehman et al., 2004; Sutherland-Smith et al., 2003). The data presented here suggest that this is not the conformation adopted by the utrophin ABD in solution and that binding to F-actin causes little or no conformational change. Paradoxically, DSC analysis suggests that binding to F-actin can occur in both an open and closed manner so it would seem that binding to F-actin by the utrophin ABD can occur in both conformations. Binding to F-actin in the locked closed conformation effectively removed ABS1 from participating with the interaction when it is known that, individually, only CH1 possesses actin-binding capabilities whereas CH2 does not (Gimona and Mital, 1998; Way et al., 1992; Winder et al., 1995). Analyses of the plectin ABD associating with F-actin suggest that initial association occurs via CH1 followed by a conformational change within the domain that allows a relative relocation of CH2 to attain the full binding potential (Garcia-Alvarez et al., 2003). It is possible that this may also occur for the utrophin ABD.

This study has presented data that have interesting implications regarding the interpretation of the current models of utrophin ABD association with F-actin. However, a more rigorous analysis of utrophin ABD cysteine mutants would yield data of further use towards the investigation of the binding interaction. This work has principally focused upon a double cysteine mutant of the utrophin ABD. During the

production of this mutant a single cysteine mutant was generated within CH1 but it would also be useful to produce the second CH domain cysteine mutation within CH2. Characterising the actin-binding properties of these mutants would be of use towards a complete determination of the effects that the cysteine mutations have upon the binding interaction. It would also be beneficial to subject all of the cysteine mutants to CD analysis to make sure that no gross structural alterations have occurred as a result of the mutations. Any structural perturbation may affect the manner in which these mutants associate with F-actin as already determined via the linker mutants. It would be of particular importance to try and visualise the binding of the locked closed utrophin ABD with F-actin using either helical reconstruction or IHRSR. CH domains have been found to be particularly stable protein folds, it would be useful to investigate the effects upon protein stability that the presence of a disulphide generates. It is likely that the disulphide bond would increase the resistance to proteolysis and may prove useful in supporting the DSC data. All of these experiments would yield information that, combined with the current models of utrophin ABD association, would be particularly useful when evaluating the current modes of association. Also, analytical ultracentrifugation may be of use to identify hydrodynamic differences between the locked closed form of the utrophin ABD and the wild type protein to help determine if there is a detectable difference in solution conformation which may complement the DSC work. It would also be of use to further map the interaction of the utrophin ABD with F-actin. The double or single cysteine mutants could be fluorescently labelled and FRET could be attempted with phalloidin labelled F-actin to try and gauge specific distances between the labels of both molecules. All of these studies would be useful in contributing to the overall understanding of how the utrophin ABD interacts with F-actin.

It would seem that utrophin association with F-actin can be quite dynamic and ambiguous when only the ABD is considered. Analyses of the isolated utrophin ABD have been preferred given the large size of the whole protein. It is known that utrophin does not associate solely with F-actin via its N-terminal ABD but also via a number of spectrin repeats immediately following the domain (Rybakova and Ervasti, 2005; Rybakova et al., 2002). The utrophin ABD and the first spectrin repeat have been modelled to bind F-actin with a 1:1 stoichiometry and affinities similar to

the isolated domain (Rybakova and Ervasti, 2005; Sutherland-Smith et al., 2003). More recent work using utrophin ABD constructs and up to ten spectrin repeats has shown that binding affinities and stoichiometries identical to the full length protein can be attained (Rybakova and Ervasti, 2005). It is clear that modelling the isolated utrophin ABD may result in ambiguous data given that this particular domain requires the presence of the neighbouring spectrin repeats to achieve an interaction with F-actin more akin to the complete protein. Given the importance of the spectrin repeats that follow the utrophin ABD to the interaction with F-actin, modelling the association of plectin and α-actinin ABDs should also be approached carefully until an understanding of the contribution that the domains that follow the ABDs of these proteins is better understood. In the case of α-actinin, the presence of adjoining spectrin repeats would be particularly important, not only for the location of the ABD and the overall binding reaction, but also to the potential regulation of the interaction with F-actin.

The work presented here has helped to further develop the understanding of how the utrophin ABD interacts with F-actin but many more questions have been raised. It is apparent, though, that continued work is required to try and determine how the utrophin ABD and those related to it interact with and bind to F-actin.

Appendices

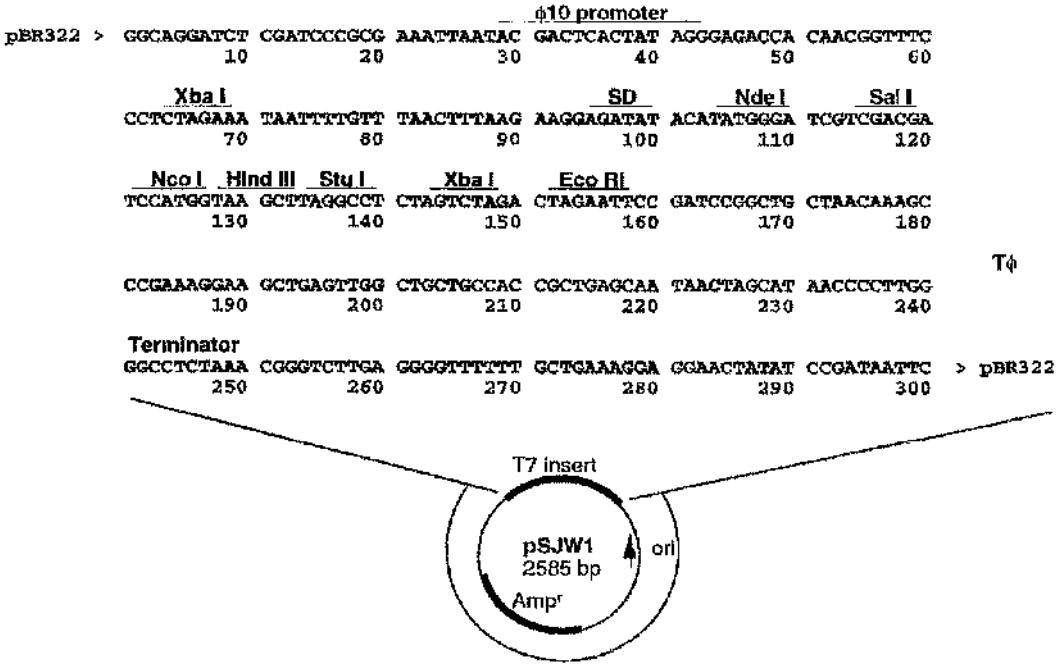

Figure A: T7 insert region pf pSJW1. The utrophin ABD construct (UTR261) was inserted into the pSJW1 vector (Winder and Kendrick-Jones, 1995) between the Nde I and Sal I restriction sites. The pSJW1 vector is based upon the pET expression vector pMW172 which was modified by the addition of a Sal I restriction site in place of an existing Bam HI site. These vectors are under the control of the T7 promoter and are particulary useful for the generation of high levels of soluble protein. An initial aliquot of pSJW1 and UTR261 construct was supplied by Professor S. Winder.

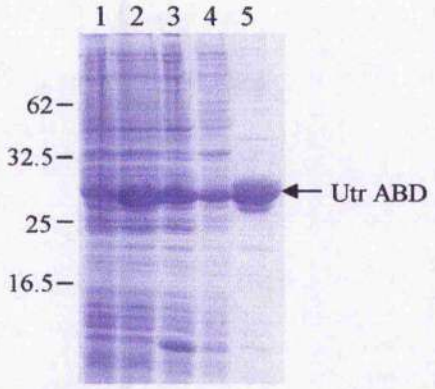

Appendix B: Expression, solubility and purification of wild type utrophin ABD. Lanes 1 and 2 represent the protein present in a pre and post induction sample of 1 ml of bacterial lysate. Lanes 4 and 5 indicate soluble and insoluble protein fractions and lane 5 represents a sample of gel purified utrophin ABD.

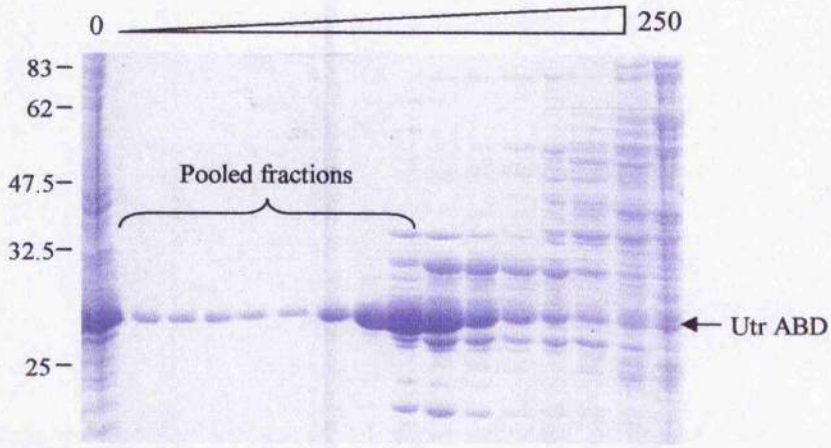

Appendix C: Sepharose™ DEAE elution profile of utrophin ABD. Bacterial lysate containing soluble utrophin ABD (lane 1) was loaded onto DEAE sepharose equilibrated with TED buffer pH 8.0. Utrophin ABD was eluted using a 0-0.5 M NaCl gradient (lanes 2-16). The most homogenous fractions were chosen to be concentrated for gel filtration.

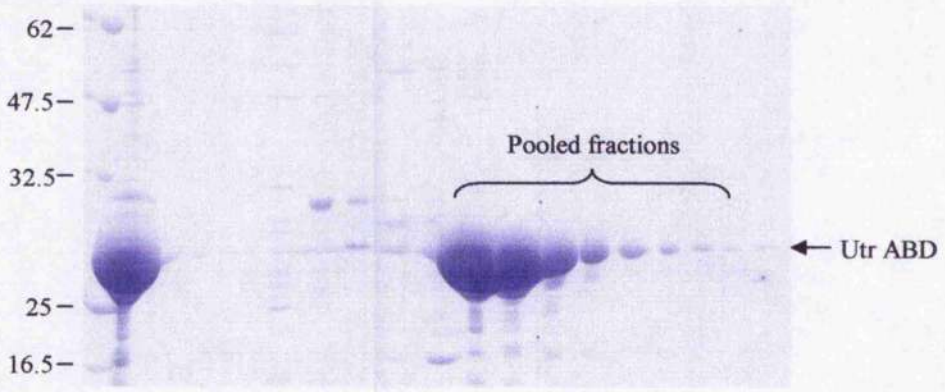

Appendix D: Gel purification of wild type utrophin ABD. Elution of utrophin ABD from a Sephacryl™ S200 gel filtration column. Homogenous fractions were selected and concentrated ready for experimental use. A sample of concentrated DEAE eluted utrophin ABD is shown on the far left of the figure for comparison with the gel purified fractions.

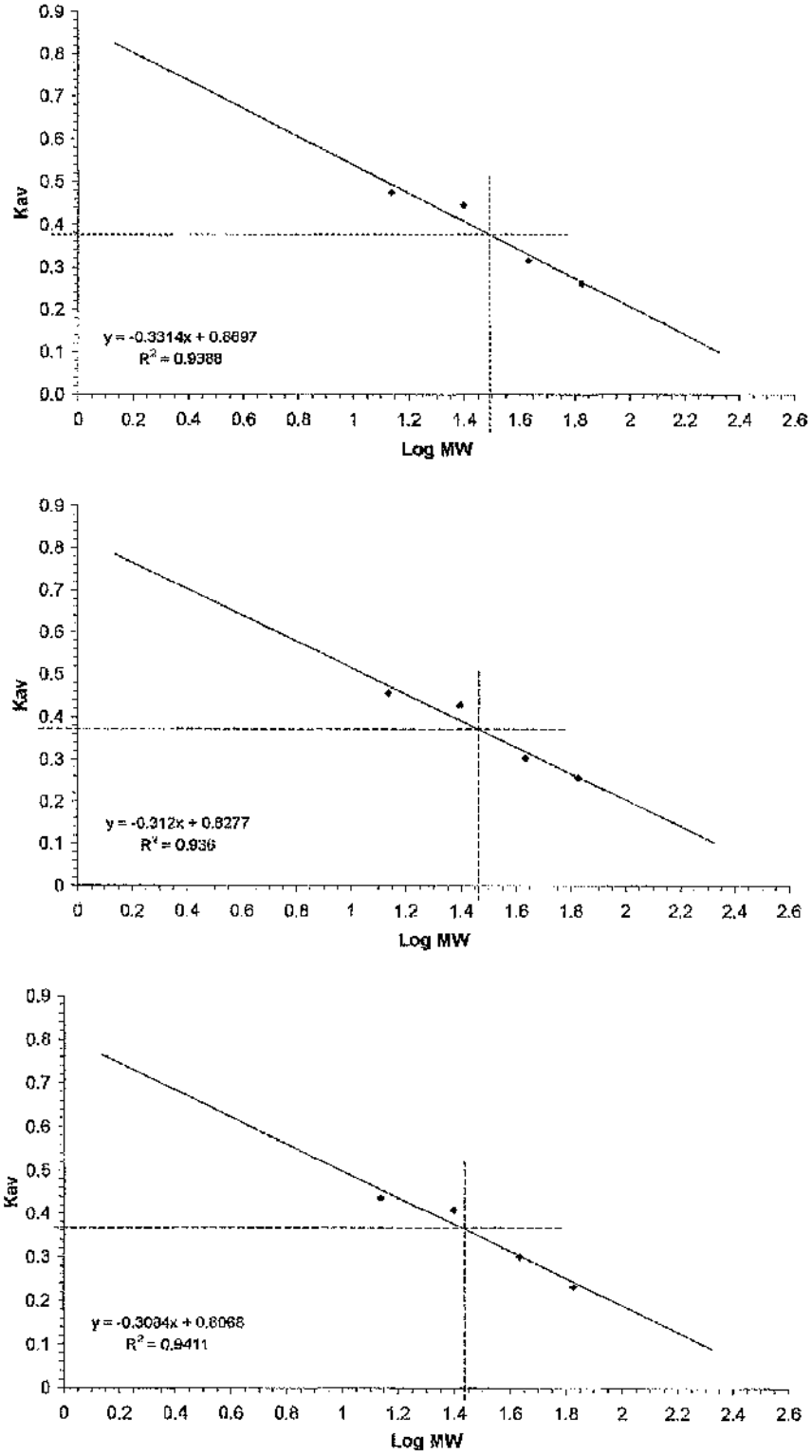

Figure E: Calibration of the Superose gel filtration column at pH 6, 8 and 10. Calibration cures were generated for the Superose™ 12 HR column at pH 6, 8 and 10 to allow accurate determination of utrophin ABD MW. The dashed lines mark the value of K_{av} calculated for utrophin ABD at each pH and the log MW to which this corresponds

20k Interference data fitted with a model for a single ideal species

approximate	pH6		pH8		pH10	
conc (au)	$M_{w,app}$ (kDa)	(+/-)	$M_{w,app}$ (kDa)	(+/-)	$M_{w,app}$ (kDa)	(+/-)
0.10			174.9	14.2	82.2	7.8
0.15	13.7	1.6	128.8	10.2	19.9	2.3
0.20	21.0	2.0	103.6	8.7	25.1	2.2
0.25	21.2	1.8	71.2	11.0	200.6	17.2
0.30	53.8	3.9	66.0	8.5	41.3	2.9
0.35	48.9	2.9	131.5	15.1	232.7	17.6
0.40	53.6	2.7	64.9	7.0	131.5	11.9
0.45	94.7	6.6	51.8	4.8	73.0	4.6
0.50	53.3	3.2	53.6	4.2	72.8	5.8

25k Interference data fitted with a model for a single ideal species

approximate	pH6		pH8		pH10	
conc (au)	$M_{w,app}$ (kDa)	(+/-)	$M_{w,app}$ (kDa)	(+/-)	$M_{w,app}$ (kDa)	(+/-)
0.10			87.6	6.7	43.9	5.1
0.15	15.3	1.4	89.8	6.1	45.1	5.3
0.20	35.1	4.5	60.0	4.1	165.4	19.6
0.25	29.3	2.7	52.8	3.2	120.9	14.6
0.30	45.0	3.8	45.0	2.2		
0.35	46.5	1.6	57.4	4.5	139.0	16.0
0.40	46.8	2.2	38.9	1.9	88.2	7.8
0.45	38.5	1.5	46.3	3.2	52.8	4.3
0.50	43.9	0.4	41.0	2.0	53.7	3.9

30k Interference data fitted with a model for a single ideal species

approximate	pH6		pH8		pH10	
conc (au)	$M_{w,app}$ (kDa)	(+/-)	$M_{w,app}$ (kDa)	(+/-)	$M_{w,app}$ (kDa)	(+/-)
0.10	40.5	3.7	74.5	4.3	53.5	2.5
0.15	35.8	3.6	59.5	2.5	55.9	3.2
0.20	41.4	1.9	24.5	1.5	73	8.2
0.25	37.6	2.4	51.8	4.9	96.8	11.6
0.30	40.9	0.8	44.9	2.8		
0.35	37.9	1.1	60.2	5.9	75.9	5.7
0.40	36.5	2.7	36.7	1.2	55.8	4.6
0.45	36.3	0.8	37.0	1.0	41.8	2.1
0.50	36.8	0.9	38.8	1.2	40.0	1.3

Figure F: Utrophin ABD interference data at 20000, 25000 and 30000 rpm, varying pH. Utrophin ABD was subjected to sedimentation equilibrium analysis at 20000, 25000 and 30000 rpm. A serial dilution of the utrophin stocks at pH 6, 8 and 10 were prepared to give nine samples ranging in concentration between 0.1 and 0.5 au at 280 nm. 100 µl of each concentration was prepared using the buffer dialysate at each pH consisting of 100 mM NaCl, 1 mM EDTA and either 20 mM Tris at pH 8 or 10 or MES at pH 6. 20 µl of each sample concentration was loaded into two 8 channel centrepieces along with a 20 µl reference buffer sample. An initial scan was recorded at 3000 rpm to check for cell leakage before running the samples at 18000, 25000 and 30000 rpm at 4 °C. Scans of sample distribution were recorded at each of these speeds and were used to calculate whole-cell apparent weight molecular masses for the utrophin ABD at each pH. The biophysical data required to determine the apparent molecular weight (buffer density, viscosity and v-bar) were calculated using the program *sednterp* (Laue, 1992). Blank cells refer to data that had not sufficiently distributed to be analysed.

25K Interference data fitted with model for single ideal species						
approximate	pH6		pH8		pH10	
conc (au)	$M_{w,app}$ (kDa)	(+/-)	$M_{w,app}$ (kDa)	(+/-)	$M_{w,app}$ (kDa)	(+/-)
0.10	65.2	11.7	226.8	30.4	192.0	45.6
0.15	47.4	5.2	12.5	1.4	59.3	11.1
0.20	27.8	2.6	20.7	2.3	231.8	7.3
0.25	36.4	3.2	56.8	7.3	190.8	6.2
0.30	32.3	2.2	61.5	6.3	215.6	9.7
0.35	34.7	1.9	50.9	9.9	137.9	9.9
0.40	24.2	1.4	26.0	2.3	45.0	2.9
0.45	23.8	1.0	36.2	1.3	28.2	1.3
0.50	32.1	1.5	37.0	2.1	31.8	1.4

30K Interference data fitted with model for single ideal species						
approximate	pH6		pH8		pH10	
conc (au)	$M_{w,app}$ (kDa)	(+/-)	$M_{w,app}$ (kDa)	(+/-)	$M_{w,app}$ (kDa)	(+/-)
0.10	61.4	9.7	100.0	17.3	175.7	24.0
0.15	31.6	3.3	29.4	3.0	33.5	3.8
0.20	33.8	2.6	25.5	2.0	202.4	7.2
0.25	34.4	2.7	39.8	3.7	187.3	5.8
0.30	31.9	1.6	40.6	2.6	163.8	20.8
0.35	30.2	1.0	33.7	2.8	119.0	3.1
0.40	32.2	1.2	26.7	1.3	38.5	1.0
0.45	27.9	1.0	32.6	0.8	32.6	0.8
0.50	31.7	0.7	31.9	0.7	31.8	1.4

Figure G: Repeated interference data of the utrophin ABD at 25000 and 30000 rpm, varying pH. Interference data of utrophin ABD at pH 6, 8 and 10 fitted with a model for a single ideal species. The experimental perameters were identical to those found in Figure F.

sample	rmsd	s20	s20,w	D	c(f)	c(au)	c(mg/ml)	M (kDa)
pH 6.0	0.1249	2.47	2.55	7.8	45.1	13.7	8.6	29.9
	0.0925	2.45	2.53	7.9	28.6	8.7	5.5	29.3
	0.0668	2.41	2.49	7.9	15.8	4.8	3.0	28.8
	cell leakage							
	0.0080	2.41	2.49	8.0	2.9	0.9	0.6	28.6
pH 8.0	0.0941	2.40	2.48	7.1	40.8	12.4	7.8	32.0
	0.0411	2.42	2.50	7.5	25.3	7.7	4.8	30.6
	cell leakage							
	0.0348	2.38	2.45	7.8	9.6	2.9	1.8	29.0
	0.0153	2.41	2.49	7.5	2.6	0.8	0.5	30.3
pH 10.0	0.1807	2.39	2.47	6.9	39.9	12.1	7.6	32.8
	0.1744	2.31	2.38	7.1	24.9	7.5	4.8	30.7
	0.0366	2.43	2.51	7.8	14.9	4.5	2.9	29.5
	0.0265	2.43	2.51	7.6	9.2	2.8	1.8	30.2
	0.0177	2.38	2.45	7.4	2.5	0.8	0.5	30.3

Figure H: Summary of utrophin ABD sedimentation velocity data at varying pH. The utrophin ABD was subjected to sedimentation velocity analysis at pH 6, 8 and 10. Protein stocks were diluted, with the respective buffers, to give a range of concentrations covering several orders of magnitude at each pH. 360 µl of each sample concentration was loaded into a two channel centrepiece along with 360 µl of buffer to serve as a reference. An initial scan was recorded at 3000 rpm to check for cell leakage. Once thermal equilibrium was attained (20 °C) the centrifuge was accelerated to 50000 rpm and 240 scans of sample distribution were recorded at 2 minute intervals. Data from the sedimentation velocity runs was analysed using the program *sedfit* (Schuck, 1998).

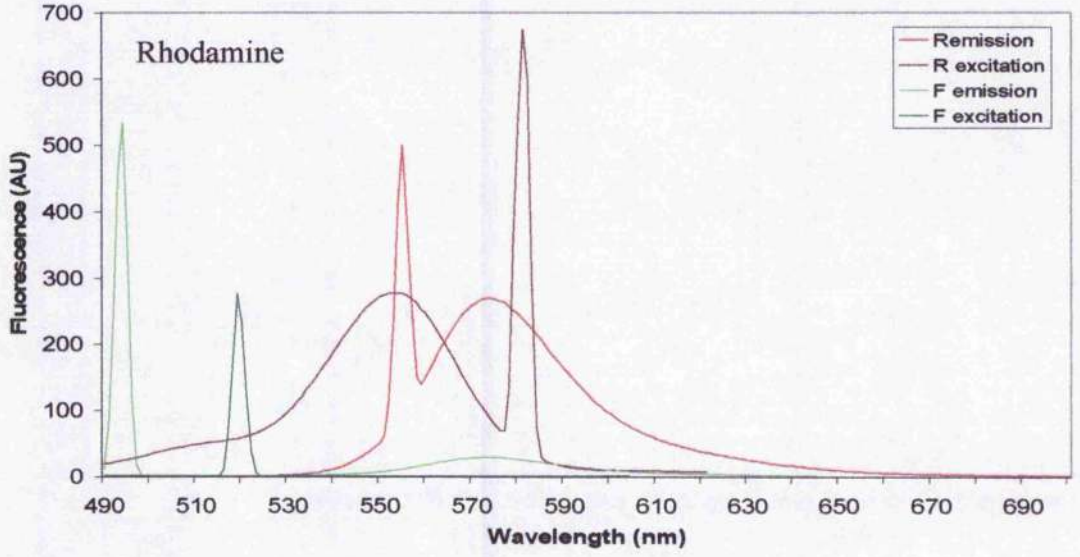

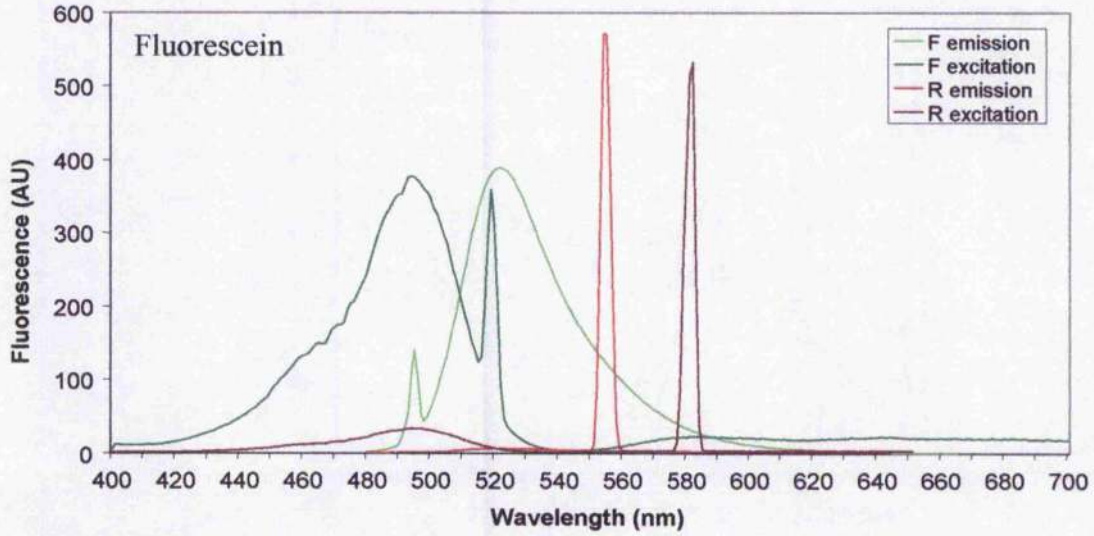

Appendix I: Confirmation of fluor conjugation using fluorescence. 30 μM samples $UTR^{T36C/S242C}$ labelled with either rhodamine or fluorescein were subjected to fluorescence analysis to confirm the presence of the conjugated fluors. Rhodamine conjugated $UTR^{T36C/S242C}$ was excited at 555 nm and emission spectra collected between 490-700 nm. Excitation spectra were also collected over the same range based on rhodamine emission at 580 nm. The rhodamine conjugated $UTR^{T36C/S242C}$ was also subjected to emission and excitation scans at the excitation (494 nm) and emission (518 nm) wavelengths of fluorescein to determine if rhodamine was stimulated at these wavelengths. Fluorescein conjugated $UTR^{T36C/S242C}$ was also subjected to emission and excitation scans at the wavelengths detailed above to confirm the presence of the fluor and if there was any stimulation by the rhodamine emission and excitation wavelengths. All scans were made at a slow scanning speed between wavelengths of 480 - 700 nm. Emission and excitation slit widths were both 1.5 nm. Fluorescence is represented in arbitrary units (AU).

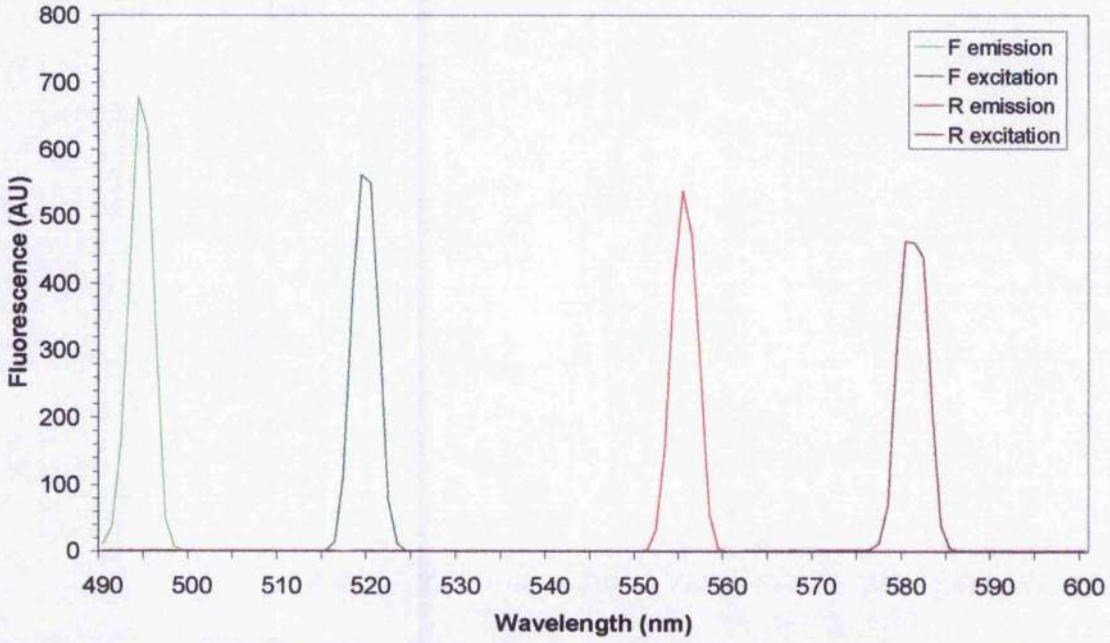

Appendix J: Actin fluorescence when scanned at the emission and excitation wavelengths of fluorescein and rhodamine. Samples of F-actin (5 μM) in TE pH 7.0 and 1 x ABB were subjected to emission and excitation scans at 555 or 494 nm and 580 or 518 nm. All scans were made at a slow scanning speed between wavelengths of 490 - 600 nm. Emission and excitation slit widths were both 1.5 nm. Fluorescence is represented as arbitrary units (AU).

References

Agre, P., Asimos, A., Casella, J. F., and McMillan, C. (1986). Inheritance pattern and clinical response to splenectomy as a reflection of erythrocyte spectrin deficiency in hereditary spherocytosis. N Engl J Med *315*, 1579-1583.

Agre, P., Casella, J. F., Zinkham, W. H., McMillan, C., and Bennett, V. (1985). Partial deficiency of erythrocyte spectrin in hereditary spherocytosis. Nature *314*, 380-383.

Amann, K. J., Guo, A. W., and Ervasti, J. M. (1999). Utrophin lacks the rod domain actin binding activity of dystrophin. J Biol Chem *274*, 35375-35380.

An, X., Guo, X., Sum, H., Morrow, J., Gratzer, W., and Mohandas, N. (2004). Phosphatidylserine binding sites in erythroid spectrin: location and implications for membrane stability. Biochemistry *43*, 310-315.

Atkinson, R. A., Joseph, C., Kelly, G., Muskett, F. W., Frenkiel, T. A., Nietlispach, D., and Pastore, A. (2001). Ca2+-independent binding of an EF-hand domain to a novel motif in the alpha-actinin-titin complex. Nat Struct Biol *8*, 853-857.

Baines, A. J. (2003). Comprehensive analysis of all triple helical repeats in beta-spectrins reveals patterns of selective evolutionary conservation. Cell Mol Biol Lett *8*, 195-214.

Banuelos, S., Saraste, M., and Carugo, K. D. (1998). Structural comparisons of calponin homology domains: implications for actin binding. Structure *6*, 1419-1431.

Baron, M. D., Davison, M. D., Jones, P., Patel, B., and Critchley, D. R. (1987). Isolation and characterization of a cDNA encoding a chick alpha-actinin. J Biol Chem *262*, 2558-2561.

Bateman, A., Birney, E., Durbin, R., Eddy, S. R., Finn, R. D., and Sonnhammer, E. L. (1999). Pfam 3.1: 1313 multiple alignments and profile HMMs match the majority of proteins. Nucleic Acids Res *27*, 260-262.

Becker, K., Robb, S. A., Hatton, Z., Yau, S. C., Abbs, S., and Roberts, R. G. (2003). Loss of a single amino acid from dystrophin resulting in Duchenne muscular dystrophy with retention of dystrophin protein. Hum Mutat *21*, 651.

Bennett, H., and Condeelis, J. (1988). Isolation of an immunoreactive analogue of brain fodrin that is associated with the cell cortex of Dictyostelium amoebae. Cell Motil Cytoskeleton *11*, 303-317.

Bennett, V., and Baines, A. J. (2001). Spectrin and ankyrin-based pathways: metazoan inventions for integrating cells into tissues. Physiol Rev *81*, 1353-1392.

Bennett, V., and Gilligan, D. M. (1993). The spectrin-based membrane skeleton and micron-scale organization of the plasma membrane. Annu Rev Cell Biol *9*, 27-66.

Berney, C., and Danuser, G. (2003). FRET or no FRET: a quantitative comparison. Biophys J *84*, 3992-4010.

Bies, R. D., Caskey, C. T., and Fenwick, R. (1992). An intact cysteine-rich domain is required for dystrophin function. J Clin Invest *90*, 666-672.

Blake, D. J., Tinsley, J. M., Davies, K. E., Knight, A. E., Winder, S. J., and Kendrick-Jones, J. (1995). Coiled-coil regions in the carboxy-terminal domains of dystrophin and related proteins: potentials for protein-protein interactions. Trends Biochem Sci *20*, 133-135.

Blake, D. J., Weir, A., Newey, S. E., and Davies, K. E. (2002). Function and genetics of dystrophin and dystrophin-related proteins in muscle. Physiol Rev *82*, 291-329.

Blanchard, A., Ohanian, V., and Critchley, D. (1989). The structure and function of alpha-actinin. J Muscle Res Cell Motil *10*, 280-289.

Blondin, L., Sapountzi, V., Maciver, S. K., Lagarrigue, E., Benyamin, Y., and Roustan, C. (2002). A structural basis for the pH-dependence of cofilin. F-actin interactions. Eur J Biochem *269*, 4194-4201.

Bonet-Kerrache, A., Fabbrizio, E., and Mornet, D. (1994). N-terminal domain of dystrophin. FEBS Lett *355*, 49-53.

Bramham, J., Hodgkinson, J. L., Smith, B. O., Uhrin, D., Barlow, P. N., and Winder, S. J. (2002). Solution structure of the calponin CH domain and fitting to the 3D-helical reconstruction of F-actin:calponin. Structure (Camb) *10*, 249-258.

Bresnick, A. R., Janmey, P. A., and Condeelis, J. (1991). Evidence that a 27-residue sequence is the actin-binding site of ABP-120. J Biol Chem *266*, 12989-12993.

Bresnick, A. R., Warren, V., and Condeelis, J. (1990). Identification of a short sequence essential for actin binding by Dictyostelium ABP-120. J Biol Chem *265*, 9236-9240.

Broderick, M. J., and Winder, S. J. (2002). Towards a complete atomic structure of spectrin family proteins. J Struct Biol *137*, 184-193.

Broderick, M. J., and Winder, S. J. (2005). Spectrin, alpha-actinin, and dystrophin. Adv Protein Chem *70*, 203-246.

Buevich, A. V., Lundberg, S., Sethson, I., Edlund, U., and Backman, L. (2004). NMR studies of calcium-binding to mutant alpha-spectrin EF-hands. Cell Mol Biol Lett *9*, 167-186.

Burridge, K., and Chrzanowska-Wodnicka, M. (1996). Focal adhesions, contractility, and signaling. Annu Rev Cell Dev Biol *12*, 463-518.

Buscaglia, M., Schuler, B., Lapidus, L. J., Eaton, W. A., and Hofrichter, J. (2003). Kinetics of intramolecular contact formation in a denatured protein. J Mol Biol *332*, 9-12.

Byers, T. J., Brandin, E., Lue, R. A., Winograd, E., and Branton, D. (1992). The complete sequence of Drosophila beta-spectrin reveals supra-motifs comprising eight 106-residue segments. Proc Natl Acad Sci U S A *89*, 6187-6191.

Byers, T. J., Husain-Chishti, A., Dubreuil, R. R., Branton, D., and Goldstein, L. S. (1989). Sequence similarity of the amino-terminal domain of Drosophila beta spectrin to alpha actinin and dystrophin. J Cell Biol *109*, 1633-1641.

Byron, O. (2000). Hydrodynamic bead modeling of biological macromolecules. Methods Enzymol *321*, 278-304.

Campbell, K. P., and Kahl, S. D. (1989). Association of dystrophin and an integral membrane glycoprotein. Nature *338*, 259-262.

Carugo, K. D., Banuelos, S., and Saraste, M. (1997). Crystal structure of a calponin homology domain. Nat Struct Biol *4*, 175-179.

Castresana, J., and Saraste, M. (1995). Does Vav bind to F-actin through a CH domain? FEBS Lett *374*, 149-151.

Chan, Y., and Kunkel, L. M. (1997). In vitro expressed dystrophin fragments do not associate with each other. FEBS Lett *410*, 153-159.

Chen, Y., and Barkley, M. D. (1998). Toward understanding tryptophan fluorescence in proteins. Biochemistry *37*, 9976-9982.

Chung, W., and Campanelli, J. T. (1999). WW and EF hand domains of dystrophin-family proteins mediate dystroglycan binding. Mol Cell Biol Res Commun *2*, 162-171.

Cicchetti, P., Mayer, B. J., Thiel, G., and Baltimore, D. (1992). Identification of a protein that binds to the SH3 region of Abl and is similar to Bcr and GAP-rho. Science *257*, 803-806.

Claudepierre, T., Rodius, F., Frasson, M., Fontaine, V., Picaud, S., Dreyfus, H., Mornet, D., and Rendon, A. (1999). Differential distribution of dystrophins in rat retina. Invest Ophthalmol Vis Sci *40*, 1520-1529.

Coffey, A. J., Roberts, R. G., Green, E. D., Cole, C. G., Butler, R., Anand, R., Giannelli, F., and Bentley, D. R. (1992). Construction of a 2.6-Mb contig in yeast artificial chromosomes spanning the human dystrophin gene using an STS-based approach. Genomics *12*, 474-484.

Corrado, K., Mills, P. L., and Chamberlain, J. S. (1994). Deletion analysis of the dystrophin-actin binding domain. FEBS Lett *344*, 255-260.

Craig, S. W., and Pardo, J. V. (1983). Gamma actin, spectrin, and intermediate filament proteins colocalize with vinculin at costameres, myofibril-to-sarcolemma attachment sites. Cell Motil *3*, 449-462.

Creighton, T. E. (1996). Proteins: Structures and molecular properties, 2nd edn (New York: W.H Freeman and Company).

Critchley, D. R. (2000). Focal adhesions - the cytoskeletal connection. Curr Opin Cell Biol *12*, 133-139.

Czurylo, E. A., Eimer, W., Kulikova, N., and Hellweg, T. (2000). Size, shape and secondary structure of calponin. Acta Biochim Pol *47*, 791-806.

Danowski, B. A., Imanaka-Yoshida, K., Sanger, J. M., and Sanger, J. W. (1992). Costameres are sites of force transmission to the substratum in adult rat cardiomyocytes. J Cell Biol *118*, 1411-1420.

Davison, M. D., and Critchley, D. R. (1988). alpha-Actinins and the DMD protein contain spectrin-like repeats. Cell *52*, 159-160.

Delaunay, J. (1995). Genetic disorders of the red cell membranes. FEBS Lett *369*, 34-37.

Delaunay, J., and Dhermy, D. (1993). Mutations involving the spectrin heterodimer contact site: clinical expression and alterations in specific function. Semin Hematol *30*, 21-33.

DeWolf, C., McCauley, P., Sikorski, A. F., Winlove, C. P., Bailey, A. I., Kahana, E., Pinder, J. C., and Gratzer, W. B. (1997). Interaction of dystrophin fragments with model membranes. Biophys J *72*, 2599-2604.

Djinovic-Carugo, K., Gautel, M., Ylanne, J., and Young, P. (2002). The spectrin repeat: a structural platform for cytoskeletal protein assemblies. FEBS Lett *513*, 119-123.

Dubreuil, R. R. (1991). Structure and evolution of the actin crosslinking proteins. Bioessays *13*, 219-226.

Dubreuil, R. R., Byers, T. J., Sillman, A. L., Bar-Zvi, D., Goldstein, L. S., and Branton, D. (1989). The complete sequence of Drosophila alpha-spectrin: conservation of structural domains between alpha-spectrins and alpha-actinin. J Cell Biol *109*, 2197-2205.

Dunn, S. D. (1980). ATP causes a large change in the conformation of the isolated alpha subunit of Escherichia coli F1 ATPase. J Biol Chem *255*, 11857-11860.

Earnest, J. P., Santos, G. F., Zuerbig, S., and Fox, J. E. (1995). Dystrophin-related protein in the platelet membrane skeleton. Integrin-induced change in detergent-insolubility and cleavage by calpain in aggregating platelets. J Biol Chem *270*, 27259-27265.

Ehmer, S., Herrmann, R., Bittner, R., and Voit, T. (1997). Spatial distribution of beta-spectrin in normal and dystrophic human skeletal muscle. Acta Neuropathol (Berl) *94*, 240-246.

Emery, A. E. (1991). Population frequencies of inherited neuromuscular diseases--a world survey. Neuromuscul Disord *1*, 19-29.

England, S. B., Nicholson, L. V., Johnson, M. A., Forrest, S. M., Love, D. R., Zubrzycka-Gaarn, E. E., Bulman, D. E., Harris, J. B., and Davies, K. E. (1990). Very mild muscular dystrophy associated with the deletion of 46% of dystrophin. Nature *343*, 180-182.

Ervasti, J. M., and Campbell, K. P. (1993). Dystrophin and the membrane skeleton. Curr Opin Cell Biol *5*, 82-87.

Ervasti, J. M., and Campbell, K. P. (1993). A role for the dystrophin-glycoprotein complex as a transmembrane linker between laminin and actin. J Cell Biol *122*, 809-823.

Evans, E. A., and Hochmuth, R. M. (1977). A solid-liquid composite model of the red cell membrane. J Membr Biol *30*, 351-362.

Fabbrizio, E., Bonet-Kerrache, A., Leger, J. J., and Mornet, D. (1993). Actin-dystrophin interface. Biochemistry *32*, 10457-10463.

Faulkner, G., Pallavicini, A., Comelli, A., Salamon, M., Bortoletto, G., Ievolella, C., Trevisan, S., Kojic, S., Dalla Vecchia, F., Laveder, P., *et al.* (2000). FATZ, a filamin-, actinin-, and telethonin-binding protein of the Z-disc of skeletal muscle. J Biol Chem *275*, 41234-41242.

Ferguson, K. M., Lemmon, M. A., Sigler, P. B., and Schlessinger, J. (1995). Scratching the surface with the PH domain. Nat Struct Biol *2*, 715-718.

Franzot, G., Sjoblom, B., Gautel, M., and Djinovic Carugo, K. (2005). The crystal structure of the actin binding domain from alpha-actinin in its closed conformation: structural insight into phospholipid regulation of alpha-actinin. J Mol Biol *348*, 151-165.

Fukami, K., Endo, T., Imamura, M., and Takenawa, T. (1994). alpha-Actinin and vinculin are PIP2-binding proteins involved in signaling by tyrosine kinase. J Biol Chem *269*, 1518-1522.

Fukami, K., Furuhashi, K., Inagaki, M., Endo, T., Hatano, S., and Takenawa, T. (1992). Requirement of phosphatidylinositol 4,5-bisphosphate for alpha-actinin function. Nature *359*, 150-152.

Fukami, K., Sawada, N., Endo, T., and Takenawa, T. (1996). Identification of a phosphatidylinositol 4,5-bisphosphate-binding site in chicken skeletal muscle alpha-actinin. J Biol Chem *271*, 2646-2650.

Galkin, V. E., Orlova, A., VanLoock, M. S., and Egelman, E. H. (2003). Do the utrophin tandem calponin homology domains bind F-actin in a compact or extended conformation? J Mol Biol *331*, 967-972.

Galkin, V. E., Orlova, A., VanLoock, M. S., Rybakova, I. N., Ervasti, J. M., and Egelman, E. H. (2002). The utrophin actin-binding domain binds F-actin in two different modes: implications for the spectrin superfamily of proteins. J Cell Biol *157*, 243-251.

Garcia-Alvarez, B., Bobkov, A., Sonnenberg, A., and de Pereda, J. M. (2003). Structural and functional analysis of the actin binding domain of plectin suggests alternative mechanisms for binding to F-actin and integrin beta4. Structure (Camb) *11*, 615-625.

Garcia De La Torre, J., Huertas, M. L., and Carrasco, B. (2000). Calculation of hydrodynamic properties of globular proteins from their atomic-level structure. Biophys J *78*, 719-730.

Gardner, K., and Bennett, V. (1987). Modulation of spectrin-actin assembly by erythrocyte adducin. Nature *328*, 359-362.

Gill, S. C., and von Hippel, P. H. (1989). Calculation of protein extinction coefficients from amino acid sequence data. Anal Biochem *182*, 319-326.

Gimona, M., Djinovic-Carugo, K., Kranewitter, W. J., and Winder, S. J. (2002). Functional plasticity of CH domains. FEBS Lett *513*, 98-106.

Gimona, M., and Mital, R. (1998). The single CH domain of calponin is neither sufficient nor necessary for F-actin binding. J Cell Sci *111 (Pt 13)*, 1813-1821.

Gimona, M., and Winder, S. J. (1998). Single calponin homology domains are not actin-binding domains. Curr Biol *8*, R674-675.

Goldberg, L. R., Hausmanowa-Petrusewicz, I., Fidzianska, A., Duggan, D. J., Steinberg, L. S., and Hoffman, E. P. (1998). A dystrophin missense mutation showing persistence of dystrophin and dystrophin-associated proteins yet a severe phenotype. Ann Neurol *44*, 971-976.

Goldsmith, S. C., Pokala, N., Shen, W., Fedorov, A. A., Matsudaira, P., and Almo, S. C. (1997). The structure of an actin-crosslinking domain from human fimbrin. Nat Struct Biol *4*, 708-712.

Gonnelli, M., and Strambini, G. B. (1995). Phosphorescence lifetime of tryptophan in proteins. Biochemistry *34*, 13847-13857.

Gratzer, W. B. (1982). Preparation of spectrin. Methods Enzymol *85 Pt B*, 475-480.

Greenfield, N., and Fasman, G. D. (1969). Computed circular dichroism spectra for the evaluation of protein conformation. Biochemistry *8*, 4108-4116.

Grum, V. L., Li, D., MacDonald, R. I., and Mondragon, A. (1999). Structures of two repeats of spectrin suggest models of flexibility. Cell *98*, 523-535.

Ha, T., Enderle, T., Ogletree, D. F., Chemla, D. S., Selvin, P. R., and Weiss, S. (1996). Probing the interaction between two single molecules: fluorescence resonance energy transfer between a single donor and a single acceptor. Proc Natl Acad Sci U S A *93*, 6264-6268.

Hanein, D., Volkmann, N., Goldsmith, S., Michon, A. M., Lehman, W., Craig, R., DeRosier, D., Almo, S., and Matsudaira, P. (1998). An atomic model of fimbrin binding to F-actin and its implications for filament crosslinking and regulation. Nat Struct Biol *5*, 787-792.

Harlan, J. E., Hajduk, P. J., Yoon, H. S., and Fesik, S. W. (1994). Pleckstrin homology domains bind to phosphatidylinositol-4,5-bisphosphate. Nature *371*, 168-170.

Haslam, R. J., Koide, H. B., and Hemmings, B. A. (1993). Pleckstrin domain homology. Nature *363*, 309-310.

Hassoun, H., and Palek, J. (1996). Hereditary spherocytosis: a review of the clinical and molecular aspects of the disease. Blood Rev *10*, 129-147.

Hassoun, H., Vassiliadis, J. N., Murray, J., Njolstad, P. R., Rogus, J. J., Ballas, S. K., Schaffer, F., Jarolim, P., Brabec, V., and Palek, J. (1997). Characterization of the underlying molecular defect in hereditary spherocytosis associated with spectrin deficiency. Blood *90*, 398-406.

Hawkins, M., Pope, B., Maciver, S. K., and Weeds, A. G. (1993). Human actin depolymerizing factor mediates a pH-sensitive destruction of actin filaments. Biochemistry *32*, 9985-9993.

Hazes, B., and Dijkstra, B. W. (1988). Model building of disulfide bonds in proteins with known three-dimensional structure. Protein Eng *2*, 119-125.

Helliwell, T. R., Ellis, J. M., Mountford, R. C., Appleton, R. E., and Morris, G. E. (1992). A truncated dystrophin lacking the C-terminal domains is localized at the muscle membrane. Am J Hum Genet *50*, 508-514.

Heyduk, T. (2002). Measuring protein conformational changes by FRET/LRET. Curr Opin Biotechnol *13*, 292-296.

Hoffman, E. P., Garcia, C. A., Chamberlain, J. S., Angelini, C., Lupski, J. R., and Fenwick, R. (1991). Is the carboxyl-terminus of dystrophin required for membrane association? A novel, severe case of Duchenne muscular dystrophy. Ann Neurol *30*, 605-610.

Huang, X., Poy, F., Zhang, R., Joachimiak, A., Sudol, M., and Eck, M. J. (2000). Structure of a WW domain containing fragment of dystrophin in complex with beta-dystroglycan. Nat Struct Biol *7*, 634-638.

Hyvonen, M., Macias, M. J., Nilges, M., Oschkinat, H., Saraste, M., and Wilmanns, M. (1995). Structure of the binding site for inositol phosphates in a PH domain. Embo J *14*, 4676-4685.

Ilsley, J. L., Sudol, M., and Winder, S. J. (2002). The WW domain: linking cell signalling to the membrane cytoskeleton. Cell Signal *14*, 183-189.

Ishikawa-Sakurai, M., Yoshida, M., Imamura, M., Davies, K. E., and Ozawa, E. (2004). ZZ domain is essentially required for the physiological binding of dystrophin and utrophin to beta-dystroglycan. Hum Mol Genet *13*, 693-702.

Izaguirre, G., Aguirre, L., Hu, Y. P., Lee, H. Y., Schlaepfer, D. D., Aneskievich, B. J., and Haimovich, B. (2001). The cytoskeletal/non-muscle isoform of alpha-actinin is phosphorylated on its actin-binding domain by the focal adhesion kinase. J Biol Chem *276*, 28676-28685.

Jacobson, G. R., Schaffer, M. H., Stark, G. R., and Vanaman, T. C. (1973). Specific chemical cleavage in high yield at the amino peptide bonds of cysteine and cystine residues. J Biol Chem *248*, 6583-6591.

James, M., Nuttall, A., Ilsley, J. L., Ottersbach, K., Tinsley, J. M., Sudol, M., and Winder, S. J. (2000). Adhesion-dependent tyrosine phosphorylation of (beta)-dystroglycan regulates its interaction with utrophin. J Cell Sci *113 (Pt 10)*, 1717-1726.

Jarrett, H. W., and Foster, J. L. (1995). Alternate binding of actin and calmodulin to multiple sites on dystrophin. J Biol Chem *270*, 5578-5586.

Johnson, D. A., Voet, J. G., and Taylor, P. (1984). Fluorescence energy transfer between cobra alpha-toxin molecules bound to the acetylcholine receptor. J Biol Chem *259*, 5717-5725.

Jung, D., Yang, B., Meyer, J., Chamberlain, J. S., and Campbell, K. P. (1995). Identification and characterization of the dystrophin anchoring site on beta-dystroglycan. J Biol Chem *270*, 27305-27310.

Kaplan, J. M., Kim, S. H., North, K. N., Rennke, H., Correia, L. A., Tong, H. Q., Mathis, B. J., Rodriguez-Perez, J. C., Allen, P. G., Beggs, A. H., and Pollak, M. R. (2000). Mutations in ACTN4, encoding alpha-actinin-4, cause familial focal segmental glomerulosclerosis. Nat Genet *24*, 251-256.

Kay, B. K., Williamson, M. P., and Sudol, M. (2000). The importance of being proline: the interaction of proline-rich motifs in signaling proteins with their cognate domains. Faseb J *14*, 231-241.

Keep, N. H., Norwood, F. L., Moores, C. A., Winder, S. J., and Kendrick-Jones, J. (1999a). The 2.0 A structure of the second calponin homology domain from the actin-binding region of the dystrophin homologue utrophin. J Mol Biol *285*, 1257-1264.

Keep, N. H., Winder, S. J., Moores, C. A., Walke, S., Norwood, F. L., and Kendrick-Jones, J. (1999b). Crystal structure of the actin-binding region of utrophin reveals a head-to-tail dimer. Structure Fold Des *7*, 1539-1546.

Kelly, S. M., and Price, N. C. (2000). The use of circular dichroism in the investigation of protein structure and function. Curr Protein Pept Sci *1*, 349-384.

Kennedy, S. P., Warren, S. L., Forget, B. G., and Morrow, J. S. (1991). Ankyrin binds to the 15th repetitive unit of erythroid and nonerythroid beta-spectrin. J Cell Biol *115*, 267-277.

Kerr, T. P., Sewry, C. A., Robb, S. A., and Roberts, R. G. (2001). Long mutant dystrophins and variable phenotypes: evasion of nonsense-mediated decay? Hum Genet *109*, 402-407.

Kingston, H. M., Harper, P. S., Pearson, P. L., Davies, K. E., Williamson, R., and Page, D. (1983). Localisation of gene for Becker muscular dystrophy. Lancet *2*, 1200.

Klein, M. G., Shi, W., Ramagopal, U., Tseng, Y., Wirtz, D., Kovar, D. R., Staiger, C. J., and Almo, S. C. (2004). Structure of the actin crosslinking core of fimbrin. Structure (Camb) *12*, 999-1013.

Knight, B., Laukaitis, C., Akhtar, N., Hotchin, N. A., Edlund, M., and Horwitz, A. R. (2000). Visualizing muscle cell migration in situ. Curr Biol *10*, 576-585.

Koenig, M., Beggs, A. H., Moyer, M., Scherpf, S., Heindrich, K., Bettecken, T., Meng, G., Muller, C. R., Lindlof, M., Kaariainen, H., and et al. (1989). The molecular basis for Duchenne versus Becker muscular dystrophy: correlation of severity with type of deletion. Am J Hum Genet *45*, 498-506.

Koenig, M., Hoffman, E. P., Bertelson, C. J., Monaco, A. P., Feener, C., and Kunkel, L. M. (1987). Complete cloning of the Duchenne muscular dystrophy (DMD) cDNA and preliminary genomic organization of the DMD gene in normal and affected individuals. Cell *50*, 509-517.

Koenig, M., Monaco, A. P., and Kunkel, L. M. (1988). The complete sequence of dystrophin predicts a rod-shaped cytoskeletal protein. Cell *53*, 219-226.

Korenbaum, E., and Rivero, F. (2002). Calponin homology domains at a glance. J Cell Sci *115*, 3543-3545.

Kosk-Kosicka, D., Bzdega, T., and Wawrzynow, A. (1989). Fluorescence energy transfer studies of purified erythrocyte Ca2+-ATPase. Ca2+-regulated activation by oligomerization. J Biol Chem *264*, 19495-19499.

Kuhlman, P. A., Hemmings, L., and Critchley, D. R. (1992). The identification and characterisation of an actin-binding site in alpha-actinin by mutagenesis. FEBS Lett *304*, 201-206.

Laemmli, U. K. (1970). Cleavage of structural proteins during the assembly of the head of bacteriophage T4. Nature *227*, 680-685.

Lagarrigue, E., Ternent, D., Maciver, S. K., Fattoum, A., Benyamin, Y., and Roustan, C. (2003). The activation of gelsolin by low pH: the calcium latch is sensitive to calcium but not pH. Eur J Biochem *270*, 4105-4112.

Lakowicz, J. R. (1999). Principles of Fluorescent Spectroscopy, 2nd edn (New York: Kluwer Academic/ Plenum Publishers).

Lamb, J. A., Allen, P. G., Tuan, B. Y., and Janmey, P. A. (1993). Modulation of gelsolin function. Activation at low pH overrides Ca2+ requirement. J Biol Chem *268*, 8999-9004.

Laue, T. M., Shah, B. D., Ridgeway, T. M. and Pelletier, S. L. (1992). Computer aided interpretation of analytical sedimentation data for proteins, In Analytical ultracentrifugation in biochemistry and polymer science, R. A. Harding SE, Horton, JC, ed. (Cambridge, UK: The Royal Society of Chemistry), pp. 90-125.

Law, R., Carl, P., Harper, S., Dalhaimer, P., Speicher, D. W., and Discher, D. E. (2003). Cooperativity in forced unfolding of tandem spectrin repeats. Biophys J *84*, 533-544.

Lazarides, E., and Burridge, K. (1975). Alpha-actinin: immunofluorescent localization of a muscle structural protein in nonmuscle cells. Cell *6*, 289-298.

Le Rumeur, E., Fichou, Y., Pottier, S., Gaboriau, F., Rondeau-Mouro, C., Vincent, M., Gallay, J., and Bondon, A. (2003). Interaction of dystrophin rod domain with membrane phospholipids. Evidence of a close proximity between tryptophan residues and lipids. J Biol Chem *278*, 5993-6001.

Lebart, M. C., Mejean, C., Boyer, M., Roustan, C., and Benyamin, Y. (1990). Localization of a new alpha-actinin binding site in the COOH-terminal part of actin sequence. Biochem Biophys Res Commun *173*, 120-126.

Lebart, M. C., Mejean, C., Roustan, C., and Benyamin, Y. (1993). Further characterization of the alpha-actinin-actin interface and comparison with filamin-binding sites on actin. J Biol Chem *268*, 5642-5648.

Lee, J. C., and Discher, D. E. (2001). Deformation-enhanced fluctuations in the red cell skeleton with theoretical relations to elasticity, connectivity, and spectrin unfolding. Biophys J *81*, 3178-3192.

Lehman, W., Craig, R., Kendrick-Jones, J., and Sutherland-Smith, A. J. (2004). An open or closed case for the conformation of calponin homology domains on F-actin? J Muscle Res Cell Motil *25*, 351-358.

Lemmon, M. A., and Ferguson, K. M. (1998). Pleckstrin homology domains. Curr Top Microbiol Immunol *228*, 39-74.

Lemmon, M. A., Ferguson, K. M., and Abrams, C. S. (2002). Pleckstrin homology domains and the cytoskeleton. FEBS Lett *513*, 71-76.

Lenk, U., Oexle, K., Voit, T., Ancker, U., Hellner, K. A., Speer, A., and Hubner, C. (1996). A cysteine 3340 substitution in the dystroglycan-binding domain of dystrophin associated with Duchenne muscular dystrophy, mental retardation and absence of the ERG b-wave. Hum Mol Genet *5*, 973-975.

Levine, B. A., Moir, A. J., Patchell, V. B., and Perry, S. V. (1990). The interaction of actin with dystrophin. FEBS Lett *263*, 159-162.

Levine, B. A., Moir, A. J., Patchell, V. B., and Perry, S. V. (1992). Binding sites involved in the interaction of actin with the N-terminal region of dystrophin. FEBS Lett *298*, 44-48.

Levitsky, D. I., Nikolaeva, O. P., Orlov, V. N., Pavlov, D. A., Ponomarev, M. A., and Rostkova, E. V. (1998). Differential scanning calorimetric studies on myosin and actin. Biochemistry (Mosc) *63*, 322-333.

Li, X., and Bennett, V. (1996). Identification of the spectrin subunit and domains required for formation of spectrin/adducin/actin complexes. J Biol Chem *271*, 15695-15702.

Liu, J., Taylor, D. W., and Taylor, K. A. (2004). A 3-D reconstruction of smooth muscle alpha-actinin by CryoEm reveals two different conformations at the actin-binding region. J Mol Biol *338*, 115-125.

Liu, Y., and Eisenberg, D. (2002). 3D domain swapping: as domains continue to swap. Protein Sci *11*, 1285-1299.

Loh, N. Y., Newey, S. E., Davies, K. E., and Blake, D. J. (2000). Assembly of multiple dystrobrevin-containing complexes in the kidney. J Cell Sci *113 (Pt 15)*, 2715-2724.

Love, D. R., Flint, T. J., Genet, S. A., Middleton-Price, H. R., and Davies, K. E. (1991). Becker muscular dystrophy patient with a large intragenic dystrophin deletion: implications for functional minigenes and gene therapy. J Med Genet *28*, 860-864.

Love, D. R., Hill, D. F., Dickson, G., Spurr, N. K., Byth, B. C., Marsden, R. F., Walsh, F. S., Edwards, Y. H., and Davies, K. E. (1989). An autosomal transcript in skeletal muscle with homology to dystrophin. Nature *339*, 55-58.

Lundberg, S., Bjork, J., Lofvenberg, L., and Backman, L. (1995). Cloning, expression and characterization of two putative calcium-binding sites in human non-erythroid alpha-spectrin. Eur J Biochem *230*, 658-665.

Lundberg, S., Lehto, V. P., and Backman, L. (1992). Characterization of calcium binding to spectrins. Biochemistry *31*, 5665-5671.

Luther, P. K. (2000). Three-dimensional structure of a vertebrate muscle Z-band: implications for titin and alpha-actinin binding. J Struct Biol *129*, 1-16.

MacDonald, R. I., and Pozharski, E. V. (2001). Free energies of urea and of thermal unfolding show that two tandem repeats of spectrin are thermodynamically more stable than a single repeat. Biochemistry *40*, 3974-3984.

Maksymiw, R., Sui, S. F., Gaub, H., and Sackmann, E. (1987). Electrostatic coupling of spectrin dimers to phosphatidylserine containing lipid lamellae. Biochemistry *26*, 2983-2990.

Markle, D. R., Evans, E. A., and Hochmuth, R. M. (1983). Force relaxation and permanent deformation of erythrocyte membrane. Biophys J *42*, 91-98.

Masaki, T., Endo, M., and Ebashi, S. (1967). Localization of 6S component of a alpha-actinin at Z-band. J Biochem (Tokyo) *62*, 630-632.

Matsudaira, P. (1991). Modular organization of actin crosslinking proteins. Trends Biochem Sci *16*, 87-92.

Matsumura, K., Ervasti, J. M., Ohlendieck, K., Kahl, S. D., and Campbell, K. P. (1992). Association of dystrophin-related protein with dystrophin-associated proteins in mdx mouse muscle. Nature *360*, 588-591.

Matsumura, K., Yamada, H., Shimizu, T., and Campbell, K. P. (1993). Differential expression of dystrophin, utrophin and dystrophin-associated proteins in peripheral nerve. FEBS Lett *334*, 281-285.

Mayer, B. J. (2001). SH3 domains: complexity in moderation. J Cell Sci *114*, 1253-1263.

Mayer, B. J., Ren, R., Clark, K. L., and Baltimore, D. (1993). A putative modular domain present in diverse signaling proteins. Cell *73*, 629-630.

McGough, A. (1998). F-actin-binding proteins. Curr Opin Struct Biol *8*, 166-176.

McGough, A., Way, M., and DeRosier, D. (1994). Determination of the alpha-actinin-binding site on actin filaments by cryoelectron microscopy and image analysis. J Cell Biol *126*, 433-443.

Michalak, M., Fu, S. Y., Milner, R. E., Busaan, J. L., and Hance, J. E. (1996). Phosphorylation of the carboxyl-terminal region of dystrophin. Biochem Cell Biol *74*, 431-437.

Mimura, N., and Asano, A. (1987). Further characterization of a conserved actin-binding 27-kDa fragment of actinogelin and alpha-actinins and mapping of their binding sites on the actin molecule by chemical cross-linking. J Biol Chem *262*, 4717-4723.

Minetti, C., Tanji, K., and Bonilla, E. (1992). Immunologic study of vinculin in Duchenne muscular dystrophy. Neurology *42*, 1751-1754.

Monaco, A. P., Bertelson, C. J., Middlesworth, W., Colletti, C. A., Aldridge, J., Fischbeck, K. H., Bartlett, R., Pericak-Vance, M. A., Roses, A. D., and Kunkel, L. M. (1985). Detection of deletions spanning the Duchenne muscular dystrophy locus using a tightly linked DNA segment. Nature *316*, 842-845.

Moores, C. A., Keep, N. H., and Kendrick-Jones, J. (2000). Structure of the utrophin actin-binding domain bound to F-actin reveals binding by an induced fit mechanism. J Mol Biol *297*, 465-480.

Moores, C. A., and Kendrick-Jones, J. (2000). Biochemical characterisation of the actin-binding properties of utrophin. Cell Motil Cytoskeleton *46*, 116-128.

Morris, G. E., Nguyen, T. M., Nguyen, T. N., Pereboev, A., Kendrick-Jones, J., and Winder, S. J. (1999). Disruption of the utrophin-actin interaction by monoclonal antibodies and prediction of an actin-binding surface of utrophin. Biochem J *337 (Pt 1)*, 119-123.

Mukai, H., Toshimori, M., Shibata, H., Takanaga, H., Kitagawa, M., Miyahara, M., Shimakawa, M., and Ono, Y. (1997). Interaction of PKN with alpha-actinin. J Biol Chem *272*, 4740-4746.

Muntoni, F., Gobbi, P., Sewry, C., Sherratt, T., Taylor, J., Sandhu, S. K., Abbs, S., Roberts, R., Hodgson, S. V., Bobrow, M., and et al. (1994). Deletions in the 5' region of dystrophin and resulting phenotypes. J Med Genet *31*, 843-847.

Musacchio, A., Gibson, T., Rice, P., Thompson, J., and Saraste, M. (1993). The PH domain: a common piece in the structural patchwork of signalling proteins. Trends Biochem Sci *18*, 343-348.

Musacchio, A., Noble, M., Pauptit, R., Wierenga, R., and Saraste, M. (1992). Crystal structure of a Src-homology 3 (SH3) domain. Nature *359*, 851-855.

Nakayama, S., and Kretsinger, R. H. (1994). Evolution of the EF-hand family of proteins. Annu Rev Biophys Biomol Struct *23*, 473-507.

Nguyen, T. M., Ellis, J. M., Love, D. R., Davies, K. E., Gatter, K. C., Dickson, G., and Morris, G. E. (1991). Localization of the DMDL gene-encoded dystrophin-related protein using a panel of nineteen monoclonal antibodies: presence at neuromuscular junctions, in the sarcolemma of dystrophic skeletal muscle, in vascular and other smooth muscles, and in proliferating brain cell lines. J Cell Biol *115*, 1695-1700.

Noegel, A., Witke, W., and Schleicher, M. (1987). Calcium-sensitive non-muscle alpha-actinin contains EF-hand structures and highly conserved regions. FEBS Lett *221*, 391-396.

Norwood, F. L., Sutherland-Smith, A. J., Keep, N. H., and Kendrick-Jones, J. (2000). The structure of the N-terminal actin-binding domain of human dystrophin and how mutations in this domain may cause Duchenne or Becker muscular dystrophy. Structure Fold Des *8*, 481-491.

Oda, T., Makino, K., Yamashita, I., Namba, K., and Maeda, Y. (2001). Distinct structural changes detected by X-ray fiber diffraction in stabilization of F-actin by lowering pH and increasing ionic strength. Biophys J *80*, 841-851.

Oosawa, F., and Kasai, M. (1962). A theory of linear and helical aggregations of macromolecules. J Mol Biol *4*, 10-21.

Otey, C. A., and Carpen, O. (2004). Alpha-actinin revisited: a fresh look at an old player. Cell Motil Cytoskeleton *58*, 104-111.

Otey, C. A., Pavalko, F. M., and Burridge, K. (1990). An interaction between alpha-actinin and the beta 1 integrin subunit in vitro. J Cell Biol *111*, 721-729.

Otto, J. J. (1994). Actin-bundling proteins. Curr Opin Cell Biol *6*, 105-109.

Palek, J., and Jarolim, P. (1993). Clinical expression and laboratory detection of red blood cell membrane protein mutations. Semin Hematol *30*, 249-283.

Pardo, J. V., Siliciano, J. D., and Craig, S. W. (1983). Vinculin is a component of an extensive network of myofibril-sarcolemma attachment regions in cardiac muscle fibers. J Cell Biol *97*, 1081-1088.

Pascual, J., Castresana, J., and Saraste, M. (1997). Evolution of the spectrin repeat. Bioessays *19*, 811-817.

Pasternak, C., Wong, S., and Elson, E. L. (1995). Mechanical function of dystrophin in muscle cells. J Cell Biol *128*, 355-361.

Pearce, M., Blake, D. J., Tinsley, J. M., Byth, B. C., Campbell, L., Monaco, A. P., and Davies, K. E. (1993). The utrophin and dystrophin genes share similarities in genomic structure. Hum Mol Genet *2*, 1765-1772.

Perkins, K. J., and Davies, K. E. (2002). The role of utrophin in the potential therapy of Duchenne muscular dystrophy. Neuromuscul Disord *12 Suppl 1*, S78-89.

Perry, S. V. (1955). Myosin Adenosine Triphosphatase, Vol 2 (New York: Academic Press).

Petrof, B. J., Shrager, J. B., Stedman, H. H., Kelly, A. M., and Sweeney, H. L. (1993). Dystrophin protects the sarcolemma from stresses developed during muscle contraction. Proc Natl Acad Sci U S A *90*, 3710-3714.

Phelps, S. F., Hauser, M. A., Cole, N. M., Rafael, J. A., Hinkle, R. T., Faulkner, J. A., and Chamberlain, J. S. (1995). Expression of full-length and truncated dystrophin mini-genes in transgenic mdx mice. Hum Mol Genet *4*, 1251-1258.

Pollard, T. D. (1984). Purification of a high molecular weight actin filament gelation protein from Acanthamoeba that shares antigenic determinants with vertebrate spectrins. J Cell Biol *99*, 1970-1980.

Pons, F., Robert, A., Fabbrizio, E., Hugon, G., Califano, J. C., Febrentz, J. A., Martinez, J., and Mornet, D. (1994). Utrophin localization in normal and dystrophin-deficient heart. Circulation *90*, 369-374.

Ponting, C. P., Blake, D. J., Davies, K. E., Kendrick-Jones, J., and Winder, S. J. (1996). ZZ and TAZ: new putative zinc fingers in dystrophin and other proteins. Trends Biochem Sci *21*, 11-13.

Porter, G. A., Dmytrenko, G. M., Winkelmann, J. C., and Bloch, R. J. (1992). Dystrophin colocalizes with beta-spectrin in distinct subsarcolemmal domains in mammalian skeletal muscle. J Cell Biol *117*, 997-1005.

Porter, J. D., Rafael, J. A., Ragusa, R. J., Brueckner, J. K., Trickett, J. I., and Davies, K. E. (1998). The sparing of extraocular muscle in dystrophinopathy is lost in mice lacking utrophin and dystrophin. J Cell Sci *111 (Pt 13)*, 1801-1811.

Prior, T. W., Bartolo, C., Pearl, D. K., Papp, A. C., Snyder, P. J., Sedra, M. S., Burghes, A. H., and Mendell, J. R. (1995). Spectrum of small mutations in the dystrophin coding region. Am J Hum Genet *57*, 22-33.

Prior, T. W., Papp, A. C., Snyder, P. J., Burghes, A. H., Bartolo, C., Sedra, M. S., Western, L. M., and Mendell, J. R. (1993). A missense mutation in the dystrophin gene in a Duchenne muscular dystrophy patient. Nat Genet *4*, 357-360.

Raae, A. J., Banuelos, S., Ylanne, J., Olausson, T., Goldie, K. N., Wendt, T., Hoenger, A., and Saraste, M. (2003). Actin binding of a minispectrin. Biochim Biophys Acta *1646*, 67-76.

Raats, C. J., van den Born, J., Bakker, M. A., Oppers-Walgreen, B., Pisa, B. J., Dijkman, H. B., Assmann, K. J., and Berden, J. H. (2000). Expression of agrin, dystroglycan, and utrophin in normal renal tissue and in experimental glomerulopathies. Am J Pathol *156*, 1749-1765.

Rafael, J. A., Cox, G. A., Corrado, K., Jung, D., Campbell, K. P., and Chamberlain, J. S. (1996). Forced expression of dystrophin deletion constructs reveals structure-function correlations. J Cell Biol *134*, 93-102.

Rando, T. A. (2001). The dystrophin-glycoprotein complex, cellular signaling, and the regulation of cell survival in the muscular dystrophies. Muscle Nerve *24*, 1575-1594.

Rebecchi, M. J., and Scarlata, S. (1998). Pleckstrin homology domains: a common fold with diverse functions. Annu Rev Biophys Biomol Struct *27*, 503-528.

Ren, R., Mayer, B. J., Cicchetti, P., and Baltimore, D. (1993). Identification of a ten-amino acid proline-rich SH3 binding site. Science *259*, 1157-1161.

Rentschler, S., Linn, H., Deininger, K., Bedford, M. T., Espanel, X., and Sudol, M. (1999). The WW domain of dystrophin requires EF-hands region to interact with beta-dystroglycan. Biol Chem *380*, 431-442.

Rief, M., Pascual, J., Saraste, M., and Gaub, H. E. (1999). Single molecule force spectroscopy of spectrin repeats: low unfolding forces in helix bundles. J Mol Biol *286*, 553-561.

Roberts, R. G. (1995). Dystrophin, its gene, and the dystrophinopathies. Adv Genet *33*, 177-231.

Roberts, R. G., Gardner, R. J., and Bobrow, M. (1994). Searching for the 1 in 2,400,000: a review of dystrophin gene point mutations. Hum Mutat *4*, 1-11.

Rubin, G. M., Yandell, M. D., Wortman, J. R., Gabor Miklos, G. L., Nelson, C. R., Hariharan, I. K., Fortini, M. E., Li, P. W., Apweiler, R., Fleischmann, W., *et al.* (2000). Comparative genomics of the eukaryotes. Science *287*, 2204-2215.

Rybakova, I. N., Amann, K. J., and Ervasti, J. M. (1996). A new model for the interaction of dystrophin with F-actin. J Cell Biol *135*, 661-672.

Rybakova, I. N., and Ervasti, J. M. (2005). Identification of spectrin-like repeats required for high affinity utrophin-actin interaction. J Biol Chem *280*, 23018-23023.

Rybakova, I. N., Patel, J. R., Davies, K. E., Yurchenco, P. D., and Ervasti, J. M. (2002). Utrophin binds laterally along actin filaments and can couple costameric actin with sarcolemma when overexpressed in dystrophin-deficient muscle. Mol Biol Cell *13*, 1512-1521.

Rybakova, I. N., Patel, J. R., and Ervasti, J. M. (2000). The dystrophin complex forms a mechanically strong link between the sarcolemma and costameric actin. J Cell Biol *150*, 1209-1214.

Sahr, K. E., Laurila, P., Kotula, L., Scarpa, A. L., Coupal, E., Leto, T. L., Linnenbach, A. J., Winkelmann, J. C., Speicher, D. W., Marchesi, V. T., and et al. (1990). The complete cDNA and polypeptide sequences of human erythroid alpha-spectrin. J Biol Chem *265*, 4434-4443.

Salmikangas, P., Mykkanen, O. M., Gronholm, M., Heiska, L., Kere, J., and Carpen, O. (1999). Myotilin, a novel sarcomeric protein with two Ig-like domains, is encoded by a candidate gene for limb-girdle muscular dystrophy. Hum Mol Genet *8*, 1329-1336.

Scheel, J., Ziegelbauer, K., Kupke, T., Humbel, B. M., Noegel, A. A., Gerisch, G., and Schleicher, M. (1989). Hisactophilin, a histidine-rich actin-binding protein from Dictyostelium discoideum. J Biol Chem *264*, 2832-2839.

Schlunegger, M. P., Bennett, M. J., and Eisenberg, D. (1997). Oligomer formation by 3D domain swapping: a model for protein assembly and misassembly. Adv Protein Chem *50*, 61-122.

Schmidt, J. M., Robson, R. M., Zhang, J., and Stromer, M. H. (1993). The marked pH dependence of the talin-actin interaction. Biochem Biophys Res Commun *197*, 660-666.

Schuck, P. (1998). Sedimentation analysis of noninteracting and self-associating solutes using numerical solutions to the Lamm equation. Biophys J *75*, 1503-1512.

Schuck, P. (2000). Size-distribution analysis of macromolecules by sedimentation velocity ultracentrifugation and lamm equation modeling. Biophys J *78*, 1606-1619.

Speicher, D. W., and Marchesi, V. T. (1984). Erythrocyte spectrin is comprised of many homologous triple helical segments. Nature *311*, 177-180.

Spudich, J. A., and Watt, S. (1971). The regulation of rabbit skeletal muscle contraction. I. Biochemical studies of the interaction of the tropomyosin-troponin complex with actin and the proteolytic fragments of myosin. J Biol Chem *246*, 4866-4871.

Sreerama, N., and Woody, R. W. (1993). A self-consistent method for the analysis of protein secondary structure from circular dichroism. Anal Biochem *209*, 32-44.

Sreerama, N., and Woody, R. W. (2000). Estimation of protein secondary structure from circular dichroism spectra: comparison of CONTIN, SELCON, and CDSSTR methods with an expanded reference set. Anal Biochem *287*, 252-260.

Stafford, W. F., 3rd, Mabuchi, K., Takahashi, K., and Tao, T. (1995). Physical characterization of calponin. A circular dichroism, analytical ultracentrifuge, and electron microscopy study. J Biol Chem *270*, 10576-10579.

Stoeckelhuber, M., Noegel, A. A., Eckerskorn, C., Kohler, J., Rieger, D., and Schleicher, M. (1996). Structure/function studies on the pH-dependent actin-binding protein hisactophilin in Dictyostelium mutants. J Cell Sci *109 (Pt 7)*, 1825-1835.

Stradal, T., Kranewitter, W., Winder, S. J., and Gimona, M. (1998). CH domains revisited. FEBS Lett *431*, 134-137.

Straub, V., Bittner, R. E., Leger, J. J., and Voit, T. (1992). Direct visualization of the dystrophin network on skeletal muscle fiber membrane. J Cell Biol *119*, 1183-1191.

Straub, V., and Campbell, K. P. (1997). Muscular dystrophies and the dystrophin-glycoprotein complex. Curr Opin Neurol *10*, 168-175.

Sutherland-Smith, A. J., Moores, C. A., Norwood, F. L., Hatch, V., Craig, R., Kendrick-Jones, J., and Lehman, W. (2003). An atomic model for actin binding by the CH domains and spectrin-repeat modules of utrophin and dystrophin. J Mol Biol *329*, 15-33.

Tanaka, M., and Shibata, H. (1985). Poly(L-proline)-binding proteins from chick embryos are a profilin and a profilactin. Eur J Biochem *151*, 291-297.

Tang, J., Taylor, D. W., and Taylor, K. A. (2001). The three-dimensional structure of alpha-actinin obtained by cryoelectron microscopy suggests a model for Ca(2+)-dependent actin binding. J Mol Biol *310*, 845-858.

Taylor, K. A., and Taylor, D. W. (1993). Projection image of smooth muscle alpha-actinin from two-dimensional crystals formed on positively charged lipid layers. J Mol Biol *230*, 196-205.

Taylor, K. A., Taylor, D. W., and Schachat, F. (2000). Isoforms of alpha-actinin from cardiac, smooth, and skeletal muscle form polar arrays of actin filaments. J Cell Biol *149*, 635-646.

Thomas, G. H., Newbern, E. C., Korte, C. C., Bales, M. A., Muse, S. V., Clark, A. G., and Kiehart, D. P. (1997). Intragenic duplication and divergence in the spectrin superfamily of proteins. Mol Biol Evol *14*, 1285-1295.

Tinsley, J. M., Blake, D. J., Roche, A., Fairbrother, U., Riss, J., Byth, B. C., Knight, A. E., Kendrick-Jones, J., Suthers, G. K., Love, D. R., and et al. (1992). Primary structure of dystrophin-related protein. Nature *360*, 591-593.

Tommasi di Vignano, A., Di Zenzo, G., Sudol, M., Cesareni, G., and Dente, L. (2000). Contribution of the different modules in the utrophin carboxy-terminal region to the formation and regulation of the DAP complex. FEBS Lett *471*, 229-234.

Trave, G., Lacombe, P. J., Pfuhl, M., Saraste, M., and Pastore, A. (1995). Molecular mechanism of the calcium-induced conformational change in the spectrin EF-hands. Embo J *14*, 4922-4931.

Tufty, R. M., and Kretsinger, R. H. (1975). Troponin and parvalbumin calcium binding regions predicted in myosin light chain and T4 lysozyme. Science *187*, 167-169.

Vainzof, M., Takata, R. I., Passos-Bueno, M. R., Pavanello, R. C., and Zatz, M. (1993). Is the maintainance of the C-terminus domain of dystrophin enough to ensure a milder Becker muscular dystrophy phenotype? Hum Mol Genet *2*, 39-42.

Viel, A. (1999). Alpha-actinin and spectrin structures: an unfolding family story. FEBS Lett *460*, 391-394.

Viel, A., and Branton, D. (1996). Spectrin: on the path from structure to function. Curr Opin Cell Biol *8*, 49-55.

Virel, A., and Backman, L. (2004). Molecular evolution and structure of alpha-actinin. Mol Biol Evol *21*, 1024-1031.

Vivian, J. T., and Callis, P. R. (2001). Mechanisms of tryptophan fluorescence shifts in proteins. Biophys J *80*, 2093-2109.

Wang, D. S., Miller, R., Shaw, R., and Shaw, G. (1996). The pleckstrin homology domain of human beta I sigma II spectrin is targeted to the plasma membrane in vivo. Biochem Biophys Res Commun *225*, 420-426.

Wang, D. S., and Shaw, G. (1995). The association of the C-terminal region of beta I sigma II spectrin to brain membranes is mediated by a PH domain, does not require membrane proteins, and coincides with a inositol-1,4,5 triphosphate binding site. Biochem Biophys Res Commun *217*, 608-615.

Wasenius, V. M., Saraste, M., Salven, P., Eramaa, M., Holm, L., and Lehto, V. P. (1989). Primary structure of the brain alpha-spectrin. J Cell Biol *108*, 79-93.

Waugh, R., and Evans, E. A. (1979). Thermoelasticity of red blood cell membrane. Biophys J *26*, 115-131.

Waugh, R. E., and Agre, P. (1988). Reductions of erythrocyte membrane viscoelastic coefficients reflect spectrin deficiencies in hereditary spherocytosis. J Clin Invest *81*, 133-141.

Way, M., Pope, B., Cross, R. A., Kendrick-Jones, J., and Weeds, A. G. (1992). Expression of the N-terminal domain of dystrophin in E. coli and demonstration of binding to F-actin. FEBS Lett *301*, 243-245.

Wells, D. J., Wells, K. E., Asante, E. A., Turner, G., Sunada, Y., Campbell, K. P., Walsh, F. S., and Dickson, G. (1995). Expression of human full-length and minidystrophin in transgenic mdx mice: implications for gene therapy of Duchenne muscular dystrophy. Hum Mol Genet *4*, 1245-1250.

Wessel, G. M., and Chen, S. W. (1993). Transient, localized accumulation of alpha-spectrin during sea urchin morphogenesis. Dev Biol *155*, 161-171.

Williams, M. W., and Bloch, R. J. (1999). Extensive but coordinated reorganization of the membrane skeleton in myofibers of dystrophic (mdx) mice. J Cell Biol *144*, 1259-1270.

Winder, S. J. (1997). The membrane-cytoskeleton interface: the role of dystrophin and utrophin. J Muscle Res Cell Motil *18*, 617-629.

Winder, S. J. (2001). The complexities of dystroglycan. Trends Biochem Sci *26*, 118-124.

Winder, S. J. (2003). Structural insights into actin-binding, branching and bundling proteins. Curr Opin Cell Biol *15*, 14-22.

Winder, S. J., Gibson, T. J., and Kendrick-Jones, J. (1995). Dystrophin and utrophin: the missing links! FEBS Lett *369*, 27-33.

Winder, S. J., Gibson, T. J., and Kendrick-Jones, J. (1996). Low probability of dystrophin and utrophin coiled coil regions forming dimers. Biochem Soc Trans *24*, 280S.

Winder, S. J., Hemmings, L., Bolton, S. J., Maciver, S. K., Tinsley, J. M., Davies, K. E., Critchley, D. R., and Kendrick-Jones, J. (1995). Calmodulin regulation of utrophin actin binding. Biochem Soc Trans *23*, 397S.

Winder, S. J., Hemmings, L., Maciver, S. K., Bolton, S. J., Tinsley, J. M., Davies, K. E., Critchley, D. R., and Kendrick-Jones, J. (1995). Utrophin actin binding domain: analysis of actin binding and cellular targeting. J Cell Sci *108 (Pt 1)*, 63-71.

Winder, S. J., Jess, T., and Ayscough, K. R. (2003). SCP1 encodes an actin-bundling protein in yeast. Biochem J *375*, 287-295.

Winder, S. J., and Kendrick-Jones, J. (1995). Calcium/calmodulin-dependent regulation of the NH2-terminal F-actin binding domain of utrophin. FEBS Lett *357*, 125-128.

Winder, S. J., and Kendrick-Jones, J. (1995). Protein production in three different expression vectors from a single polymerase chain reaction product. Anal Biochem *231*, 271-273.

Winder, S. J., and Walsh, M. P. (1990). Structural and functional characterization of calponin fragments. Biochem Int *22*, 335-341.

Winnard, A. V., Klein, C. J., Coovert, D. D., Prior, T., Papp, A., Snyder, P., Bulman, D. E., Ray, P. N., McAndrew, P., King, W., and et al. (1993). Characterization of translational frame exception patients in Duchenne/Becker muscular dystrophy. Hum Mol Genet *2*, 737-744.

Wu, P., and Brand, L. (1994). Resonance energy transfer: methods and applications. Anal Biochem *218*, 1-13.

Xia, H., Winokur, S. T., Kuo, W. L., Altherr, M. R., and Bredt, D. S. (1997). Actinin-associated LIM protein: identification of a domain interaction between PDZ and spectrin-like repeat motifs. J Cell Biol *139*, 507-515.

Yao, J., Le, T. C., Kos, C. H., Henderson, J. M., Allen, P. G., Denker, B. M., and Pollak, M. R. (2004). Alpha-actinin-4-mediated FSGS: an inherited kidney disease caused by an aggregated and rapidly degraded cytoskeletal protein. PLoS Biol *2*, 787-794.

Ylanne, J., Scheffzek, K., Young, P., and Saraste, M. (2001). Crystal structure of the alpha-actinin rod reveals an extensive torsional twist. Structure (Camb) *9*, 597-604.

Young, P., Ferguson, C., Banuelos, S., and Gautel, M. (1998). Molecular structure of the sarcomeric Z-disk: two types of titin interactions lead to an asymmetrical sorting of alpha-actinin. Embo J *17*, 1614-1624.

Zarrinpar, A., and Lim, W. A. (2000). Converging on proline: the mechanism of WW domain peptide recognition. Nat Struct Biol *7*, 611-613.

Zhang, M., Tanaka, T., and Ikura, M. (1995). Calcium-induced conformational transition revealed by the solution structure of apo calmodulin. Nat Struct Biol *2*, 758-767.

Zhang, P., Talluri, S., Deng, H., Branton, D., and Wagner, G. (1995). Solution structure of the pleckstrin homology domain of Drosophila beta-spectrin. Structure *3*, 1185-1195.

Zhou, M. M., Ravichandran, K. S., Olejniczak, E. F., Petros, A. M., Meadows, R. P., Sattler, M., Harlan, J. E., Wade, W. S., Burakoff, S. J., and Fesik, S. W. (1995). Structure and ligand recognition of the phosphotyrosine binding domain of Shc. Nature *378*, 584-592.

Zimmerle, C. T., and Frieden, C. (1988). Effect of pH on the mechanism of actin polymerization. Biochemistry *27*, 7766-7772.

Zucker, S., Buttle, D. J., Nicklin, M. J., and Barrett, A. J. (1985). The proteolytic activities of chymopapain, papain, and papaya proteinase III. Biochim Biophys Acta *828*, 196-204.

Zuellig, R. A., Bornhauser, B. C., Knuesel, I., Heller, F., Fritschy, J. M., and Schaub, M. C. (2000). Identification and characterisation of transcript and protein of a new short N-terminal utrophin isoform. J Cell Biochem *77*, 418-431.